Investigation of the Role of Toll-like and Interleukin-6 Receptors in Peritoneal Inflammatory Responses to Infection

Chantal Sophie Françoise Colmont

Thesis submitted for the degree of Philosophiae Doctor

2014

Institute of Nephrology
School of Medicine
Cardiff University
Heath Park Campus
Cardiff University
CF14 4XN
United Kingdom

DECLARATION

This work has not previously been accepted in substance for any degree and is not concurrently submitted in candidature for any degree.

Signed …… (candidate) Date ……

STATEMENT 1

This thesis is being submitted in partial fulfillment of the requirements for the degree of ……(insert MCh, MD, MPhil, PhD etc, as appropriate)

Signed …… (candidate) Date ……

STATEMENT 2

This thesis is the result of my own independent work/investigation, except where otherwise stated.
Other sources are acknowledged by explicit references.

Signed …… (candidate) Date ……

STATEMENT 3

I hereby give consent for my thesis, if accepted, to be available for photocopying and for inter-library loan, and for the title and summary to be made available to outside organisations.

Signed …… (candidate) Date ……

STATEMENT 4: PREVIOUSLY APPROVED BAR ON ACCESS

I hereby give consent for my thesis, if accepted, to be available for photocopying and for inter-library loans **after expiry of a bar on access previously approved by the Graduate Development Committee.**

Signed …… (candidate) Date ……

ACKNOWLEDGEMENTS

I wish to express my gratitude to my supervisors Professor Nick Topley, Dr Donald Fraser and Dr Mario Labéta for the opportunity to undertake this research and their support throughout my time in research. I am particularly indebted to Dr Mario Labéta, who helped and supported me during the writing period and who enabled the completion of this PhD.

I express my appreciation and gratitude to Dr Ceri Fielding for his help and support from the beginning of the project and throughout my time in research and for carrying out the *in vivo* experiment described in section 2.1.7. A very special thank you to Dr Anne-Catherine Raby who carried out the luciferase assay experiments described in section 2.1.5, the Western blot of section 2.2.1 and for her help performing some *in vivo* experiments. I want to thank Prof Arthur Tzianabos (Department of Microbiology and Molecular Genetics, Harvard Medical School, Boston, USA) for welcoming me in his laboratory and allowing me to perform preliminary experiments before setting up the *in vivo* model of bacterial infection in Cardiff, and Dr Ronald Panzo for conducting the experiment with me. Due to the magnitude and technological demand required to set up the mouse model of peritoneal bacterial infection, the experiments of section 2.4 were carried out with Mrs Barbara Coles and Dr Ann Kift-Morgan. I would like to thank them both for performing the animal experiments and analysing the results with me. I would like to thank Dr Claudia Consoli from Central Biotechnology Services (School of Medicine, Cardiff University) for her technical support with RNA extraction from murine peritoneal membranes and performing some of the qRT-PCR. I wish to thank Dr Vincent Dioszeghy who helped me with immunocytochemistry experiments. A special acknowledgement and thank you goes to Dr Ola Krupa for her help with primer design and real-time PCR work and for her friendship. I wish to thank Professor Simon Jones for his help during the writing period. I also want to thank Dr Kieron Donovan for his critical reading of the clinical section on peritoneal dialysis.

I am very grateful to Dr Rachel McLoughlin for teaching me *in vivo* work and for her guidance when I first arrived in the laboratory, Dr John Martin and Dr Robert Jenkins for their help in the laboratory and everybody in the Institute of Nephrology, in particular Kim Abberley and Cheryl Ward for proof reading part of this manuscript.

Thank you to Andrew (*aka* LD) for helping me focus, for your support and constant encouragements. I wish to thank Anne-Catherine for her friendship and support during all these years in the laboratory, and on the climbing wall !

I want to specially thank my sister Béatrice for supporting and pushing me to finish my thesis and for regularly checking up on me to make sure I was not going crazy (merci beaucoup Béa de tes appels réguliers, pour ton aide morale, et tes encouragements), Blandine for her nice Paris postcards, as well as all my family and friends, in Cardiff and France.

ABSTRACT

Bacterial infection is a feature of long-term peritoneal dialysis (PD) and a cause of loss of peritoneal function and treatment failure. Understanding how local inflammation is initiated and peritoneal host defence mechanisms are activated in PD patients is key to reducing the detrimental consequences of peritonitis. The capacity of human peritoneal mesothelial cells (HPMC) to ingest bacteria has been described, and the ability of the Toll-like family of innate immune receptors (TLR) to trigger inflammatory responses to pathogens has been demonstrated. However, the pathogen recognition ability, the potential role of TLRs, the specific role in the early inflammatory response, and the regulation of HPMC' putative ability for pathogen recognition have not been fully investigated. To address these issues, the present study aimed at characterising TLR expression and responses in HPMC and evaluating the capacity of modulators of pro-inflammatory responses, namely soluble TLR2 (sTLR2) and the IL-6/sIL-6R complex, to regulate TLR-mediated HPMC and peritoneal responses *in vitro* and *in vivo*. HPMC were found to respond to an array of bacterial pathogens *via* expression and function of a specific set of TLRs. HPMC responses were susceptible to modulation by sTLR2 and sIL-6R, resulting in inhibition of TLR2-driven HPMC responses. *In vivo*, sTLR2 and IL-6/sIL-6R reduced neutrophil influx partly by inhibiting NF-κB activation in stromal cells of the peritoneum. IL-6 signalling counteracted TLR2-mediated responses by reducing peritoneal leukocyte recruitment and chemokine production. Notably, following the establishment of a mouse model of peritoneal bacterial infection, IL-6 signalling was confirmed to be beneficial to bacterial clearance. The results of this thesis confirm and extend the knowledge of the pivotal role that HPMC play in peritoneal responses to infection. The capacity of sTLR2 and IL-6/sIL-6R to modulate peritoneal responses demonstrated in this study may inform the design of new therapeutic strategies to reduce PD-associated peritonitis and thus improve treatment outcomes.

PUBLICATIONS and PRESENTATIONS

Publications

Fielding CA, Jones GW, McLoughlin RM, McLeod L, Hammond VJ, Uceda J, Williams AS, Lambie M, Foster TL, Liao CT, Rice CM, Greenhill CJ, Colmont CS, Hams E, Coles B, Kift-Morgan A, Newton Z, Craig KJ, Williams JD, Williams GT, Davies SJ, Humphreys IR, O'Donnell VB, Taylor PR, Jenkins BJ, Topley N, Jones SA. Interleukin-6 signaling drives fibrosis in unresolved inflammation. *Immunity*. 2014 Jan 16;40(1):40-50.

Raby AC, Holst B, Le Bouder E, Diaz C, Ferran E, Conraux L, Guillemot JC, Coles B, Kift-Morgan A, Colmont CS, Szakmany T, Ferrara P, Hall JE, Topley N, Labéta MO. Targeting the TLR co-receptor CD14 with TLR2-derived peptides modulates immune responses to pathogens. *Sci Transl Med*. 2013 May 15;5(185):185ra64.

Part of the work described in this thesis has been published:
Colmont CS, Raby AC, Dioszeghy V, Lebouder E, Foster TL, Jones SA, Labéta MO, Fielding CA, Topley N. Human peritoneal mesothelial cells respond to bacterial ligands through a specific subset of Toll-like receptors. *Nephrol Dial Transplant*. 2011 Dec;26(12):4079-90.

Raby AC, Holst B, Davies J, Colmont C, Laumonnier Y, Coles B, Shah S, Hall J, Topley N, Köhl J, Morgan BP, Labéta MO. TLR activation enhances C5a-induced pro-inflammatory responses by negatively modulating the second C5a receptor, C5L2. *Eur J Immunol*. 2011 Sep;41(9):2741-52.

Raby AC, Le Bouder E, Colmont C, Davies J, Richards P, Coles B, George CH, Jones SA, Brennan P, Topley N, Labéta MO. Soluble TLR2 reduces inflammation without compromising bacterial clearance by disrupting TLR2 triggering. *J Immunol*. 2009 Jul 1;183(1):506-17.

Dioszeghy V, Rosas M, Maskrey BH, Colmont C, Topley N, Chaitidis P, Kühn H, Jones SA, Taylor PR, O'Donnell VB. 12/15-Lipoxygenase regulates the inflammatory response to bacterial products in vivo. *J Immunol*. 2008 Nov 1;181(9):6514-24.

Fielding CA, McLoughlin RM, McLeod L, Colmont CS, Najdovska M, Grail D, Ernst M, Jones SA, Topley N, Jenkins BJ. IL-6 regulates neutrophil trafficking during acute inflammation via STAT3. *J Immunol*. 2008 Aug 1;181(3):2189-95.

Hams E, Colmont CS, Dioszeghy V, Hammond VJ, Fielding CA, Williams AS, Tanaka M, Miyajima A, Taylor PR, Topley N, Jones SA. Oncostatin M receptor-beta signaling limits monocytic cell recruitment in acute inflammation. *J Immunol*. 2008 Aug 1;181(3):2174-80.

McCully ML, Fairhead T, Colmont CS, Beasley FC, Heinrichs DE, Blake PG, Topley N, Madrenas J. Receptor-Interacting Protein-2 Deficiency Delays Macrophage Migration and Increases Intracellular Infection during Peritoneal Dialysis-Associated Peritonitis. *Am J Nephrol*. 2008 Jun 20;28(6):879-889.

Fielding CA, McLoughlin RM, Colmont CS, Kovaleva M, Harris DA, Rose-John S, Topley N, Jones SA. Viral IL-6 Blocks Neutrophil Infiltration during Acute Inflammation. *J Immunol*. 2005 Sep 15;175(6):4024-9.

Presentations:

Poster presentation at the 16th International Cytokine Society (ICS) annual meeting, Montreal, Canada, October 2008. "Regulation of TLR-mediated responses in the peritoneal cavity."

Oral presentation at the 2nd Euro PD annual meeting, Prague, Czech Republic, October 2005. "Regulation of TLR-mediated responses in the peritoneal cavity."

Oral presentation at the " Infection, Immunity and Inflammation Interdisciplinary Research Group (I^3IRG) Summer Meeting, Gregynog Hall, Newtown, Wales, July 2005. "Regulation of Toll-like receptor expression on mesothelium"

Poster presentation at the 12th International Cytokine Society (ICS) annual meeting, Puerto Rico, USA, October 2004. "Regulation of TLR-mediated responses in the peritoneal cavity."

ABBREVIATIONS

Ab	Antibody
AGE	Advanced Glycation End Products
AIM2	Absent in melanoma-2
APC	Antigen-presenting cell
BSA	Bovine serum albumin
CAPD	Continuous Ambulatory Peritoneal Dialysis
CARD	Caspase activation and recruitment domain
CCL	CC chemokines lignad
CD	Cluster of differentiation
CFU	Colony Forming Unit
CLR	C-type lectin receptor
CpG	2'-deoxyribo(cytidine–phosphate–guanosine)
CXCL	CXC chemokine ligand
DAI	DNA-dependent activator of IRF
DAMP	Danger-associated molecular patterns
DCs	Dendritic cells
DCC	Differential Cell Counting
DMEM	Dulbecco's modified Eagle medium
DNA	Desoxyribonucleic Acid
dsRNA	Double-stranded RNA
DTT	Dithiothreitol
E. coli	*Escherichia coli*
ECM	Extracellular matrix
EDTA	Ethylenediaminetetraacetic acid
ELISA	Enzyme-Linked Immunosorbant Assay
EMSA	Electrophoretic Mobility Shift Assay
ESRD	End Stage Renal Disease
FACS	Fluorescence-activated cell sorting
FBS	Foetal Bovine Serum
FCS	Foetal Calf Serum
GAPDH	Glyceraldhyde 3-Phosphate Dehydrogenase
GDP	Glucose Degradation Products
G-CSF	Granulocyte Colony-Stimulating Factor
GRP94	Glucose-regulated protein of 94 kDa
gp130	Glycoprotein 130
HA	Hyaluronan

HD	Haemodialysis
HDS	HYPER-DS-sIL-6R
HEK	Human embryonic kidney
HEPES	(4-(2-hydroxyethyl)-1-piperazineethanesulfonic acid)
HLA-DR	Human leukocyte antigen serotype DR
HMGB	High-mobility group box
HPMC	Human Peritoneal Mesothelial Cell
hToll	Human homologue of Toll
ICAM-1	Intracellular Cell Adhesion Molecule-1
iE-DAP	D-glutamyl-meso-diaminopimelic acid
IFNγ	Interferon γ
IL	Interleukin
IL-6R	IL-6 receptor
i.p.	intra peritoneal
IPAF	ICE protease-activating factor
IRAK	IL-1R-associated kinase
IRF	IFN regulatory factor
JAK	Janus kinase
KO	Knock-out
LDL	Lipoprotein
LPS	Lipopolysaccharide
LRR	Leucine-rich repeats
LTA	Lipoteichoic acid
mAb	monoclonal antibody
MAC	Membrane Attack Complex
MAL	MyD88 adaptor-like protein
MALP	Macrophage-activating lipopeptide from *Mycoplasma fermentans*
MAMP	Microbe-associated molecular patterns
MAPK	Mitogen-activated protein kinase
MD	Myeloid differentiation protein
MDA	Melanoma differentiation associated gene
MDP	Muramyl dipeptide
MHC	Major histocompatibility complex
miR	Micro RNA
MMP	Matrix metalloproteinase
MNC	Mononuclear cells
MPMC	Murine peritoneal mesothelial cells
mRNA	Messenger RNA
Myd88	Myeloid differentiation primary response gene 88
NAIP	Neuronal apoptosis inhibitory protein

NALP	NACHT-LRR-PYD-containing protein
NF-κB	Nuclear factor-kappa B
NK	Natural killer
NLR	NOD-like receptor
NOD	Nucleotide-binding oligomerisation domain
OD	Optical Density
OSM	Oncostatin M
PAMP	Pathogen-associated molecular patterns
Pam_2Cys	Dipalmitoyl-cysteinyl-seryl-$(lysil)_3$-lysine (Pam_2-Cys-Ser-Lys_4)
Pam_3Cys	Tripalmitoyl-cysteinyl-seryl-$(lysil)_3$-lysine (Pam_3-Cys-Ser-Lys_4)
PBMC	Peripheral blood mononuclear cell
PBS	Phosphate buffer saline
PCR	Polymerase chain reaction
PD	Peritoneal dialysis
pDC	Plasmacytoid dendritic cell
PE	Phycoerythrin
PECAM	Platelet endothelial cell adhesion molecule
PGN	Peptidoglycan
PI3K	Phosphatidylinositol 3 kinase
PMN	Polymorphonuclear leukocyte
PMSF	Phenylmethylsulphonyl fluoride
Poly (dIdC)	Poly (2' deoxyinosinic-2'-deoxycytidylic acid) sodium salt
Poly IC	Polyinosinic-polycytidylic acid
PRR	Pattern recognition receptor
qRT-PCR	Quantitative reverse transcription polymerase chain reaction
RIG	Retinoic acid-inducible gene
RIP	Receptor-interacting protein
RLR	RIG-I-like receptor
RNA	Ribonucleic Acid
RRF	Residual renal function
RRT	Renal replacement therapy
RT	Room temperature
RT	Reverse transcription
s	Soluble
SAA	Serum amyloid A
SD	Standard deviation
S. aureus	*Staphylococcus aureus*
S. epi.	*Staphylococcus epidermidis*
SEM	Standard error of the mean
SES	*Staphylococcus epidermidis* cell-free supernatant

SHP	Src homology 2 (SH2)-domain-containing tyrosine phosphatase
siRNA	Small interfering RNA
SOCS	Suppressor of cytokine signaling
SOP	Standard operating procedure
ssRNA	Single-stranded RNA
STAT	Signal transducer and activator of transcription
TANK	TNFR-associated factor family member-associated NF-κB activator
TGF	Transforming growth factor
TICAM	TIR domain-containing adapter molecule
TIMP	Tissue inhibitor of metalloproteinase
TIR	Toll-IL-1 resistance/receptor
TIRAP	TIR domain-containing adapter protein
t-GPI-mucins	Glycosylphosphatidylinositol-mucin
TLR	Toll-like receptor
TNF	Tumor necrosis factor
TRAF	TNFα receptor-associated factor
TRAM	TRIF-related adapter molecule
TRIF	TIR-containing adapter inducing IFNβ
TRIL	TLR4 interactor with leucine-rich repeats
VCAM	Vascular cell adhesion molecule
vs.	Versus
WT	Wild-type

TABLE OF CONTENTS

DECLARATION ii

ACKNOWLEDGEMENT iii

ABSTRACT iv

PUBLICATIONS and PRESENTATIONS v

ABBREVIATIONS vii

CHAPTER I: INTRODUCTION 1

1.1 RENAL REPLACEMENT THERAPY 2

1.1.1 RENAL FAILURE 2

1.1.2 PERITONEAL DIALYSIS *VS*. HAEMODIALYSIS 2

1.1.3 HISTORY OF PERITONEAL DIALYSIS 3

1.1.4 PERITONEAL DIALYSIS 3

1.1.4.1 The technique 3

1.1.4.2 Peritoneal dialysis modalities 3

1.1.5 COMPLICATIONS AND TREATMENT FAILURE 3

1.1.5.1 Inflammation 3

1.1.5.2 Infection 4

1.2 THE PERITONEAL CAVITY AND PERITONEUM 4

1.2.1 STRUCTURE OF THE PERITONEAL CAVITY 4

1.2.1.1 Visceral-Parietal 4

1.2.1.2 Mesentery adipose tissue 5

1.2.1.3 Omenta and milky spots 5

1.2.1.4 Immunocompetent resident cells 5

1.2.2 THE PERITONEAL MEMBRANE 5

1.2.2.1 Anatomy of the peritoneal membrane 6

1.2.2.2 Loss of peritoneal membrane function with time on PD 6

a. Bioincompatible PD solutions 6

b. Peritonitis 7

1.3 MESOTHELIAL CELLS 8

1.3.1 MESOTHELIUM ANATOMY 8

1.3.2 MESOTHELIAL CELLS 8

1.3.2.1 Morphology 8

1.3.2.2 Typical features of HPMC 8
1.3.3 PHYSIOLOGICAL FUNCTIONS OF THE MESOTHELIUM 9
1.3.3.1 Protection barrier 9
1.3.3.2 Transport and communication 9
1.3.3.3 Peritoneal clearance 9
1.3.3.4 Procoagulant and fibrinolytic activities 10
1.3.3.5 Tissue repair and extracellular matrix remodelling 10
1.3.3.6 Epithelial-to-mesenchymal transition 10
1.4 PERITONEAL IMMUNITY 11
1.4.1 IMMUNOCOMPETENT CELLS OF THE PERITONEAL CAVITY 11
1.4.1.1 Role of the mesothelium in inflammation 11
a. Ingestion of bacteria 11
b. Antigen presentation 11
c. Expression of complement factors 12
d. Role of HPMC-secreted glycosaminoglycans 12
e. Expression of cytokines and chemokines 12
f. Immunomodulatory role of HPMC 13
g. Expression of adhesion molecules 13
1.4.1.2 Peritoneal macrophages 14
1.4.1.3 Peritoneal lymphocytes and dendritic cells 14
1.4.1.4 Other cells with immune activity in the peritoneal cavity 15
1.4.2 THE ROLE OF IL-6 IN INFLAMMATION AND ITS MECHANISM OF ACTION 15
1.4.3 LEUKOCYTE RECRUITMENT DURING PERITONEAL INFLAMMATION 17
1.4.4 RESOLUTION OF THE EARLY PHASE OF PERITONEAL INFLAMMATION 18
1.5 THE INNATE IMMUNE SYSTEM AND PERITONEAL IMMUNITY 19
1.5.1 OVERVIEW OF THE INNATE AND ADAPTIVE IMMUNE RESPONSES 19
1.5.2 COMPONENTS OF THE INNATE IMMUNE SYSTEM 20
1.5.2.1 Mucosal epithelia 21
1.5.2.2 Eosinophils, basophils and mast cells 21
1.5.2.3 Phagocytes 22
a. Neutrophils 22
b. Macrophages 22
1.5.2.4 NK cells and DCs 22
1.5.2.5 Antimicrobial peptides, proteins and enzymes 23
1.5.2.6 Complement 24

1.5.2.7 Additional components 25

a. Acute phase proteins 25

b. Lipid mediators 25

c. Inflammasomes 25

1.6 RECEPTORS OF THE INNATE IMMUNE SYSTEM 26

1.6.1 SOLUBLE PRRS 26

1.6.2 ENDOCYTIC RECEPTORS 27

1.6.2.1 C-type lectin receptors (CLRs) 27

1.6.2.2 Scavenger receptors 28

1.6.3 SIGNALLING RECEPTORS 28

1.6.3.1 Nucleotide-binding oligomerisation-domain protein (NOD)-like receptors (NLRs) 28

1.6.3.2 Retinoic-acid-inducible protein I (RIG-I)-like receptors (RLRs) 29

1.6.3.3 Additional receptors 29

1.7 THE TOLL-LIKE RECEPTOR FAMILY 30

1.7.1 TISSUE DISTRIBUTION OF TLRS 31

1.7.2 CELLULAR LOCALISATION OF TLRS 32

1.7.3 TLR LIGANDS, CO-RECEPTORS AND ACCESSORY MOLECULES 32

1.7.3.1 TLR1, TLR2 and TLR6 33

1.7.3.2 TLR4 34

1.7.3.3 TLR5 34

1.7.3.4 TLR3 35

1.7.3.5 TLR7 and TLR8 35

1.7.3.6 TLR9 35

1.7.4 STRUCTURE AND ACTIVATION 36

1.7.5 TLR SIGNALLING PATHWAYS 38

1.7.5.1 The MyD88-dependent pathway 38

1.7.5.2 The TRIF-dependent pathway 39

1.7.6 REGULATION OF TLR SIGNALLING 39

1.7.6.1 Soluble TLRs 39

1.7.6.2 Transmembrane and intracellular modulators 40

1.7.7 TLR INTERACTION WITH OTHER SIGNALLING PATHWAYS 41

1.8 HYPOTHESES, AIMS AND OBJECTIVES OF THE PROJECT 42

CHAPTER II: RESULTS 43

2.1 EXPRESSION AND ACTIVITY OF TLRS IN HUMAN PERITONEAL MESOTHELIAL CELLS 44

2.1.1 TLR EXPRESSION IN HPMC 44

2.1.2 HPMC RESPONSES TO TLR2, TLR4 AND TLR5 LIGANDS 45

2.1.3 HPMC RESPONSES TO TLR3 AND TLR7/8 LIGANDS 46

2.1.4 FURTHER EVALUATION OF HPMC RESPONSES TO SES 47

2.1.5 EXAMINATION OF THE INVOLVEMENT OF CD14 IN HPMC RESPONSES TO SES 47

2.1.6 EVALUATION OF THE EFFECT OF INFLAMMATORY CYTOKINES AND TLR LIGANDS ON HPMC TLR2 EXPRESSION 48

2.1.7 DISCUSSION 49

2.2 MODULATION OF TLR2-MEDIATED HUMAN PERITONEAL MESOTHELIAL CELL RESPONSES: EFFECT OF SOLUBLE TLR2 AND IL-6 RECEPTOR ACTIVATION 52

2.2.1 PRODUCTION OF SOLUBLE TLR2 BY HPMC AND ITS DETECTION IN PD FLUID 52

2.2.2 EFFECT OF SOLUBLE TLR2 ON CYTOKINE RELEASE AND NF-κB ACTIVATION IN MESOTHELIAL CELLS 52

2.2.3 EFFECT OF IL-6 TRANS-SIGNALLING ON TLR2-MEDIATED HPMC RESPONSES 53

2.2.4 EFFECT OF SOLUBLE TLR2 ON STAT ACTIVATION 55

2.2.5 DISCUSSION 55

2.3 ROLE OF TLR2, SOLUBLE TLR2 AND IL-6 SIGNALLING IN PERITONEAL INFLAMMATION AND INFECTION *IN VIVO* 58

2.3.1 EFFECT OF SOLUBLE TLR2 ON SES-INDUCED LEUKOCYTE RECRUITMENT AND CYTOKINE PRODUCTION 58

2.3.2 EFFECT OF SOLUBLE TLR2 ON SES-INDUCED NF-κB AND STAT ACTIVATION 59

2.3.3 EFFECT OF SOLUBLE TLR2 ON *S. EPI.*-INDUCED PERITONEAL INFECTION 59

2.3.4 EFFECT OF IL-6 SIGNALLING ON *S. EPI.*-INDUCED INFLAMMATION AND INFECTION 61

2.3.5 DISCUSSION 63

2.4 DEVELOPMENT OF AN *IN VIVO* MODEL OF BACTERIAL PERITONITIS 67

2.4.1 METHOD 68

2.4.1.1 Reagents and Equipment 68

2.4.1.2 Animals 68

2.4.1.3 General aseptic technique 68

2.4.1.4 Bacteria 68

2.4.1.5 Agar plate inoculation and incubation 68

2.4.1.6 First and second broth inoculation and incubation 68

2.4.1.7 Bacteria preparation for inoculation 69

2.4.1.8 Inoculum verification 69
a. OD measurement 69
b. Bacterial counts on agar plate 69
c. ATP bioassay 70
2.4.1.9 Preparation of injection 70
a. Mice body temperature readings 70
b. Anaesthetisation of mice 70
2.4.1.10 Intra peritoneal injection of anaesthetised mice 70
2.4.1.11 Mice body temperature readings and culling process 70
2.4.1.12 Blood retrieval by cardiac puncture 70
2.4.1.13 Peritoneal lavages 71
2.4.1.14 Peritoneal membrane recovery for bacterial count 71
2.4.1.15 Kidney recovery for bacterial count 71
2.4.1.16 Sample processing 71
a. Technical issue: haemocytometer *vs.* cell counter counts 71
b. Technical issue: Differential cell counting by cytospin *vs.* flow cytometry 72
c. Technical issue: manual *vs.* spiral plating of bacteria 72
2.4.1.17 Microbiology, dilutions, plating, incubation and counting 72
2.4.2 RESULTS 73
2.4.2.1 Standardisation-Bacterial growth 73
a. Staphylococcus epidermidis 73
b. Staphylococcus aureus 74
c. Escherichia coli 75
2.4.2.2 Staphylococcus epidermidis infection 75
a. Pilot study 1: Aseptic techniques and bacterial dissemination 75
b. Pilot study 2: Dose determination 76
c. Pilot study 3: Toxicity-survival 76
d. Pilot study 4: Bacterial dose optimisation for a 24h study 77
e. Pilot study 5: Bacterial dose optimisation for a 96h study 78
2.4.2.3 Pilot study to establish a mild peritonitis model with S. aureus 79
2.4.2.4 Pilot study of E. coli - induced peritonitis 80
2.4.3 DISCUSSION 81
CHAPTER III: DISCUSSION AND FUTURE WORK 83
CHAPTER IV: MATERIALS AND METHODS 93

4.1 ANTIBODIES, REAGENTS AND EQUIPMENT **94**

4.2 CELL AND TISSUE CULTURE **95**

4.2.1 HPMC ISOLATION, GROWTH CONDITIONS AND SUB-CULTURE 95

4.2.2 SV40-TRANSFORMED HPMC 96

4.2.3 ISOLATION AND CULTURE OF PERIPHERAL BLOOD MONONUCLEAR CELLS 96

4.2.4 CULTURE OF TRANSFECTED HUMAN EMBRYONIC KIDNEY CELLS 96

4.3 CELL ACTIVATION **97**

4.3.1 ACTIVATION OF HPMC 97

4.3.2 ACTIVATION OF PBMC 98

4.3.3 STIMULATION OF TRANSFECTED HUMAN EMBRYONIC KIDNEY CELLS 98

4.4 DETECTION OF TLR EXPRESSION BY IMMUNOCYTOCHEMISTRY **98**

4.5 FLOW CYTOMETRY ANALYSIS **98**

4.6 RNA ANALYSIS **99**

4.6.1 RNA ISOLATION FROM HPMC AND MOUSE PERITONEAL MEMBRANE 99

4.6.2 NUCLEIC ACID QUANTIFICATION AND RNA INTEGRITY ASSESSMENT METHODS 99

4.6.3 REVERSE TRANSCRIPTION 100

4.7 DNA ANALYSIS **101**

4.7.1 PRIMER DESIGN AND PCR 101

4.7.2 QUANTITATIVE REAL-TIME PCR 101

4.8 NF-κB REPORTER ASSAY **102**

4.9 PREPARATION OF NUCLEAR EXTRACTS **102**

4.9.1 HPMC NUCLEAR EXTRACTS 102

4.9.2 NUCLEAR EXTRACTS FROM MURINE PERITONEAL MEMBRANE 103

4.10 ELECTROPHORETIC MOBILITY SHIFT ASSAY (EMSA) **103**

4.10.1 ANNEALING OF PRIMERS AND RADIO-LABELLING OF OLIGONUCLEOTIDE PROBES 103

4.10.2 ANALYSIS OF DNA-PROTEIN COMPLEXES BY ELECTROPHORESIS 103

4.10.3 ANALYSIS OF TRANSCRIPTION FACTOR SUBUNITS 104

4.11 SDS-PAGE AND WESTERN BLOTTING **104**

4.12 PREPARATION OF *S. EPI*. CELL-FREE SUPERNATANT (SES) **105**

4.13 *IN VIVO* EXPERIMENTS **105**

4.14 STATISTICAL ANALYSIS **106**

BIBLIOGRAPHY **107**

Chapter I

INTRODUCTION

1.1 Renal replacement therapy

1.1.1 Renal failure

End-stage renal disease (ESRD) is a condition in which a patient's kidneys have stopped functioning and renal replacement therapy (RRT) is required. There are two major forms of RRT available following kidney failure: renal transplant or dialysis. Kidney transplant is the best possible option available for some patients, but there are not enough donor kidneys for all patients and not always suitable recipients. About 23% of ESRD patients have a renal transplant (Grassmann et al., 2005), leaving the remaining patients relying on dialysis therapy.

1.1.2 Peritoneal dialysis *vs*. haemodialysis

There are mainly two types of dialysis therapies: haemodialysis (HD), the most common dialysis method, and peritoneal dialysis (PD). The latter is the method used for about 11% of patients worldwide (Jain et al., 2012), with a higher rate in some countries such as the UK, where 16.8% of RRT consists of PD (Byrne et al.).

HD takes place at the hospital or at home, where the patient's blood is pumped and passed through an artificial kidney to be filtered.

PD, for which the internal lining of the abdomen acts as the artificial kidney, is carried out at home. Dialysis fluid is instilled into the peritoneal cavity via a catheter surgically installed in the cavity (Fig 1.1). An exchange of water and solutes takes place across the peritoneum between the capillary blood and the dialysate (see detailed description of the technique below, section 1.1.4.). PD potentially offers several advantages over HD, including a better preservation of the residual renal function (RRF) (Jansen et al., 2002) and a lower cost. RRF is an important parameter when considering the success of the dialysis process, and PD appears to have a survival advantage in the first 2 to 4 years (Saxena and West, 2006; Sinnakirouchenan and Holley, 2011). This technique also allows a greater flexibility for the patient, who can continue to work and travel and have less dietary restrictions, therefore contributing to a better quality of life (Saxena and West, 2006). Most patients stay only a few years on PD. The main causes of PD treatment failure are peritonitis, the structural and functional changes of the peritoneal membrane and the loss of RRF (Saxena and West, 2006). Globally, there is a 6 to 7% annual increase in ESRD patients, with an increase in both HD and PD quite variable depending on the country (Grassmann et al., 2005). In the UK, the prevalence of patients on RRT has increased by about 4% over the last two decades (Byrne et al., 2010), with HD increasing while PD decreases. It is essential to give the best possible choice for the patient as well as providing a cost effective treatment.

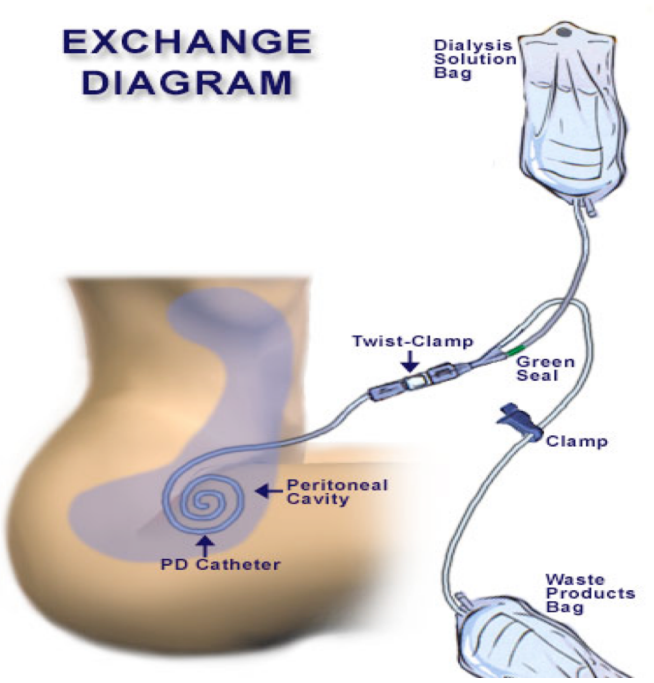

Figure 1.1. Schematic representation of fluid exchange during PD.

1.1.3 History of peritoneal dialysis

It was in 1923 that the first description of a saline solution being infused into the peritoneal cavity of a woman, whose condition then improved, was published (Ganter, 1923). Over the next 50 years, this method was developed and refined in patients as well as animals (Boen, 1988). Initially known as equilibrium peritoneal dialysis technique, Continuous Ambulatory Peritoneal Dialysis (CAPD) was introduced in 1976 by Popovitch (Popovich et al., 1978). It marked the transition from using PD only for acute renal failure to chronic renal failure (Krediet, 2007).

1.1.4 Peritoneal dialysis

1.1.4.1 The technique

When the peritoneal membrane is bathed in fluid, waste products can diffuse from the capillary blood vessels into the fluid. Thereby, blood toxins such us urea, creatinine, phosphates, among other molecules, can be removed as they diffuse into the dialysate. Excess body water is also removed during PD by ultrafiltration. This is achieved by adding an osmotically active agent, typically glucose, to the PD fluid to make it hypertonic compared to blood. During peritoneal dialysis, 2-3 litres of dialysis fluid is infused into the peritoneal cavity where it remains for several hours, whilst waste products diffuse into it, and it is then drained out. This process, repeated several times a day, can effectively replace some of the excretory functions of the kidney.

1.1.4.2 Peritoneal dialysis modalities

Over the years, different types of PD schedules have been established, with procedures being manual or automated, continuous or intermittent (Saxena and West, 2006). CAPD is the most common regimen, and is usually the manual performance of 3 exchanges during the day and an overnight long dwell. An alternate procedure with shorter and more frequent dwells, termed Automated Peritoneal Dialysis, uses a mechanised cycler which infuses and drains peritoneal dialysate at night for faster fluid exchanges (Ryckelynck et al., 2005). The choice of regimen will depend on the peritoneal membrane transport kinetics.

1.1.5 Complications and treatment failure

Despite presenting advantages over HD, including improved well-being due to continuous removal of waste products, PD has long-term complications such as inflammation, infection, vasculopathy and fibrosis within the peritoneal membrane (de Lima et al., 2013).

1.1.5.1 Inflammation

Even in the absence of infection, an inflammatory status is a feature of chronic kidney disease, even at early stages. Although it may pre-exist the treatment, it often worsens due to uremia, the presence of waste products, as well as mechanical stress and the existence of

comorbidities. Macrophages and cytokines have been found in the peritoneal cavity of PD patients, indicating a state of chronic inflammation (de Lima et al., 2013).

1.1.5.2 Infection

Microbial-induced peritonitis remains a leading complication of PD, occurring at a variable rate depending on centers and countries. Immediate consequences can be hospitalisation, transfer to HD and increased mortality, while longer-term problems include membrane failure and cardiovascular morbidity (Lam et al., 2007). Patients usually present with abdominal pain and "cloudy" dialysis fluid. The diagnosis is subsequently confirmed by the finding of > 100 white blood cells/mm^3 of dialysate (with at least 50% of neutrophils). The most common pathogenic organisms involved in peritonitis in PD patients are skin commensals such as Gram-positive *Staphylococci*. In particular, *Staphylococcus epidermidis* and *Staphylococcus aureus* are found in 30-50% of peritoneal infections (Szeto et al., 2005). Over the past decade, however, a growing feature of this mode of treatment is the clinically more severe infections with Gram-negative organisms, resulting in increased rate of treatment failure and poor patient outcomes (Szeto and Chow, 2007). The wide spectrum of organisms responsible for PD-associated infections is summarised in Table 1.1.

Other detrimental factors impairing PD, such as bioincompatible PD solutions (described in section 1.2.2.2) affect the peritoneal membrane, which functions as a permeability barrier across which diffusion and ultrafiltration occur. The maintenance of this function is critical to the technique success.

1.2 The peritoneal cavity and peritoneum

1.2.1 Structure of the peritoneal cavity

The abdominal or peritoneal cavity is the space circumscribed by the peritoneal membrane or peritoneum. It comprises the digestive system (stomach and intestines) as well as the liver, pancreas, spleen, kidneys and bladder. It also includes the peritoneal reflections which are the peritoneal ligaments, mesenteries and omenta, fatty tissue that connects the spleen, stomach, pancreas and colon (Healy and Reznek, 2000). A thin layer of serous fluid (up to 100 ml) maintains the surface of the peritoneum moist and smooth, protecting it from frictional damage (Raftery et al., 1989). The following is a brief description of the different parts of the peritoneal cavity and their main roles.

1.2.1.1 Visceral-Parietal

The peritoneum can be divided into the parietal peritoneum lining the abdominal wall and the visceral peritoneum around the abdominal organs (Healy and Reznek, 2000). In PD, it is mainly

Table 1.1 Organisms associated with PD infections

Organisms	Frequency
Gram-positive bacteria	
Staphylococcus epidermidis	50-90%
Staphylococcus aureus	30-40%
Streptococcus viridians	5-10%
Streptococcus fecalis	5-10%
Gram-negative bacteria	
Escherichia coli	5-10%
Klebsiella/Enterobacter spp.	5%
Pseudomonas spp.	< 10%
Acinetobacter spp.	< 5%
Mycobacterium spp.	< 5%
Other	< 5%
Fungi	
Candida spp. Other Fungi	1-10%
Culture negative	5-20 (up to 30) %

Adapted from (Munib 2006, Akoh 2012)

the parietal peritoneum which is effectively involved in the exchanges of water and solutes (Saxena and West, 2006).

1.2.1.2 Mesentery adipose tissue

There are four mesenteries adipose tissue in the peritoneal cavity (small bowel mesentery, transverse mesocolon, sigmoid mesocolon and mesoappendix), which are folds of peritoneum connecting various organs to each other or to the abdominal wall (Healy and Reznek, 2000). Clusters of lymphocytes, able to proliferate and secrete an array of cytokines in response to stimulation, have recently been observed in both mouse and human mesentery (Moro et al., 2010).

1.2.1.3 Omenta and milky spots

Among the two omenta, the lesser and greater omentum, the latter is the largest peritoneal fold and plays an important role in immunity (Healy and Reznek, 2000). It has been referred to as the “abdominal policeman”. Within the greater omentum, anatomist Ranvier described in 1874 small white aggregates of cells of lymphoid origin that he named milky spots (Broche and Tellado, 2001). In a resting state, milky spots are mainly composed of macrophages and B1 lymphocytes as well as few T lymphocytes (Rangel-Moreno et al., 2009). Following expression of various adhesion molecules (ICAM-1, VCAM-1) on the peritoneal membrane, the leukocytes can migrate from the bloodstream through the milky spots into the peritoneal cavity. This phenomenon occurs in both resting and stimulated conditions, providing the supply of peritoneal macrophages to the cavity (Cui et al., 2002). Rapidly following the start of PD, the number and size of milky spots increase (Beelen et al., 2005).

1.2.1.4 Immunocompetent resident cells

Resident peritoneal macrophages constitute the main leukocyte cell population in the cavity (70-90%), which also contains B and T lymphocytes (5-10%). The presence of small proportions of natural killer (NK) cells and dendritic cells (DC) has also been reported (Broche and Tellado, 2001; Sammour et al., 2010). In addition, mesothelial cells greatly contribute to host defence. Their role as well as the role of the different immunocompetent cells of the peritoneal cavity, including fibroblasts and adipocytes, will be described in section 1.4.

1.2.2 The peritoneal membrane

The peritoneum has been studied since antiquity, as the first mention of lymph vessels (lacteals-milk, white fluid) in the peritoneum is from Erasistratus, a Greek physician who died in 280 BC (Robinson, 1897). Most of the research was done from the 16th century by various European anatomists and surgeons. Notably, Bichat (1771-1808) first established that the peritoneum had a structure (anatomy) and function (physiology) and called it a serous membrane (Robinson, 1897). In 1897, Robinson writes that the function of the peritoneum is “to

regulate fluid for nutrient and mechanical purposes. Its anatomical utility is chiefly mechanical, ie. to allow limited action, to facilitate motion, to economise friction and conduct vessels and nerves to viscera" (Robinson, 1897). There has been a renewed interest in the study of the peritoneum since the introduction of PD as a treatment of ESRD.

1.2.2.1 Anatomy of the peritoneal membrane

The name peritoneum comes from the Greek periteino, which means to stretch around (Arnold and Bryce, 2010). The peritoneum, which is the largest serous membrane of the body, has a surface area equal to that of the skin with 1-2 m^2. It consists of two layers, the mesothelium and the tunica propria.

1) mesothelium: a simple squamous epithelium resting on a basal lamina (basement membrane or sub-mesothelial compact zone).

2) tunica propria: a layer of vascular loose connective tissue formed by a complex network of extracellular matrix (ECM), which consists of macromolecules of collagen, elastin and fibronectin as well as hydrated gel made of different glycosaminoglycans (Hyaluronan (HA), sulphated proteoglycans). Some large and small blood vessels are found in a deeper loosen adipose layer. Draining lymphatics are mainly in the interstitium of the sub-diaphragmatic peritoneal membrane, whereas the extracellular fluid is found throughout the ECM. Fibroblasts, macrophages and mast cells are also present (Nagy and Jackman, 1998; Raftery et al., 1989) (Fig 1.2).

1.2.2.2 Loss of peritoneal membrane function with time on PD

This is one of the main causes of treatment failure. Although the precise biological mechanisms responsible for the changes are still not well defined, it is generally assumed that alterations in peritoneal function are related to structural changes in the membrane. These changes include loss or degeneration of the mesotelium, increase in the thickness of the sub-mesothelial compact zone and various vascular changes, such as small vessel atherosclerosis (Williams et al., 2002; Williams et al., 2003b). These modifications in membrane structure are generally described as fibrosis. Studies showed that over time on PD, the membrane thickness increases from an average of 50-100 μm up to 700-1000 μm (Williams et al., 2002; Williams et al., 2003a; Williams et al., 2003b). These changes are associated with a loss of ultrafiltration and decrease of solute clearance. Encapsulating peritoneal sclerosis is a serious complication, characterised by gross fibrotic changes leading to bowel obstruction, whose frequency increases with time on PD (Lambie et al., 2010). Although multi-factorial, membrane fibrosis is mainly thought to be due to exposure to bioincompatible PD solutions and to recurrent infections.

a. Bioincompatible PD solutions

The precise etiology is still speculative, but studies suggested that the continuous exposure to dialysis fluids is associated with membrane fibrosis. These fluids have a detrimental effect due to their low pH (which prevents the caramelisation of glucose during sterilisation), the high

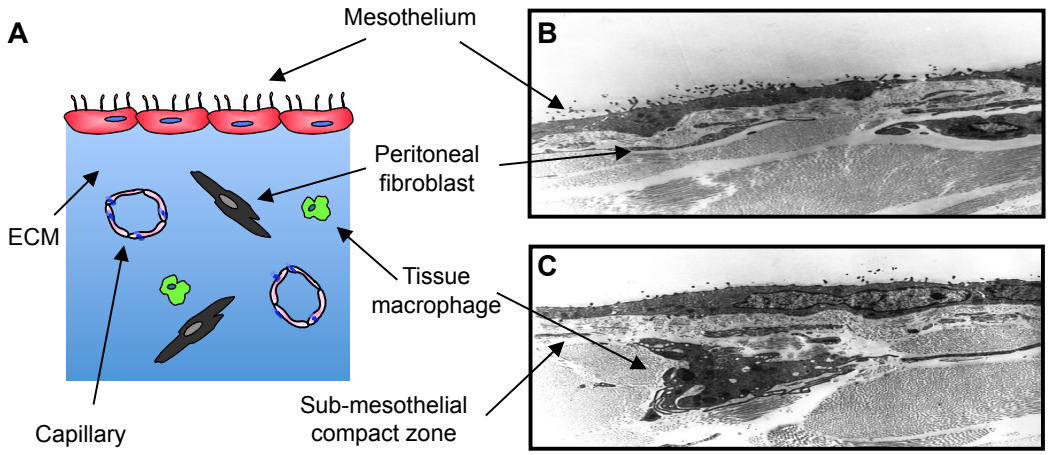

Figure 1.2. Structure of the peritoneal membrane.
Cross section of the peritoneal membrane shown schematically **(A)**, and following transmission electron microscopy **(B, C)**. The mesothelium is covered with microvilli. Tissue macrophage and peritoneal fibroblast are indicated. ECM, extracellular matrix.

concentration of glucose, glucose degradation products (GDP) and lactate. These fluids are referred to as “bioincompatible”. Glucose is a potent activator of human peritoneal mesothelial cells (HPMC), inducing production of fibronectin and Transforming Growth Factor β (TGFβ), both drivers of fibrosis (Ha et al., 2001). PD fluids may also contribute to membrane damage via the presence of GDP and the formation of advanced glycation end products (AGE) (Honda et al., 1999). *In vitro* studies show that certain GDP inhibit mesothelial wound healing (Morgan et al., 2003), whilst *in vivo* mouse studies suggest that they contribute to angiogenesis and fibrosis. Glucose, AGE and lactate have also been implicated in cellular pathways involved in fibrosis (Saxena, 2008; ter Wee et al., 2003). Upon experimental PD and exposure to PD fluids, mast cells were found to accumulate in the omentum in proximity of blood vessels and produce angiogenic and profibrotic factors, suggesting a role in omental tissue remodelling in long-term PD (Zareie et al., 2006). To prevent these adverse effects, new PD fluids have been developed with a physiological pH, a bicarbonate buffer and low GDP content. Despite being less cytotoxic, a beneficial effect for patient outcomes remains to be demonstrated.

b. Peritonitis

A correlation between the peritoneal membrane thickness and the number of peritonitis episodes has been demonstrated, as well as the increased TGFβ production by HPMC following pro-inflammatory cytokines secretion (Kang et al., 1999). In addition, the degree of associated peritoneal inflammation has been shown to influence the changes in peritoneal kinetics (Davies et al., 1996). With time on CAPD, the accumulation of AGE was also shown to be increased with the number of peritonitis episodes (Park et al., 2000), which might in turn have a detrimental effect on the membrane. Furthermore, following exposure to bioincompatible solutions, the inflammatory response has been shown to be impaired, with a lower viability of leukocytes and mesothelial cells, a defect in cytokines and chemokines secretion, decreased phagocytosis, respiratory burst and bacterial killing, increasing the detrimental effect of infection (Mackenzie et al., 2003; Mortier et al., 2004). Notably, treatment of a mesothelial cell line with glucose-based solutions decreased Toll-like receptor 2 (TLR2) and TLR4 expression and tumour necrosis factor α (TNFα) and interleukin 1β (IL-1β) secretion following stimulation with TLR ligands (Wu et al., 2010), potentially impairing the peritoneal response to bacterial peritonitis.

Of note, infection has a profound effect on its own by impairing the physiological properties of the membrane, and by contributing to fibrosis.

The combination of inflammation and angiogenesis occurring in the sub-mesothelial compact zone simultaneously to fibrosis, results in an impaired exchange of solutes and water between dialysis solution and blood, leading to ultrafiltration failure, in particular in long-term PD patients. The mesothelial cells lining the peritoneal membrane greatly contribute to these events because of their versatile roles.

1.3 Mesothelial cells

1.3.1 Mesothelium anatomy

The monolayer of cells covering the surface of the peritoneum originates from the mesoderm and looks like an epithelium, therefore was named mesothelium by Minot (Minot, 1880). It extends over several regions, including the abdominal cavity (peritoneum), the chest cavity (pleura), and pericardium (heart) (Mutsaers, 2004). Stomata are 4-10 μm openings between mesothelial cells, located on the mesothelium lining of the diaphragm as well as the omental, mesenteric and pelvic peritoneum (Yao et al., 2003). They represent an important channel of communication between the peritoneal cavity and the lymphatic system (Sammour et al., 2010).

1.3.2 Mesothelial cells

1.3.2.1 Morphology

Mesothelial cells constitute one of the most numerous cell types of the peritoneal cavity, with about 1 x 10^9 cells (Nagy and Jackman, 1998). They show a predominantly flattened and squamous aspect, but can also appear cuboidal in specific areas (Fig 1.3) - notably around milky spots - and each type has a different metabolic state. The cuboidal mesothelial cells are more active, with a cytoplasm rich in mitochondria, rough endoplasmic reticulum, Golgi apparatus and microtubules (Mutsaers, 2002; Yao et al., 2003).

HPMC are between 0.5 μm to 2 μm thick and about 30 μm in diameter, with the cytoplasm raised over the nucleus region and a thinner surrounding region, where HPMC are in contact with each other to form a continuous sheet (Mutsaers, 2004; Raftery et al., 1989). The integrity of the mesothelium is provided in part by the overlapping of cells, but mainly by a number of cell-cell and cell-matrix interactions. Adherens junctions and desmosomes form anchoring junctions to attach HPMC to each other or to the basement membrane; gap junctions allow chemical and electrical signals between HPMC (Mutsaers, 2004; Nagy and Jackman, 1998). The apical, luminal, surface is covered with microvilli, which can increase the cell surface area up to 40 m^2. Microvilli can adapt to the physiological conditions by increasing their length and number (Raftery et al., 1989; Yung and Chan, 2009). Cilia, up to five times longer than microvilli, can also be observed on the apical surface, which in addition to a protective role as part of the peritoneal barrier might play a role in the cells' polarity and adhesion, as well as in matrix proteins synthesis (van der Wal and Jeekel, 2007).

1.3.2.2 Typical features of HPMC

HPMC express specific mesenchymal intermediate filaments such as vimentin and desmin, but also cytokeratin 6, 8 and 18, which are characteristic of epithelial cells (Broche and Tellado, 2001; Mutsaers, 2004). Constitutive expression of ICAM-1, VCAM-1 and Platelet Endothelial Cell Adhesion Molecule 1 (PECAM-1) is also characteristic of HPMC (Broche and Tellado,

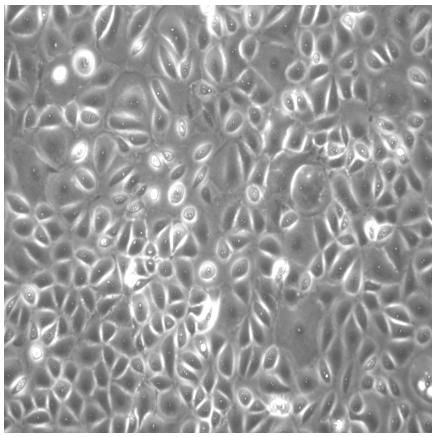

Figure 1.3. Mesothelial cells
Confluent monolayer of HPMC showing polygonal shape and typical “cobblestone” appearance (magnification x250).

2001; Nagy and Jackman, 1998). The mesothelium has the ability to slowly regenerate itself in resting conditions (0.16-0.5% of cells), but can greatly increase to 30-80% in case of injury, at the edge of the wound (Mutsaers, 2004). Cancer Antigen 125, a detection marker of ovarian cancer, is highly expressed in HPMC and characteristic of their integrity (Visser et al., 1995a).

It is now well documented that the mesothelium performs diverse functions, both physiological and in disease.

1.3.3 Physiological functions of the mesothelium

1.3.3.1 Protection barrier

Initially, the function of the peritoneal membrane was considered to be mainly passive. By trapping some fluid and creating a slippery surface, the peritoneum creates a smooth environment for the movement of organs. The network of ECM and hydrated gel of glycosaminoglycans produced by HPMC - in particular hyaluronan (HA) which is one of the main constituent - in conjunction with the microvilli and cilia, forms a protective barrier against physical damage and invading organisms (Mutsaers, 2004; Raftery et al., 1989; Yung and Chan, 2009).

Beside their primary function of providing a non-adhesive, frictionless, protective barrier, HPMC are also capable of producing and secreting a variety of macromolecules and peptides that contribute to the structural and functional integrity of the underlying basement membrane.

1.3.3.2 Transport and communication

The mesothelium is actively involved in the passage of soluble substances and cells across the membrane through the action of microvilli, gap junctions, pinocytic vesicles and stomata (Mutsaers, 2004). The aqueous phase of the interstitium allows the transport of water, nutrients electrolytes, hormones, waste metabolites and gases between the cells within the ECM and the blood capillaries (Nagy and Jackman, 1998). A prominent rough endoplasmic reticulum with numerous intra-cytoplasmic lipid inclusions reflect the active role of the mesothelial cells in intercellular communication and secretion of protein and lipid mediators to their environment (Broche and Tellado, 2001).

1.3.3.3 Peritoneal clearance

The stomata can increase their number and their size up to 20 μm during inflammation, and eliminate contaminants into the lymphatic vessels lying underneath. The microvilli can also increase their size and number in response to peritoneal insult. It only takes a few minutes for this process to start clearing contaminants, showing the capacity of the mesothelium to adapt in order to improve the peritoneal clearance (Mutsaers, 2004; Yao et al., 2003).

1.3.3.4 Procoagulant and fibrinolytic activities

HPMC are involved in the coagulation cascade through the expression of tissue factor (an activator of coagulation), leading to fibrin deposit (Nagy and Jackman, 1998; van der Wal and Jeekel, 2007). Fibrin deposit and clearance is a constant process in the serosal cavities. HPMC play a role in the fibrinolytic process of the peritoneal cavity through their capacity to express both tissue plasminogen activator and urokinase type plasminogen activator and inhibitors (type 1 and type 2 plasminogen activator inhibitors, PAI-1 and PAI-2). Tissue plasminogen activator and urokinase type plasminogen activator can activate the plasmin-mediated fibrinolytic cascade. In normal conditions, the mesothelium has a fibrinolytic activity, to prevent the formation of fibrous adhesions between peritoneal surfaces. When injury or inflammation occurs, the balance between activators and inhibitors of the fibrinolytic process can be modified by various stimuli (cytokines, growth factors), and the fibrinolytic activity is altered or abolished to allow repair (Mutsaers, 2004; Nagy and Jackman, 1998; Sammour et al., 2010).
During peritonitis, coagulation takes place in parallel with a decrease in the fibrinolytic activity, leading to the deposit of fibrin and formation of peritoneal adhesions and sclerotic thickening. In PD patients, these events can lead to a loss of efficiency of the peritoneal membrane as a filter, resulting in treatment failure (Nagy and Jackman, 1998).

1.3.3.5 Tissue repair and extracellular matrix remodelling

HPMC synthesise a number of ECM molecules (collagen I, III & IV, elastin, fibronectin, laminin, HA, dermatan and chondroitin sulfates), and can organise them into complex structures (Mutsaers, 2004). In turn, this ability is balanced by the action of matrix metalloproteinases (MMP) and their inhibitors (TIMP), some of which are expressed by HPMC (MMP-2, MMP-3, MMP-9, TIMP-1, TIMP-2 and TIMP-3) (Martin et al., 2000). Through their ability to secrete these different categories of molecules, HPMC participate in the ECM turnover and regulation. The balance between these processes is influenced by the production of cytokines and growth factors. The resulting sub-mesothelial ECM forms gels with pores of different sizes and charge densities, controlling the traffic of macromolecules and cells across the membrane (Nagy and Jackman, 1998). A controlled deposition of ECM is part of the normal peritoneal membrane repair, whereas its excessive accumulation results in adhesion formation and fibrosis (Mutsaers, 2004; Nagy and Jackman, 1998). Notably, HPMC play an important role in fibrosis via their secretion of TGFβ following injury or infection (Mutsaers, 2004; Nagy and Jackman, 1998).

1.3.3.6 Epithelial-to-mesenchymal transition

HPMC have the ability to modify their phenotype in what is called epithelial-to-mesenchymal transition, where reduced intercellular adhesions and increased motility occur. It is an essential and reversible process in embryogenesis and wound healing, characterised by the loss of epithelial markers such as E-cadherin and up-regulation of mesenchymal ones. Several molecules (growth factors and in particular TGFβ and intermediates of its signalling pathway) regulate this complex process. There is increasing evidence of this phenomenon occurring

during PD, with an involvement in fibrosis as well as angiogenesis. Episodes of peritonitis and bioincompatible PD fluids seem to affect this process, with a detrimental effect on the peritoneal membrane function (Devuyst et al., 2010; Lai and Leung, 2010a; Mutsaers, 2004; Yung and Chan, 2009).

The specific roles of mesothelial cells in inflammation will be described in the following section.

1.4 Peritoneal immunity

The peritoneal cavity is home to a variety of cell types with immune properties as listed previously in section 1.2.1.4. The characteristics of these cell types and roles are described below as well as their interaction with some specific components of the peritoneal inflammatory response.

1.4.1 Immunocompetent cells of the peritoneal cavity

1.4.1.1 Role of the mesothelium in inflammation

The mesothelium plays a role in various diseases including endometriosis, gastric and ovarian cancer and mesothelioma by being involved in ECM remodelling, fibrosis and epithelial-to-mesenchymal transition (Izzi et al., 2012; Tsukada et al., 2012; Young et al., 2013), but the focus here will be on its specific role in microbial-induced inflammation.

a. Ingestion of bacteria

Being the most numerous cells in the peritoneal cavity, HPMC are exposed more frequently to microorganisms invading the cavity than resident peritoneal macrophages, whose numbers are low in the uninfected cavity (10^4-10^5 macrophages/ml) (Topley and Williams, 1994). HPMC are able to ingest, digest and kill some bacteria, although not equally among all strains. *Staphylococci* ingestion and digestion induce CXCL8 secretion, which triggers neutrophil recruitment, whereas *Escherichia coli* ingestion leads to a less efficient digestion, no chemokine secretion, disintegration of the cells and extracellular proliferation (Visser et al., 1996). This might partly explain why peritonitis caused by Gram-negative bacteria have worse outcomes.

b. Antigen presentation

Antigen presentation and T cell activation are the first steps in the generation of a specific adaptive immune response. In addition to their role in innate immune responses, HPMC are also involved in antigen presentation, and are recognised as non-professional antigen-presenting cells (APC). Upon stimulation with IFNγ, HPMC secrete IL-15, a growth factor and activator of T cells, and express major histocompatibility complex class II molecules (i.e. HLA-DR), which present foreign antigens to T-helper cells, leading to the release of potent immune mediators. CD154 (CD40L) expression on T cells and its cross-link with CD40 on APC is a central event in antigen presentation and regulation of cytokine secretion. Basal expression of

CD40 by HPMC was found increased following IFNγ and TNFα stimulation, and the CD40-CD154 interaction was shown to trigger IL-15 and CCL5 secretion by HPMC. HPMC also express high levels of the adhesion molecule ICAM-1, a major accessory molecule for antigen presentation (Basok et al., 2001; Hausmann et al., 2000; Yao et al., 2003). Given their antigen presentation capacity and ability to respond to T cells by producing immune mediators, HPMC are involved in a positive feedback loop, further supporting the immune response during peritonitis.

c. Expression of complement factors

The anaphylatoxins C3 to C9 of the complement pathway (detailed in section 1.5.2.6) have been detected in the supernatant of HPMC and in the peritoneal cavity of PD patients, suggesting an immunoregulatory role for the complement in the peritoneal cavity. CD59, which regulates the formation of the membrane attack complex, is also expressed on the HPMC membrane (Barbano et al., 1999; Tang et al., 2004). In addition, HPMC contain lamellar bodies that produce surfactant, which work synergistically with complement by promoting phagocytosis of bacteria, (Yao et al., 2003), thus contributing to mesothelial cell-mediated peritoneal defence.

d. Role of HPMC-secreted glycosaminoglycans

Glycosaminoglycans on basement membranes have been shown to bind to chemokines and participate in their function by activating and stabilising them. They regulate cytokine activity and create a chemotactic gradient, and could potentially play a role in leukocyte recruitment in peritoneal inflammation. In addition HA, which HPMC secrete in large amounts, contribute to regulate inflammation by sequestering free radicals. Its synthesis is increased during inflammation, signalling to resident and infiltrating cells to initiate tissue survival and repair. HA is a macromolecule that participates in the resolution of inflammation. However, HA degradation products, resulting from HA turnover during tissue injury and present in the peritoneal cavity of PD patients, have pro-inflammatory activity, including induction of cytokine and chemokine secretion (CXCL8 and CCL2) by HPMC, and thus need to be removed in a timely fashion (Haslinger et al., 2001; Yung and Chan, 2009).

e. Expression of cytokines and chemokines

It was demonstrated in the 1990's that HPMC stimulated with inflammatory mediators such as IL-1β and TNFα, and also with whole bacteria including *Staphylococcus epidermidis* and *Staphylococcus aureus*, secrete several cytokines and chemokines including IL-1β, IL-6, CXCL8, CCL2 and CCL5. This demonstrated the potential role of HPMC in regulating inflammatory responses in the peritoneal cavity (Goodman et al., 1992; Li et al., 1998; Topley et al., 1993b; Visser et al., 1995b). Importantly, a polarised - predominantly apical - secretion of CXCL8 and other chemokines by HPMC was demonstrated (Li et al., 1998; Nasreen et al., 2001). This emphasises the role played by HPMC in neutrophil (and other leukocytes) migration across the membrane during peritoneal inflammation.

HPMC showed the capacity to secrete CXCL1, a neutrophil chemoattractant, and also granulocyte colony-stimulating factor (G-CSF) in response to IL-17 - a cytokine mainly produced by T cells that induces neutrophil maturation and release from the bone marrow (Chien et al., 2013). This capacity was synergistically increased in the presence of TNFα, secreted early in peritonitis, and likely contributes to neutrophil maturation and recruitment to the peritoneal cavity (Witowski et al., 2000; Witowski et al., 2007).

As described below in section 1.4.3, HPMC secrete the mononuclear cell (MNC) chemoattractants CCL2 and CCL5, following stimulation with IL-6 in combination with soluble IL-6 receptor. In addition, HPMC express the CD40 receptor, a member of the TNF family of receptors whose ligand CD154 is found on activated MNC. It was demonstrated that, when stimulated with IFNγ, IL-1β or TNFα, CD40 expression on HPMC increases and that CD40-CD154 ligation triggers CCL2 and CCL5 production (Man et al., 2003). This further demonstrates the important role played by HPMC in leukocyte recruitment in the peritoneal cavity during an inflammatory episode.

f. Immunomodulatory role of HPMC

TGFβ is not only a potent pro-fibrotic agent, but also an anti-inflammatory cytokine capable of suppressing uncontrolled immune responses (Wynn and Ramalingam, 2012). In resting HPMC, the TGFβ signalling pathway has been demonstrated to be involved in suppressing cytokine production by γδ T cells - a small proportion of circulating T cells with an important role in the early phase of the immune response. HPMC-secreted TGFβ similarly inhibited $CD4^+$ and $CD8^+$ αβ T cells (Lin et al., 2013a). Furthermore, TGFβ-induced suppression of γδ T cell proliferation in the presence of the γδ T cell specific activator (E)-4-hydroxy-3-methyl-but-2-enyl pyrophosphate in PD effluent of non-infected patients, has also been demonstrated (Lin et al., 2013a).

g. Expression of adhesion molecules

ICAM-1 and VCAM-1 expression in HPMC has been demonstrated to be important in neutrophil and MNC adherence to HPMC, respectively. During peritonitis, ICAM-1 and VCAM-1 expression increases in the microvilli, allowing binding and movement of leukocytes into the peritoneal cavity (Yao et al., 2003). Following the creation of a chemokine gradient across the mesothelium, up-regulation of ICAM-1 expression occurs on HPMC allowing migration of leukocytes (Li et al., 1998).

HPMC are able to express and release a number of immune mediators, many of them are detailed above and are also listed in Table 1.2 (includes human and murine mesothelial cells).

Notably, HPMC also interact with all other immunocompetent cells of the peritoneal cavity, being resident or infiltrating cells, which are described below.

Table 1.2 Immune mediator production by Peritoneal Mesothelial Cells

Molecule	Stimulus
Cytokines	
IL-1	EGF, TNFα,
IL-6	TNFα, IL-1
IL-15	IFNγ
CSF (G, M, GM)	IL-1, TNFα, EGF, LPS
Chemokines	
CXCL8	IL-1, TNFα, LPS, macrophage CM, asbestos, talc
CCL2	IL-1, TNFα, IFNγ, LPS
CCL5	IL-1, TNFα, IFNγ
CXCL1	IL-1, TNFα, IFNγ
CXCL10	IL-1, TNFα, IFNγ
CCL11	IL-4, TNFα
Leukotriene B4	IL-1α, TNFα, IFNγ
Growth factors	
TGFβ	IL-1, hypoxia
PDGF, HGF	unknown
FGF	IL-1, TGFβ
HB-EGF	IL-1, TNFα
VEGF	IL-1, TNFα, TGFβ
ECM-related molecules	
Collagen I	IL-1, TNFα, EGF, PDGF
Collagen III	TGFβ, EGF, PDGF, hypoxia
Fibronectin	IL-1
Hyaluronan	IL-1, EGF, PDGF
Surfactant, Biglycan, Decorin	unknown
MMP-2, 3, 9	TGFβ, PMA
TIMP-1-3	TGFβ, PMA
Integrins (α1–6, β1, β3, α4β3)	EGF
Coagulation cascade proteins	
Tissue factor	unknown
tPA	TNFα
uPA	TGFβ
PAI	IL-1, TNFα, TGFβ, thrombin, LPS
Adhesion molecules	
ICAM	IL-1, TNFα, IFNγ
VCAM	IL-1, TNFα, IFNγ, LPS
E-Cadherin, N-Cadherin	unknown
Other molecules	
Cyclo-oxygenase/ prostaglandins	IL-1, TNFα, thrombin, macrophage, CM
HSP	IL-1, TNFα
NO	Combinations of IL-1, TNFα, IFNγ, LPS
Reactive species scavengers	Asbestos

Abbreviations: EGF, PDGF, FGF, HGF: epidermal, platelet-derived, fibroblast, hepatocyte growth factor, respectively; G-, M-, GM-CSF: granulocyte, macrophage and granulocyte-macrophage colony stimulating factor, respectively; LPS, lipopolysaccharide; CM, conditioned media; PMA, phorbol myristate acetate; HB-EGF, VEGF, heparin-binding and vascular EGF, respectively; tPA, uPA: tissue and urokinase plasminogen activators, respectively; HSP, heat shock protein; NO, nitric oxide. (Adapted from Goodman et al. 1992; Mutsaers 2002)

1.4.1.2 Peritoneal macrophages

The most abundant resident leukocyte population, the macrophages, are a heterogeneous and multipotential cell population. Tissue-resident macrophages are of prenatal origin or blood monocytes-derived (Davies et al., 2013). Macrophages are often functionally divided into the M1 and M2 classes, where classically activated M1 present a pro-inflammatory profile - secreting IL-1β, TNFα and other pro-inflammatory cytokines and reactive oxygen species - that can be observed early in inflammation, whereas alternatively activated M2 display anti-inflammatory and tissue repair properties. However, the 'M1-M2 paradigm' is a simplified concept as macrophage differentiation and activation depends on regulatory signals from the local environment, and their functional phenotype can shift in response to changes in the milieu (Davies et al., 2013; Fieren, 2012). Macrophages are mostly free-floating cells, but tissue macrophages also reside in the peritoneal membrane close to the mesothelial basement membrane and in the perivascular regions (Nagy and Jackman, 1998). During peritonitis, their main functions are: 1) the production of pro-inflammatory cytokines, with IL-1β and TNFα playing a key role in the initiation of the inflammatory response; 2) phagocytosis of invading pathogens and 3) antigen presentation (Sammour et al., 2010; Topley et al., 1996b). With time on PD, macrophages progressively display a more immature phenotype, a decreased phagocytic activity and impaired cytokine production, changes that appear to be heightened with recurrent episodes of peritonitis (Broche and Tellado, 2001; Lin and Huang, 1990; McGregor et al., 1996).

1.4.1.3 Peritoneal lymphocytes and dendritic cells

The peritoneal lymphocyte population consists of 95-97% T cells and 3-5% B cells. The T cells display distinct properties compare to the intrathymically differentiated T cells, and express markers of activation such as CD69 and HLA-DR. A high proportion of T cells are $CD45RO^+$, indicating a memory/effector phenotype (Broche and Tellado, 2001; Davies et al., 1989; Sammour et al., 2010). There is evidence of a key role of T cells in the peritoneal inflammatory response, suggested notably by the early detection of elevated levels of the T cell-derived IFNγ, and by knock-out (KO) mice studies demonstrating a critical role of IFNγ in leukocyte recruitment (McLoughlin et al., 2003).

Two B cell subsets are found in the peritoneum: 1) B1a cells, which develop from progenitors in the omentum and 2) B2 cells, which migrate either directly from the circulation using $\alpha4\beta1$ integrins or through the milky spots and involving a different set of integrins ($\alpha4\beta7$). They predominantly produce IgM, but $CD8^+$ T cells also provide B cell helper function to synthesise IgG and IgA (Sammour et al., 2010).

NK cells that can destroy virally infected cells and tumour cells are present in the resting peritoneum in small numbers and increase following cytokine stimulation. This tissue-specific subset of innate immune cells has a distinct phenotype and regulatory functions in the mouse (Gonzaga et al., 2011; Sammour et al., 2010).

DC represent up to 5-6% of the total peritoneal cell numbers, and are composed of several subsets. They have a higher capacity to activate T cell proliferation, and are better equipped as APC than macrophages. In PD patients, another subset of $CD14^+CD4^+$ cells representing approximately 2% of the peritoneal cells and with the characteristics of DC precursors has been described. Their number increases during peritonitis, and their recruitment occurs more rapidly with Gram-positive than with Gram-negative infections, suggesting a role in adaptive immune responses (Broche and Tellado, 2001; McCully and Madrenas, 2006).

1.4.1.4 Other cells with immune activity in the peritoneal cavity

Peritoneal mast cells, located in the proximity of blood capillaries, have been shown to be involved in neutrophil infiltration through their capacity to release leukotrienes. Degranulation of mast cells releases vasoactive substances, complement and opsonins, which coat bacteria and promote phagocytosis (Sammour et al., 2010). Mast cells also have a role in tissue repair following peritoneal membrane damage (Ramos et al., 1991; Zareie et al., 2006).

Fibroblasts, a major resident cell type in the peritoneal membrane, have the capacity to release pro-inflammatory cytokines and chemokines (IL-6, CXCL1, CXCL8, G-CSF and CCL2) potentially contributing to the cytokine network and leukocyte recruitment of the inflammatory response (Witowski et al., 2009; Witowski et al., 2001). Through the secretion of macromolecules of the ECM and of various factors, fibroblasts also have a role in tissue repair and fibrosis (Nagy and Jackman, 1998). More recently, a potential inflammatory role of peritoneal adipocytes has been recognised, as they were found to secrete a variety of adipokines, including the cytokines TNFα and IL-6 and growth factors such as TGFβ, as well as expressing their receptors (Lai and Leung, 2010b).

1.4.2 The role of IL-6 in inflammation and its mechanism of action

IL-6 is a pleiotropic cytokine with a wide range of metabolic functions, including induction and differentiation of lymphocytes, cell proliferation and survival, involvement in haematopoiesis, bone metabolism and sexual reproduction. IL-6 has a crucial role in host defence due to its varied immune activities, including its ability to induce proteins of the acute phase response, C-reactive protein (opsonin that binds to phosphocholine in bacterial surface molecules) and serum amyloid A (SAA, involved in leukocyte recruitment during infection). IL-6 has been implicated in various disease processes such as rheumatoid arthritis and other autoimmune conditions, Alzheimer's disease, myocardial infarction, osteoporosis, various cancers and inflammation. IL-6 is secreted by a number of different cell types, and its blood and tissue levels are elevated in numerous infections, inflammatory and autoimmune diseases (Trikha et al., 2003). IL-6 was demonstrated to be a good prognostic marker, with high plasma levels associated with poor outcomes in CAPD patients (Pecoits-Filho et al., 2002). High levels of IL-6 are also found in PD effluent of patients, and are associated with up-regulation of intra-peritoneal inflammatory and angiogenic mediators (Oh et al., 2010). Membrane function can be assessed by the peritoneal solute transport rate (PSTR). In CAPD patients, high PSTR appears

to be associated with worse survival, and increased levels of IL-6 are linked to increased PSTR but do not determine survival, indicating the importance of membrane function over the inflammation parameter (Lambie et al., 2013; Pecoits-Filho et al., 2006). These findings emphasise the potential detrimental role of IL-6, and thus the relevance of studying this cytokine in the context of PD.

IL-6 belongs to a family of cytokines that promote cellular responses through a receptor complex consisting of at least one member of the ubiquitously expressed signal-transducing glycoprotein gp130. On target cells, IL-6 first binds to a specific membrane-bound IL-6 receptor (IL-6R), and the IL-6/IL-6R complex associates with gp130, inducing its dimerisation and subsequent intracellular signal transduction (Rose-John et al., 2006).

Unlike gp130, IL-6R is mainly expressed by hepatocytes, neutrophils, monocytes/ macrophages and some lymphocytes (Scheller et al., 2013). A naturally occurring soluble form of the IL-6R (sIL-6R), found in various bodily fluids, is generated either by alternative RNA splicing (1-10%) or by shedding from the membrane IL-6R (90-99%). sIL-6R binds to IL-6 and then associate with gp130, activating target cells which do not express IL-6R and would otherwise not be responsive to IL-6. Of note, the IL-6/sIL-6R complex possesses agonistic properties, unlike other soluble receptors such as those for IL-1 or TNFα, which inhibit the cellular effects of their ligands. Activation of cells only expressing gp130 via the IL-6/sIL-6R complex is called trans-signalling, whereas classic signalling defines the membrane-bound IL-6R activation (Fig 1.4) (Chalaris et al., 2011). Both sIL-6R isoforms elicit common cellular events via gp130 (McLoughlin et al., 2004). Several cell types have been shown to respond to IL-6 exclusively via trans-signalling, among them embryonic stem cells, smooth muscle cells, many neural cells, endothelial cells and HPMC (Chalaris et al., 2011; McLoughlin et al., 2004).

Binding of IL-6 to its receptor and to gp130 results in gp130 homodimerisation and activation of cytoplasmic, constitutively-associated, Janus kinases (JAKs), which phosphorylate tyrosine residues on gp130. This activates SH2-domain-containing tyrosine phosphatase (SHP) 2 and subsequently SHP2-mediated activation of mitogen activated protein kinase (MAPK) and phosphatidylinositol 3-kinase (PI3K) signalling pathways. Signal transducer and activator of transcription (STAT) 1 and STAT3 proteins are also activated. They directly bind to phospho-tyrosine residues on gp130, resulting in their tyrosine phosphorylation, homo- and/or hetero-dimerisation, nuclear translocation and transcriptional activation of target genes (Fig 1.4). By using different downstream signalling pathways linked to distinct intracellular regions of the gp130 receptor subunit, ligand- and tissue-specific activation of distinct set of target genes occurs, resulting in distinct physiological effects of IL-6 *in vivo* (Jenkins et al., 2007). This in turn is under the control of several negative-feedback mechanisms, notably the STAT-dependent transcriptional induction of the two suppressor of cytokine signalling, the (SOCS) 1 and 3 proteins, which inhibit JAK phosphorylation of substrates (Fig 1.4). In addition, the transcriptional activity of STAT1 and STAT3 is repressed by their sequestration into complexes formed with STAT-specific members of the family of protein inhibitors of activated STAT (PIAS)

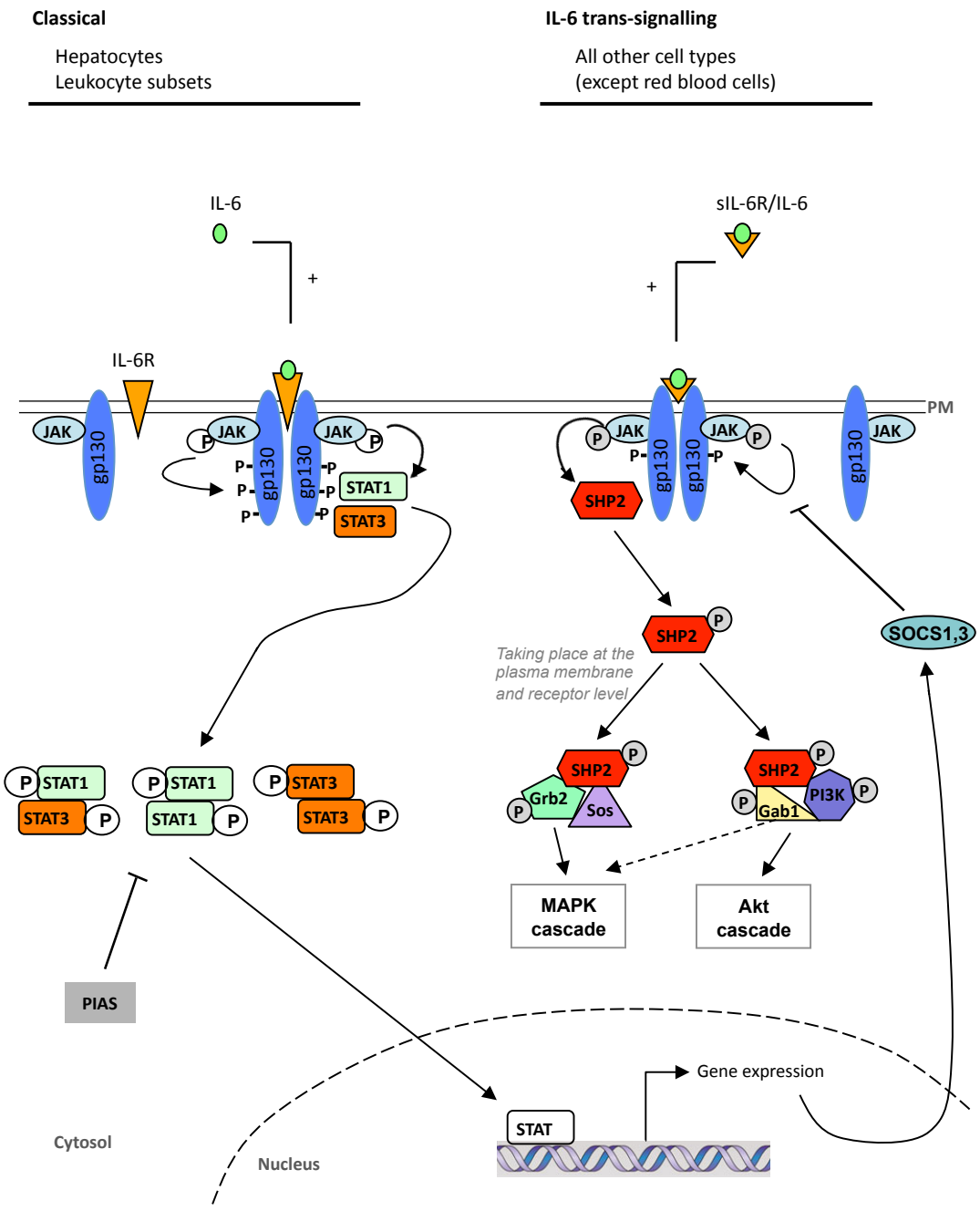

Figure 1.4. Modes of IL-6 signalling and activation of the STAT or MAPK pathways through gp130-mediated pathways.
IL-6 binds to its membrane-bound receptor (IL-6R, classical pathway) and to the soluble form of IL-6R (sIL-6R, trans-signalling pathway). Cytokine binding induces homodimerisation of the signal transducer unit, gp130, resulting in binding and activation of Janus kinases (JAKs). Activated JAKs phosphorylate tyrosine residues on the intracellular domain of gp130, creating docking sites for signal transducer and activator of transcription (STAT) proteins or SH2-domain-containing tyrosine phosphatase (SHP2). Following JAK phosphorylation of STAT monomers, homo- or hetero-dimerisation of STAT proteins occurs, leading to their translocation to the nucleus and transcription of their target genes. At the membrane level, receptor-bound SHP2 is phosphorylated by JAKs, leading to its association with one of two complexes, as indicated on the figure, and the activation of the MAPK or Akt cascades in a cell-type specific manner. IL-6 signalling is controlled by several negative-feedback mechanisms, which include the activity of the STAT-dependent transcriptional induction of suppressor of cytokine signalling (SOCS) 1 and 3 (inhibit JAK phosphorylation of substrates) and the repression of STAT1 and STAT3 transcriptional activity by their sequestration into complexes formed with STAT-specific members of the family of protein inhibitors of activated STAT (PIAS). Abbreviations: PM, plasma membrane; Grb2, growth factor-receptor-bound protein; Sos, Son of Sevenless; Gab1, Grb2-associated-binder-1; PI3K, phosphatidylinositol 3-kinase; MAPK, mitogen-activated protein kinase. (Adapted from Heinrich 2003, Ernst 2004, Eulenfeld 2012)

(Ernst and Jenkins, 2004; Heinrich et al., 2003). A soluble form of gp130, notably found in high levels in blood (250-400 ng/ml), is a natural antagonist of IL-6 trans-signalling. Soluble gp130 specifically binds to the IL-6/sIL-6R complex while leaving membrane-bound IL-6 classic signalling unaffected (Jostock et al., 2001; Scheller et al., 2013). Soluble gp130 has been used to determine the physiological involvement of IL-6 trans-signalling *in vivo* and represents a potential therapeutic agent in chronic inflammatory conditions such as Crohn's disease and rheumatoid arthritis, where IL-6 trans-signalling is detrimental, and is now tested in clinical phase I studies (Rose-John et al., 2006; Scheller et al., 2013).

The activity of IL-6 is of particular interest in the context of the present study, as it plays pro- and anti-inflammatory roles. Indeed, it has been associated with infection, trauma and inflammatory events, but studies have also demonstrated a protective role in septic shock and its ability to promote resolution of inflammation, conferring both beneficial and detrimental properties to this cytokine (Diao and Kohanawa, 2005; Hurst et al., 2001; Jones et al., 2005). Identification of the diverse roles of IL-6 is partly due to a better understanding of sIL-6R properties and of the interplay between IL-6 and other inflammatory mediators (Jones, 2005).

1.4.3 Leukocyte recruitment during peritoneal inflammation

Patients' data and animal models have shown that peritonitis is characterised by an initial influx of PMN into the peritoneal cavity, cleared in 4 to 6 days in humans and 48h in mice, replaced and followed by a more sustained population of mononuclear cells, namely monocytes and lymphocytes (Hurst et al., 2001). The transition from the PMN to the MNC population is the hallmark of a successful inflammation/infection resolution (Jones, 2005) (Fig 1.5).

Resident cell populations orchestrate the peritoneal inflammatory response with a specific sequence of events occurring to allow movement of leukocytes across the capillary endothelium into the interstitial space, across the mesothelium into the peritoneal cavity and to the site of inflammation.

Expression of specific pro- and anti-inflammatory cytokines and chemokines and their receptors, and specific adhesion molecules, guarantees the appropriate leukocyte infiltration pattern (McLoughlin, 2005). Cytokines and chemokines regulate leukocyte trafficking in and out of the peritoneal cavity, thus they are involved in a variety of physiological and pathological processes and control many immune functions.

Belonging to the cytokine family, chemokines are a specific class of small, secreted molecules with chemotactic properties. Most chemokines have four conserved N-terminal cysteines and are divided into two major subgroups based on the arrangement of their two first cysteines: CXC, when the cysteines have an amino acid (X) between them or CC, when they are adjacent. A further subdivision has been made in the CXC group to differentiate the chemokines containing the ELR amino acid motif (ELR^+) from the ELR^- ones. Selective neutrophil recruitment is due to specific ELR^+ CXC chemokines, whereas CC chemokines confer selectivity to monocytes/macrophages and T cells recruitment (Zlotnik and Yoshie, 2000).

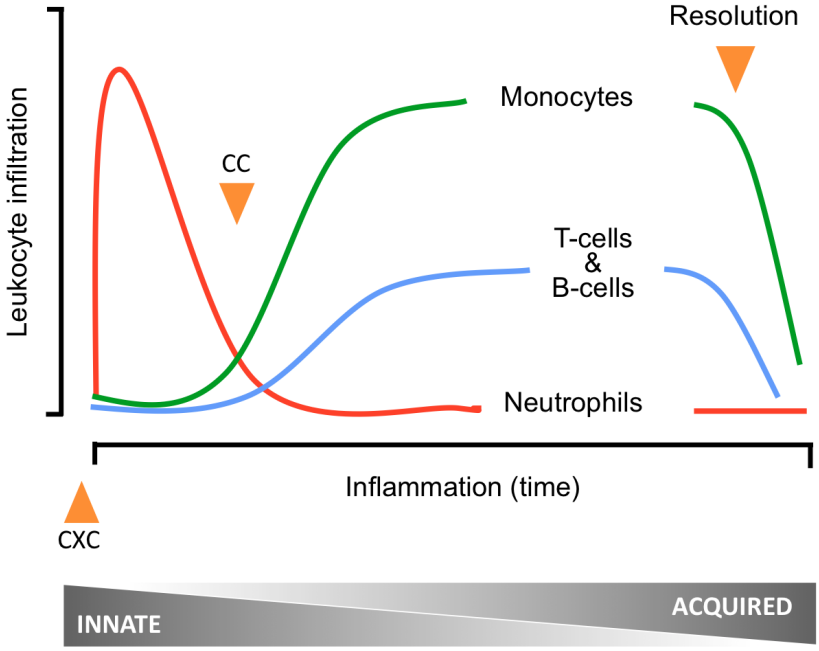

Figure 1.5. Typical kinetics pattern of leukocyte infiltration in the peritoneal cavity.
Successful resolution of acute inflammation requires a transition from ELR^+ CXC chemokine-driven neutrophil recruitment to CC chemokine-induced mononuclear cells infiltration .

Exposure to invading pathogens activates resident macrophages, triggering the release of pro-inflammatory cytokines, and shortly following the onset of infection, IL-1β and TNFα cytokines are found in the peritoneal cavity. In addition to direct sensing of the infecting agents, this process drives HPMC to secrete CXCL8 and increase expression of ICAM-1 (Li et al., 1998). This results in neutrophil recruitment from the capillaries of the peritoneal membrane. Given the high numbers of HPMC, this process represents an amplification step, which is crucial for the resolution of inflammation (Topley and Williams, 1994). IFNγ, observed early in the infected peritoneal cavity, is also an important player. IFNγ controls the initial neutrophil recruitment by affecting IL-1β local activities and promoting IL-6 secretion (McLoughlin et al., 2003).

In addition to macrophages, HPMC are the main producers of IL-6 within the peritoneal cavity. IL-6 signalling, via its sIL-6R, has been demonstrated to play a central role in peritoneal inflammation and in the typical transition from a neutrophil-rich population to mononuclear cell dominance (Hurst et al., 2001). Studies with IL-6 deficient mice (IL-6-KO mice) have shown that in the absence of IL-6 there is accumulation of neutrophils at sites of inflammation (McLoughlin et al., 2003; Xing et al., 1998). Furthermore, as stromal cells are mainly $gp130^{+}IL\text{-}6R^{-}$, the local concentration of sIL-6R is responsible for IL-6 signalling activity, with a correlation between infiltrating neutrophil accumulation in the peritoneal cavity and sIL-6R levels. These levels are increased by inflammatory chemokines and other chemotactic agents that activate neutrophils, promoting sIL-6R shedding (Marin et al., 2001; McLoughlin et al., 2004). IL-6 will subsequently combine with sIL-6R to stimulate HPMC secretion of CCL2 and CCL8, which drive mononuclear cells recruitment (Marin et al., 2001; Modur et al., 1997; Romano et al., 1997).

1.4.4 Resolution of the early phase of peritoneal inflammation

The transition from innate to adaptive immunity is the pivotal event towards the resolution of inflammation, with the removal of inflammatory leukocytes and replacement by a mononuclear cell population. This modifies the environment, with increasing concentration of anti-inflammatory molecules and initiates tissue repair. In chronic inflammation, high levels of neutrophils and pro-inflammatory cytokines are still present in the peritoneal cavity for several weeks, even after clinical remission (Lai and Leung, 2010a). This prolongs the detrimental effects of the inflammatory status, as aberrant trafficking is characteristic of chronic inflammation, and retention of activated leukocytes at site of infection leads to tissue damage. IL-6 trans-signalling inhibits the IL-1β- and TNFα-induced production of CXCL1 and CXCL8, modulates the expression of ICAM-1 and VCAM-1 (Modur et al., 1997; Romano et al., 1997) and participates, with IFNγ acting upstream of IL-6, in neutrophil apoptosis through a caspase-3 mechanism (McLoughlin et al., 2003). Furthermore, trans-signalling might be involved in bacterial clearance and in improved survival through an increased macrophage recruitment and phagocytosis activity of both neutrophils and macrophages (Onogawa, 2005; Onogawa et al., 2013).

Once this primary phase of the inflammatory process is ongoing, a secondary one takes place with the activity of infiltrating monocytes/macrophages and lymphocytes. IL-6 influences the inflammatory outcome by affecting both types of cells. Briefly, IL-6 is involved in skewing the differentiation of monocytes away from a dendritic lineage to a macrophage phenotype (Jones, 2005). Furthermore, studies suggest that sIL-6R controls the homing capacity of T cells by affecting both T cell migration and adhesion (Chen et al., 2004; McLoughlin et al., 2005).
Amongst other players, IL-6 is critical in orchestrating the transition from innate to acquired immunity. In chronic disorders, IL-6 role seems to be more detrimental and its interplay with other signalling pathways and pro-inflammatory mediators such as IFNγ and TGFβ might affect its activity (Jones, 2005).

Figure 1.6 recapitulates the initial events of an inflammatory response taking place in the peritoneal cavity at the onset of infection.

An overview of the role of the different players involved in innate immunity follows.

1.5 The innate immune system and peritoneal immunity

The inflammatory response is a coordinated sequence of events triggered by infection and tissue injury that aims to eradicate the insult and restore normal tissue function. At the centre of this response is the activity of the innate immune system. Many different types of inducers, exogenous and endogenous, can trigger the inflammatory response, but here the focus will be on microbial pathogens.

1.5.1 Overview of the innate and adaptive immune responses

In jawed vertebrates, the two arms of the immune system: the innate and adaptive immune systems, are characterised by the type of receptors utilised to recognise pathogens. The innate immune system uses pattern recognition receptors (PRRs), which are germline-encoded and recognise a broad array of conserved and invariant features of microorganisms. They will be described below, in section 1.6 and 1.7. The adaptive or acquired immune system utilises antigen receptors (Medzhitov, 2007), the T- and B-cell receptors, which are expressed on T- and B-lymphocytes, respectively. They are generated through gene recombination to provide an extensive variation of receptor specificity with unique antigen recognition capacity (Litman et al., 2010). Adaptive immunity is characterised by antigen-specific responses with clonal expansion of lymphocytes following the recognition of, and activation by antigens, resulting in long-term memory. This provides a faster and stronger response in the event of encountering the same antigen again. This highly specific arm of the immune system is not immediately available, as several days are required to mount an adaptive response following first encounter with an antigen. Therefore, the two systems must cooperate, and the activity of the innate immune system, through the use of ready-made receptors, is critical to a prompt and efficient pro-

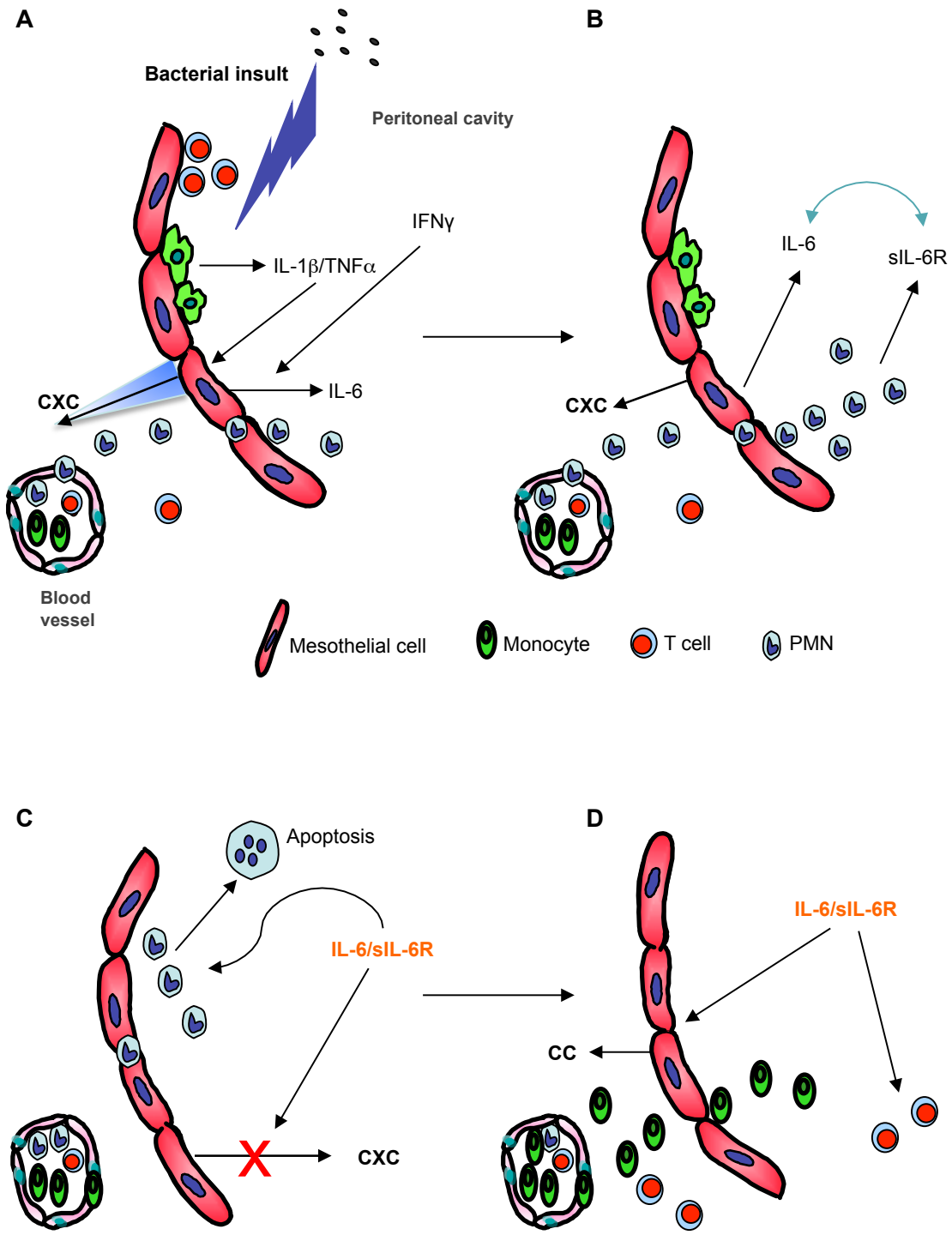

Figure 1.6. IL-6 trans-signalling directs the temporal transition from neutrophils to mononuclear cells in the peritoneal cavity.
(A) Upon bacterial insult, resident macrophages produce IL-1β and TNFα which stimulate HPMC to secrete CXC chemokines, notably CXCL8. A chemotactic gradient is created, attracting neutrophils from the blood stream into the peritoneal cavity. IFNγ, secreted early in inflammation, also stimulates HPMC to secrete IL-6. **(B)** In the peritoneal cavity, neutrophils shed sIL-6R - following migration and activation - which combines with IL-6 to form the IL-6/sIL-6R complex. **(C)** This complex is responsible for the transition from the initial influx of neutrophils to the subsequent mononuclear cell recruitment by inhibiting CXCL8 secretion and stopping the neutrophil influx. **(D)** The IL-6/sIL-6R complex also induces CC chemokine secretion, therefore promoting mononuclear cell recruitment. In addition, the IL-6/sIL-6R complex is involved in neutrophil apoptosis, a crucial event to avoid detrimental damage of the peritoneal membrane.

inflammatory response against a microbial challenge. This is a response to pathogens devoid of memory component (Medzhitov, 2008).

Not only innate, but also adaptive immune responses play an important role in peritoneal immunity. The focus, however, of this thesis is on innate responses. Innate immunity is the most universal and most rapidly acting, with dynamic mechanisms that have been refined over hundreds of millions of years to achieve the three prime goals of recognising a vast array of pathogens, killing the pathogens once recognised and sparing the host tissues (Beutler, 2004). It was initially accepted that the innate immune response was an early event, whereas elements of the adaptive immune response took place later on. It is now clear that some cells participating in the later phase are also part of the innate immune system whereas some T cells (the hallmark “adaptive” cells) may play an important role in the early phase. In addition, traditional components of the innate immune system, such as NK cells, have been described to play a role in the adaptive arm, challenging the established dogma of two distinct systems (Biron, 2010).

The inflammatory response initiates with the recognition of infection or tissue damage by either professional or non-professional immune cells. It is mostly mediated by tissue macrophages and mast cells, and triggers the activation and recruitment of other cells in conjunction with the secretion and release of a variety of pro-inflammatory mediators, including cytokines, chemokines, free radicals, hormones, vasoactive amines, eicosanoids and products of the proteolytic and complement cascades and other small molecules (Medzhitov, 2008). During an acute inflammatory response, controlled recruitment of leukocytes from the circulation to the site of infection is a critical step. Their subsequent timely removal is necessary to eliminate infection and achieve a successful resolution of inflammation while minimising the damage to host tissues. The different players of this early, innate, inflammatory phase will be described here.

1.5.2 Components of the innate immune system

Innate immunity is composed of an afferent and efferent arm, each of these arms further divided into cellular and humoral components. They form a complex network, and the precise distinction between sensors and effectors can be difficult to achieve, as some molecules such as cytokines have no direct effect on microbes but attract cells capable of killing them. Furthermore, a fine balance needs to be struck between harming the invading organism and preserving the normal function of the host.

The cellular components of the innate immune system are composed of the mucosal epithelia, the first line of defence of the body and organs against invading pathogens, and the various leukocytes attracted to the site of infection following the action of cytokines and chemoattractants. Leukocytes subsequently signal, target and kill microorganisms, via the expression of a vast array of soluble molecules, direct destruction and phagocytosis. Hepatocytes and epithelial cells are also involved in the early phase of the immune response through the secretion of diverse antimicrobial molecules, cytokines and chemokines.

1.5.2.1 Mucosal epithelia

The epithelium provides a tissue barrier against all external dangers. Epithelial cells of the airways, the intestinal tract and the skin represent the first line of defence, as they are the main interface between the host and the microbial world. They are polarised cells with apical and basolateral surfaces. The apical surface presents cilia and microvilli, involved in motility and transport of substances, respectively. The epithelium of the airways is covered by a surface fluid contributing to the mucociliary escalator, essential for the clearance of microbes and other particles. The basolateral surface is characterised by the expression of tight and adherens junctions, critical structures to maintain the structural integrity of the epithelium, and separate the lumen from the tissue compartment. Besides its mechanistic role, the epithelium can produce antimicrobial peptides to limit the growth of microorganisms, pathogens or commensals that colonise these sites. Through the secretion of a plethora of soluble mediators, epithelial cells also interact with cells in their environment and participate in defence mechanisms. The involvement of epithelial cells in the pathogenesis of inflammatory bowel disease, asthma, lung diseases and cancer, emphasises the central role of the epithelial barrier function (Shaykhiev and Bals, 2007; Tosi, 2005).

1.5.2.2 Eosinophils, basophils and mast cells

Eosinophils and basophils belong to the polymorphonuclear leukocyte group and are key players to contain infection, notably with an array of effector functions. Rare cells, eosinophils and basophils are recruited from the circulation and produce mediators thereby creating the inflammatory milieu. Their number can greatly increase, in particular with a parasitic infection or during an allergic response (Beutler, 2004).

Mast cells, tissue-dwelling descendants of the myeloid lineage and important mediators of allergic responses, are distributed throughout tissues, notably near surfaces exposed to the environment, where they are sentinels likely to encounter pathogens and allergens. They are also strategically located near blood and lymphatic vessels. Mast cells, long-lived cells capable of surviving for months and years, greatly contribute to controlling a wide range of pathogenic infections, including those by parasites and bacteria. They are characterised by their ability to store and secrete different types of proteases and proteoglycans, and have the potential to respond to an invading pathogen within seconds to minutes, acting as first responders. Upon activation by various stimuli, mast cells can proliferate and secrete a wide range of biologically active products with pro- or anti-inflammatory activities. They express diverse types of receptors, which allow mast cells to recognise pathogens, and through chemokine secretion are involved in leukocyte recruitment, in particular eosinophils and NK cells (Abraham and St John, 2010; Galli et al., 2011).

1.5.2.3 Phagocytes

Neutrophils and macrophages are professional phagocytes with a common precursor; they are essential to eliminate pathogenic insults and to remove damaged tissue. The effectiveness of the phagocytes in regulating innate immunity depends on their mutual co-operation during the successive phases of the inflammatory response, from leukocyte recruitment to resolution.

a. Neutrophils

Neutrophils are short-lived cells (few hours, to potentially a few days, before undergoing apoptosis) and the most abundant circulating phagocytes. Unlike most other phagocytes and leukocytes, neutrophils are mature cells and do not proliferate (Galli et al., 2011). They engage in three major functions: migration to the site of infection, recognition and ingestion of microorganisms followed by the killing and the digestion of these organisms (Beutler, 2004; Tosi, 2005). Neutrophils are equipped with granules, which store reactive oxygen species and nitric oxide species, proteinase 3, cathepsin G and elastase as well as antimicrobial polypeptides. Other toxic molecules are generated by neutrophils to kill microorganisms by their rapid action on diverse molecular targets, which include lipids, proteins and nucleic acids (Beutler, 2004; Medzhitov, 2008; Soehnlein and Lindbom, 2010). This potent killing and non-specific activity needs to be tightly regulated to avoid tissue damage and is partly counterbalanced and complemented by the activity of macrophages.

b. Macrophages

Morphologically and functionally diverse, macrophages are distributed throughout the body and likely to encounter invading organisms. One of their primary roles is to phagocytose and kill microbes, although they are less cytotoxic than neutrophils. But macrophages also have active roles in the induction of the innate immune response, by alerting and recruiting other cells to the site of infection, as well as in the resolution phase, via the generation of chemotactic cytokines, lipid mediators and the expression of a variety of molecules, including many types of receptors to sense infection (Beutler, 2004; Soehnlein and Lindbom, 2010). Macrophages participate – with the collaboration of other resident cells – in neutrophil trafficking to the site of infection and, following removal of foreign entities, to the inhibition of neutrophil recruitment and their elimination (Soehnlein and Lindbom, 2010).

1.5.2.4 NK cells and DCs

NK cells are specialised lymphocytes that do not express clonally distributed receptors, and play an important role in innate immunity. They contain viral infections before the development of adaptive immune responses and control malignant tumours. NK cells are found in the circulation, the spleen and bone marrow; they are recruited by diverse chemoattractants - CXCL8, CX3CL1, leukotrienes, chemerin and C5a (Gregoire et al., 2007; Parolini et al., 2007)- to sites of infection, where they induce apoptosis of target cells in two different ways: 1) granule exocytosis, which kills infected or malignant cells by releasing perforin or granzymes from

storage compartments, and 2) by death receptor engagement on target cells, leading to the activation of downstream intracellular pathways and apoptosis (Degli-Esposti and Smyth, 2005; Tosi, 2005). NK cells interact with other cells and express inhibitory receptors that bind MHC class I molecules present on the host cells but not on pathogens. NK cell inhibitory receptor binding to MHC class I molecules blocks their effector functions - cytotoxicity and cytokine production - providing protection for target cells expressing normal level of MHC class I molecules on their surface. Although MHC class I receptors play a key role in NK cell regulation, a low level of expression is not a prerequisite and in some circumstances, signals from activating receptors are sufficient to stimulate NK cells (Smyth et al., 2005). NK cells interact with DCs, which greatly influence their proliferation and activation. Following activation, NK cells secrete diverse cytokines and chemokines, notably IFNγ, affecting and defining the environment in which subsequent immune interactions occur. It has been demonstrated that IFNγ secretion by NK cells requires the formation of an immunological synapse and DC-derived cytokine production, emphasising the importance of the interaction between these two cell types (Borg et al., 2004; Degli-Esposti and Smyth, 2005).

Of myeloid origin, DCs represent a minority population located in peripheral organs and mucosal surfaces, where they sample the environment for antigens. After antigen uptake, and following a maturation programme initiated by direct interaction with pathogens, DCs are highly efficient at antigens presentation to naïve T lymphocytes. Direct interaction with other immune cells also results in DC maturation. In this regard, NK cells affect DC functions and maturation. The complex bidirectional crosstalk between DCs and NK cells influences the nature of the response as well as its outcome. The initial stimulus received by DCs determines which cytokines they produce and, through differential receptor engagement, influences NK cells properties and effector functions - cytotoxicity, proliferation, survival and migration. In turn, soluble factors secreted by NK cells and cell-cell contact can induce maturation or kill immature DCs, potentially skewing the inflammatory response towards adaptive immunity (Degli-Esposti and Smyth, 2005; Wilson et al., 1999).

The various cells participating in innate peritoneal immunity and their functions are summarised in Figure 1.7.

1.5.2.5 Antimicrobial peptides, proteins and enzymes

There are several major families of antimicrobial peptides, including α- and β-defensins, cathelicidins (expressed notably by leukocytes and epithelia), histatins in the saliva and dermcidin on the skin. They show broad-spectrum antimicrobial activities against a vast array of bacteria, fungi and viruses. They are small molecules, 20-50 amino acids long, mostly positively charged that act by creating membrane pores, through membrane disruption via electrostatic interaction with the membrane lipids, or by accumulating at the membrane surface resulting in membrane dissolution. They can also target intracellular cell components and act as metabolic inhibitors (Nguyen et al., 2011; Tavares et al., 2013). These peptides have also been shown to

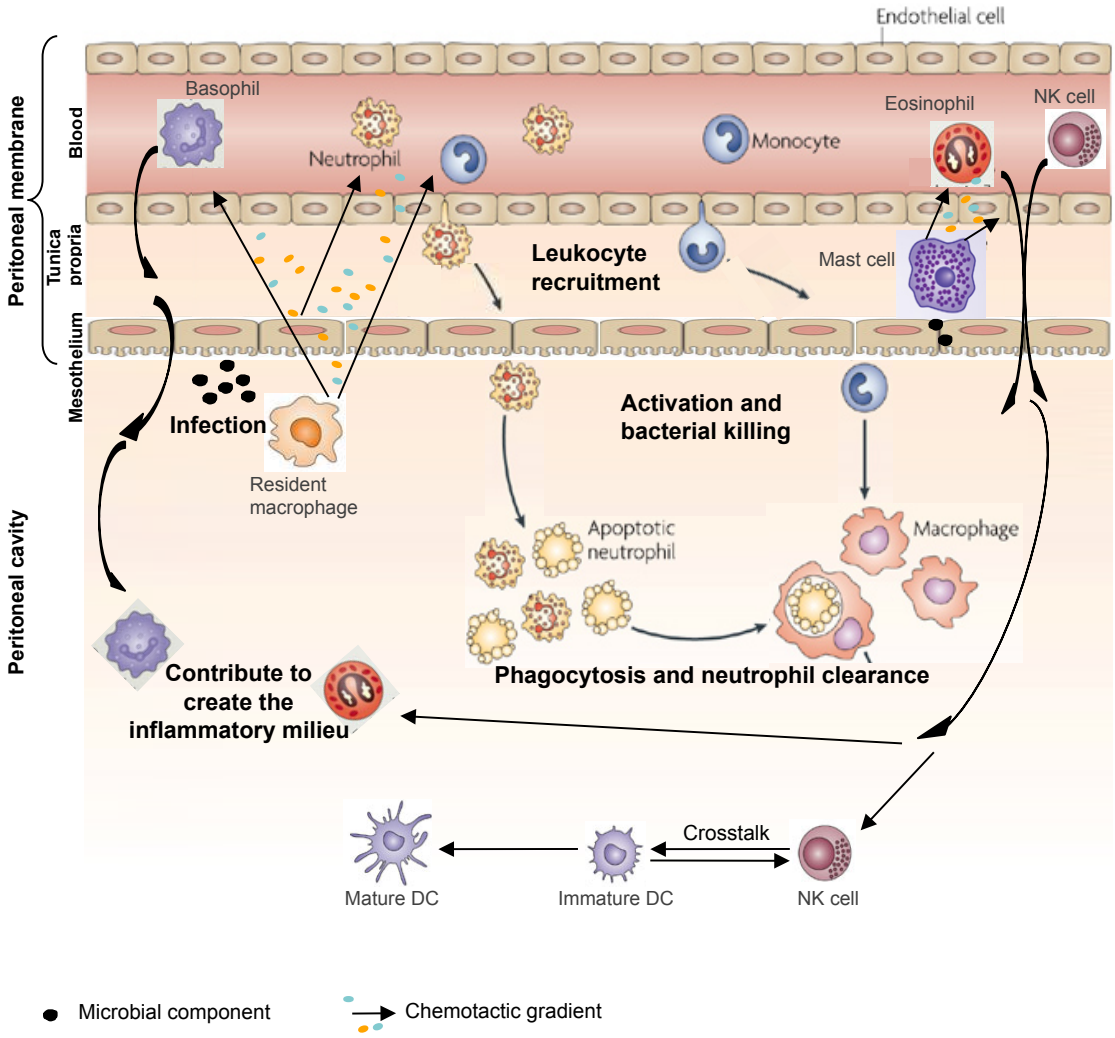

Figure 1.7. Schematic representation of the early events in peritoneal inflammation and the immunocompetent cells involved.
Following pathogen invasion, resident macrophages, epithelial cells and mast cells sense PAMPs and secrete cytokines and chemokines to alert patrolling monocytes, neutrophils and other leukocytes present in the blood. This leads to neutrophil, inflammatory monocyte, NK cell, basophil and eosinophil recruitment to the infected tissue. This is facilitated by cytokine-induced increased vascular permeability and expression of adhesion molecules by epithellial cells. All cell types have the capacity to express a variety of receptors and soluble mediators and interact with other cells. Basophils, eosinophils and NK cells contribute to create the inflammatory milieu. The NK cell-DC interaction is crucial for both cell activation and function. Following bacterial killing and phagocytosis, neutrophil clearance is primordial to avoid host tissue damage (See description of the specific role of each cell type in the text). (Adapted from Degli-Esposti 2005, Serhan 2008, Soehnlein 2010, Abraham 2010, Galli 2011)

play immunomodulatory roles, including chemotactic activity (Gallo and Hooper, 2012; Tosi, 2005).

Lysozyme, a glycosidase contained in the primary and secondary neutrophil granules and in epithelial cells, hydrolyses peptidoglycan (PGN) of bacteria cell walls. Lactoferrin, also present in neutrophil granules, alters the mobility of certain bacteria (e.g., *Pseudomonas aeruginosa*) and their ability to form biofilms, presumably also causing their destruction (Beutler, 2004; Gallo and Hooper, 2012).

Other proteins present antimicrobial activities, such as cathepsin G and elastase in neutrophil granules. They play diverse roles in oxygen species formation, opsonisation, endotoxin neutralisation, iron sequestering and leukocyte activation (Nguyen et al., 2011). C-type lectins form another group of proteins with antimicrobial activities and will be discussed in section 1.6.2.1.

1.5.2.6 Complement

The complement system plays a key role in innate immunity and in the development of an effective inflammatory response. It consists of 35 to 40 proteins and glycoproteins present in blood and on cell surfaces. The plasma proteins are mostly produced in the liver, and many are also secreted by a variety of cell types, notably monocytes and macrophages. Beside a role in homeostasis, the role of complement in immunity is to recognise and promote the elimination of microorganisms (bacteria, viruses and fungi) by generating active peptides including anaphylatoxins (complement components 3a (C3a), C4a and C5a). They have a wide range of pro-inflammatory and immunomodulatory properties including lysis and opsonisation of pathogens, induction of chemotaxis, anaphylatoxic effect, as well as generation of oxygen and nitrogen species by phagocytic cells and cytokine and chemokine production (Carroll and Sim, 2011; Tang et al., 2004). Activation of the complement cascade leads to three main outcomes: 1) opsonisation of microbes via the activation and binding of C3b; 2) recruitment of phagocytes through generation of the inflammatory and chemotactic molecules C4a and C5a; 3) direct killing of pathogens via the formation of the membrane-attack complex, leading to cell lysis and phagocytosis by macrophages (Carroll and Sim, 2011). Normally inactive, soluble complement proteins circulate in the blood where they encounter and recognise target molecules, leading to their activation and conformational change, which triggers a catalytic cascade resulting in the rapid generation of activated complement products. Activation occurs via any of three canonical pathways: classical, alternative and lectin. All three result in the activation of the most abundant component C3, leading to the activation of the terminal pathway. This pathway starts with the cleavage of C5 and the subsequent assembly of several complement proteins, namely C5b, C6, C7 and C8. The C5b678 complex, bound to plasma membranes, binds to 1-18 C9 molecules, forming a ring-shaped assembly of proteins subunits called the membrane-attack complex that can lyse bacteria and inactivate viruses through disruption of the proton gradient across the membrane (Beutler, 2004; Carroll and Sim, 2011; Podack, 1984; Podack and Tschopp, 1984). The existence of a fourth pathway has been suggested in phagocytic cells, where C3a and C5a

are generated independently of the canonical pathways, and directly activated by proteases of the coagulation cascade (Amara et al., 2008; Huber-Lang et al., 2006). Another important role of the complement is the activation of the adaptive immune system following ligation of complement receptors on B cells and DCs (Fearon, 1998).

1.5.2.7 Additional components

a. Acute phase proteins

The acute phase response is an early event during the innate immune response to infection that involves the generation of proteins such as haptoglobin, fibrinogen, C-reactive protein and SAA as well as an array of secondary effects such as fever. Acute phase proteins are secreted by hepatocytes in response to the pro-inflammatory cytokines IL-1β and IL-6. They have defensive functions by binding to microbes and signal their presence, or isolating the infectious agent in the case of fibrinogen. Their concentration increases markedly following infection, and they act together with the complement system and soluble receptors (discussed in the next section) (Beutler, 2004; Medzhitov, 2007).

b. Lipid mediators

Lipid mediators such as eicosanoids, platelet-activating factors and prostaglandins, play an important role in initiating events of the inflammatory response, ranging from inducing fever, controlling the blood flow as wells as inducing vasodilatation needed for leukocytes recruitment. Some lipid mediators also have chemotactic activities, such as the leukotriene B_4. Recently, a prominent role has been attributed to the anti-inflammatory lipoxins, resolvins and protectins in the switch from neutrophil to monocyte recruitment, phagocytosis and tissue repair (Medzhitov, 2008; Serhan et al., 2008).

c. Inflammasomes

The inflammasome is a protein complex that activates inflammatory caspase-1 and triggers the processing of pro-IL-1β, pro-IL-18 and probably pro-IL-33, resulting in the secretion of their mature forms (Elinav et al., 2011; Martinon et al., 2002). Known inflammasomes are generally composed of at least one nucleotide-binding oligomerisation-domain protein (NOD)-like receptor protein (NLR, e.g. NALP-3, IPAF) or absent in melanoma-2 (AIM2) that function as sensors of endogenous or exogenous PAMPs or DAMPs, the apoptosis-associated speck-like protein containing a CARD (ASC) and pro-caspase-1 (Fig 1.8). Inflammasome components and the activation of downstream signalling pathways depend on the nature of the stimuli (Elinav et al., 2011; Petrilli et al., 2007). Inflammasomes play a role in the very early stages of the inflammatory response, as IL-1β is one of the first cytokines to be produced and initiate host defence. Inflammasomes can be activated by various ligands from bacterial origin (PGN, flagellin), viral single stranded and double stranded RNA (ssRNA and dsRNA, respectively), fungi and parasites, crystalline or aggregated substances (including silica, uric acid, asbestos) or even by molecules produced as a result of the infection (potassium efflux and reactive

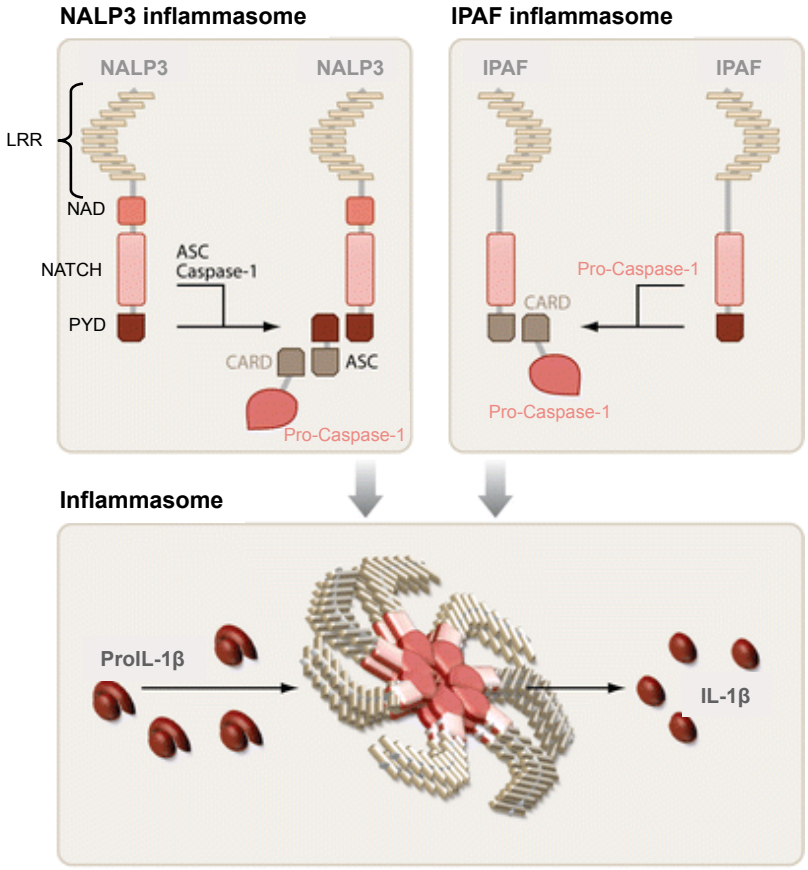

Figure 1.8. Structural organisation of NALP3 and IPAF inflammasomes.
The core structure of the NALP3 inflammasome is formed by NALP3, the adaptor ASC, and pro-caspase-1. PYD-PYD and CARD-CARD homotypic interactions are crucial to the recruitment and activation of the adaptor ASC and the inflammatory caspases, respectively (upper left panel). In the IPAF inflammasome, IPAF recruits pro-caspase-1 directly via CARD-CARD interactions (upper right panel). The leucine-rich repeats of NALP3 and IPAF are proposed to sense the activating signals, leading to oligomerisation of the NACHT domain, and initiating the formation of the donut-shaped inflammasome. Based on the structure of the apoptosome, the caspases and IL-1β processing activity most likely face toward the inside of the donut (lower panel). Abbreviations: NALP, NACHT-LRR-PYD-containing protein; ASC, apoptosis-associated speck-like protein containing a CARD; IPAF, ICE-protease-activating factor; LRR, leucine-rich repeats; PYD, pyrin domain; CARD, caspase recruitment domain; NAD, NACHT-associated domain. (Adapted from Martinon 2009, Terlizzi 2014)

oxygen species production) (Elinav et al., 2011; Martinon et al., 2009). Even though some proteins of the NLR family (discussed in section 1.6.3.1) activate inflammasomes, not all of those proteins directly recognise activating ligands but rather utilise adaptor molecules. Activation usually requires two steps, the first being the transcription of the various elements of the inflammasome, and the second the interaction between the activators and the relevant sensor, leading to inflammasome assembly and cleavage of its substrate (Elinav et al., 2011).

1.6 Receptors of the innate immune system

The activity of the innate immunocompetent cells and the release of the innate immune mediators detailed above depend heavily on the capacity of an array of innate immune receptors (PRRs) to sense pathogens or danger signals.

PRRs are involved in microbe internalisation by phagocytes (soluble PRRs and endocytic receptors) and/or cell activation (signalling PRRs). They can be either soluble or cell-associated, expressed at the cell surface or intracellular. Pathogen detection by PRRs is achieved not only by immune cells but also by non-immune cells including epithelial cells, fibroblasts, and endothelial cells. This recognition leads to innate immune and inflammatory responses in the infected tissues. PRRs detect highly conserved motifs expressed by large families of microbes; they are called pathogen- or microbe-associated molecular patterns (PAMPs or MAMPs). In addition to recognising PAMPs/MAMPs, PRRs also sense danger signals by binding endogenous molecules whose presence in the extracellular milieu indicates host injury (danger-associated molecular patterns, DAMPs) as well as cell apoptosis or death. Based on their functions PRRs can be classified in three families: (i) Soluble PRRs, (ii) Endocytic receptors and (iii) Signalling receptors (Hoffmann and Akira, 2013; Jeannin et al., 2008). The PRR families are represented in Figure 1.9.

1.6.1 Soluble PRRs

Direct contact between microbes and extracellular molecules of the host, which recognise specific residues on the surface of microorganisms, allows activation of downstream mechanisms (Beutler, 2004). Sometimes called soluble pattern recognition molecules, they are numerous, belong to different molecular families and represent the functional ancestors of antibodies (ante-antibodies). The three main families of soluble PRRs are the collectins, ficolins and pentraxins (Fig 1.9).

Collectins and ficolins, produced in the liver, lung and by phagocytes, facilitate the recognition and elimination of their ligands by phagocytes through opsonisation of foreign particles via sugar recognition. Collectins include mannose-binding lectin and surfactant protein A and D; they share structural and functional homology with C1q, a member of the classical complement pathway (Jeannin et al., 2008).

The pentraxin superfamily is composed of short pentraxins, serum amyloid P component and C-reactive protein - produced in the liver - and long pentraxin 3, produced at sites of inflammation

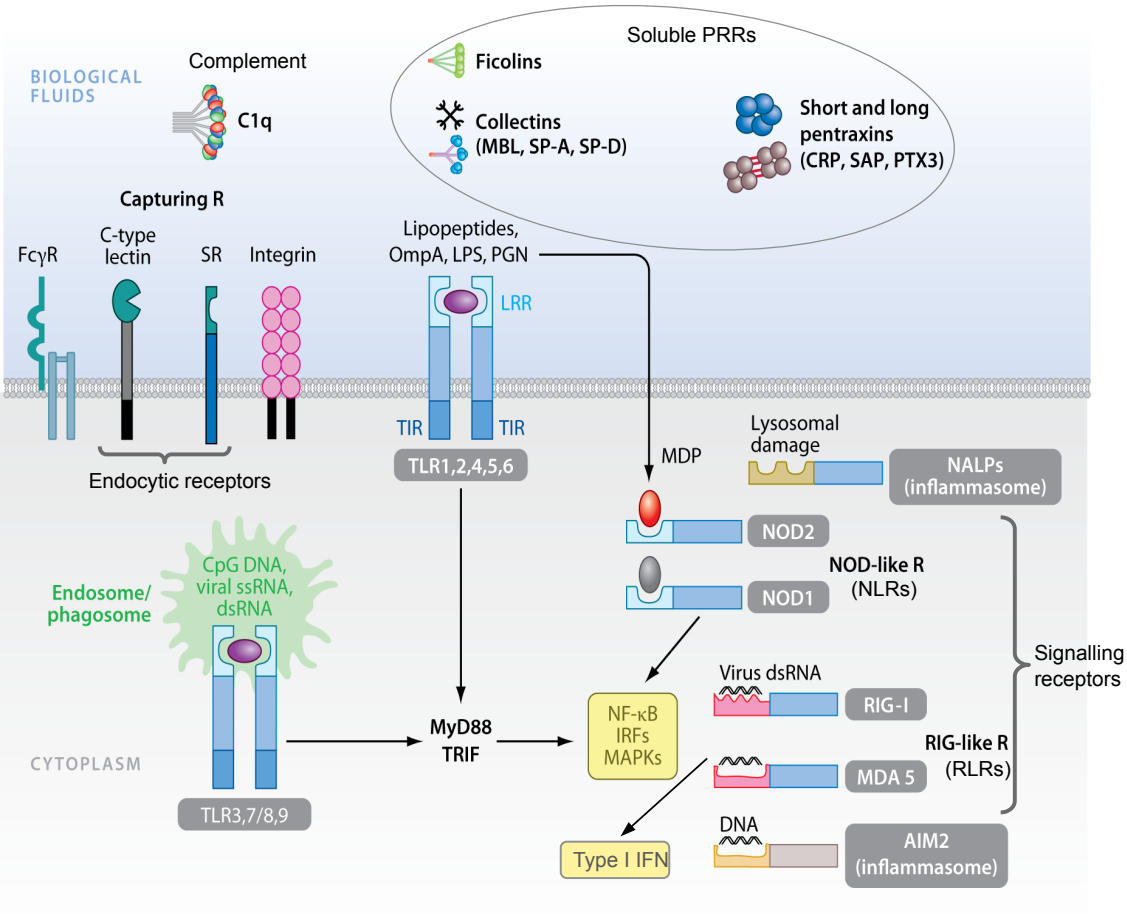

Figure 1.9. Schematic view of soluble and cell-associated pattern recognition receptors.
Soluble PRRs belong to different molecular families, including collectins, ficolins, C1q, and pentraxins. Cell-associated PRRs are strategically located in different cellular compartments (plasma membrane, endosomes, cytoplasm) and belong to different molecular classes (e.g., TLRs, scavenger receptors, lectin receptors), some of which are shown here. The TLRs, the NOD- and RIG-like receptors are signalling receptors that induce activation of transcription factors, including NF-κB, IRFs, and MAPKs. The scavenger receptors, C-type lectins, integrins, and FcγR are capturing receptors. Peptidoglycan-derived fragments (e.g., MDP) are recognized by NODs (MDP, by NOD2) and by NALP3, a component of the inflammasome. NALP containing inflammosomes are activated by different danger signals, including lysosomal damage, whereas the AIM2 inflammosome and RIG-like receptors recognise viral DNA and dsRNA, respectively (see detailed description in the text). Abbreviations: CRP, C reactive protein; LPS, lipopolysaccharide; LRR, leucine-rich repeat; MAPK, mitogen-activated protein kinase; MBL, mannan-binding lectin; MDA5, melanoma-differentiation-associated gene 5; MDP, muramyl dipeptide; NALPs, NACHT-LRR-PYD-containing proteins; NF-κB, nuclear factor-κB; NOD, nucleotide-binding oligomerization domain; OmpA, Outer membrane protein A; PGN, peptidoglycan; PTX3, pentraxin 3; RIG-I, retinoic acid–inducible gene I; SAP, serum amyloid P component; SP-A/-D, surfactant protein A/D; SR, scavenger receptor; TIR, Toll/interleukin-1 receptor domain; TLR, Toll-like receptor; TRIF, Toll-IL-1 receptor domain-containing adaptor-inducing interferon-β; IRFs, IFN-regulatory factors. (Adapted from Bottazzi 2010)

by many different cell types. They are proteins of the acute phase response, with plasma C-reactive protein concentration increasing greatly following the onset of inflammation in response to pro-inflammatory mediators, mainly IL-6 (Manfredi et al., 2008). Soluble PRRs have also been called opsonins, due to their capacity to facilitate target recognition and effector function of phagocytes. Collectins and ficolins are involved in the activation of the lectin pathway of the complement system, while pentraxins activate the classical pathway. Some members of different families of soluble PRRs interact with each other to form heterocomplexes, such as L- and M-ficolins, which are ligands for the short pentraxins. This cooperation is likely to increase their repertoire of recognition and actions. Soluble PRRs also play an important role in the elimination of apoptotic cells by recognising damaged cells and their constituents. C-reactive protein binds to membranes of damaged and apoptotic cells during late phase of apoptosis via various phospholipids, and also binds to chromatin/nucleolar components that redistribute to the plasma membrane. Several other members of the pentraxin family, collectins and ficolins bind apoptotic cells. This leads to phagocytosis and clearance of apoptotic cells (Bottazzi et al., 2010; Jeannin et al., 2008).

Many other molecules can serve as soluble PRRs, such as SAA, induced by pro-inflammatory cytokines (IL-1β, TNFα and IL-6) and mainly synthesised by the hepatocytes on the onset of an inflammatory response. SAA recognises a variety of pathogens (bacteria and virus) and opsonise them to facilitate the response of phagocytic cells with cytokines and reactive oxygen production. SAA also has cytokine-like properties, induces the production of chemokines, MMPs, nitric oxide and oxygen species and can interact with TLR2 to trigger nuclear factor-κB (NF-κB) activation (Bottazzi et al., 2010; He et al., 2009; O'Reilly et al., 2014).

The description and modulatory activity of soluble PRRs of the Toll-like receptor family will be discussed in section 1.7.6.1.

1.6.2 Endocytic receptors

Endocytic receptors, expressed at the cell surface, mediate the internalisation and recognition of microbes or microbial components. The recognition can be direct or mediated via heteromultimeric complexes. There are two main types of endocytic receptors: C-type lectin and scavenger receptors (Fig 1.9).

1.6.2.1 C-type lectin receptors (CLRs)

CLRs constitute a superfamily that recognises a variety of ligands, including sugar moieties of bacteria and fungi (mannose, mannose- and fucose-glycans, galactose or αmannans, among others) and oxidised lipids or self-ligands from damaged or dead cells. They are expressed mainly on myeloid cells (Sancho and Reis e Sousa, 2012). Dectin-1, one of the prototypes of the C-type lectin family is a transmembrane receptor that binds β-glucan, and is expressed on DCs and macrophages. Dectin-1 has an important role in antifungal defence, being involved in

phagocytosis of fungal pathogens and the production of antimicrobial molecules (Medzhitov, 2007). Another typical CLR, the mannose receptor, mediates recognition and phagocytosis of a range of viral, bacterial, fungal and protozoan pathogens by binding to mannose residues [Sancho and Reis e Sousa 2012]. In general, CLR activation promotes microbicidal activity, engages the phagocytic machinery to engulf microbes or viruses, and triggers pro- or anti-inflammatory processes. CLRs also interact with other PRR families to modulate and adapt the response to infection (Sancho and Reis e Sousa, 2012).

1.6.2.2 Scavenger receptors

Scavenger receptors (SR) are multidomain proteins, which were first described to bind oxidised low-density lipoproteins (LDL), but not native ones (Brown and Goldstein, 1979). It has since been shown that SR mediate the uptake of a diverse range of ligands including modified LDL, various polyanionic ligands, microorganisms, apoptotic and necrotic cells, and self-components such as ECM molecules. SR such as SR-A, CD36, LOX-1 and macrophage receptor with a collagenous structure (MARCO), form a heterogenous group with a common function. SRs are divided into 8 classes (SR-A to -H, including class C, which is only present in *Drosophila melanogaster*) on the basis of the structure of their extracellular domains (Canton et al., 2013). They are mainly expressed at the cell surface of macrophages, DCs and specific endothelial cells. Recognition of SR ligands is followed by their rapid internalisation, resulting either in accumulation (generation of foam cells after oxidised-lipoprotein internalisation) and/or destruction (endosome–lysosome fusion after microorganism internalisation) (Jeannin et al., 2008). SR have a broad range of other functions as they are thought to be involved in phagocytosis and antigen presentation, among others, but their exact mechanism of action remains unclear as they do not have a signalling domain (Canton et al., 2013).

1.6.3 Signalling receptors

Signalling receptors trigger cell activation in response to recognition of diverse microbial components, such as proteins, glycans, lipoproteins, and nucleic acids. They are expressed at the surface of the cells or intracellularly (Fig 1.9).

1.6.3.1 Nucleotide-binding oligomerisation-domain protein (NOD)-like receptors (NLRs)

NLRs are one class of intracellular and cytoplasmic proteins that sense bacterial components present in the cytoplasm. The NLR family consists of more than 20 members, including NOD1 and 2, the NACHT-LRR-PYD-containing protein (NALP or NLRP) family - the largest subfamily of NLRs - NAIP, IPAF (NLRC4) and CIITA, which respond to various PAMPs, including bacterial motifs and flagellin (NAIP5 and IPAF). NLRs also trigger pro-inflammatory responses following recognition of non-PAMP particles and cellular stress (Kawai and Akira, 2011). Notably, several NLR members (NALP1, NALP3 and IPAF) form the caspase-1 activating complexes called inflammasomes (discussed in section 1.5.2.7c) (Akira et al., 2006; Elinav et al., 2011).

NOD1 and NOD2, the namesake of the NLRs, are crucial for innate immune responses to specific bacterial infections. NOD1 is expressed in diverse cell types, whereas NOD2 expression is restricted to myeloid and lymphoid cells of the haematopoietic compartment. However, its expression in intestinal epithelial cells and Paneth cells of the intestinal crypts has been reported. NOD2 is being extensively studied, as it is one of the genetic risk factors for the development of Crohn's disease (Hugot et al., 2001; Philpott et al., 2014). NOD1 and NOD2 lack transmembrane domains, but are recruited to the plasma membrane and detect bacteria at the entry point. Both NOD1 and NOD2 recognise and directly bind intracellular fragments of bacterial PGN. NOD1 detects D-glutamyl-meso-diaminopimelic acid (iE-DAP), a dipeptide present in a PGN mainly found in Gram-negative bacteria and certain categories of Gram-positive bacteria, including *Listeria* spp. and *Bacillus* spp. NOD2 senses muramyl dipeptide (MDP), ubiquitously found in bacterial PGN. Their activation triggers their auto-oligomerisation, forming the NOD signalosome, which activates receptor-interacting protein-2. This is followed by NF-κB and MAPK activation and downstream signalling, leading to the production of pro-inflammatory mediators (TNF, IL-6, CXCL8, CCL2) and antimicrobial factors, such as defensins (Martinon et al., 2009; Philpott et al., 2014).

1.6.3.2 Retinoic-acid-inducible protein I (RIG-I)-like receptors (RLRs)

Also located in the cytoplasm, RLRs are important in antiviral defence, as they can sense RNA species generated during viral replication. RLRs, which include RIG-I, MDA5 and LGP2, are RNA helicases with an ATP-binding motif. RIG-I recognises ssRNA and short dsRNA, whereas MDA5 detects long dsRNA, structural features absent from cellular RNA, thus allowing discrimination between viral from self-RNA. LGP2 has been suggested to regulate RIG-I/MDA5, but whether in a negative or positive manner it is still a matter of debate (Kawai and Akira, 2009). Cardif (also known as IPS1/MAVS/VISA), another member of the NLR family, is a crucial adaptor of RIG-I and MDA5-mediated downstream signalling, with a C-terminal end that is required for mitochondrial targeting, suggesting a role of the mitocondria in innate immunity and IFN responses (Meylan et al., 2005; Seth et al., 2005). Activation of these proteins results in the production of type I IFNs (IFNα and IFNβ) and IFN-inducible genes, thereby inducing a broad range of antiviral activities (Medzhitov, 2007). Several NLRs also activate NF-κB and MAPK, leading to the expression of an array of immune and inflammatory genes (Kawai and Akira, 2009; Meylan et al., 2005; Seth et al., 2005).

HPMC have been shown to express RIG-1 and MDA5, whose stimulation triggers the up-regulation of pro-inflammatory cytokines and chemokines and type I IFNs, thus indicating a role of these cells in immunity against viral infection (Wornle et al., 2009).

1.6.3.3 Additional receptors

Other cytosolic proteins, not belonging to the NLR or RLR families, such as DAI, IFI16, DDX41 and AIM2, have been reported to be involved in the recognition of cytosolic DNA or retrovirus

infection, inducing the production of type I IFN and IL-1β secretion (Kawai and Akira, 2011). Many of these DNA binding proteins are ubiquitous and have the potential to engage endogenous DNA. It is therefore crucial that the DNA recognition process is tightly regulated. When mitochondrial DNA is released from a damaged mitochondria, caspase-1 activation is not dependent on AIM2, which is part of the AIM2 inflammasome, but instead it depends on the NALP3 inflammasome, potentially leading to a different response (Holm et al., 2013).

Another important family of signalling PRRs, the toll-like receptors (TLRs), is of particular relevance to this thesis and will be described in more detail in the following section.

1.7 The Toll-like receptor family

TLRs were the first PRRs to be discovered, and represented the missing link between innate and adaptive immunity. TLRs mediate a phylogenetically primitive, non-clonal mechanism of pathogen recognition based on binding to structurally conserved PAMPs.

It all started in the late 1980's, with the identification of the IL-1R type 1 (Sims et al., 1988). IL-1 is a pleiotropic pro-inflammatory cytokine involved in the initiation of the acute phase response, pyrogenicity, promotion of cartilage breakdown and T cell activation (Dinarello, 1991). The IL-1R type 1 signalling mechanism was not known, as there was no recognisable signalling motif in its cytoplasmic domain. In 1991, it was reported that the IL-1R cytoplasmic domain shared some homology with the cytoplasmic domain of a *Drosophila melanogaster* protein called Toll (Gay and Keith, 1991). Toll was initially known to promote dorsoventral polarity during fly development, involving a protein, Dorsal, which contains a REL domain with homology with members of the NF-κB family of transcription factors (Anderson et al., 1985; Steward, 1987). NF-κB was emerging as an important player in gene transcription, as many genes with a role in inflammation and infection were reported to be regulated by NF-κB. Notably, lipopolysaccharide (LPS) – a main component of the Gram-negative bacterial cell wall – was demonstrated to activate NF-κB, as did IL-1 (Baeuerle and Henkel, 1994; Sen and Baltimore, 1986). This suggested a common signalling mechanism between *Drosophila melanogaster* development and pro-inflammatory signalling in mammals. In 1994, a plant protein providing resistance to tobacco mosaic virus - the N protein - was characterised. The N protein presented some homology with the cytoplasmic domains of Toll and IL-1R type 1, indicating that a conserved region within the cytoplasmic domain had a role in host defence in the plant and animal kingdoms, emphasising its importance. It was therefore initially called the Toll-IL-1-resistence (TIR) domain and later renamed Toll/IL-1 receptor domain (Whitham et al., 1994). Parallel work unravelled mechanism of action of NF-κB, demonstrating that its activation triggered the production of antimicrobial peptides (Ip et al., 1993). This led to Jules Hoffmann's laboratory to investigate a potential role of Toll in immune gene expression. Hoffmann and colleagues demonstrated that following fungal infection, the antimicrobial peptide Drosomycin was expressed through activation of the Toll pathway (Lemaitre et al., 1996). The first human

homologue of Toll, called hToll was cloned in 1997 and showed to activate NF-κB and NF-κB-dependent genes (Medzhitov et al., 1997). Importantly, hToll triggered the expression of CD80, a protein involved in co-stimulation of T cells, providing one of the first links between innate and adaptive immunity. More Toll homologues were then cloned and named Toll-like receptors, and hToll was renamed TLR4 (Chiang and Beachy, 1994; Rock et al., 1998).

The discovery of the TLR family is paralleled and linked to the search for the LPS receptor, as LPS (the main component of bacterial endotoxin) was being extensively studied due to its role as the causative agent of Gram-negative bacteria-induced sepsis. A spontaneous mutation in the C3H/HeJ mouse strain rendered these mice resistant to LPS. This mutation was shown to be due to a single autosomal gene named *Lps*^{d}, which Bruce Beutler's group positionally cloned in 1998 and identified as being *Tlr4*. Notably, Beutler and his colleagues demonstrated that a single point mutation in the cytoplasmic domain of *Tlr4* (P 712 H) was responsible for the LPS resistance in the C3H/HeJ mice, thus defining TLR4 as the signalling receptor of LPS (Poltorak et al., 1998). In the following two years, *Lps*^{d} was also reported to be *Tlr4* by another group using a similar approach (Qureshi et al., 1999), and a TLR4 KO mouse strain was shown to fail to respond to LPS, confirming that TLR4 was indeed the LPS signalling receptor (Hoshino et al., 1999). The subsequent identification of co-receptors and understanding of the molecular mechanism of LPS recognition established TLR4 as a PRR. Ten TLR genes have now been identified in humans and twelve in mice (O'Neill et al., 2013).

1.7.1 Tissue distribution of TLRs

When the first human TLRs were cloned (TLR1-5), they were shown to be expressed differentially in a variety of organs and tissues, with TLR1 expressed ubiquitously, TLR2 mainly expressed in the heart, brain, lung and muscle, like TLR3, which was also found in the pancreas and placenta. TLR4 was only found in placenta, and TLR5 in ovaries and peripheral blood monocytes (Rock et al., 1998). Most tissue tested since then have shown to express at least one TLR, if not all (Sandor and Buc, 2005). An extensive study observed that the most diverse repertoire of TLRs was present in tissues involved in immune functions (spleen and peripheral blood leukocytes) and in organs most likely to encounter microbes (lung, small intestine, colon). The pancreas, placenta and ovary also displayed some variety (Zarember and Godowski, 2002). Notably, leukocytes were found to express the greatest variety of TLRs (Table 1.3).

TLRs are also expressed on non-haematopoietic cells. Notably, they are widely present on epithelial cells of the skin, lungs and intestines, tissues in direct contact with microorganisms, as mentioned above. Keratinocytes express TLR1, TLR2, TLR3, TLR5 but not TLR7, TLR8, TLR9, whereas data on TLR4, TLR6 and TLR10 are conflicting (Kollisch et al., 2005; Sandor and Buc, 2005). TLR2 and TLR4 are expressed throughout the epithelium of the airways, with some cell type specificity. Intestinal epithelial cells also express TLR2, TLR4 and TLR5. Despite constant exposure to the commensal flora in the gut, homeostasis is maintained, and TLR ligands do not necessarily trigger pathologic inflammation. This is achieved in part by their localisation (e.g.

Table 1.3 Expression of TLRs on leukocytes

TLR / Cell type	TLR1	TLR2	TLR3	TLR4	TLR5	TLR6	TLR7	TLR8	TLR9	TLR10
Neutrophils	+	+	-	+	+	+	+	+	+	+
Monocytes	+	+++	-	++	+	+	+	+	+	+
Macrophages	+	+	-	+	+	+	+	+	+	+
Eosinophils	+	+	-	+	-	+	+	-	-	+
Basophils	ND	+/-	ND	+/-	ND	ND	ND	ND	ND	ND
Mast cells	+	+	+	+	+	+	+	ND	+	ND
NK cells	+	+	+	+	+	+	+	+	+	-
pDC	+	+/-	-	+/-	-	+	++	-	++	+/-
iDC	+	+	-	++	+	-	-	+	+	+
mDC	+	+	+	+	+	+	+/-	+	-	+/-
*CD4 T cells	ND	+	+	+	+	ND	+	+	+	ND
*CD8 T cells	ND	+	+	+	+	ND	+	+	+	ND
*T reg	ND	+	+/-	+	+	ND	+	+	+	ND
*$\gamma\delta$ T cell	+	+	++	+/-	+	+	+	+	+	ND
*B1 cells	+	+/-	-	+/-	-	+	+/-	-	+	+
*Marginal zone B cells	+	+/-	-	+/-	-	+	+/-	-	+	+

*Of note, TLR expression on B and T cells is highly variable depending on their subset and level of differentiation and activation. Abbreviations: pDC, iDc, mDC, plasmacitoid, immature and myeloid DC, respectively; ND, not determined. (Adapted from Muzio, Bosisio et al. 2000; Jarrossay, Napolitani et al. 2001; Hornung, Rothenfusser et al. 2002; Sabroe, Jones et al. 2002; Chalifour, Jeannin et al. 2004; Kokkinopoulos, Jordan et al. 2005; Sandor and Buc 2005; Kabelitz 2007; Cole, Georgiou et al. 2010; Kulkarni, Behboudi et al. 2011; Rawlings, Schwartz et al. 2012)

TLR5: basolateral expression, not apical), low or potential expression (mRNA, but not protein) or by triggering signalling pathways by commensal bacteria different from those induced by pathogens (Melmed et al., 2003; Sandor and Buc, 2005). TLRs expression on HPMC has also been investigated, mainly at the mRNA expression level, showing a potential expression of most TLRs. However, only the HPMC expression of TLR3 and its responses to TLR3-specific agonists was clearly demonstrated (Wornle et al., 2009). TLRs expression in vessels depends on the location. Smooth muscle cells constitutively express TLR1, TLR3 TLR4 and TLR6, while TLR2 can be induced by *Chlamydia pneumoniae* (Cole et al., 2010). Normal vessels only express low levels of TLRs, but TLR1, TLR2 and TLR4 protein expression is increased in atherosclerotic vessels, while TLR2 is detected in endothelial cells in atheroprone regions, with a detrimental role in the initiation and development of atherosclerotic lesions such as leukocyte recruitment and foam cell formation (Cole et al., 2010). TLR expression depends on various factors, including the presence of pathogens, cytokines and environmental stress signals.

1.7.2 Cellular localisation of TLRs

TLRs can be divided into two groups according to their cellular localisation. TLR1, TLR2, TLR4, TLR5 and TLR6 are mainly expressed at the cell surface, while TLR3, TLR7, TLR8 and TLR9 are intracellular receptors, expressed on vesicles such as the endosome, lysosome, endolysosome and endoplasmic reticulum (Beutler, 2009; Kawai and Akira, 2009; Miggin and O'Neill, 2006). This suggests that the TLR system is not used to detect pathogens that are in the cytosol, these pathogens are detected by cytoplasmic PRRs (described in section 1.6.3). The intracellular localisation of some TLRs enables them to recognise nucleic acids delivered to the intracellular compartments after the uptake of viral particles or after viral or bacterial infections. By contrast, host nucleic acids are normally confined to the nucleus or cytoplasm and are not present in endosomes, thus avoiding TLR recognition. Thus, compartmentalisation permits avoiding unwanted TLR activation (Barton and Kagan, 2009; Kawai and Akira, 2011; Takeuchi and Akira, 2010).

1.7.3 TLR ligands, co-receptors and accessory molecules

Based on their primary sequence, TLRs can be further divided into subfamilies, which recognise related ligands: TLR1, TLR2 and TLR6 recognise mainly lipids whereas the highly related TLR7, TLR8 and TLR9 recognise nucleic acids. TLRs however are able to recognise a wide variety of structurally unrelated ligands. Cell-surface TLRs - TLR1, TLR2, TLR4, TLR5, TLR6, TLR10 - recognise mainly microbial membrane components, including lipoproteins, glycolipids and proteins, whereas intracellular TLRs - TLR3, TL7, TLR8, TLR9 - sense different types of nucleic acids. Therefore, many microbes such as bacteria, fungi or viruses are sensed by several TLRs, recognising the various PAMPs of a given pathogen (Akira et al., 2006). TLRs and their ligands are summarised in Table 1.4.

Table 1.4 TLRs agonists and co-receptors

TLR	Ligand	Origin of ligand	Accessory molecule and co-receptor
TLR1-TLR2	Triacyl lipopeptides Soluble factors Pam_3Cys	Bacteria and mycobacteria *Neisseria meningitides* Synthetic compounds	CD14, CD36, Dectin1
TLR2	Lipoprotein/lipopeptides Peptidoglycan Lipoteichoic acid Lipoarabinomannan Phospholipomannan Phenol-soluble modulin Glycoinositolphospholipids Glycolipids Porins Atypical lipopolysaccharide Atypical lipopolysaccharide Zymosan t-GPI-mucins Haemagglutinin protein Heat-shock protein 60 Heat-shock protein 70 HMGB1	Various pathogens Gram-positive bacteria Gram-positive bacteria Mycobacteria *Candida albicans* *Staphylococcus epidermidis* *Trypanosoma cruzi Treponema maltophilum* *Neisseria* *Leptospira interrogans* *Porphyromonas gingivalis* Fungi *Trypanosoma* Measles virus Host Host Host	
TLR2-TLR6	Diacyl lipopeptides Lipoteichoic acid Zymosan Pam_2Cys	*Mycoplasma* Gram-positive bacteria Fungi Synthetic compounds	CD14, CD36, Dectin1
TLR3	Double-stranded RNA Poly (I:C)	Viruses Synthetic compounds	CD14, TRIL, HMGB
TLR4	Lipopolysaccharide Fusion protein Envelope protein Mannan Heat-shock protein 60 Heat-shock protein 70 Type III repeat extra domain A of fibronectin Oligosaccharides of HA Polysaccharide fragments of heparan sulphate Fibrinogen β-Defensin HMGB1	Gram-negative bacteria Respiratory syncytial virus Mouse mammary-tumour virus *Candida albicans* Host Host Host Host Host Host Host Host	CD14, MD2, CD36, TRIL
TLR4-TLR6	Oxydised LDL Amyloid-β fibrils	Host Host	
TLR5	Flagellin	Bacteria	
TLR7	Single-stranded RNA Imidazoquinoline Loxoribine Bropirimine	Viruses Synthetic compounds Synthetic compounds Synthetic compounds	CD14, LL37, HMGB1, HMGB3
TLR8	Single-stranded RNA Imidazoquinoline Resiquimod	Viruses Synthetic compounds Synthetic compounds	CD14, LL37
TLR9	CpG-containing DNA Haemozoin CpG-A, CpG-B, CpG-C	Bacteria and viruses *Plasmodium falciparum* Synthetic compounds	CD14, progranulin, HMGB1, LL37
TLR10	Peptidoglycan	ND	Might heterodimerise with TLR2

Abbreviations: ND, not determined; Pam_3Cys, Pam_3-Cys-Ser-$(Lys)_4$; t-GPI-mucins, glycosylphosphatidylinositol-mucin; HMGB, High-mobility group box; Pam_2Cys, Pam_2-Cys-Ser-$(Lys)_4$; poly I:C, polyinosine-deoxycytidylic acid; HA, hyaluronan; MD2, myeloid differentiation protein 2; TRIL, TLR4 interactor with leucine-rich repeats; LDL, low-density lipoproteins. (Adapted from Akira and Takeda 2004; Akira, Uematsu et al. 2006; Guan, Ranoa et al. 2010; Lee, Avalos et al. 2012; Mulla, Myrtolli et al. 2013)

1.7.3.1 TLR1, TLR2 and TLR6

TLR2 recognises a wide range of components derived from bacteria, mycoplasma, fungi, parasites and viruses. Bacteria can be classified into Gram-positive and Gram-negative bacteria depending on the characteristics of their cell walls, and some of their unique components constitute PAMPs that are recognised by specific TLRs. Lipoteichoic acid (LTA, of Gram-positive bacteria), lipoproteins and PGN (both present in Gram-positive and Gram-negative bacteria) and mycobacteria, are potent immunostimulants (Fig 1.10). TLR2 plays a major role in detecting Gram-positive bacteria, including *Staphylococcus aureus* (*S. aureus*), *S. epidermidis* and *Streptococcus pneumoniae* (Echchannaoui et al., 2002; Takeuchi et al., 2000), and is involved in the recognition of LTA, lipoproteins and PGN. To achieve the recognition of various ligands, TLR2 is able to heterodimerise with TLR1 or TLR6, allowing discrimination between subtle changes in the lipid portion of lipoproteins (Alexopoulou et al., 2002; Ozinsky et al., 2000; Takeuchi et al., 2001; Takeuchi et al., 2002). The resulting TLR1/TLR2 heterodimer recognises triacyl lipopeptides from bacteria and mycobacteria - including *Mycobacterium leprae* and its triacylated 19 kDa and 33 kDa lipoproteins (Krutzik et al., 2003) - as well as synthetic lipopeptides such as Pam_3-Cys-Ser-$(Lys)_4$ (Pam_3Cys) (Nakata et al., 2006). By contrast, TLR6/TLR2 recognises diacyl lipoproteins from bacteria, or its synthetic counterpart Pam_2Cys as well as zymosan from fungi, LTA and macrophage-activating lipopeptide 2 (MALP2) from *Mycoplasma fermentans*. Additional cell wall components from diverse organisms detected by TLR2 include lipoarabinomannan from mycobacteria such as *Mycobacterium smegmatis* (Gilleron et al., 2003) and β-glucan from fungi, including *Candida albicans* and *Aspergillus fumigatus* (Netea et al., 2004). TLR2 is also involved in parasite recognition, such as *Trypanosoma*-derived glycosylphosphatidylinositol-mucin (Gazzinelli et al., 2004), and is able to sense viral components including measles virus hemaglutinin protein, human cytomegalovirus and herpex simplex virus 1 (Akira et al., 2006; Lee et al., 2012).

Several molecules act as co-receptors/cofactors for TLR2, allowing discrimination between, and facilitating recognition of, diverse agonists. TLR2 has been shown to use CD36 - a scavenger receptor found in lipid rafts - to discriminate between ligands. CD36 uniquely enhances immune responses to TLR2/TLR6 ligands, namely LTA and MALP2, and its deficiency results in increased susceptibility to *S. aureus* (Hoebe et al., 2005; Stuart et al., 2005). CD14, another TLR co-receptor, is a glycoprotein present in soluble form in plasma and other biological fluids as well as a glycosylphosphatidylinositol-anchored membrane protein on myeloid cells (Durieux et al., 1994; Haziot et al., 1988). It interacts with TLR ligands and enhances their ability to activate TLRs. CD14 is an important co-receptor for several TLRs, mediating pro-inflammatory cytokine production induced by TLR2/TLR6 ligands such as Pam_2Cys, zymosan, LTA and MALP2. LPS-binding protein (described below), a TLR cofactor, can bind to LTA, PGN and lipopeptides and transfer them to CD14, indicating an assisting role in TLR1, TLR2 and TLR6 activation (Lee et al., 2012). In addition, Dectin-1, a C-type lectin receptor (described in section

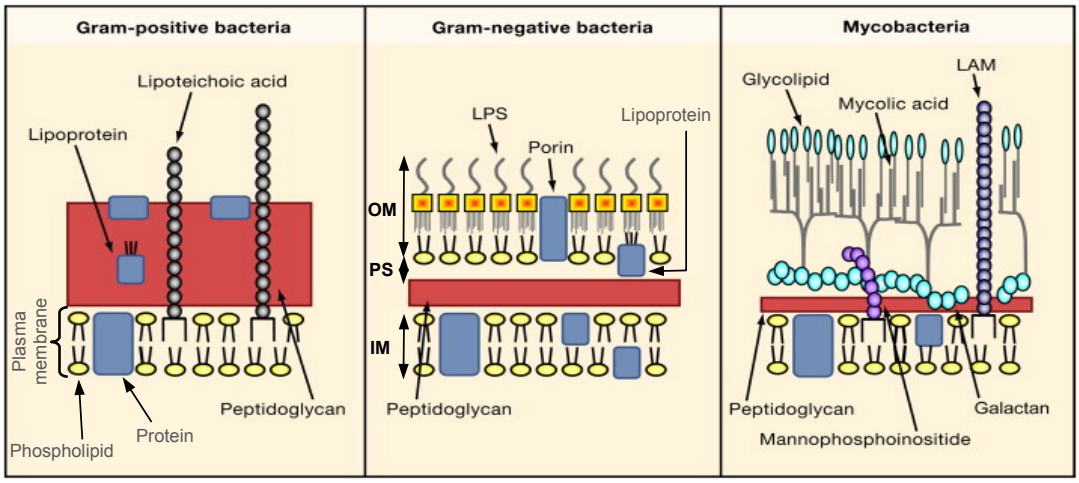

Figure 1.10. Schematic representation of bacterial cell walls.
Gram-positive bacteria have a thick porous layer of peptidoglycan (PGN). Lipoteichoic acids and lipoproteins are embedded in this cell wall. Gram-negative bacteria is characterized by the presence of LPS in the outer layer covering a thinner PGN layer. Mycobacteria produce a thick hydrophobic layer containing mycolyl arabinogalactan and dimycolate, in addition to a lipid bilayer and a PGN layer. Lipoarabinomannan (LAM) is a major cell-wall-associated glycolipid. Lipoproteins are common structures for various types of bacteria. Abbreviations: OM, outer membrane; IM, inner membrane; PS, periplasmic space. (Adapted from Akira 2006)

1.6.2.1), can collaborate with TLR2 to elicit a strong inflammatory response to yeast β-glucan and zymosan (Gantner et al., 2003).

Based on sequence similarity, TLR10 is related to TLR1 and TLR6 and one report showed that it could form a complex with TLR2 (Guan et al., 2010). TLR10 could be involved in PGN sensing (Mulla et al., 2013) but no definite ligand has been identified so far.

1.7.3.2 TLR4

TLR4 recognises, among other PAMPs, the main constituent of the outer membrane of Gram-negative bacteria, LPS (Fig 1.10) (Poltorak et al., 1998), and in particular its lipid portion called lipid A, which is responsible for most of the pathogenic effects associated with LPS and Gram-negative bacterial infection. LPS forms micelles poorly recognised by TLR4. Therefore it requires co-receptors and accessory molecules to detect it as well as to bind and activate signal transduction. LPS first associates with high affinity with LPS-binding protein, an acute phase protein present in the bloodstream. This interaction facilitates the disaggregation of LPS and its transfer to CD14 (Hailman et al., 1994). CD14 then chaperones LPS from LPS-binding protein to myeloid differentiation protein 2 (MD2) (Shimazu et al., 1999), a secreted protein that is bound to the extracellular domain of TLR4 and is part of the TLR4 receptor complex. LPS binding to MD2 leads to TLR4 oligodimerisation and downstream signalling (Akira et al., 2006; Lee et al., 2012). CD14 is also involved in LPS-induced endocytosis of TLR4, which is required for TRIF-mediated signalling (described in section 1.7.5.2) (Zanoni et al., 2011).

TLR4 participate in antifungal immunity - as initially suggested by its homology with *Drosophila melanogaster* Toll - by detecting fungal PAMPs in the cell wall or on the cell surface of *Candida albicans* and *Aspergillus fumigatus* (Netea et al., 2004). In addition, TLR4 is involved in the detection of respiratory syncytial virus fusion protein, the envelope protein of mouse mammary tumor virus, *Streptococcus pneumoniae* pneumolysin, some lipomannan from mycobacterial cell wall and parasite *Trypanosoma*-derived glycoinositolphospholipids (Akira et al., 2006). Additional co-receptors have been described for TLR4, including: 1) CD36, which mediates responses to oxidised LDL and amyloid-β fibrils through the assembly of a TLR4-TLR6 heterodimer (Stewart et al., 2010) and 2) TLR4 interactor with leucine-rich repeats, a transmembrane protein highly expressed in the brain, which can be induced by LPS and mediates TLR4 signalling and has been suggested to be involved in ligand delivery (Carpenter et al., 2009).

1.7.3.3 TLR5

TLR5 detects flagellin, the main protein constituent of bacterial flagella, the motility apparatus used by many microbial pathogens, and a potent activator of innate immune responses. TLR5 specifically recognises a relatively conserved domain of flagellin, the constant domain D1 in *Salmonella*, amongst other flagellated bacteria (Andersen-Nissen et al., 2007; Hayashi et al., 2001). *Helicobacter pylori* and *Campylobacter jejuni* are able to produce different types of

flagellins, enabling them to evade the flagellin-specific host immune responses (Andersen-Nissen et al., 2005).

1.7.3.4 TLR3

TLR3 recognises dsRNA, a major component of many viruses that mediates the activation of NF-κB and type I IFN signalling pathways. dsRNA can be generated during viral infection as a replication intermediate for ssRNA viruses, such as respiratory syncytial virus, encephalomyocarditis virus and West Nile virus, or as a by-product of symmetrical transcription of DNA viruses (Akira et al., 2006). TLR3 senses the genomic RNA of reoviruses and can also recognise a synthetic analogue of dsRNA, polyinosine-deoxycytidylic acid (poly I:C) (Alexopoulou et al., 2001). TLR3 has been shown to associate with CD14, which mediates ligand trafficking and enhances immune responses to TLR3 ligands (Lee et al., 2006). TLR4 interactor with leucine-rich repeats also appears to be able to mediate TLR3 signalling (Carpenter et al., 2011). High-mobility group box (HMGB) proteins form a family of nuclear proteins associated with chromatin and involved in transcription regulation by facilitating DNA access. HMGB proteins bind to RNA and are required for signalling downstream of TLR3 by mediating RNA delivery to the receptor, although their mechanism of action has not been elucidated (Yanai et al., 2009).

1.7.3.5 TLR7 and TLR8

TLR7 and TLR8 are highly homologue and detect ssRNA from RNA viruses – vesicular stomatitis virus, influenza A virus and human immunodeficiency virus - as well as purine analogue compounds with antiviral activity (imidazoquinolins). TLR8 also recognises uridin-rich or uridin/guanosin-rich ssRNA of both viral and host origin (Diebold et al., 2004; Hemmi et al., 2002). Many enveloped viruses traffic into the cytosol through the endosomal compartment, but in the phagolysosome (an acidic compartment containing degradation enzymes), viral particles can be damaged and ssRNA released, enabling its recognition by TLR7 and TLR8 and the subsequent production of potent anti-viral type I IFNs. TLR7 can also detect RNA species from bacteria such as group B *Streptococcus* (Kawai and Akira, 2010). Co-receptors and accessory molecules act also in concert with TLR7 and 8. CD14 acts as a co-receptor for TLR7 and TLR8, and probably promotes the general internalisation of nucleic acids (Baumann et al., 2010). LL37 - an amphipathic peptide activated through the cleavage of cathelicidin antimicrobial peptide - has been shown to form complexes with self RNA and to mediate its delivery to endosomal TLRs. LL37-self RNA complexes initiate TLR7- and TLR8-dependent signal transduction (Lee et al., 2012). HMGB1 and HMGB3 also facilitate ligand delivery to TLR7 and are required for type I IFN and pro-inflammatory cytokine production in response to RNA (Yanai et al., 2009).

1.7.3.6 TLR9

TLR9 senses unmethylated 2'-deoxyribo (cytidine-phosphate-guanosine) (CpG) DNA motifs that are frequent in bacteria and viruses but rare in mammalian cells. These motifs are found in

genomic DNA from bacteria, mycobacteria and parasites, as well as viral DNA from DNA viruses such as murine cytomegalovirus and herpex simplex virus 1 (Gazzinelli et al., 2004; Hemmi et al., 2000; Hochrein et al., 2004; Krieg, 2002; Tabeta et al., 2004). Synthetic oligonucleotides containing the CpG motif mimic bacterial DNA, thus activating TLR9 (Akira et al., 2006). TLR9 was also reported to recognise hemozoin, a crystalline metabolite of haemoglobin produced by the malaria parasite *Plasmodium falciparum* (Coban et al., 2005). However, it was later demonstrated that TLR9 senses not hemozoin, but the parasite DNA (highly pro-inflammatory) present in purified hemozoin; this haemoglobin metabolite appears to target the parasite DNA to endosomes (Parroche et al., 2007). Similar to other TLRs, TLR9 activation benefits from the collaboration of co-receptors and accessory molecules. Indeed, CD14 associates with TLR9 and mediates ligand trafficking (Baumann et al., 2010), while LL37 has been reported as a TLR9 accessory molecule. LL37 is implicated in the delivery of self-DNA to TLR9, via the formation of LL37-DNA complexes, which are internalised and localise to early endosomes to mediate TLR9-dependent signalling (Lande et al., 2007). HMGB1 is a pro-inflammatory molecule, as it is a TLR2 and TLR4 ligand (Andersson and Tracey, 2011), and has also been described as a TLR9 cofactor based on its ability to bind CpG DNA, interact with TLR9 and enhance TLR9 delivery to endosomes in response to its ligand (Tian et al., 2007). HMGB proteins may be universal mediators of innate immunity, as they are required for normal inflammatory responses to nucleic acids. The multifunctional protein granulin is present at high levels in serum as progranulin. Granulin processing is required for subsequent contribution to TLR9 signalling, as granulin fragments help deliver CpG DNA to the appropriate compartment to promote TLR9 responses (Park et al., 2011).

The use of diverse co-receptors and accessory molecules (summarised in Table 1.4), although sometimes common to different TLRs, but used in various combinations, increases the complexity of the mechanisms of ligand recognition and TLR signalling and allows ligand discrimination by different TLRs.

As described above, TLRs can also recognise endogenous ligands - generated by tissue injury, damaged or dying cells as well as tumour cells - that trigger inflammatory responses (Table 1.4). Endogenous ligands include degradation products of the ECM such has hyaluronan fragments, heat shock proteins, HMGB1 and self nucleic acids (Kawai and Akira, 2010). SAA, an acute phase protein whose concentration can increase up to 1,000-fold early upon onset of inflammation, has been reported to be a TLR2 ligand, leading to NF-κB activation (Cheng et al., 2008) and IL-6 secretion (O'Reilly et al., 2014). MicroRNAs (described in section 1.7.6.2) have also been reported to be intracellular TLR ligands (Fabbri et al., 2012).

1.7.4 Structure and activation

All TLRs share a conserved modular structure. They are type I transmembrane proteins - N-terminal is outside the membrane - composed of three major domains: 1) the ectodomain,

mostly composed of blocks of leucine-rich repeats that mediate ligand recognition; 2) a single transmembrane α-helix domain and 3) an intracellular domain, containing the TIR domain required to trigger downstream signal transduction following receptor engagement. About 80% of the polypeptide chain is above the plasma membrane (for TLRs 1, 2, 4, 5 and 6) or into the endosomal vesicle (for TLRs 3, 7, 8 and 9). The leucine-rich repeat units adopt a curved, solenoid shape, with conserved residues forming the hydrophobic core of each leucine-rich repeat. The inner surface of the solenoid, where specific molecular recognition takes place, presents side chains of variable residues, generating a wide range of binding specificities for diverse biological molecules (Beutler, 2009; Gay et al., 2006).
Ligand recognition and binding is a crucial step to initiate the homo- or heterodimerisation of the receptor, which induces a series of conformational changes in the receptor. The first conformational change following receptor crosslinking takes place in the C-terminal region of the ectodomain, allowing stable receptor-receptor interactions. This in turn promotes the rearrangement of the transmembrane helices, and allows signal transduction to occur. The intracellular TIR domain is required for coupling extracellular dimerisation to downstream signalling adaptor molecules (Gay et al., 2006).

A number of proteins play important roles in TLR expression and activation. Glucose-regulated protein of 94 kDa (GRP94) - found in the endoplasmic reticulum - mediates protein folding, and is necessary for the function of TLR1, TLR2, TLR4, TLR5, TLR7 and TLR9. GRP94 is required for the surface expression of TLR1, TLR2 and TLR4, and for the maturation and cleavage of TLR9. By mediating the folding and maturation of TLRs, GRP94 allows them to exit the endoplasmic reticulum. Protein associated with TLR4 A is also important for the maturation of multiple TLRs and may act as a co-chaperone for GRP94, because these two proteins interact to ensure that the unique requirements of TLR folding are fulfilled (Lee et al., 2012).
TLR3, TLR7, TLR8 and TLR9 are sequestered in the endoplasmic reticulum and are delivered to the endosomes via the Golgi apparatus. In the endosomes, they are processed by lysosomal proteases including cathepsins and asparagine endopeptidase, and become functional receptors that encounter and respond to their specific ligands (Blasius and Beutler, 2010; Kawai and Akira, 2011). Uncoordinated 93 homolog B1 is an endoplasmic reticulum-resident membrane glycoprotein required for endosomal TLR responses that associates with nucleic acid-sensing TLRs via their transmembrane domains and mediates their delivery to endolysosomes. Another protein involved in TLR trafficking is adaptor protein 3, member of a family of tetrameric complexes that mediate the sorting of membrane proteins in the secretory and endocytic pathways (Nakatsu and Ohno, 2003). Adaptor protein 3 recruits cargo proteins into endosomes for delivery to lysosomes and lysosome-related organelles. A mutation in a subunit of adaptor protein 3 reduced IFN expression in response to CpG, suggesting a role for adaptor protein 3 in recruiting TLR9 to lysosomes (Sasai et al., 2010). Whether other endosomal TLRs also require adaptor protein 3 for trafficking is not yet known (Lee et al., 2012).

1.7.5 TLR signalling pathways

TIR-containing receptors do not have enzymatic activity and rely on the adaptor proteins to trigger the inflammatory response. Once TLRs are activated, they recruit a specific set of adaptor proteins that form distinct complexes, tailoring a specific response to a particular ligand. Adaptors also contain TIR domains, which are rearranged following receptor dimerisation, providing the binding specificity required to recruit the appropriate adaptors (Gay et al., 2006). The TIR-domain-containing adaptor proteins involved in TLR signalling pathways are: 1) myeloid differentiation gene product 88 (MyD88), 2) MyD88 adaptor-like protein (MAL or TIR domain-containing adaptor protein (TIRAP)), 3) TIR domain-containing inducing IFNβ (TRIF or TIR-containing adaptor molecule 1 (TICAM1)) and 4) TRIF-related adaptor molecule (TRAM or TICAM2) (O'Neill and Bowie, 2007).

1.7.5.1 The MyD88-dependent pathway

MyD88 is a TIR-containing adaptor protein used by all TLRs except TLR3 (Kawai and Akira, 2011). MyD88 recruitment to TLR2 and TLR4 requires another TIR domain-containing adaptor called MAL, which is a bridging adaptor that links MyD88 to the TLR (Fitzgerald et al., 2001; Horng et al., 2001). MyD88 also possesses a death domain, involved in its interaction with IL-1R-associated kinase 4 (IRAK4) death domain (Flannery and Bowie, 2010). The conformational changes induced by receptor crosslinking leads to the sequential recruitment of several layers of MyD88, IRAK4 and IRAK2 monomers, forming the Myddosome signalling complex (Gay et al., 2011; Lin et al., 2010). IRAK1 is next recruited and activated, leading to its dissociation from the Myddosome and association with TNFα receptor-associated factor 6 (TRAF6). Further downstream signalling proteins associate with TRAF6, ultimately leading to NF-κB activation as well as MAPK and downstream transcription factors activation (Fig 1.11) (Kawai and Akira, 2010; O'Neill et al., 2013). The TIR domain plays a crucial role in the activation of TLR-induced signalling. This is emphasised by the fact that some pathogens have developed innate immune-evasion strategies by producing molecules containing homologues of the TIR domain that interfere with TLR2-MyD88-MAL signalling pathway (Askarian et al., 2014).

TLR7/8 and TLR9 also signal through the MyD88-dependent pathway and this can either lead to NF-κB activation or alternatively - and exclusively in plasmacytoid DCs TLR7 and TLR9 (Gilliet et al., 2008) - to the induction of type I IFN via binding of IFN-regulatory factor 7 (IRF7) to MyD88 (Kawai and Akira, 2010; O'Neill et al., 2013) (Fig 1.11).

Typically, TLR2 stimulation induces the production of pro-inflammatory cytokines via NF-κB activation. However, it has been reported that a MyD88-, IRF3- and IRF7-dependent type I IFN production - requiring TLR2 internalisation - is triggered by viral infection exclusively in inflammatory monocytes, suggesting a cell-type and ligand-specific response (Barbalat et al., 2009).

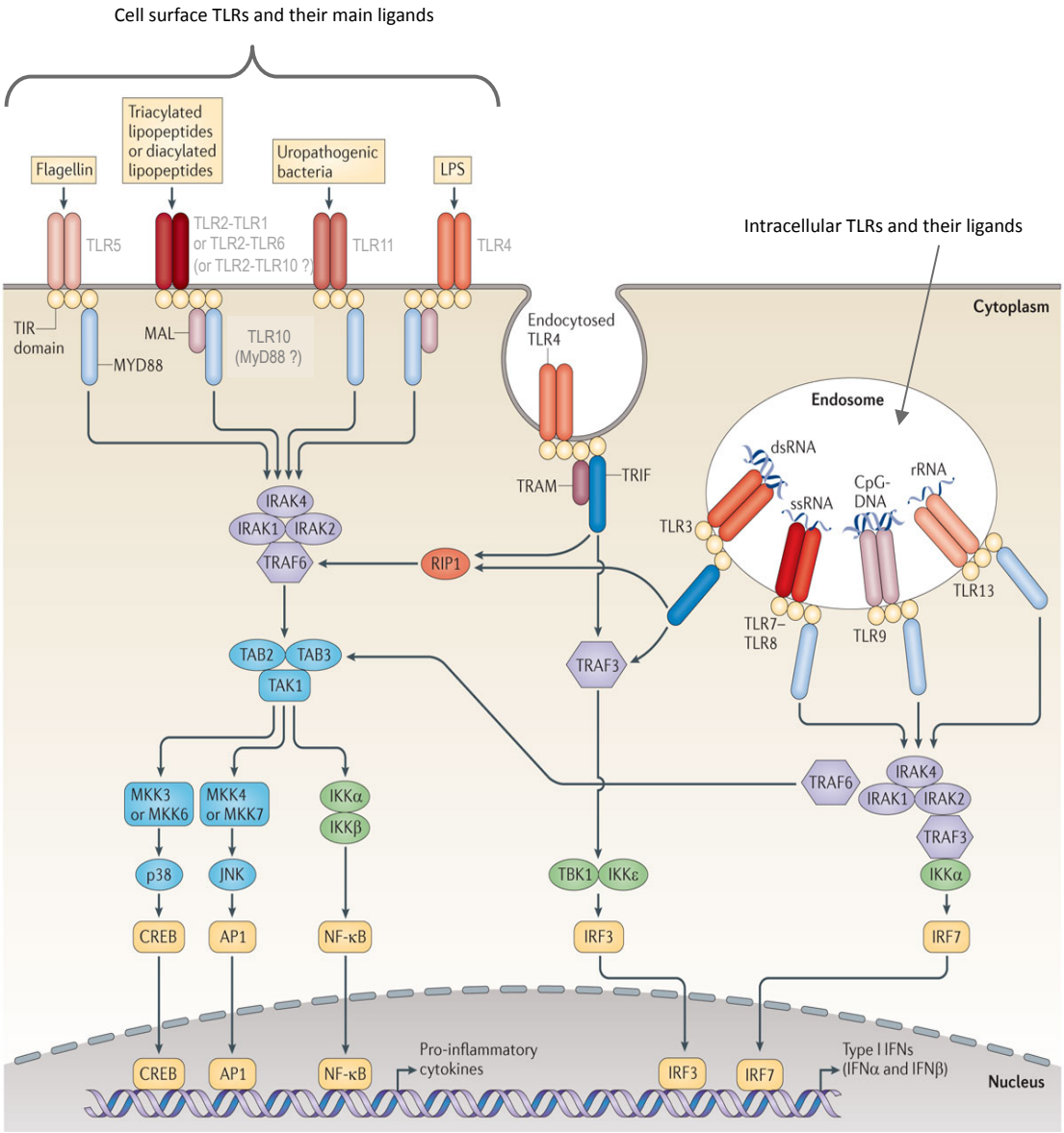

Figure 1.11. TLR signalling pathways in humans and mice.
TLR5, TLR11, TLR4, and the heterodimers of TLR2-TLR1 or TLR2-TLR6 – and potentially TLR2-TLR10 - bind to their respective ligands at the cell surface, whereas TLR3, TLR7–TLR8, TLR9 and TLR13 localise to the endosomes, where they sense microbial and host-derived nucleic acids. TLR4 is found expressed in both the plasma membrane and the endosomes. TLR signalling is initiated by ligand-induced dimerisation of the receptor. Subsequently, the Toll–IL-1-receptor (TIR) domains of TLRs engage TIR domain-containing adaptor proteins (either myeloid differentiation primary-response protein 88 (MyD88) and MyD88-adaptor-like protein (MAL), or TIR domain-containing adaptor protein inducing IFNβ (TRIF) and TRIF-related adaptor molecule (TRAM)). TLR4 moves from the plasma membrane to the endosomes in order to switch signalling from MyD88 to TRIF. Engagement of the signalling adaptor molecules stimulates downstream signalling pathways that involve interactions between IL-1R-associated kinases (IRAKs) and the adaptor molecules TNF receptor-associated factors (TRAFs), leading to the activation of the mitogen-activated protein kinases (MAPKs), JUN N-terminal kinase (JNK) and p38, and transcription factors. Two important families of transcription factors that are activated downstream of TLR signalling are nuclear factor-κB (NF-κB) and the interferon-regulatory factors (IRFs), but other transcription factors, such as cyclic AMP-responsive element-binding protein (CREB) and activator protein 1 (AP1), are also important. A major consequence of TLR signalling is the induction of pro-inflammatory cytokines, and in the case of the endosomal TLRs, the induction of type I interferons (IFNs). Additional abbreviations: dsRNA, double-stranded RNA; IKK, inhibitor of NF-κB kinase; LPS, lipopolysaccharide; MKK, MAP kinase kinase; RIP1, receptor-interacting protein 1; rRNA, ribosomal RNA; ssRNA, single-stranded RNA; TAB, TAK1-binding protein; TAK, TGFβ-activated kinase; TBK1, TANK-binding kinase 1; TLR, Toll-like receptor. (Adapted from O'Neil 2013)

Studies using MyD88 KO mice showed that type I IFN induction via the transcription factor IRF3 and the delayed NF-κB activation that are downstream of TLR4 were MyD88-independent (Yamamoto et al., 2002), suggesting the existence of an alternative signalling pathway.

1.7.5.2 The TRIF-dependent pathway

In contrast to the MyD88-dependent pathway, TLR3 and TLR4 activate a distinct signalling pathway, where TRIF is recruited to the receptor instead of MyD88 (Hoebe et al., 2003; Oshiumi et al., 2003a; Yamamoto et al., 2003a; Yamamoto et al., 2002). TRIF recruits either TRAF6, which activates the NF-κB and MAPK pathways, or TRAF3, activating IRF3 and the induction of type I IFN genes (Fig 1.11).

In the case of TLR4, an additional TIR domain-containing molecule, TRAM, is used as the bridging molecule, which helps recruit TRIF to the TLR4 TIR domain (Fitzgerald et al., 2003; Oshiumi et al., 2003b; Yamamoto et al., 2003b). TLR4 is the only TLR activating both the MyD88- and TRIF-dependent pathways. TLR4 activates sequentially the MAL-MyD88 pathway to trigger NF-κB and MAPK activation and the TRAM-TRIF pathway to induce IRF3 as well as the late-phase activation of NF-κB and MAPK. The TRIF-dependent pathway relies on endocytosis of TLR4 and its trafficking to the endosome, where it forms a signalling complex with TRAM and TRIF, rather than MAL and MyD88 (Barton and Kagan, 2009). As a consequence, TLR4 activates the MyD88-dependent pathway earlier than the TRIF-dependent pathway. This emphasises the importance of subcellular localisation for differential signalling by TLRs (Kawai and Akira, 2010; O'Neill et al., 2013).

TLR10 recruits MyD88, but its signalling pathway has not been elucidated yet, and one report failed to show the activation of NF-κB- or IFNβ-driven reporters, suggesting that TLR10 could trigger activation of alternative signalling pathways (Guan et al., 2010).

The TLR signalling pathways are summarised in Figure 1.11.

1.7.6 Regulation of TLR signalling

TLR activation is essential to initiate innate immune responses and modulate the quality and extent of the adaptive immunity. However, overactivation or dysregulation of TLRs and molecules involved in their signalling pathway may lead to severe acute and chronic inflammatory conditions and autoimmunity. A negative regulation of TLR-induced responses is therefore necessary to reduce inflammation and avoid its deleterious effects. Many negative regulators have been identified and can be soluble, membrane bound or intracellular (Kawai and Akira, 2010; Liew et al., 2005b). They are summarised in Table 1.5.

1.7.6.1 Soluble TLRs

The first reported, and best-described, naturally-occurring soluble form of a TLR is sTLR2, which was found to modulate TLR2-mediated responses. It corresponds to the extracellular domain of membrane-bound TLR2. sTLR2 was first found in human plasma and breast milk as

Table 1.5 Negative regulators of TLRs in humans

Regulator	Expression and induction	Targeted TLR	Suggested mechanism
sTLR2	Constitutively expressed in breast milk, plasma, saliva and amniotic fluid	TLR2	Blocks interaction of TLR2 with its ligands (decoy receptor) and co-receptor CD14
sTLR4	Constitutively expressed in saliva	TLR4	Blocks interaction of TLR4 and MD2
sTLR9	ND	TLR9	Blocks interaction of TLR9 with its ligands (decoy receptor)
RP105	LPS-induced in several cell types	TLR4	Inhibits LPS binding to TLR4-MD2
ST2	LPS-induced expression in macrophages	TLR2,4,9	Sequesters MyD88 and MAL
SIGIRR	Mainly expressed by epithelial cells and immature DCs, but downregulated by activation	TLR4,9	Interacts with TRAF6 and IRAK
TRAILR	Constitutively expressed in most cells	TLR2,3,4	Stabilises Iκ-Bα
MyD88s	LPS-induced expression, mainly in spleen	TLR4	Inhibits phosphorylation of IRAK1
IRAKM	LPS-induced expression by monocytes	TLR4,9	Inhibits phosphorylation of IRAK1
IRAK1c	ND	ND	Interferes with TLR signalling
IRAK2c/d	ND	ND	Prevent recruitment of MyD88
SARM	LPS-induced	TLR3,4	Inhibits TRIF-dependant signalling
TAG	LPS-induced	TLR4	Disrupts TRIF-TRAM complex and promotes TLR4 degradation
SOCS1	LPS- and CpG-induced expression in macrophages	TLR4,9	Mediates MAL degradation
TRIAD3A	Constitutively expressed in most cells and tissues	TLR4,9	Ubiquitylates TLRs
β-arrestin	LPS-induced	TLR4	Prevents TRAF6 oligomerisation
PI3K	Constitutively expressed by most cells	TLR2,3,4,5,9	Inhibits p38, JNK and NF-κB function
TOLLIP	Constitutively expressed in most tissues	TLR2,4	Autophosphorylates IRAK1
TRAF1	ND	TLR3	Inhibits TRIF-dependant signalling
TRAF4	ND	TLR2,3,4,9	Inhibits TRIF- and TRAF6-dependent signalling
A20	LPS-induced expression in macrophages	TLR2,3,4,5,9	De-ubiquitylates TRAF6, Suppresses TRAF6 and RIP1
TANK	Ligand-induced in macrophages, B cells, cDCs and glomeruli	TLR2,4,5,6,7,9	Inhibits TRAF6 ubiquitination
SHP-1	AMPK-induced expression in macrophages and splenocytes	TLR1,2,3,4,5,6	Suppresses IRAK1 and IRAK2- Inhibits TRAF6 ubiquitination and suppresses p65
WWP1	ND	TLR4	Ubiquitylates and mediates TRAF6 degradation
BCAP	Agonist-induced in B cells and DCs	TLR2,4,9	Binds PI3K and inhibits TLR responses
CYLD	Inducible in T and B cells	ND	Inhibits TRAF 2 (and to a lesser extent TRAF6) ubiquitination
TRIM30α	Agonists-induced	TLR4	Targets TAB2 and TAB3 for degradation
Atg16L1	Inducible in Paneth cells	TLR3,4	Suppresses inflammasome activation
Zc3h12a	Inducible in macrophages and cDCs	Several TLRs	Affects IL-6 and IL-12p40 mRNA stability
Tristeraprolin	Inducible in macrophages and cDCs	Several TLRs	Affects TNF mRNA stability
ATF3	Inducible in macrophages and cDCs	TLR4	Affects mRNA stability and prevents IL-6 and IL-12p40 transcription
Pin1	Agonist-induced in macrophages	TLR3	Degrades IRF3
DUBA	Agonist-induced	TLR3,4,9	Suppresses IRF3 and IRF7
miR-105	Many cell types	TLR2	Decreases receptor mRNA levels
miR-223	Many cell types	TLR3,4	Decreases receptor mRNA levels
let7i, let7e	Many cell types	TLR4	Decreases receptor expression

Abbreviations: ND, not determined; RP105, radioprotective 105; ST2, Suppressor of tumorigenicity 2; SIGIRR, single immunoglobulin IL-1R-related molecule; TRAF6, TNF receptor-associated factor 6; TRAILR, TNF-related apoptosis-inducing ligand; IRAK1, interleukin receptor-associated kinase1; SARM, sterile alpha and HEAT-Armadillo motifs; TAG, TRAM adaptor with GOLD domain; SOCS1, suppressor of cytokine signaling 1; TRIAD3A, Triad-domain containing protein 3A; PI3K, phosphoinostol-3-kinase; JNK, c-jun N-terminal Kinase; p38, p38 mitogen activated protein kinase; TOLLIP, Toll-interacting protein; TANK, TRAF family member-associated NF-κB activator; SHP-1, Src homology-2 containing tyrosine phosphatase-1; AMPK, AMP-activated protein kinase; WWP1, WW domain containing E3 ubiquitin protein ligase 1; BCAP, B-cell adapter for PI3K; CYLD, tumor suppressor cylindromatosis; TRIM30α, tripartite-motif 30α. ATF3, activating transcription factor; peptidyl-prolyl isomerase Pin1; DUBA, Deubiquitylating enzyme A. (Adapted from Trompouki, Hatzivassiliou et al. 2003; Liew, Liu et al. 2005; Liew, Xu et al. 2005; Saitoh, Tun-Kyi et al. 2006; Hazeki, Nigorikawa et al. 2007; Kawai and Akira 2007; Kayagaki, Phung et al. 2007; Brikos and O'Neill 2008; Kenny and O'Neill 2008; Shi, Deng et al. 2008; Sun 2008; Kawagoe, Takeuchi et al. 2009; Zunt, Burton et al. 2009; Kawai and Akira 2010; McGettrick and O'Neill 2010; Chockalingam, Cameron et al. 2011; Yuk, Shin et al. 2011; Ni, MacFarlane et al. 2012; Troutman, Hu et al. 2012; Virtue, Wang et al. 2012; Lin, Xu et al. 2013).

well as in pig and mouse plasma (LeBouder et al., 2003), and later reported present in amniotic fluid and saliva (Dulay et al., 2009; Kuroishi et al., 2007). sTLR2 is secreted by monocytes upon stimulation of TLR2 or other TLRs, or by non-TLR mediated cell activation, and data suggested that it originates from proteolytic cleavage of membrane-bound TLR2 (LeBouder et al., 2003). sTLR2 was demonstrated to exert an anti-inflammatory effect *in vitro* and *in vivo* by inhibiting TLR2-mediated CXCL8, CCL2, CXCL1/KC (murine counterpart of human CXCL3), TNFα secretion as well as NF-kB activation. It exerts its modulatory effect by sequestering the ligand (decoy receptor) and by disrupting the interaction between TLR2 and its co-receptor CD14, as sTLR2 was found to associates with CD14 (Kuroishi et al., 2007; LeBouder et al., 2003; Raby et al., 2009). Iwami et al. reported the existence of an alternatively spliced variant of mouse TLR4 mRNA that, when transiently transfected in CHO cells, expressed a partially secreted soluble form of TLR4 (Iwami et al., 2000). The existence of four human TLR4 splice variants was later described (Jaresova et al., 2007), and a functional sTLR4 was found in saliva with a modulatory effect on TNFα secretion (Zunt et al., 2009). Two other negative modulators, a naturally-occurring sTLR9 (Chockalingam et al., 2011) and sTLR3 generated by cloning of the extracellular domain of TLR3 (Sun et al., 2006) have been described. By contrast, a naturally occurring sTLR5, only found in fish, has shown some synergistic activity with the membrane-bound TLR5 (Tsoi et al., 2006; Tsujita et al., 2006).

1.7.6.2 Transmembrane and intracellular modulators

TLR signalling pathways are modulated at multiple levels and by molecules assuming various functions, including splice variants for adaptors or related proteins, ubiquitin ligases, deubiquitinases, transcriptional regulators and microRNAs. Regulators include PI3K, TOLLIP, SOCS1, A20, SIGRR, TRIAD3A, TANK and TRAILR, and the ligand-induced MyD88s, IRAKM and ST2L. They are constitutively expressed in diverse cells and tissues. Negative regulators act by a variety of ways, for example, by direct suppression of a TLR signalling pathway protein activity (ST2L), by inhibiting signal intermediate ubiquitination (TANK), by inhibiting transcription factor activity (SOCS1) or by affecting messenger RNA stability such as the zinc-finger RNAse Zc3h12a (Kawai and Akira, 2010; Liew et al., 2005b).

MicroRNAs are small (21-24 nucleotides) RNA molecules and are important regulators of gene expression. MicroRNAs decrease target mRNA levels - through either mRNA decay or translational inhibition - and control the protein content of a cell. Their expression is highly regulated, and they function as immunomodulators. Indeed, microRNAs can control TLR expression and target many TLR signalling proteins, transcription factors, cytokines and chemokines. In turn, targets can reciprocally control the expression and function of microRNAs. While some microRNAs are ubiquitous, such as miR-155, miR-146 and miR-21, TLR activation seems to result in the sequential induction of important microRNAs that can control the strength and longevity of an inflammatory response (Huntzinger and Izaurralde, 2011; O'Neill et al., 2011). TLR negative regulators are summarised in Table 1.5.

Cooperation and synergy between various TLRs has been demonstrated (Trinchieri and Sher, 2007). TLR signal transduction can also be affected, in a negative or positive way, by the activity, interaction and crosstalk with other signalling pathways.

1.7.7 TLR interaction with other signalling pathways

In addition to their first-responder roles in inducing an inflammatory response to invading pathogens, TLRs can network with other components of the innate or adaptive immune system. Many reports studying the involvement of TLRs, NLRs, CLRs and other PRRs in the recognition of various pathogens, including mycobacteria, viruses and fungi - notably using KO mice - have demonstrated that none of them is responsible for the full innate immune response but rather act in synergy to mount an appropriate response and circumvent pathogen evasion mechanisms (Kawai and Akira, 2011; O'Neill, 2008). Notably, dectin-1 collaborates with TLR2 or TLR4 to trigger cytokine production upon recognition of *C. albicans* and zymosan (Goodridge and Underhill, 2008). Synergy has also been shown between TLRs and the complement system to produce pro-inflammatory molecules. In particular, TLRs showed a positive modulatory effect on C5a-induced responses by targeting a negative modulator of C5a receptor (Raby et al., 2011). Similarly, signal transduction crosstalks exist between TLRs and other signalling pathways. Notably in macrophages, IFNγ - and its downstream JAK/STAT signalling pathway - has been reported to enhance TLR responses by increasing TLR expression or blocking TLR-induced feedback-inhibition loops, such as the suppression of TLR-mediated IL-10 expression and downstream STAT3 activation (Hu et al., 2006; Schroder et al., 2006; Spiller et al., 2008).
TLR and IL-6 signalling pathways are also inter-connected. While IL-6 is an obvious downstream transducer of TLR-driven pro-inflammatory responses, several endogenous TLR agonists, such as SAA and HMGB1, are regulated by STAT3, downstream of IL-6 (Tye and Jenkins, 2013). IL-6 trans-signalling via STAT3 has been shown to play an important role in modulating TLR4-driven pro-inflammatory responses (Greenhill et al., 2011). TLR and IL-6 have been the particular focus of interest in cancer - notably in cancers of the liver, colon, lung and pancreas - where there is a recurrent dysregulated co-activation of STAT3 and NF-κB, the archetypal downstream transcription factors of the IL-6 and TLR families. These transcription factors are of particular interest due to their ability to propagate inflammation, which plays a crucial role in the promotion of carcinogenesis (Mansell and Jenkins, 2013). In gastric cancer, IL-6 signalling has been shown to modulate TLR responses by a STAT3-driven upregulation of TLR2, promoting tumorigenesis independently of tumour inflammation (Tye et al., 2012).

1.8 Hypotheses, aims and objectives of the project

The work conducted to date in humans and mice, and discussed in previous sections, demonstrated the pivotal role that peritoneal mesothelial cells play in the initiation, progression and resolution of inflammatory responses in the peritoneal cavity. Their activity is critical to maintaining the integrity of the peritoneal membrane, which is required for an efficient PD therapy. The critical role that the TLR family of innate immune receptors and the IL-6 cytokine and its receptors play in the inflammatory response has been well documented, and discussed previously. However, the expression of TLRs in HPMC and their role in HPMC-mediated pro-inflammatory responses to infection have not been investigated. Similarly, the capacity of IL-6 and its receptors to modulate microbial-induced peritoneal inflammation and TLR-mediated peritoneal responses remained to be fully evaluated.

Given the pivotal role that HPMC play in peritoneal inflammation, it was hypothesised in the present study that HPMC express TLRs, and that these receptors are critical to HPMC-mediated pro-inflammatory responses to most common pathogens affecting PD. Furthermore, it was hypothesised that IL-6 and its receptors may modulate the putative expression and activity of TLRs in HPMC. The putative activity of TLRs and IL-6 and its receptors in HPMC-mediated responses may contribute to guaranteeing a prompt, strong and efficient response to the microbial challenge and a rapid clearance of infection, and thus may impact on PD outcomes. The aim of the project was therefore to evaluate the role that TLRs and IL-6/ IL-6 receptors play in peritoneal inflammatory responses to infection, with particular emphasis on the responses of HPMC *in vitro* and *in vivo*.

Objectives

This study sought to:

1. Characterise the expression of TLRs in HPMC.
2. Evaluate the capacity of HPMC *in vitro* to mount pro-inflammatory responses to microbial components through TLRs and its main co-receptor, CD14.
3. Study the modulation of the putative expression of TLRs in HPMC.
4. Evaluate the capacity of well-documented modulators of pro-inflammatory responses, soluble TLR2 (sTLR2) and the IL6/sIL6R, to modulate TLR-mediated HPMC responses *in vitro*.
5. Evaluate further the effect of sTLR2 on peritoneal inflammation by using mouse models of peritoneal inflammation and infection.
6. Study in more detail how the IL-6/sIL-6R trans-signalling complex contributes to peritoneal responses *in vivo*.
7. Develop a suitable *in vivo* model of bacterial peritonitis to address some of the questions detailed above.

Chapter 2

RESULTS

2.1 Expression and activity of TLRs in human peritoneal mesothelial cells

The ability of HPMC to directly respond to a bacterial challenge has been suggested, but the responses have not been fully characterised (Kato et al., 2004; Visser et al., 1995b). As discussed previously (Introduction, section 1.7.1), only HPMC expression of TLR3 and responses to TLR3-specific agonists were clearly demonstrated (Wornle et al., 2009). Therefore, a full characterisation of the expression of TLR family members by primary HPMC remained to be conducted, and the capacity of HPMC to mediate inflammatory responses via TLRs following stimulation with Gram-positive and Gram-negative bacteria remained to be evaluated.

Therefore, the first part of this study aimed to evaluate the potential involvement of TLRs in HPMC-mediated microbial recognition and responses during a peritonitis episode. To this end, the expression of different TLR family members in HPMC as well as the ability of TLR-specific ligands to induce chemokine expression by HPMC was investigated. Furthermore, the effect of a clinically relevant bacterial-derived preparation on HPMC's pro-inflammatory responses and its dependence on TLR activity was examined, as well as the effect of inflammatory cytokines and TLR ligands on TLR expression in HPMC.

2.1.1 TLR expression in HPMC

In order to fully characterise TLR family expression (TLR1-TLR10) in HPMC, real-time PCR (qRT-PCR) analysis of both growth arrested un-stimulated mesothelial cells and cells growing in medium containing 0.1% (v:v) or 10% (v:v) FCS was performed. This analysis showed a range of relative Tlr mRNA expression, from the most highly expressed members (Tlrs 1-3), those which were expressed at low to moderate levels (Tlrs 4-6) to barely detectable or undetectable levels (Tlrs 7-10) (Fig 2.1.1). A comparison with Tlr mRNA expression in peripheral blood mononuclear cells (PBMC) revealed lower levels of all Tlrs in HPMC, except for Tlr3 (Table 2.1.1).

In order to evaluate the capacity of HPMC to respond to Gram-positive bacteria through TLR2 and Gram-negative bacteria through TLR4, confirmation of the qRT-PCR results for TLR2 and TLR4 expression by RT-PCR and flow cytometry was sought first (Fig 2.1.2A and 2.1.2B, respectively). TLR1 and TLR6 expression was also tested, as both receptors are capable of forming heterodimers with TLR2 thereby allowing the recognition of triacyl (TLR2/TLR1) and diacyl lipopeptides (TLR2/TLR6) (Kawai and Akira, 2010). Clear bands corresponding to Tlr2 (632 pb) and Tlr6 (500 bp) were obtained by RT-PCR, but no band was observed for Tlr4 (781 bp) (Fig 2.1.2A). The presence of TLR1 and TLR2 on the cell surface of HPMC was confirmed by flow cytometric analysis (Fig 2.1.2B); no cell-surface expression of TLR6 was detectable, in

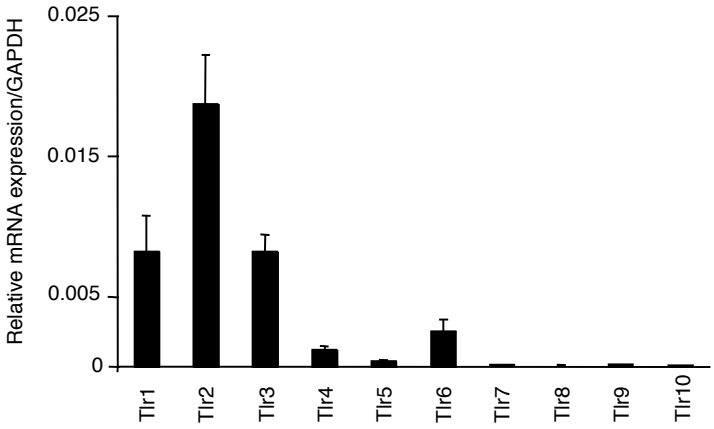

Figure 2.1.1. TLR expression in primary HPMC.
Analysis of Tlr1-Tlr10 mRNA expression in HPMC was performed by qRT-PCR. Specific primers were used to amplify human Tlr1-Tlr10 cDNAs prepared from total RNA extracted from non-stimulated HPMC. Expression of each mRNA was determined by calculating the $2^{-\Delta Ct}$, as described under Materials and Methods, and was expressed relative to the expression of the housekeeping gene GAPDH. Results (±SD) presented are representative of five experiments performed using primary cells from different donors.

Table 2.1.1. Relative TLR expression in HPMC

Tlr gene	Tlr ($2^{-\Delta Ct}$) HPMC	Tlr ($2^{-\Delta Ct}$) PBMC	Relative expression to PBMC
Tlr1	0.0041	0.0547	0.0749
Tlr2	0.0134	0.2943	0.0455
Tlr3	0.0089	0.0010	**8.9**
Tlr4	0.0018	0.0330	0.0545
Tlr5	0.0003	0.0033	0.0909
Tlr6	0.0012	0.0351	0.0342
Tlr7	$2.13e^{-05}$	0.0022	0.0097
Tlr8	$2.37e^{-06}$	0.0540	$4.39e^{-05}$
Tlr9	$4.55e^{-05}$	0.0029	0.0157
Tlr10	$7.96e^{-06}$	0.0037	0.0022

qRT-PCR evaluation of Tlr1 to Tlr10 mRNA expression in HPMC (as shown in Figure 2.1.1) and PBMC. Results are expressed as the ratio of the Tlr gene ($2^{-\Delta Ct}$) to the housekeeping gene GAPDH ($2^{-\Delta Ct}$) for each cell type as described under Materials and Methods, and as the relative expression of each Tlr in HPMC to that in PBMC (HPMC/PBMC). Results shown are of one experiment representative of four experiments performed using HPMC and PBMC from different donors.

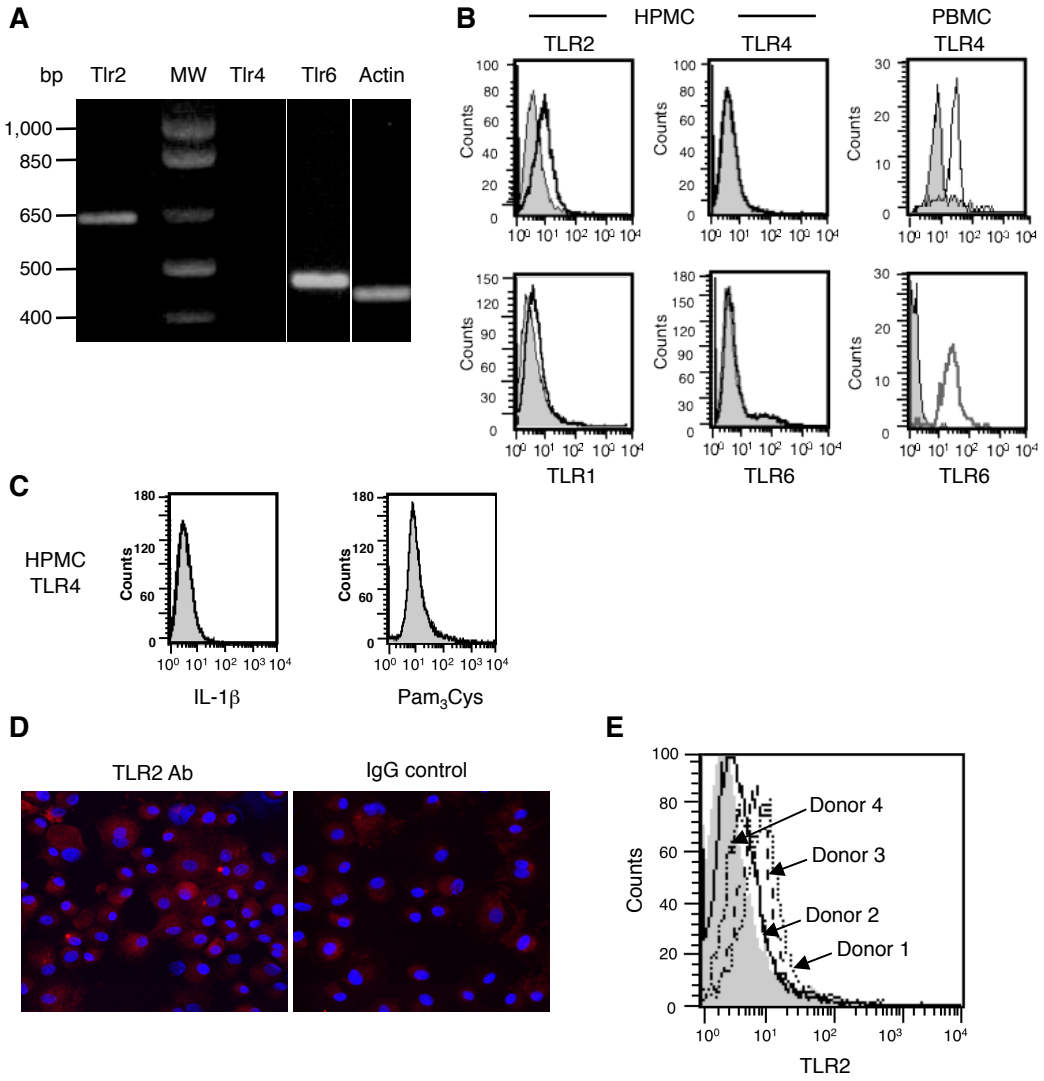

Figure 2.1.2. Analysis of TLR1, TLR2, TLR4 and TLR6 expression in primary HPMC.
(A) TLR2, TLR4, TLR6 and β-actin mRNA expression in non-stimulated HPMC was assessed by RT-PCR followed by agarose gel electrophoresis using specific primer pairs, as described under Materials and Methods. **(B)** Cell-surface expression of TLR2, TLR4, TLR1 and TLR6 was assessed by flow cytometry in growth-arrested HPMC using specific antibodies (open plots). Control fluorescent histogram profiles corresponding to the immunostaining with isotype-matched control antibodies are also shown (shaded plots). Results are representative of seven different cell lines from individual donors. In each experiment, human PBMC were used as a positive control for TLR4 and TLR6 expression. **(C)** In addition to (B), the cell-surface expression of TLR4 in HPMC was assessed by flow cytometry following cell stimulation with IL-1β (100 pg/ml) and Pam_3Cys (2 μg/ml). Data presented are representative of five experiments performed with HPMC derived from five different donors. **(D)** Non-stimulated HPMC were tested for TLR2 expression by immunocytochemistry using the TLR2-specific mAb TLR2.5. An isotype-matched antibody was used as a staining control. Results are representative of immunostaining of two different primary cells. **(E)** Primary HPMC originating from four different donors were tested for TLR2 expression by flow cytometry using the TLR2-specific mAb TLR2.1. The negative control staining with the isotype control antibody (shaded plot) was identical for all donors.

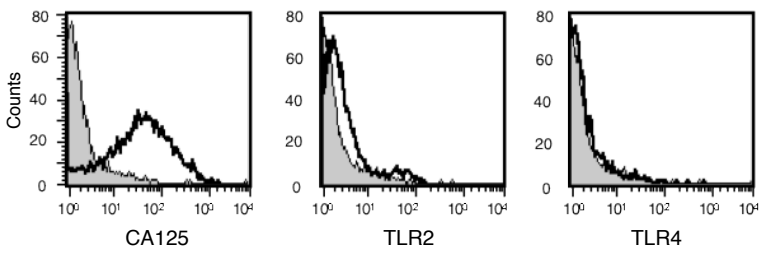

Figure 2.1.3. Analysis of TLR2 and TLR4 expression in freshly-isolated primary HPMC.
Mesothelial cells were tested for TLR2 and TLR4 cell-surface expression immediately after tryptic digestion of omental tissue. Cells were stained for TLR2, TLR4 and the HPMC-specific marker CA125, and analysed by flow cytometry. Results shown are representative of four experiments performed using primary cells from different donors.

spite of the positive detection of Tlr6 mRNA. Similarly, no TLR4 protein expression could be detected on the mesothelial HPMC surface, either on growth-arrested cells (Fig 2.1.2B) or following stimulation with various stimuli such as the pro-inflammatory cytokine IL-1β and the specific TLR2 and TLR4 ligands Pam_3-Cys-Ser-$(Lys)_4$ (Pam_3Cys) and LPS, respectively (Fig 2.1.2C and data not shown). By contrast, TLR6 and TLR4 cell-surface expression was readily detectable by flow cytometry in resting PBMC used as controls (Fig 2.1.2B). TLR2 expression was also consistently detected in HPMC by immunocytochemistry (Fig 2.1.2D), although expression levels showed a substantial inter-subject variation, as indicated by the flow cytometric analysis of individual HPMC isolates obtained from different donors (Fig 2.1.2E).

The phenomenon of 'LPS tolerance' is associated with loss of LPS responsiveness, partly as a consequence of TLR4 down-modulation following persistent exposure to endotoxin challenge (Nomura et al., 2000). Thus, to test the possibility that LPS tolerance might have been responsible for the lack of detection of TLR4 in cultured HPMC, cells were tested by flow cytometry for TLR4 expression immediately following their isolation by tryptic digestion of normal omental tissue, instead of after 1-2 weeks in cell culture. HPMC displayed high cell surface expression of the HPMC-specific marker CA125 (Visser et al., 1995a) as expected. TLR2 expression was also detectable, as observed previously, but TLR4 was not detectable on the cell surface of HPMC primary isolates (Fig 2.1.3).

2.1.2 HPMC responses to TLR2, TLR4 and TLR5 ligands

To characterise HPMC responses to Gram-positive and Gram–negative bacteria, HPMC were treated with known ligands of TLR2/1 (Pam_3Cys, PGN) and TLR4 (LPS) and a well-characterised cell-free supernatant derived from a clinical isolate of *Staphylococcus epidermidis* termed SES, which has been previously used to investigate the regulation of *Staphylococcal spp.*-induced inflammation *in vivo* (Hurst et al., 2001; McLoughlin et al., 2003). The production of the CXCL8 and CCL2 chemokines and inflammatory cytokines TNFα and IL-6 was assessed. SES and the synthetic TLR2 ligand Pam_3Cys induced a dose-dependent increase in CXCL8, IL-6, CCL2 and TNFα levels (Fig 2.1.4). HPMC were also found to respond to PGN (Fig 2.1.4). The TLR4 ligand LPS had no effect on CXCL8, IL-6, CCL2 or TNFα secretion by HPMC (Fig 2.1.4), even in the presence of LPS concentrations as high as 5 μg/ml (Fig 2.1.5A). As mentioned previously, cells may lose responsiveness to LPS, but certain genes have been reported to be resistant to LPS tolerance (Foster et al., 2007). The chemokine CCL5 belongs to this class of 'non-toleriseable' gene products, but its levels were not up-regulated following stimulation of HPMC by LPS at any dose tested (Fig 2.1.5B).

Stimulation with the diacyl lipopeptide Pam_2Cys (MALP-2 analogue, a TRL2/TLR6 ligand), also triggered a dose-dependent increase in CXCL8 secretion (Fig 2.1.6A), despite the undetectable cell-surface expression of TLR6 on HPMC. Zymosan is another TLR2/6 ligand, however HPMC did not respond to zymosan stimulation (Fig 2.1.6B). This result might be explained by a lack of

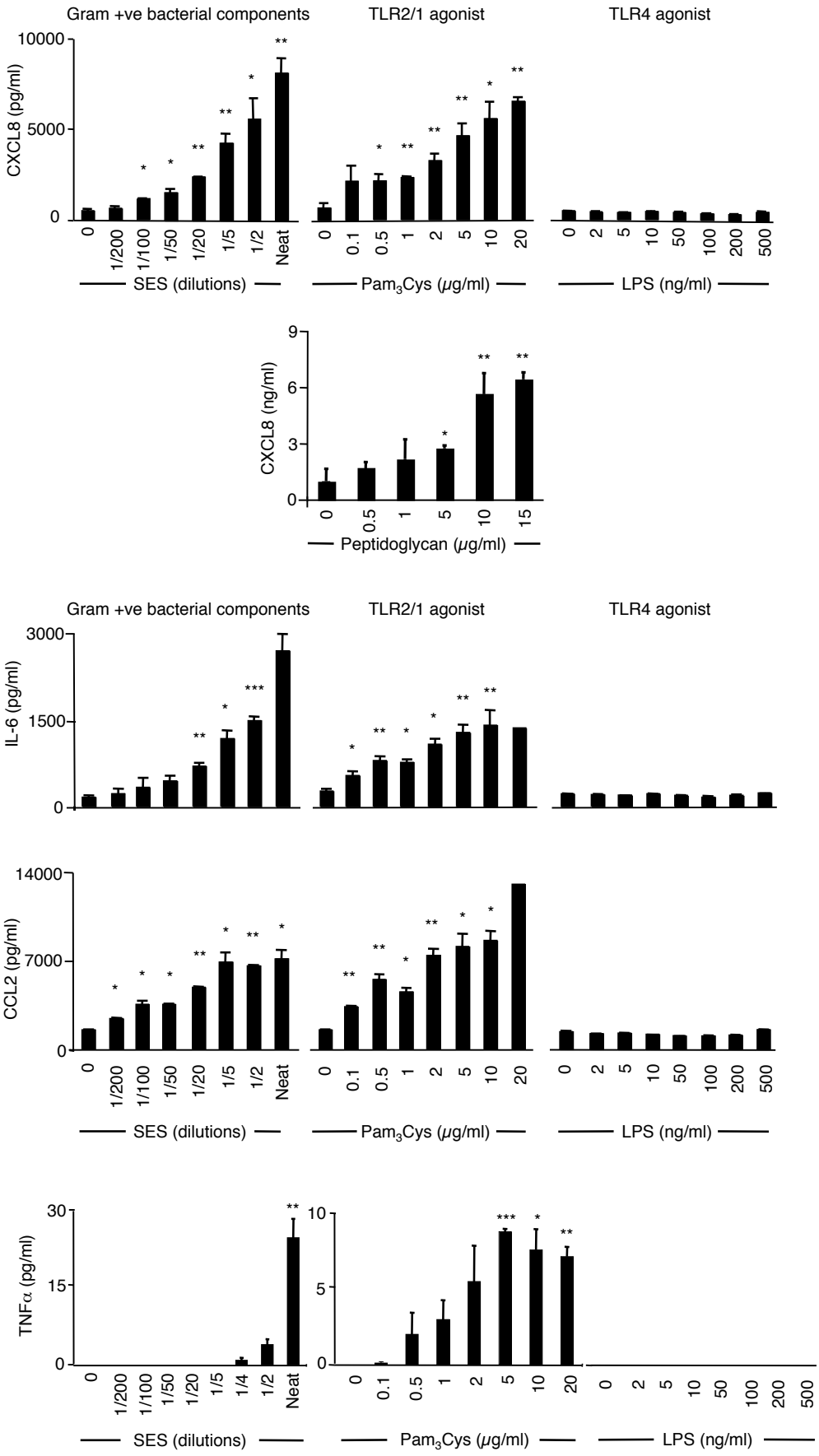

Figure 2.1.4. Response of HPMC to bacterial-derived TLR2 and TLR4 agonists.
HPMC were stimulated for 24h with the indicated serial dilutions of SES and concentrations of Pam_3Cys, LPS or Peptidoglycan. Following incubation, CXCL8, IL-6, CCL2 and TNFα levels in the cell-free culture supernatants were quantified by ELISA. TNFα was undetectable in the supernatants of cells incubated with LPS. Data shown are results (±SD) representative of at least three experiments performed using primary cells from different donors (*, $p < 0.05$; **, $p < 0.01$; ***, $p < 0.001$; non-stimulated *vs*. stimulated cells).

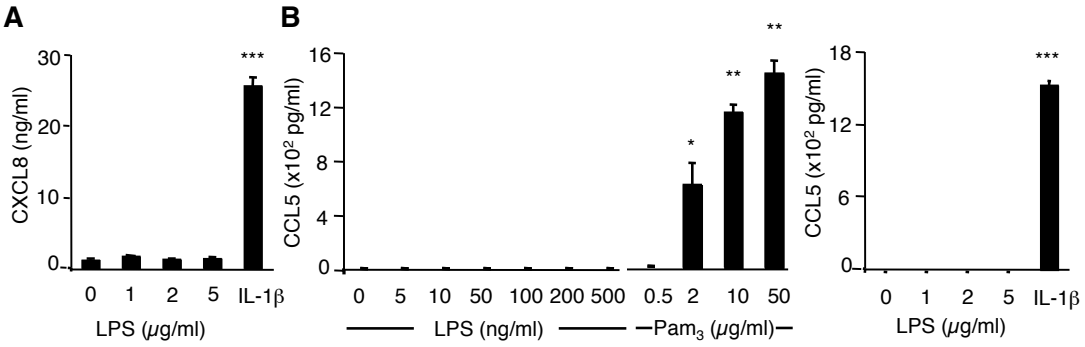

Figure 2.1.5. Response of HPMC to LPS.
(A and **B)** HPMC were treated with the indicated concentrations of LPS. Pam_3Cys and IL-1β (100 pg/ml) were used as positive controls. After 24h incubation, CXCL8 and CCL5 levels in the cell-free culture supernatants were quantified by ELISA. Results (±SD) shown are of one experiment representative of four experiments performed using primary cells from different donors (* *p,* < 0.05; ** *p,* < 0.01; ***, *p* < 0.001 stimulated *vs.* non-stimulated cells).

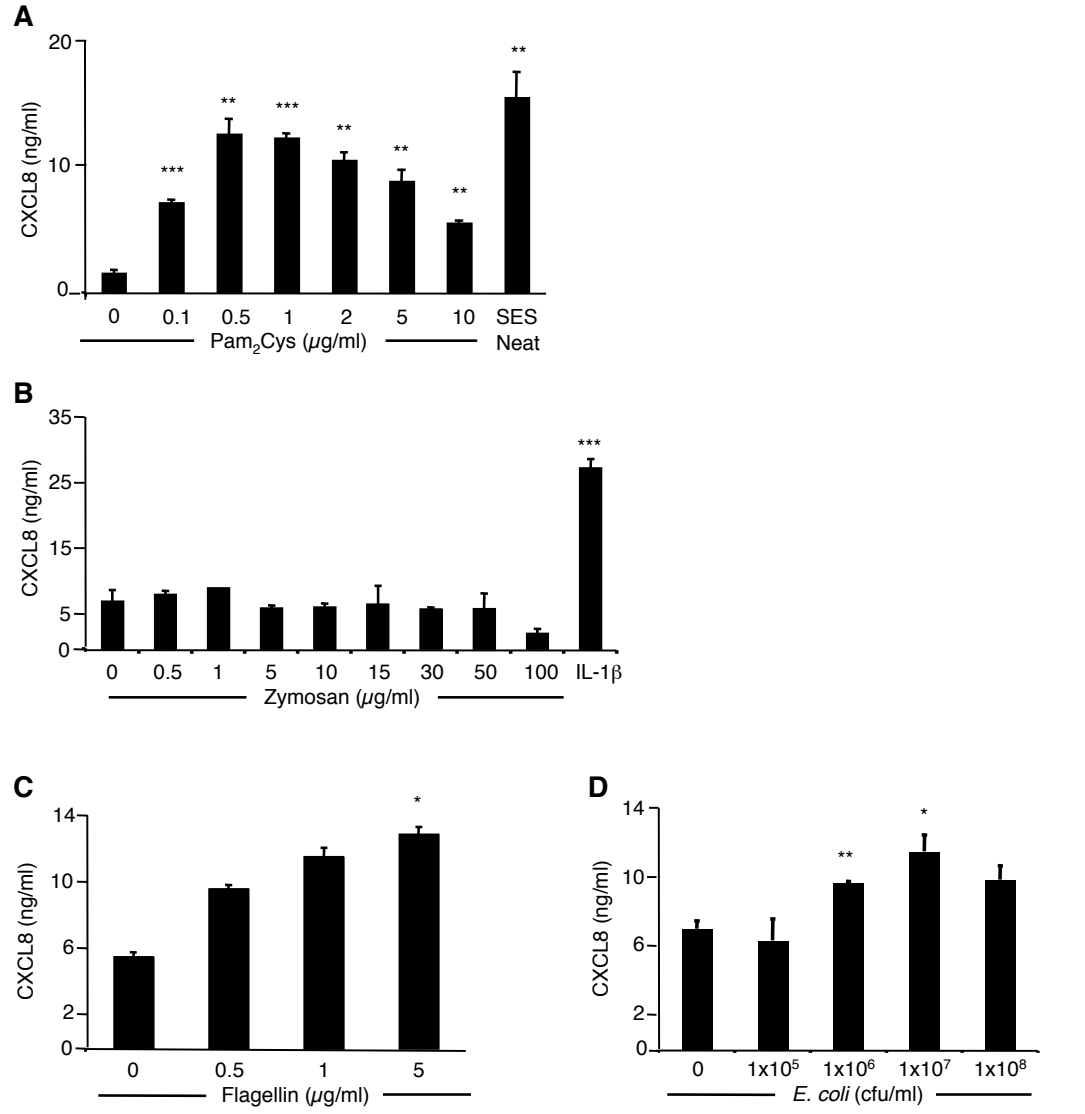

Figure 2.1.6. Response of HPMC to TLR agonists.
(A-D) HPMC were stimulated for 24h with the indicated concentrations of Pam_2Cys (TLR2/6 ligand), neat SES (with 0.1% FCS), Zymosan (TLR2/6 ligand), IL-1β (100 pg/ml), Flagellin (TLR5 ligand) or heat-killed *E. coli*. Following incubation, CXCL8 levels in the cell-free culture supernatants were quantified by ELISA. Data presented are results (±SD) representative of four (Pam_2Cys, SES), five (Zymosan, IL-1β), or two (Flagellin, *E. coli*) experiments performed using primary cells from different donors (*, *p* < 0.05; **, *p* < 0.01; ***, *p* < 0.001; non-stimulated *vs.* stimulated cells).

Dectin-1 expression in HPMC, the co-receptor required for zymosan-mediated responses in concert with TLR2/6 (Ikeda et al., 2008), and/or the extremely low levels of TLR6 expression in these cells, but this would require further investigation.

The data previously presented demonstrated that although HPMC responded to Gram-positive bacterial ligands through TLR2, they were unable to respond to the TLR4 agonist and main component of the Gram-negative cell wall, LPS (Fig 2.1.4 and 2.1.5), as they lack TLR4 expression (mRNA and protein). qRT-PCR data suggested low expression levels of TLR5 (Fig 2.1.1), which is capable of recognising flagellin, a protein component of bacterial flagellum, commonly found in many Gram-negative bacteria (Hayashi et al., 2001). Therefore, the capacity of HPMC to respond to flagellin was tested. Flagellin induced a dose-dependent increase in CXCL8 secretion (Fig 2.1.6C), indicating that HPMC can mediate a selective response to Gram-negative bacteria through TLR5 recognition of flagellin, but not through recognition of LPS. The ability of mesothelial cells to recognise Gram-negative bacteria was later confirmed when HPMC were stimulated with heat-killed *E. coli* bacteria and showed a dose-dependent (moderate) release of CXCL8 (Fig 2.1.6D).

NF-κB activation downstream of TLR signalling was measured by electrophoretic mobility shift assay (EMSA) in nuclear extracts prepared from HPMC that had been treated with LPS, Pam_3Cys, SES or Pam_2Cys for different time intervals. The results of NF-κB activation experiments were consistent with the selective response of HPMC to TLR ligands described previously. NF-κB activation was sustained over a 3-4h period following stimulation with Pam_3Cys, SES or Pam_2Cys (Fig 2.1.7A). LPS stimulation however did not up-regulate NF-κB DNA-binding signal above that observed for the control growth-arrested non-stimulated cells (Fig 2.1.7A, top panel). To examine the NF-κB subunits activated by TLR2 signalling in HPMC, a 'supershift' EMSA analysis was performed using antibodies directed against specific NF-κB family members. This analysis identified NF-κB DNA-binding complexes consisting of the p50 and p65 subunits for Pam_3Cys, SES and Pam_2Cys stimulations (Fig 2.1.7B).

2.1.3 HPMC responses to TLR3 and TLR7/8 ligands

To examine HPMC responses to viruses, HPMC were treated with known ligands for TLR3 (Poly I:C, synthetic mimetic of dsRNA) and TLR7/8 (Imiquimod, synthetic mimetic of ssRNA), and the production of the chemokine CXCL8 was assessed. Poly I:C induced a response as strong as that to IL-1β, used as a positive control (Fig 2.1.8A). By contrast, imiquimod failed to induce CXCL8 release (Fig 2.1.8B), consistent with the lack of TLR7/8 mRNA expression in HPMC observed by using qRT-PCR (Fig 2.1.1).

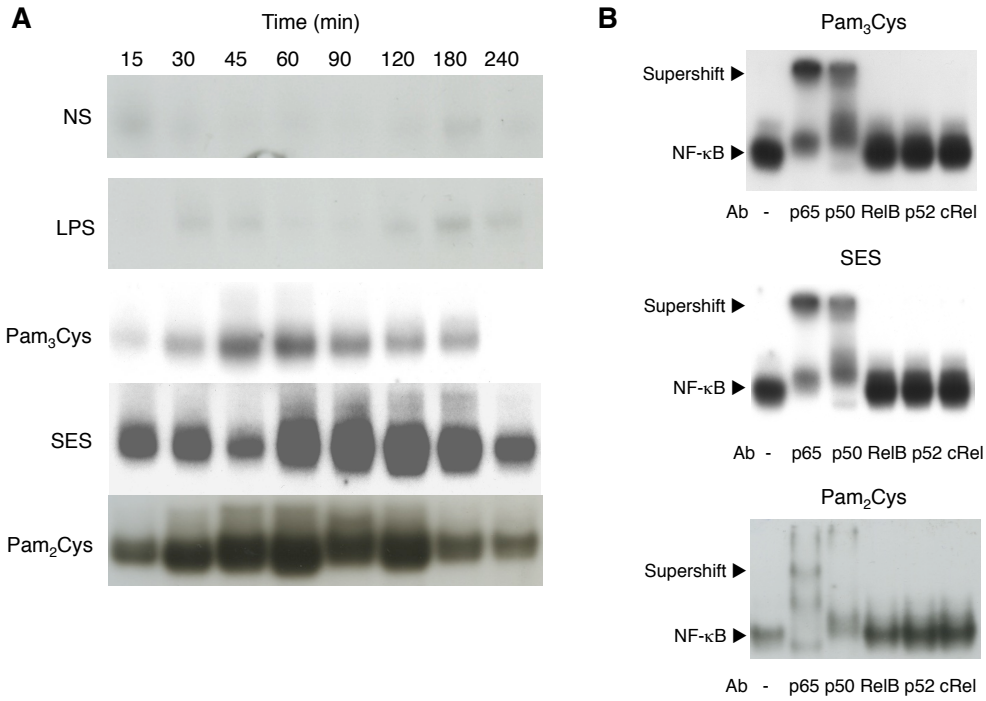

Figure 2.1.7. Activation of NF-κB in HPMC by TLR ligands.
(A) HPMC were stimulated for up to 4h with LPS (500 ng/ml), Pam_3Cys (2 μg/ml), SES (neat), Pam_2Cys (1 μg/ml) or left untreated (NS). At the indicated time points, nuclear extracts were prepared and NF-κB activation was analysed by EMSA, as described under Materials and Methods. Data presented is a representative result of three experiments performed using primary cells from different donors. **(B)** The composition of the NF-κB DNA binding complexes in HPMC stimulated with Pam_3Cys, SES or Pam_2Cys was determined by supershift EMSA analysis of nuclear extracts by using specific antibodies for the p65, p50, Rel-B, p52 and c-Rel subunits of NF-κB. Control samples without the addition of antibody are shown, and 'supershifted' complexes are indicated. Data presented is a representative result of three experiments performed using primary cells from different donors.

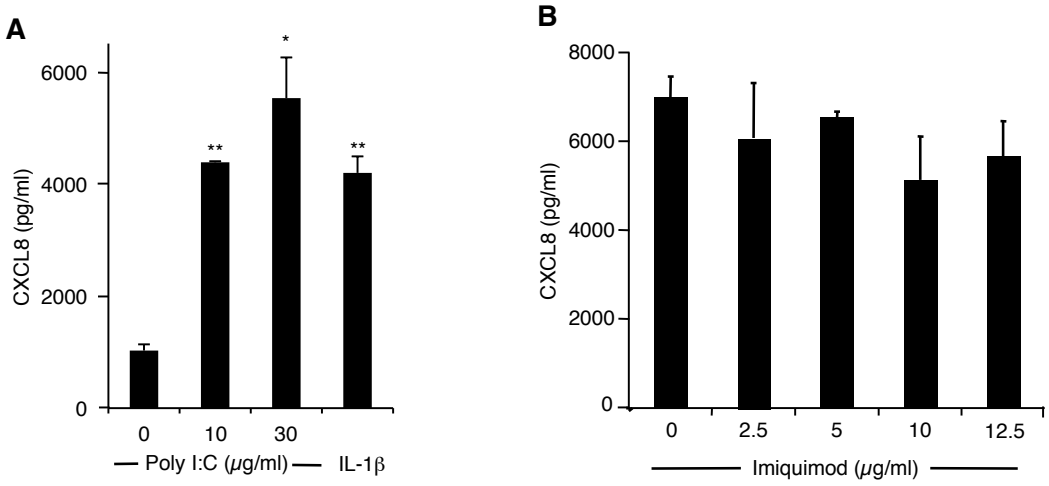

Figure 2.1.8. Response of HPMC to viral TLR agonists.
(A and **B)** HPMC were cultured for 24h in the presence of the indicated concentrations of poly I:C (TLR3 agonist) or Imiquimod (TLR7/8 agonist). Following incubation, CXCL8 levels in the cell-free culture supernatants were quantified by ELISA. Data presented are results (±SD) representative of two independent experiments performed using primary cells from different donors (*, $p < 0.05$; **, $p < 0.01$ non-stimulated *vs.* stimulated cells).

2.1.4 Further evaluation of HPMC responses to SES

Given the clinical relevance of the SES preparation in the context of *Staphylococcal spp.*-induced peritoneal inflammation in PD patients, the mechanism used by SES to stimulate mesothelial cells was investigated further. HEK293 cells stably transfected with either TLR2 (HEK-TLR2) or mock-transfected with a plasmid control (HEK-pDR2) were used. No TLR2 was detectable in the mock-transfected cells (Fig 2.1.9A, left panel), consistent with the well-documented lack of constitutive expression of TLR2 (and TLR4) in these cells (Erridge et al., 2007). By contrast, TLR2 was found highly expressed in HEK-TLR2 cell transfectants (Fig 2.1.9A, right panel and 2.1.9B). The mock-transfected cells did not respond to SES stimulation at any dose tested (Fig 2.1.9C). The presence of serum, added as a source of sCD14 (HEK293 cells do not express this TLR co-receptor), had no effect on the response of the mock-transfected cells (Fig 2.1.9C).

The TLR2-transfected cells responded to SES stimulation in a dose-dependent manner (Fig 2.1.9C), which suggested that SES stimulation of HPMC is mediated at least in part by TLR2. The response of the TLR2-transfected cell line was increased in the presence of serum, suggesting that one or several serum components are involved in SES-induced TLR2 signalling (Fig 2.1.9C). An NF-κB reporter assay was used to further confirm the involvement of TLR2 in SES signalling. Whereas HEK-TLR2 cells did not show any NF-κB reporter activity in the absence of SES, regardless of the presence of serum, all SES concentrations tested triggered a 7-fold increase in NF-κB activation (Fig 2.1.10A). In contrast, HEK cells transfected with TLR4 and its cofactor MD2 (HEK-TLR4/MD2), and expressing high levels of TLR4 (Fig 2.1.10A, inset), showed no increase in NF-κB reporter activity in the absence or presence of SES and serum (Fig 2.1.10A), indicating a lack of involvement of TLR4 in governing responsiveness to SES. The HEK-TLR4 cell transfectants showed however a dose-dependent response to LPS (Fig 2.1.10B).

SES may activate other pattern recognition pathways, in particular the NLRs NOD1 and NOD2. NOD1 and NOD2 recognise dipeptides derived from bacterial peptidoglycan (NOD1, Gram-negative and several Gram-positive bacteria; NOD2, all Gram-negative and Gram-positive bacteria) (Inohara et al., 2001; Kawai and Akira, 2009). An analysis of HPMC responses to NOD1 and NOD2 specific agonists (D-glutamyl-meso-diaminopimelic acid/iE-DAP and muramyl dipeptide/MDP, respectively) revealed a modest induction of CXCL8 in response to iE-DAP and no induction or a slight inhibition in response to MDP (Fig 2.1.11A and B). These results are similar to the findings of Park et al. in murine mesothelial cells, which identified responses to NOD1, but not to NOD2 (Park et al., 2007).

2.1.5 Examination of the involvement of CD14 in HPMC responses to SES

In order to test whether CD14 was required for TLR2-mediated responses to SES in HPMC, first, the cell-surface expression of CD14 was analysed by flow cytometry. No cell-surface

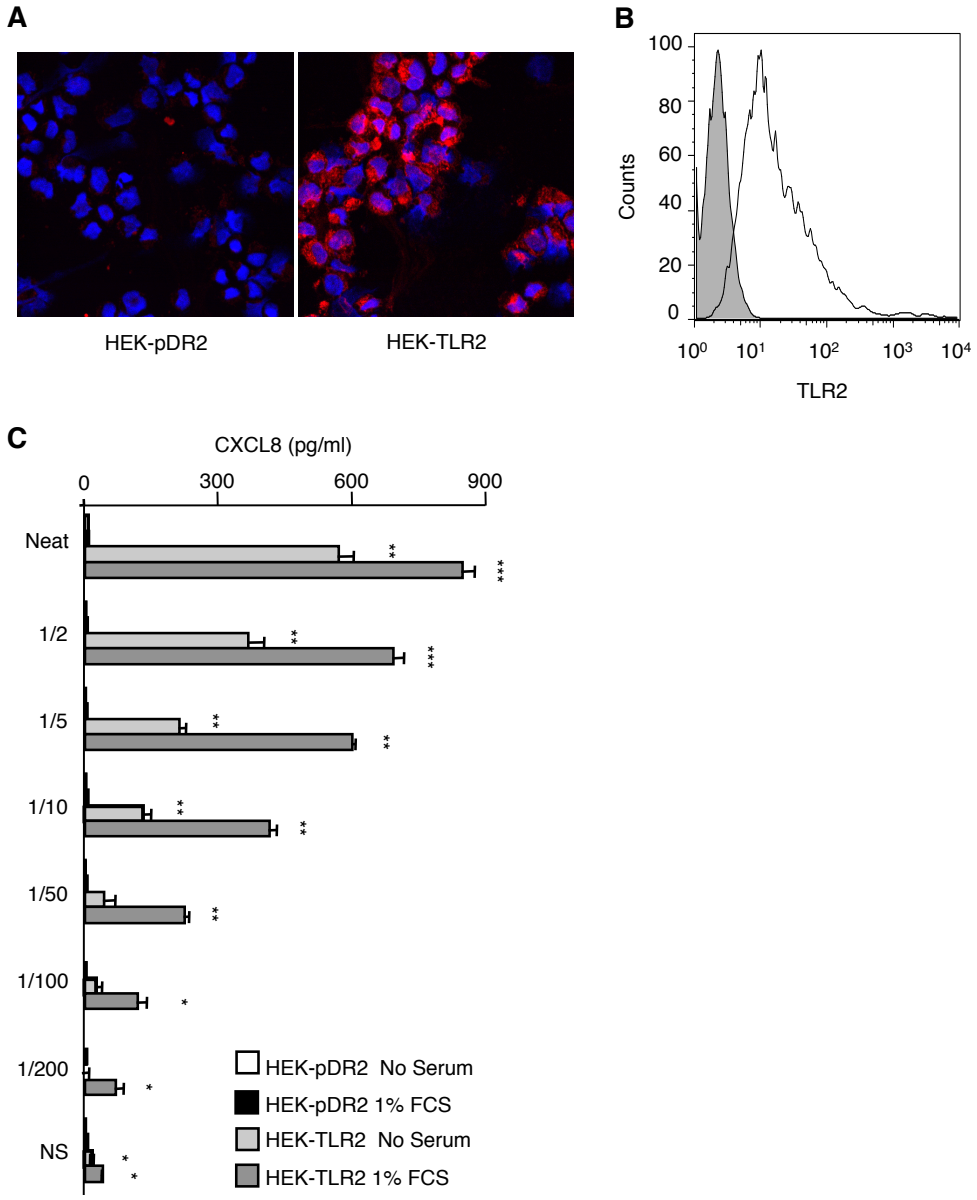

Figure 2.1.9. TLR2 and TLR4 expression by HEK cell transfectants.
(A) TLR2 expression detected by immunocytochemistry using the TLR2.5 mAb in HEK293 cells stably transfected with a TLR2 expression vector (HEK-TLR2). HEK293 cells transfected with the empty plasmid vector (HEK-pDR2) were used to confirm the specificity of the staining. **(B)** Fluorescence profile of TLR2 expression in the HEK-TLR2 cell transfectants obtained by staining with the PE-conjugated anti-TLR2 mAb TLR2.1, or its isotype-matched control IgG (shaded histogram), and analysis by flow cytometry. **(C)** HEK-pDR2 and HEK-TLR2 cell transfectants were stimulated for 15h with the indicated serial dilutions of SES in the presence or absence of 1% FCS. CXCL8 levels in the cell-free culture supernatants were quantified by ELISA. Data presented is a representative result of three experiments (±SD) performed in triplicate (*, $p < 0.05$; **, $p < 0.01$; ***, $p < 0.001$ HEK-pDR2 no serum *vs.* HEK-TLR2 no serum, and HEK-TLR2 no serum *vs* HEK-TLR2 1% FCS).

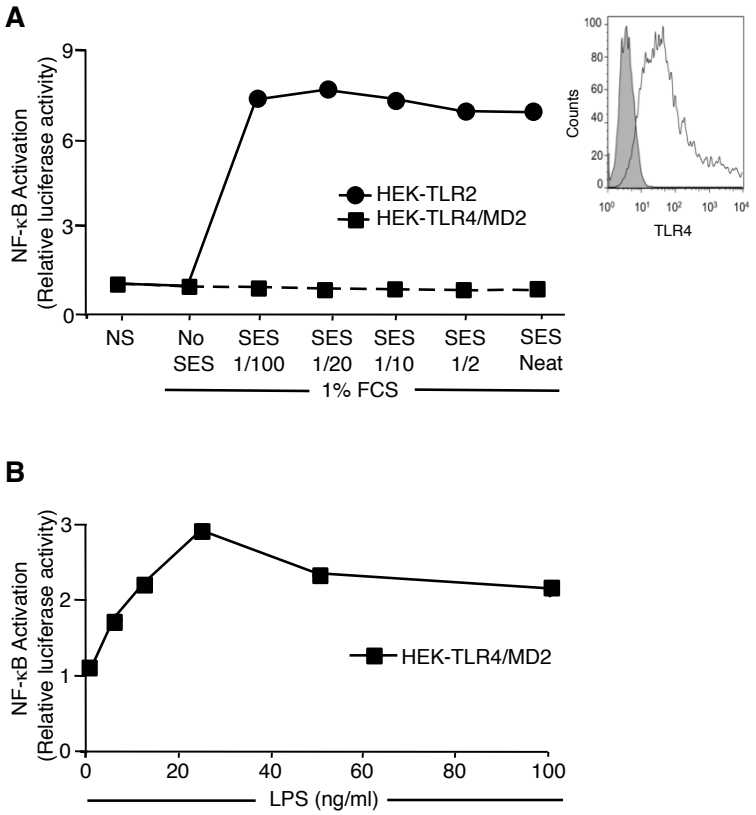

Figure 2.1.10. NF-κB acivationin HEK-TLR2 and HEK-TLR4/MD2 cell transfectants.
(A and **B)** HEK-TLR2 and HEK-TLR4/MD2 stable cell transfectants were transiently transfected with an NF-κB luciferase Firefly reporter and constitutive Renilla luciferase vectors and after 48h in culture they were stimulated (16h) with the indicated serial dilutions of SES **(A)** and concentrations of LPS in the presence of sCD14 and LBP (0.5 μg/ml and 0.1 μg/ml respectively) **(B)**. NS, non-stimulated cells. Dual luciferase activity was subsequently assayed and the Firefly reporter results normalised against the Renilla signal obtained as the fold-change above the control. **(A inset)** Fluorescence profile of TLR4 expression in the HEK-TLR4 cell transfectants obtained by staining with the non-conjugated anti-TLR4 mAb HTA125, or its isotype-matched control IgG (shaded histogram), followed by incubation with a secondary PE-conjugated anti-mouse Ab and analysis by flow cytometry. Result are representative of three experiments.

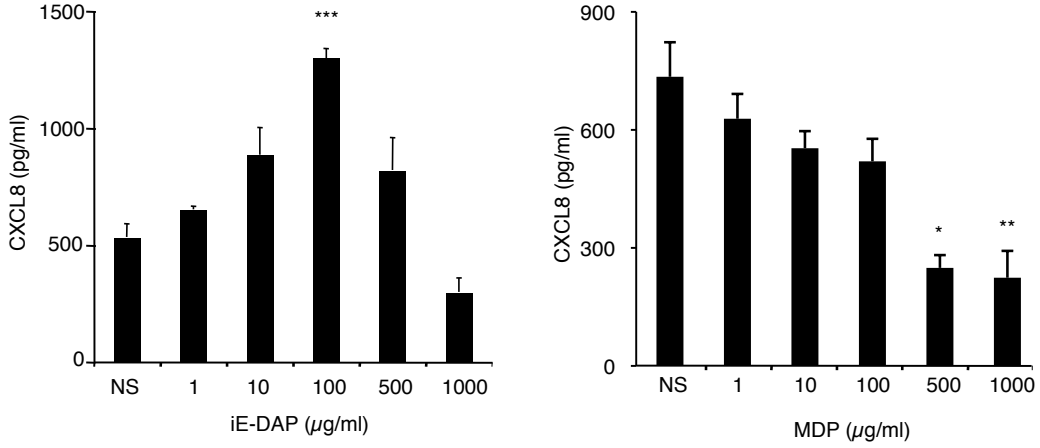

Figure 2.1.11. Response of HPMC to NOD agonists.
(A and **B)** HPMC were cultured for 24h in the presence of the indicated concentrations of D-glutamyl-meso-diaminopimelic acid (iE-DAP, Nod1 ligand) or muramyl dipeptide (MDP, Nod2 ligand). Following incubation, CXCL8 levels in the cell-free culture supernatants were quantified by ELISA. NS, non-stimulated cells. Data presented are results (±SD) representative of two independent experiments (*, $p < 0.05$; **, $p < 0.01$; ***, $p < 0.001$ non-stimulated *vs.* stimulated cells).

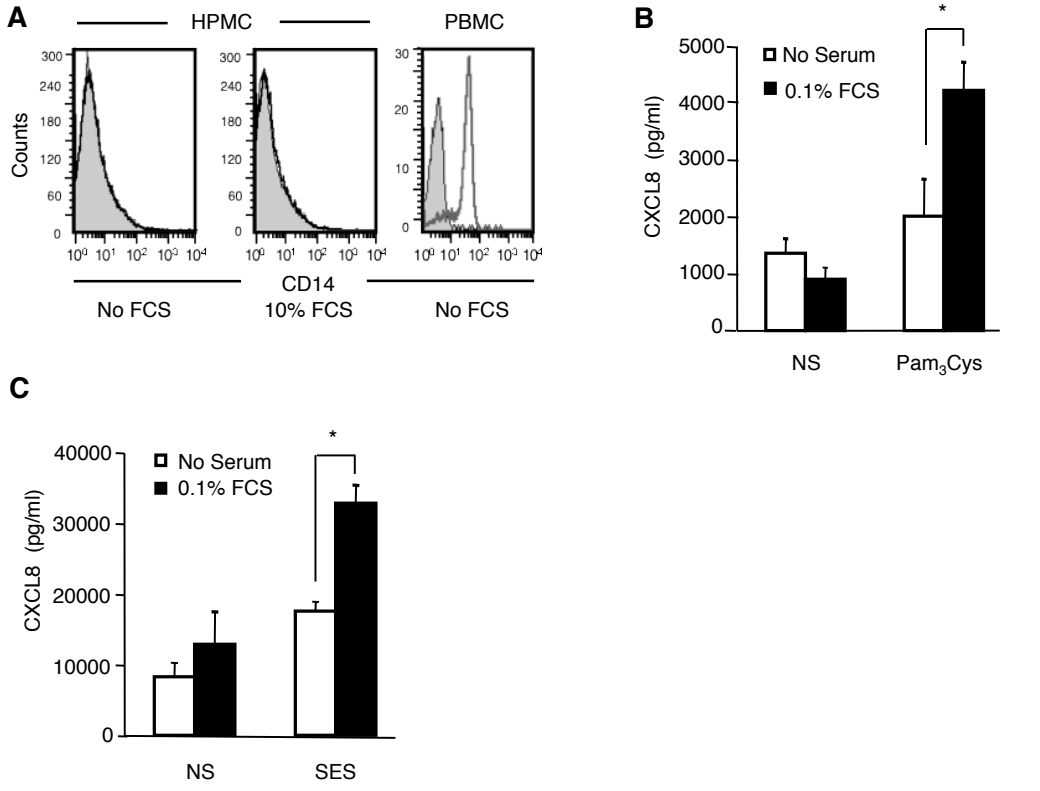

Figure 2.1.12. Evaluation of the role of serum and CD14 in HPMC and leukocyte stimulation.
(A) Flow cytometric analysis of HPMC immunostained with a PE-conjugated CD14 mAb in the presence or absence of 10% fœtal calf serum (FCS). Human PBMC were used as a positive control of CD14 expression; isotype-matched control antibody staining is shown as shaded histograms. Data presented are results representative of six experiments performed with primary cells derived from separate donors. **(B** and **C)** HPMC were stimulated for 24h with Pam_3Cys (2 μg/ml, **B**) or SES (neat, **C**) in the presence or absence of 0.1% FCS. NS, non-stimulated cells. Following incubation, CXCL8 levels in the cell-free culture supernatants were quantified by ELISA. NS, non-stimulated cells. Data presented are representative of three experiments performed in triplicate (±SD) with primary cells derived from three different donors (*, $p < 0.05$; no serum *vs*. 0.1% serum).

expression of CD14 was detected in HPMC regardless of serum, unlike PBMC, which expressed high levels of cell-surface CD14 (Fig 2.1.12A). This finding implied that if TLR2 requires CD14 for efficient signalling in HPMC, the soluble form of the TLR co-receptor (sCD14) may be involved. CXCL8 production was therefore measured in HPMC treated with Pam_3Cys and SES with or without serum, as a source of sCD14. Pam_3Cys and SES triggered a significantly higher response in the presence of serum (Fig 2.1.12B and C). To investigate whether serum sCD14 was involved in enhancing the TLR2-mediated responses, stimulation experiments in the presence of serum using an anti-CD14 blocking antibody were performed. The anti-CD14 blocking antibody had no effect on SES-induced CXCL8 in HPMC (Fig 2.1.13A), while it significantly reduced CXCL8 production induced by both SES and LPS in PBMC (Fig 2.1.13B). To directly investigate the role of sCD14 in the HPMC responses to SES, the cells were stimulated in the presence or absence of purified human natural sCD14. As shown in Fig 2.1.13C, SES-induced CXCL8 secretion was not altered by the addition of sCD14. Therefore, these results indicated that CD14 is required for fully efficient SES-induced responses of PBMC, but not for those of HPMC. These observations however do not exclude the possibility that serum component(s) other than sCD14 may play a role in enhancing SES-induced signalling in HPMC.

2.1.6 Evaluation of the effect of inflammatory cytokines and TLR ligands on HPMC TLR2 expression

In view of the involvement of TLR2 in HPMC responses to Gram-positive bacteria-derived components demonstrated previously, and the capacity of this TLR to recognise a wide range of PAMPS and DAMPs, the modulation of TLR2 expression in HPMC was studied next. TLR2 expression can be modulated in a diversity of cell types following activation with various stimuli, in particular cytokines and microbial ligands (Faure et al., 2001; Homma et al., 2004). Here, HPMC TLR2 cell-surface expression was examined by flow cytometry following treatment with different cytokines and the TLR2 ligand Pam_3Cys. An up-modulation of TLR2 expression was detected following treatment for 1h or 30 min with IL-1β or IFNγ, respectively (Fig 2.1.14A and B), but not with Pam_3Cys or TNFα at any time point tested (Fig 2.1.14C and D). To further characterise TLR2 modulation, experiments were subsequently carried out in which Tlr2 mRNA expression in HPMC was analysed by qRT-PCR. Tlr2 mRNA expression was significantly up-regulated upon stimulation (3h) with the pro-inflammatory cytokine IL-1β and the TLR2 ligand Pam_3Cys (Fig 2.1.15A), as previously described for epithelial cells (Sakai et al., 2004) and mouse pleural mesothelial cells (Hussain et al., 2008). The up-regulation of TLR2 protein upon stimulation with Pam_3Cys was confirmed by immunocytochemistry (Fig 2.1.15B). By contrast, the pro-inflammatory cytokine TNFα and the TLR4 ligand LPS did not show any significant effect on TLR2 expression (Fig 2.1.15A). A similar examination of Tlr1 and Tlr6 mRNA expression following stimulation with a number of cytokines and TLR ligands failed to show any significant major changes compared to the level of expression of non-stimulated cells (Fig

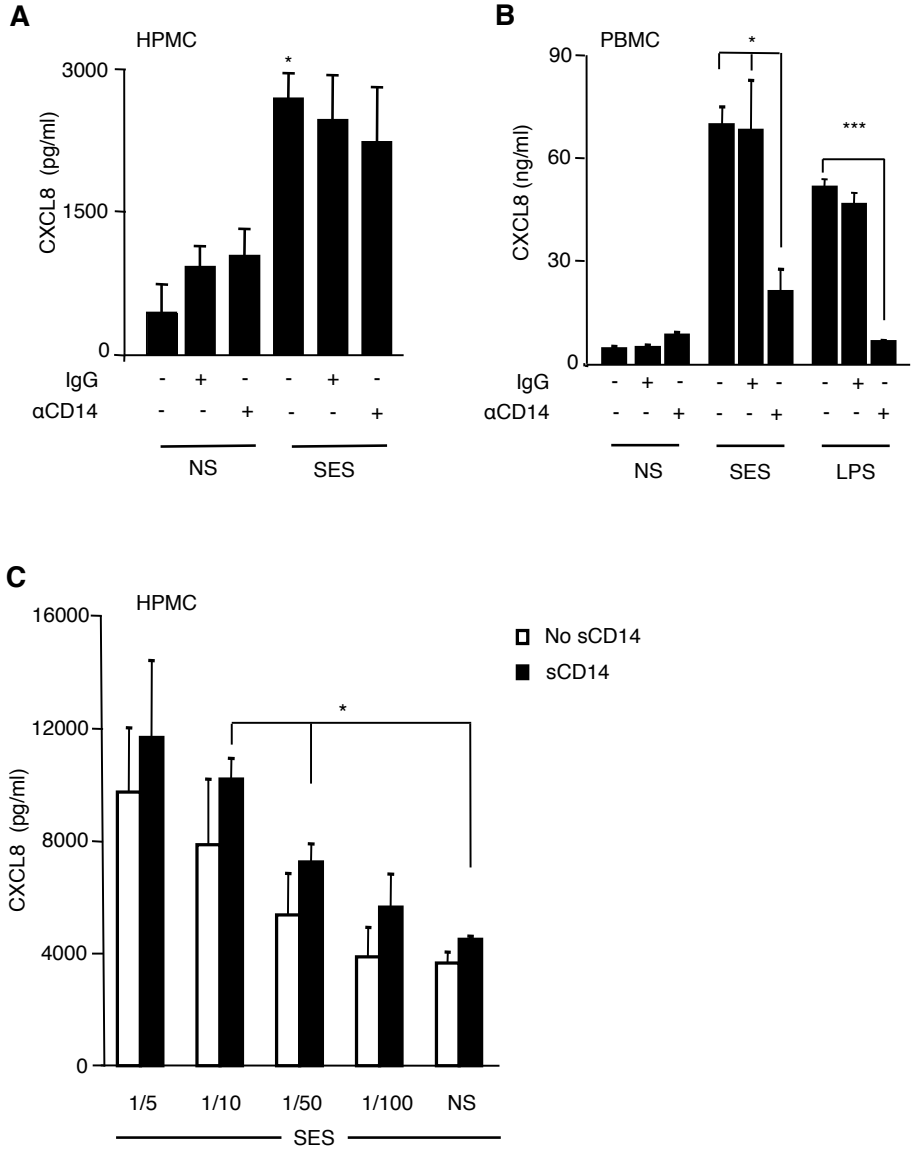

Figure 2.1.13. Evaluation of the role of CD14 as a TLR co-receptor in HPMC stimulation.
(A) HPMC were stimulated for 24h in medium containing 0.1% FCS and SES (1/10 dilution) in the presence or absence of an anti-CD14 blocking mAb (10 µg/ml). CXCL8 levels were quantified in the cell-free culture supernatants by ELISA. NS, non-stimulated cells. Shown are results (±SD) representative of three experiments performed with HPMC derived from different donors (*, $p < 0.05$ non-stimulated *vs.* stimulated cells). **(B)** PBMC were cultured overnight in medium containing 0.5% human AB serum, LPS (50ng/ml) or SES (1/80 dilution) in the presence or absence of an anti-CD14 blocking mAb (10 µg/ml). CXCL8 levels were quantified in the cell-free culture supernatants by ELISA. NS, non-stimulated cells. Data presented are representative of three experiments (±SD) performed with PBMC derived from three different donors (*, $p < 0.05$; ***, $p < 0.001$; stimulated cells in the absence *vs.* presence of anti-CD14 blocking mAb). **(C)** HPMC were stimulated for 24h with the indicated dilutions of SES in medium without serum, supplemented or not with purified human natural sCD14 (500 ng/ml). CXCL8 levels were quantified in the cell-free culture supernatants by ELISA. Data presented are representative of three experiments performed in triplicate (±SD) with HPMC derived from three different donors (*, $p < 0.05$ non-stimulated *vs.* stimulated cells).

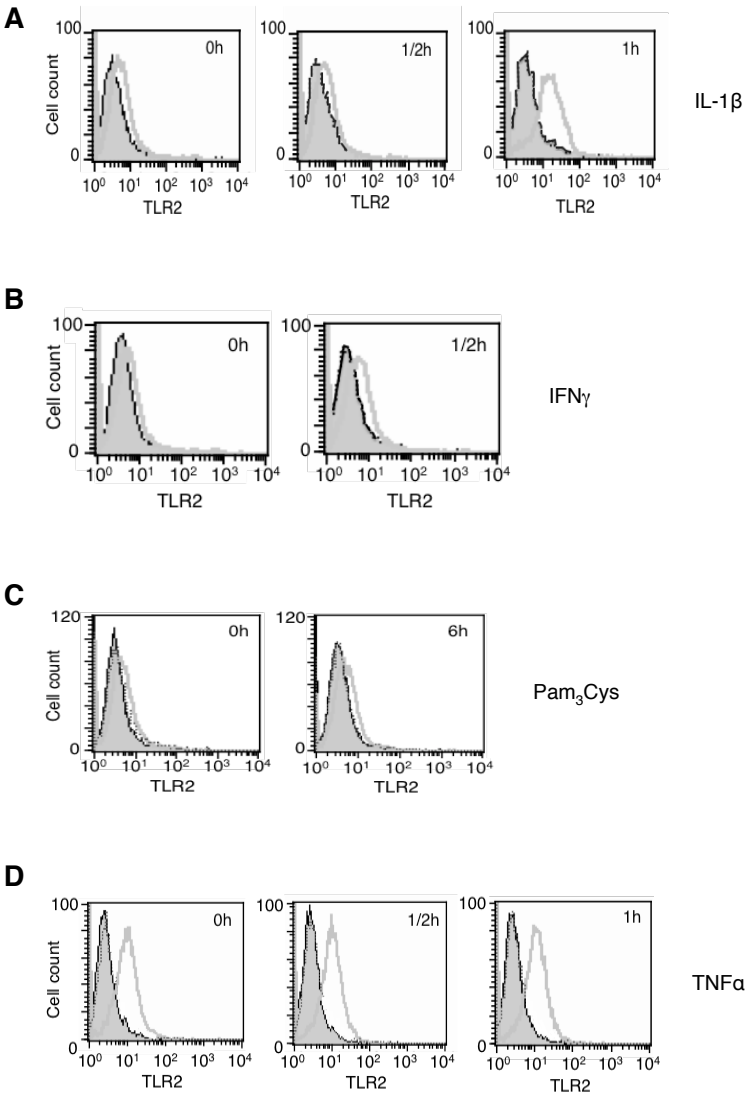

Figure 2.1.14. Modulation of TLR2 cell-surface expression on HPMC by pro-inflammatory stimuli.
The cell-surface expression of TLR2 in HPMC was assessed by flow cytometry following cell stimulation with Pam_3Cys (2 μg/ml), IL-1β (100 pg/ml), IFNγ (10 ng/ml) or TNFα (100 pg/ml) for the indicated times. Control profiles, which correspond to immunostaining with the isotype-matched control antibody are also shown (shaded plots). Data presented are representative of five experiments performed with HPMC derived from five different donors.

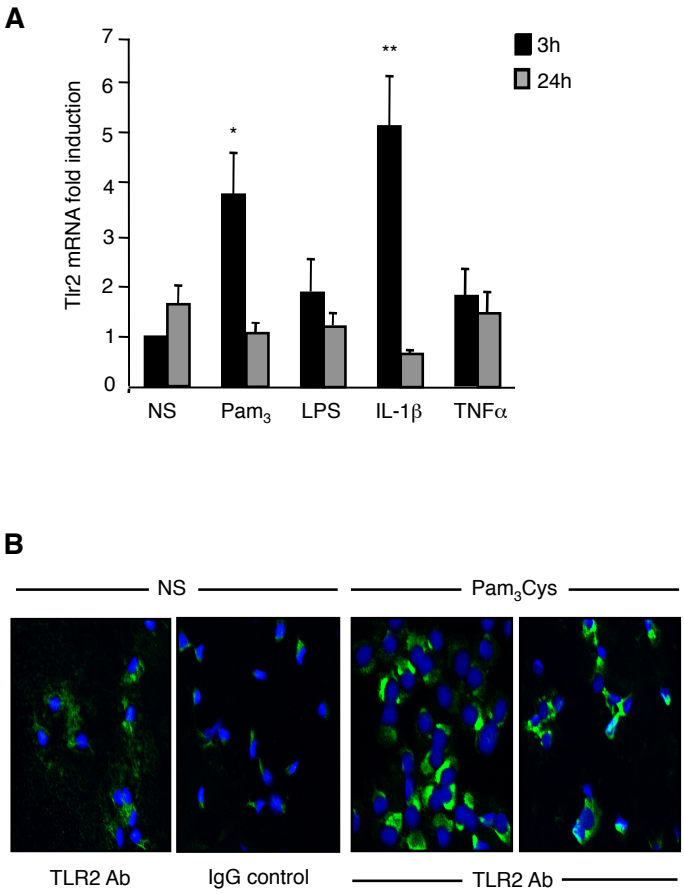

Figure 2.1.15. Analysis of the TLR2 modulation in HPMC by pro-inflammatory stimuli.
(A) Tlr2 mRNA expression assessed by qRT-PCR following stimulation of HPMC for 3h or 24h with Pam_3Cys (2 μg/ml), LPS (250 ng/ml), IL-1β (100 pg/ml) or TNFα (100 pg/ml); NS, non-stimulated cells. Fold inductions were determined as described under Materials and Methods. Data presented are representative of three experiments performed in triplicate (±SD) with primary cells derived from three different donors (*, $p < 0.05$; **, $p < 0.01$; stimulated *vs*. non-stimulated). **(B)** TLR2 expression in HPMC detected by immunocytochemistry using the TLR2.5 mAb following cell stimulation (2h) with Pam_3Cys (5 μg/ml). NS, non-stimulated cells. Control staining was carried out using an isotype-matched control antibody. Shown are HPMC staining results representative of two donors.

2.1.16A and B). Similarly, TLR4 mRNA expression did not show any significant change upon HPMC stimulation, and its basal level was very low (Fig 2.1.16C).

The IFNγ and TLR signalling pathways are known to interact to regulate macrophage function (Hu et al., 2006), and IFNγ has been demonstrated to up-regulate several TLR family's mRNAs, including Tlr2 (Faure et al., 2001; Homma et al., 2004). Given the crucial role played by IFNγ in regulating the immune response in the peritoneal cavity (McLoughlin et al., 2003; Robson et al., 2001), and its positive effect on HPMC TLR2 surface expression described previously (Fig 2.1.14C), its effect on HPMC Tlr2 expression was analysed in more detail by qRT-PCR. Additionally, the effect of SES on TLR2 mRNA was tested in parallel. HPMC stimulation with IFNγ over a 24h period showed a 7-fold increase in Tlr2 mRNA at the 6h time point, followed by a return to baseline levels by 12h (Fig 2.1.17A). A similar pattern, but with an earlier kinetics, was observed following stimulation with SES, with a peak (8-fold Tlr2 mRNA increase) at 3h followed by a drop by 6h and subsequent return to basal level of expression by 12h (Fig 2.1.17A). The effect of SES was studied further in a peritoneal model of inflammation that closely resembles the clinical situation (Hurst et al., 2001; McLoughlin et al., 2003) and complemented the *in vitro* observations. Biopsies of the parietal peritoneal membrane were taken at various time points following injection of SES into the peritoneal cavity of mice. qRT-PCR analysis of RNA extracted from the peritoneal membrane of one mouse showed a rapid and transient increase of Tlr2 mRNA expression (Fig 2.1.17B). A 3-fold increase in Tlr2 expression above the baseline level at 1h was observed, and followed by a down-regulation below the baseline level from 3h up to 12h.

2.1.7 Discussion

Repeated peritonitis, a feature of PD treatment, is predominantly caused by Gram-positive bacteria, especially *Staphylococcus* species (Szeto et al., 2005). However, Gram-negative bacterial infections also represent a significant problem and, overall, have a worse prognosis in terms of patient outcomes (Szeto and Chow, 2007). It is believed that host defences are compromised in PD patients as a result of exposure to dialysis solution, dilution of humoral factors, and alteration in the function of resident and recruited leukocytes (Devuyst et al., 2010; Topley and Williams, 1994). The initial peritoneal immune response, however, involves contributions not only from resident peritoneal leukocytes (Cailhier et al., 2005; Roberts et al., 2009), but also from the peritoneal mesothelial cells, lining the parietal and visceral peritoneum (Yung and Chan, 2009). Therefore, the expression of TLRs, critical mediators of initial immune responses, was examined in HPMC and the responses of these cells to bacterial products characterised.

The analysis of TLR expression by HPMC identified expression of a restricted subset of TLR family members (TLR1-6), which was in agreement with findings in mouse peritoneal mesothelial cells (Kato et al., 2004; Park et al., 2007). However, experiments examining the

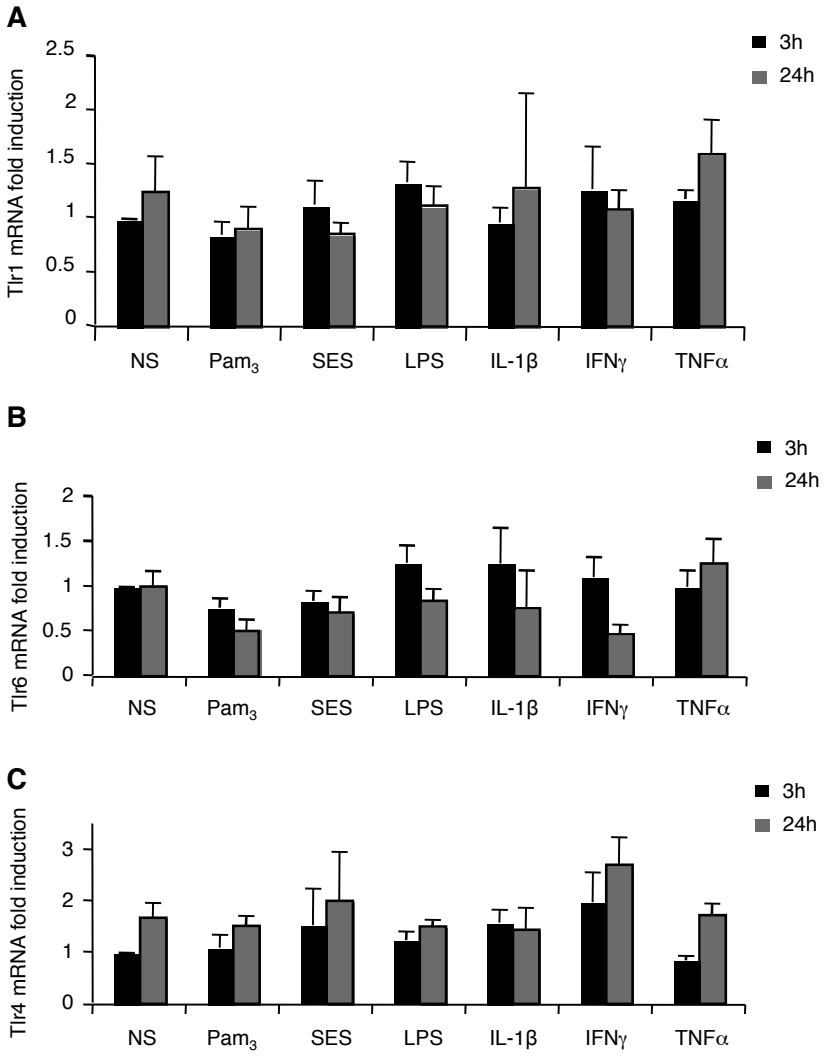

Figure 2.1.16. Modulation of HPMC TLR1/4/6 mRNA expression by pro-inflammatory cytokines and TLR ligands.
Tlr1 **(A)**, Tlr6 **(B)** and Tlr4 **(C)** mRNA expression was assessed by qRT-PCR following stimulation of HPMC for 3h or 24h with Pam_3Cys (2 μg/ml), SES (neat), LPS (250 ng/ml), IL-1β (100 pg/ml), IFNγ (10 ng/ml) or TNFα (100 pg/ml). NS, non-stimulated cells. Fold inductions were determined as described under Materials and Methods. Data presented are representative of four or five experiments (±SD) performed with primary cells derived from different donors.

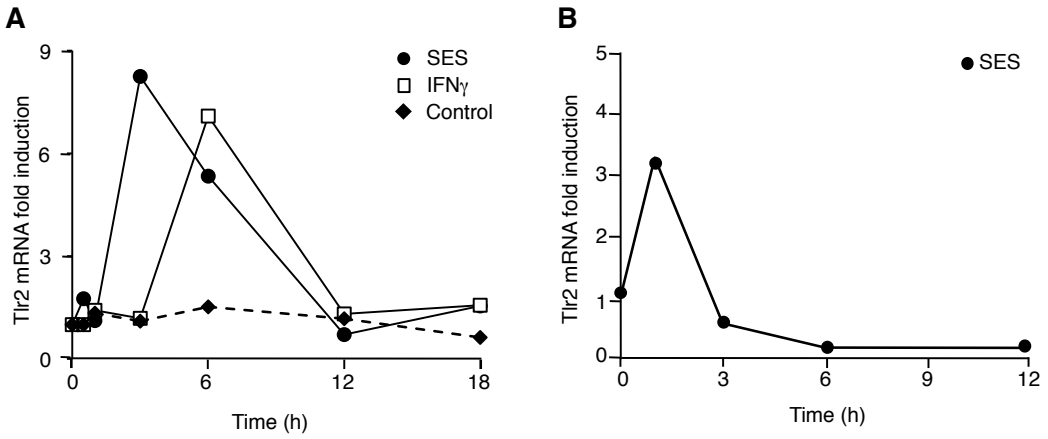

Figure 2.1.17. Kinetics of TLR2 mRNA expression *in vitro* and *in vivo*.
(A) Tlr2 mRNA expression in HPMC was assessed by qRT-PCR following cell culture for 24h in the presence or absence (Control) of SES (neat) or IFNγ (10 ng/ml). Data presented is a representative result of three experiments performed using primary cells derived from different donors. **(B)** The mouse was i.p. injected with neat SES, and at the indicated time points, Tlr2 mRNA expression levels were quantified by qRT-PCR following total RNA extraction from samples of parietal peritoneal membrane. Fold inductions were determined as described under Materials and Methods. The data represents the results of one experiment.

responsiveness of HPMC to bacterial TLR agonists revealed important differences between human and mice. Although HPMC, like mouse cells, responded to TLR2/1, TLR2/6 and TLR5 ligands, the human cells did not respond to the TLR4 agonist LPS, unlike mouse cells (Kato et al., 2004; Park et al., 2007). In the present study great care was taken (using differential sub-cultures) to ensure that HPMC cultures were not contaminated with peritoneal fibroblasts or residual resident macrophages that might contribute to apparent TLR4 expression (Lang and Topley, 1998; Topley et al., 1993a; Topley et al., 1993b; Topley et al., 1994).

Lack of TLR4 responsiveness may also be due to TLR4 down-regulation at the cell surface, which is known to contribute to 'LPS tolerance' (Nomura et al., 2000). Analysis of the response of freshly-isolated mesothelial cells and the absence of the tolerisation-resistant chemokine CCL5 (Foster et al., 2007), in the supernatants of LPS-treated HPMC appears to exclude tolerance as a reason for the TLR4 unresponsiveness of these cells. Poor responses to TLR4 ligands in airway smooth muscle cells were overcome by co-culture with PBMC in an IL-1β-dependent manner (Morris et al., 2005). Therefore, peritoneal macrophages may act as important sensors of Gram-negative bacterial infections, indirectly activating mesothelial cells (Devuyst et al., 2010; Topley et al., 1996a; Topley and Williams, 1994). The lack of mesothelial cell responsiveness to LPS may be beneficial to avoiding excessive inflammation. In this respect, intestinal epithelial cells lose their ability to respond to LPS after birth, a phenomenon interpreted as one way to avoid excessive inflammatory responses to the microbial flora (Lotz et al., 2006). Overall, the data suggest that HPMC respond to bacterial infections mainly through TLR2 (Gram-positive bacteria) and TLR5 (flagellated bacteria, predominantly Gram-negative) and possibly through NOD1 (PGN components), and to viral pathogens via TLR3 recognition of double-stranded RNA (Wornle et al., 2009). These data do not exclude the possibility that other pattern recognition receptor families may play a role in pathogen recognition by HPMC (Kawai and Akira, 2009).

TLR5 mediates recognition of flagellin, a flagellum component, present on many motile bacteria (Hayashi et al., 2001). Interestingly, TLR5 expression in the intestinal epithelium is limited to the basolateral surface, and is activated upon bacterial invasion of the gut wall (Gewirtz et al., 2001a; Gewirtz et al., 2001b). TLR5-deficient mice develop a TLR4-dependent spontaneous colitis, suggesting a critical role for TLR5 in maintaining the host-microflora balance within the gastro-intestinal tract (Vijay-Kumar et al., 2007). TLR5 expression on mesothelial cells may therefore be critical in sensing invasion of flagellated bacteria into the peritoneal cavity. Translocation of intestinal bacteria is a potential cause of infection in PD patients, along with access through the intra-peritoneal catheter (Szeto and Chow, 2007). Most flagellated bacteria found in PD-associated peritonitis patients are Gram-negative species, which are associated with poor outcomes (Szeto et al., 2005), hence the need for efficient, but not excessive, sensing of these pathogens.

TLR2, but not TLR4, expression was critical for the recognition of a *Staphylococcus epidermidis* (*S. epi.*)-derived cell-free supernatant (SES), which has been extensively utilised to model acute peritoneal inflammation (Hurst et al., 2001; McLoughlin et al., 2003). Similarly, Strunk *et al.* recently demonstrated that TLR2 is required for cellular responses to and clearance of *S. epi.* (Strunk et al., 2010). TLR2 is known to recognise microbial components by forming heterodimers with TLR1 and TLR6, depending on the ligand. The expression in HPMC of these two TLR2 partners for bacterial recognition and signalling was also investigated in this study. Of note, the response of HPMC to the TLR2/TLR6 ligand Pam_2Cys suggested that, although undetectable by flow cytometry, TLR6 is expressed and functional in HPMC, as suggested by the results of qRT-PCR and RT-PCR studies. TLR2 may also act in concert with co-receptors e.g. Dectin-1, CD36 or CD14, the latter a co-receptor for both TLR2 and TLR4 (Kawai and Akira, 2010; Yoshimura et al., 1999). CD14 blockade significantly reduced SES-induced responses in PBMC indicating that, in leukocytes, TLR-mediated responses are highly CD14-dependent. Notably, HPMC lacked cell surface expression of CD14, and although serum, a source of soluble CD14, had a significantly positive effect on SES-mediated responses of HPMC, purified sCD14 did not. These results indicate that (i) the requirement for CD14 in TLR2 activation is cell-specific and (ii) there may be other soluble cofactors in serum that co-operate with TLR2 signalling.

The modulation of TLR2 expression in HPMC in response to both TLR2-specific agonists and pro-inflammatory cytokines as well as in response to *in vitro* and *in vivo* SES stimulation was also studied. It is well documented through work with other cell types that both TLR and cytokine signalling may influence TLR expression and responsiveness (Faure et al., 2001; Homma et al., 2004; Hussain et al., 2008; Sakai et al., 2004; van Aubel et al., 2007). This is supported by the findings of the present study showing up-modulation of TLR2 expression by using a number of cytokines, TLR ligands and also the SES preparation. In particular, van Aubel *et al.* described a differential cross-talk between TLRs 2, 4 and 5 (van Aubel et al., 2007), and TLR4-induced IFNγ production leading to a sensitisation of TLR2-dependent activation in a model of Gram-negative sepsis (Spiller et al., 2008). Interestingly, the induction of TLR2 expression *in vivo* coincides with the peak of neutrophil-attracting chemokine expression (Fielding et al., 2008; Hurst et al., 2001; McLoughlin et al., 2003), suggesting the involvement of TLR2 in these critical early immune activation events.

Mesothelial cells are a major resident cell type within the peritoneal cavity, and are therefore likely to encounter infecting bacteria, triggering local inflammation and host defence (Topley et al., 1996a). Therefore, understanding how TLRs mediate HPMC responses during peritonitis will help to improve compromised host defense of PD patients, reducing infection and improving clinical outcome. To this end, in the next phase of this study the modulatory mechanisms controlling TR2-mediated HPMC responses were examined.

2.2 Modulation of TLR2-mediated human peritoneal mesothelial cell responses: effect of soluble TLR2 and IL-6 receptor activation

The study of the mechanisms controlling TLR2-mediated HPMC responses focused on two potential modulatory pathways: 1) the activity of soluble TLR2, and 2) the activation of the IL-6-IL-6 receptor pathway. The TLR2-mediated responses of HPMC may be controlled by modulating cell membrane receptor expression, as described in the previous section. However, the presence of a naturally-occurring soluble form of human TLR2 (sTLR2) in biological fluids such as human plasma, breast milk and saliva and its activity as a decoy microbial receptor and modulator of membrane-bound TLR2-mediated responses of human monocytes (Kuroishi et al., 2007; LeBouder et al., 2003; Raby et al., 2009), prompted the examination of its role as a modulator of HPMC-mediated responses. Furthermore, a critical checkpoint in the resolution of inflammation is the transition from innate to adaptive immunity (Hoebe et al., 2004). Inflammatory cytokines regulate this immunological switch by controlling the recruitment, activation and apoptotic regulation of leukocytes (Hoebe et al., 2004; Jones, 2005); one such cytokine is IL-6. The contribution of IL-6 signalling in peritoneal inflammation has been reported, in particular the critical role of IL-6 trans-signalling in the initiation of the resolution phase by regulating the transition from a neutrophil-rich population to a mononuclear cell dominance (Hurst et al., 2001). This therefore led to investigate the potential effect of IL-6 signalling on TLR2-mediated responses in HPMC.

2.2.1 Production of sTLR2 by HPMC and its detection in PD fluid

In order to assess the relevance of sTLR2 as a modulator of HPMC responses to infection, first, its production by HPMC and presence in PD fluid was investigated. The presence of sTLR2 in the serum-free culture supernatants of HPMC that had been stimulated with Pam_3Cys, SES or left untreated was tested by Western blot. sTLR2 polypeptides were not detected in the culture supernatants of non-stimulated or stimulated HPMC (Fig 2.2.1A, left panel). PD effluent of patients in stable condition and during a peritonitis episode was also tested for sTLR2. Unlike the culture supernatants of HPMC, the typical 66-kDa sTLR2 polypeptide previously identified in human plasma (LeBouder et al., 2003), was readily detectable in both the PD effluent of stable and peritonitis patients (Fig 2.2.1A, right panel).

2.2.2 Effect of sTLR2 on cytokine release and NF-κB activation in mesothelial cells

Although sTLR2 was not detected in HPMC culture supernatants, its presence in the PD effluent suggested that peritoneal sTLR2 (most likely myeloid derived) may modulate HPMC pro-inflammatory responses to pathogens. To test this possibility, HPMC were stimulated with Pam_3Cys or SES in the absence or presence of human recombinant sTLR2, and CXCL8 levels

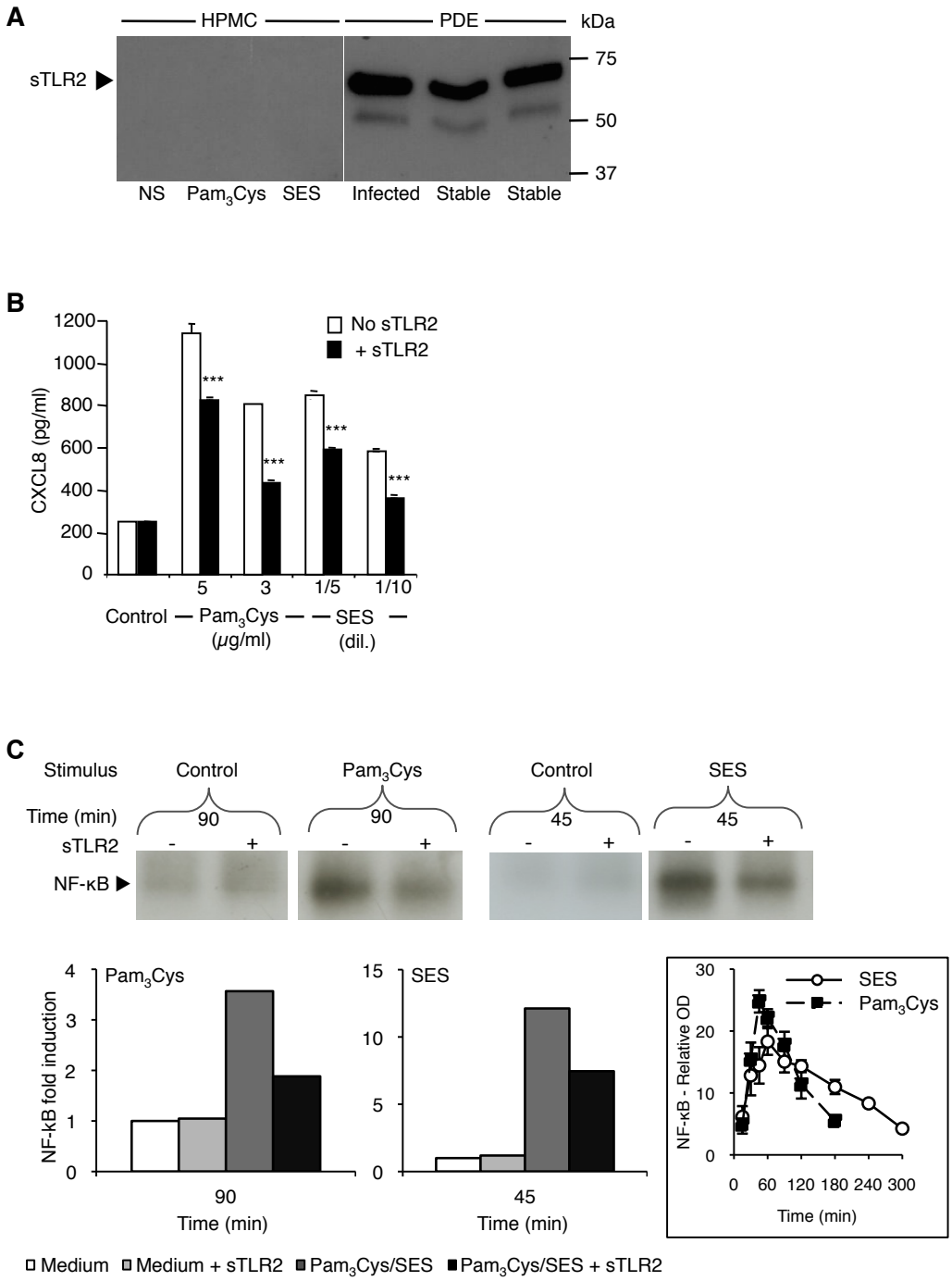

Figure 2.2.1. Detection of sTLR2 and its effect on cytokine release and NF-κB activation in HPMC.
(A) PD effluents (PDE) from stable and infected patients, the cell-free culture supernatants of non-stimulated, Pam_3Cys (10 μg/ml)- and SES (neat)-stimulated HPMC were tested for sTLR2 by Western blot, as described under Materials and Methods. **(B)** HPMC were stimulated (24h) with the indicated concentrations of Pam_3Cys or dilutions of SES in the absence or presence of recombinant human soluble TLR2 (sTLR2, 5 μg/ml), and CXCL8 levels in the cell-free culture supernatants were quantified by ELISA. Results shown (±SD) are of one experiment representative of three independent experiments (***, $p < 0.001$; sTLR2-treated *vs* non-treated cells). **(C)** HPMC were treated with medium alone, Pam_3Cys (3 μg/ml) or SES (1/10 dilution) in the absence or presence of sTLR2 (5 μg/ml) for the indicated times, nuclear extracts were then prepared and NF-κB activation monitored by EMSA, as described under Materials and Methods. The fold induction relative to non-stimulated cells (control) was calculated following densitometry scanning analysis of the EMSA gels. Data presented is representative of three different donors. Inset in C shows NF-κB activation kinetics in HPMC stimulated with Pam_3Cys (3 μg/ml) or SES (1/10 dilution) for up to 5h. At the indicated time points, nuclear extracts were prepared, NF-κB activation evaluated by EMSA and NF-κB relative ODs (to control) estimated as described in (C). Values are expressed as the mean (± SEM) of three independent experiments.

in the cell culture supernatants were quantified by ELISA. The TLR2-mediated release of CXCL8 by HPMC was found reduced in the presence of sTLR2 (Fig 2.2.1B).

TLR2 triggering in HPMC leads to NF-κB activation, as shown in Figure 2.1.7, which in turn induces the transcription of a wide range of pro-inflammatory and immunomodulatory cytokines, including CXCL8 (Doyle and O'Neill, 2006). To test the magnitude of the inhibitory effect of sTLR2 on mesothelial cells, NF-κB activation was measured by EMSA in nuclear extracts of HPMC that had been stimulated with Pam_3Cys or SES in the presence or absence of sTLR2. In order to maximise the sensitivity of the experiments, the effect of sTLR2 was tested at time points when the levels of NF-κB activation were sub-optimal, as indicated by preliminary studies on the kinetics of Pam_3Cys- and SES-induced NF-κB activation (Fig 2.2.1C, inset). Notably, HPMC stimulation with Pam_3Cys (Fig 2.2.1C, left panel) or SES (Fig 2.2.1C, right panel) in combination with sTLR2 substantially reduced the extent of NF-κB activation, when compared with that induced by Pam_3Cys or SES alone.

2.2.3 Effect of IL-6 trans-signalling on TLR2-mediated HPMC responses

Next, the potential effect of IL-6 signalling on TLR2-mediated responses in HPMC was investigated. HPMC do not express the membrane-bound IL-6R (McLoughlin et al., 2004), therefore require the sIL-6R to respond to IL-6 by IL-6 trans-signalling. The inability of HPMC to produce sIL-6R, which is generated mainly (90-99%) by proteolytic cleavage of membrane IL-6R (Scheller et al., 2013), indicates that they depend on the sIL-6R released by other cells from their environment. Infiltrating neutrophils are the main source of sIL-6R in the peritoneal cavity and resident leukocytes may constitute an additional source of sIL-6R. To test whether sIL-6R was present in the mesothelial cells environment, PD effluent of patients in stable condition was tested for sIL-6R by ELISA. Significant levels of sIL-6R was detected in the PD effluent, confirming previous findings (Oh et al., 2010; Pecoits-Filho et al., 2006), whereas sIL-6R was undetectable in the supernatant of resting or activated HPMC (Fig 2.2.2A). In addition to sIL-6R, IL-6 trans-signalling requires the expression and activity of the signal transducer gp130, thus, its expression on HPMC was also tested. Immunostaining and flow cytometry analysis of primary cultures of HPMC revealed a strong expression of the IL-6 signal transducer (Fig 2.2.2B), confirming previous findings (McLoughlin et al., 2004).

To test whether TLR2-mediated responses were affected by IL-6 trans-signalling pathway activation, HPMC were simultaneously stimulated with the TLR2 ligands Pam_3Cys or SES in combination with increasing concentrations of IL-6, sIL-6R or IL-6/sIL-6R, and CXCL8 expression levels were determined in the cell culture supernatants by ELISA (Fig 2.2.3A and B). The IL-6/sIL-6R complex caused a significant dose-dependent inhibition of basal, Pam_3Cys- and SES-induced CXCL8 production (Fig 2.2.3A and B). The inhibitory activity of 100 ng/ml IL-6/sIL-6R on basal CXCL8 secretion was 56 ± 44% (range of 12-88%; n=5); on Pam_3Cys-induced CXCL8, 78 ± 8% (range of 61-88%; n=4) and on the SES response, 54 ± 59% (range of 45-57%; n=3) (Fig 2.2.3A and B). Notably, the inhibitory activity of the IL-6/sIL-6R complex on

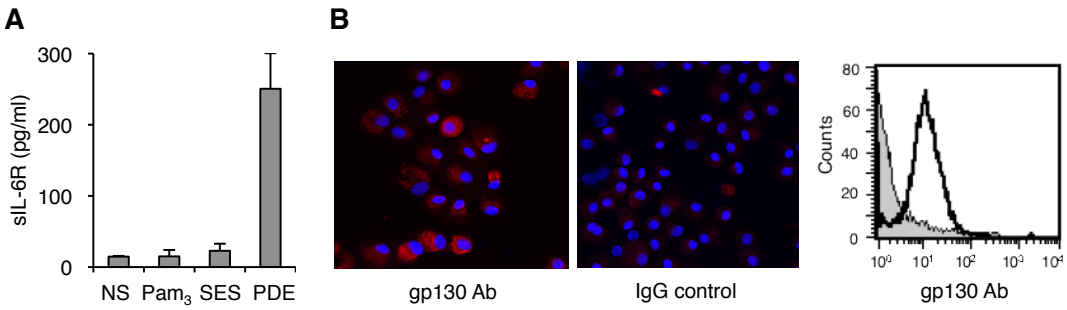

Figure 2.2.2. Production of sIL-6R and expression of gp130 by HPMC.
(A) HPMC were stimulated (24h) with Pam_3Cys (10 μg/ml) or SES (neat), and sIL-6R levels in the cell-free culture supernatants were quantified by ELISA. sIL-6R in PD effluent from a stable patient was used as a positive control. Results shown are of one experiment (±SD) representative of two. **(B,** left panel**)** Non-stimulated HPMC were tested for gp130 expression by immunocytochemistry. An isotype-matched antibody was used as a staining control. Results are representative of immunostaining of two different primary cells. **(B,** right panel**)** Cell-surface expression of gp130 was assessed by flow cytometry in freshly-isolated HPMC using a gp130 specific antibody (open plot). Control fluorescence histogram profile corresponding to the immunostaining with isotype-matched control antibody is shown (shaded plot). The result is representative of seven different cell lines from individual donors.

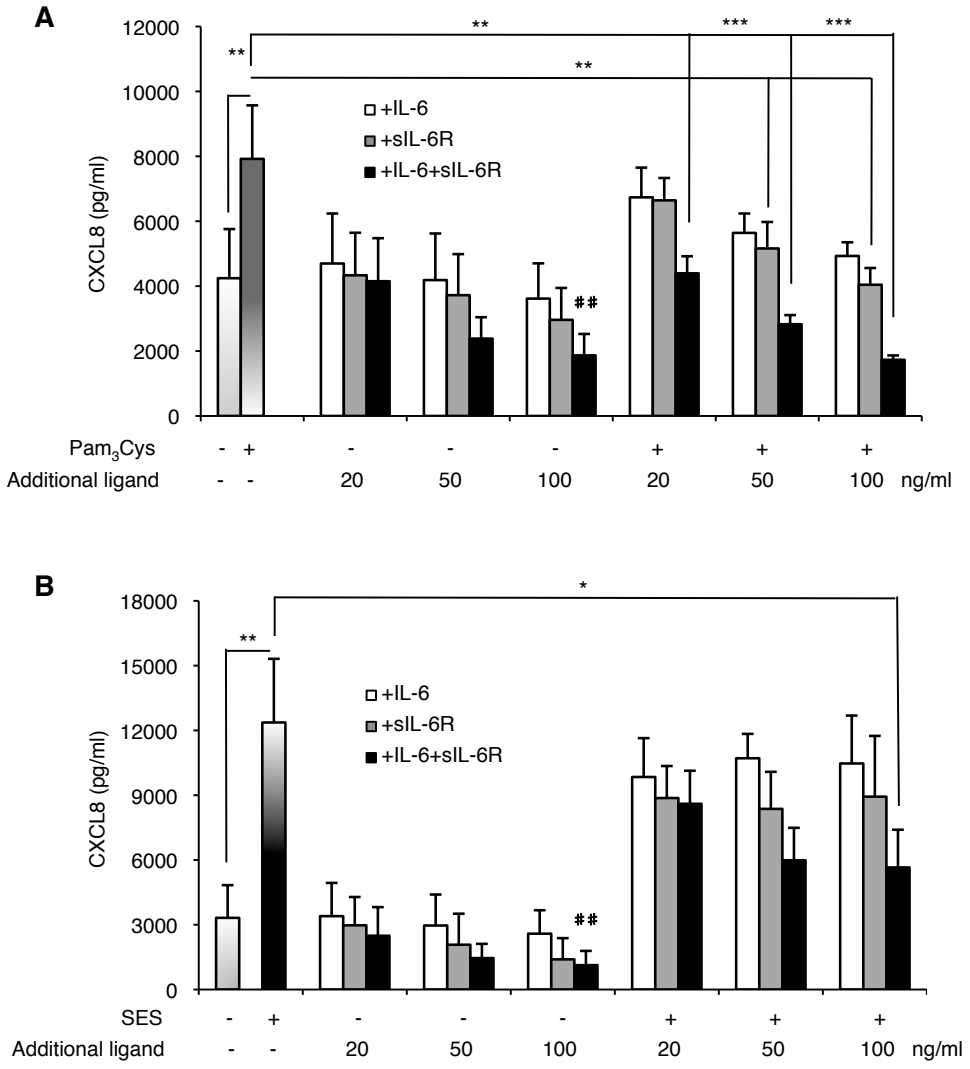

Figure 2.2.3. Effect of IL-6 trans-signalling on TLR2-induced CXCL8 release by HPMC.
HPMC were stimulated for 24h with Pam_3Cys (0.5 μg/ml) **(A)**, SES (1/5 dilution) **(B)** or left untreated (-). The culture were supplemented with the indicated concentrations of IL-6, sIL-6R or IL-6 + sIL-6R and CXCL8 levels in the cell-free culture supernatants were quantified by ELISA. Results are means (±SEM) of three (Pam_3Cys) and five (SES) independent experiments (*, $p < 0.05$; **, $p < 0.01$; ***. $p < 0.001$; non-stimulated *vs.* stimulated cells or Pam_3Cys- or SES-treated *vs.* indicated conditions; **##**, $p < 0.01$; non-stimulated *vs.* IL-6/sIL-6R stimulated cells).

SES-induced CXCL8 production was significant only at the 100 ng/ml dose (Fig 2.2.3 B). Although addition of IL-6 alone had no effect on Pam_3Cys- and SES-induced CXCL8 secretion, sIL-6R alone significantly inhibited Pam_3Cys-induced CXCL8 production (Fig 2.2.3A), suggesting that the documented basal release of IL-6 by HPMC (Witowski et al., 1996) was sufficient to facilitate the formation of an active IL-6/sIL-6R complex and IL-6 trans-signalling. This finding also indicates that IL-6 signalling in HPMC can be triggered mainly when both IL-6 and sIL-6R are present.

Pam_3Cys and SES stimulation of HPMC also results in a dose-dependent increase in CCL2 production, as previously shown in Fig 2.1.4. This finding, together with the documented capacity of IL-6/sIL-6R signalling to induce secretion of CCL2 in many cell types (Jones and Rose-John, 2002), and the modulatory effect of IL-6 trans-signalling on Pam_3Cys- and SES-induced CXCL8 described previously, posed the question of whether IL-6/sIL-6R signalling modulates Pam_3Cys- and/or SES-induced CCL2 secretion in HPMC. To address this question, HPMC were stimulated with Pam_3Cys or SES in the absence or presence of IL-6, sIL-6R or IL-6/sIL-6R, and the levels of CCL2 in the cell culture supernatants were determined by ELISA. Unlike the inhibitory effect on Pam_3Cys- and SES-induced CXCL8 described previously, IL-6/sIL-6R exerted a significant positive modulatory effect on CCL2 production by HPMC, when they were stimulated with a combination of Pam_3Cys or SES and 50 or 100 ng/ml of IL-6/sIL-6R (Fig 2.2.4A and B). These findings were consistent with previously reported work showing release of CCL2 by activation of both IL-6- and TLR2 signalling pathways, and when HPMC were stimulated with IL-6/sIL-6R in combination with IL-1β (Hurst et al., 2001).

Effect of IL-6 signalling on TLR2-mediated NF-κB activation

To establish whether the modulatory effect of IL-6 trans-signalling on TLR2-driven CXCL8 production occurs at the level of the signal transduction pathway, NF-κB activation was examined by EMSA. Addition of IL-6, sIL-6R or IL-6/sIL-6R did not significantly increase NF-κB basal activation, when considering the sensitivity of the technique (Fig 2.2.5A). The Pam_3Cys-triggered NF-κB activation previously shown in Figure 2.1.7 was not modified by addition of IL-6 or sIL-6R alone (Fig 2.2.5A). By contrast, Pam_3Cys-mediated NF-κB activation was attenuated by the addition of IL-6/sIL-6R, which correlated with the CXCL8 inhibition previously observed (Fig 2.2.2). Conversely, SES-induced NF-κB activation showed a slight attenuation with the addition of IL-6 or sIL-6R, but no change with the addition of IL-6/sIL-6R (Fig 2.2.5A). To examine the NF-κB subunits activated by TLR2 signalling in combination with IL-6 trans-signalling in HPMC, a 'supershift' EMSA study was performed using antibodies directed against specific NF-κB family members. This analysis identified the involvement of NF-κB DNA-binding complexes consisting of the p50 and p65 NF-κB subunits for Pam_3Cys and SES in combination with IL-6/sIL-6R (Fig 2.2.5B and C), as previously described for Pam_3Cys and SES alone (Fig 2.1.7B and Fig 2.2.5B and C).

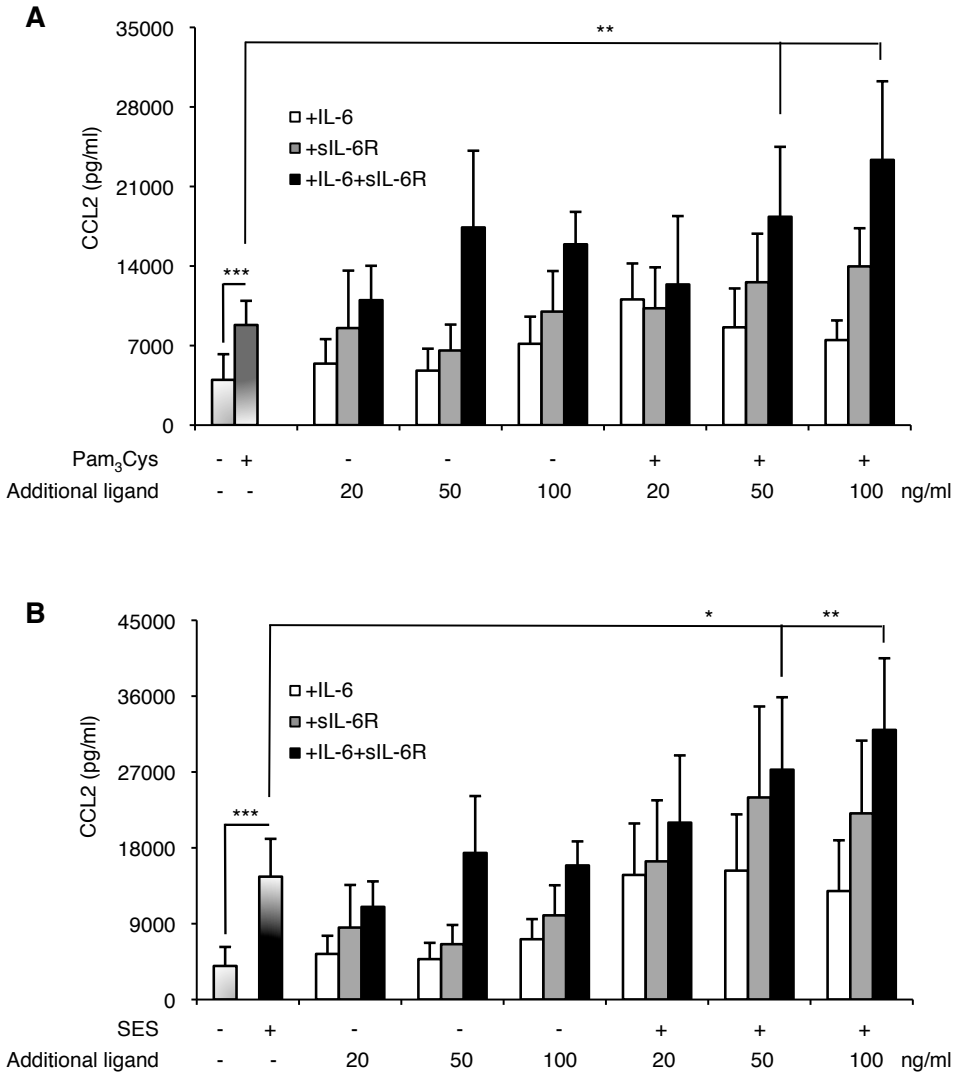

Figure 2.2.4. Effect of IL-6 trans-signalling on TLR2-induced CCL2 release by HPMC.
HPMC were stimulated for 24h with Pam_3Cys (0.5 μg/ml) **(A)**, SES (1/5 dilution) **(B)** or left untreated (-). The culture were supplemented with the indicated concentrations of IL-6, sIL-6R or IL-6 + sIL-6R and CCL2 levels in the cell-free culture supernatants were quantified by ELISA. Values are expressed as the mean (±SEM) of three independent experiments (***, $p < 0.001$ non-stimulated *vs* stimulated cells; *, $p < 0.05$; **, $p < 0.01$; Pam_3Cys- or SES-treated *vs* indicated conditions).

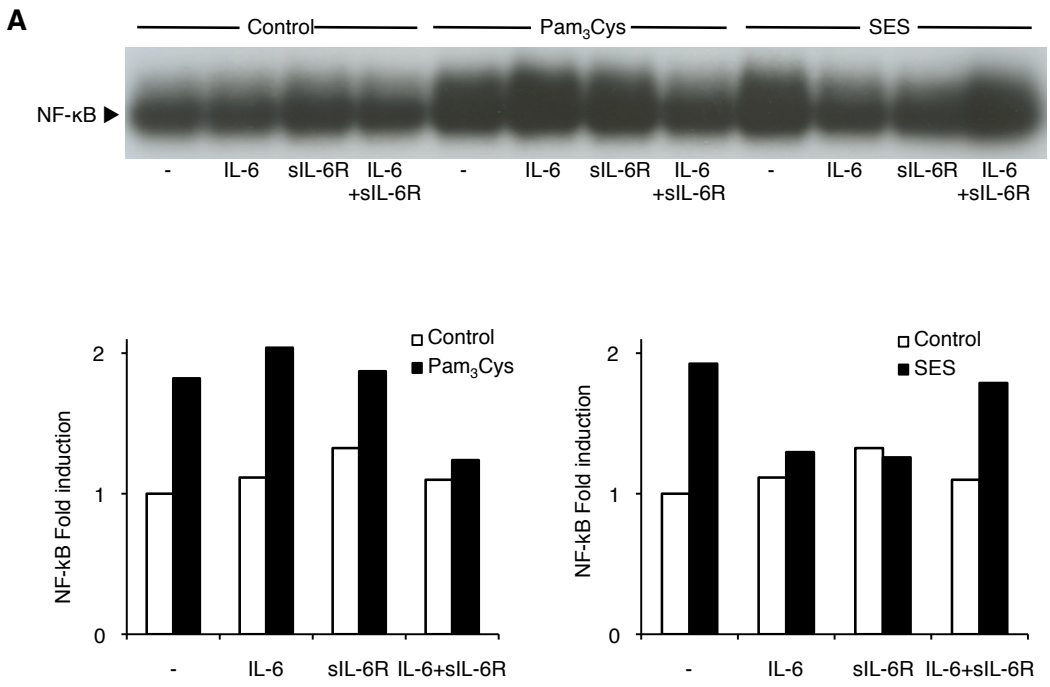

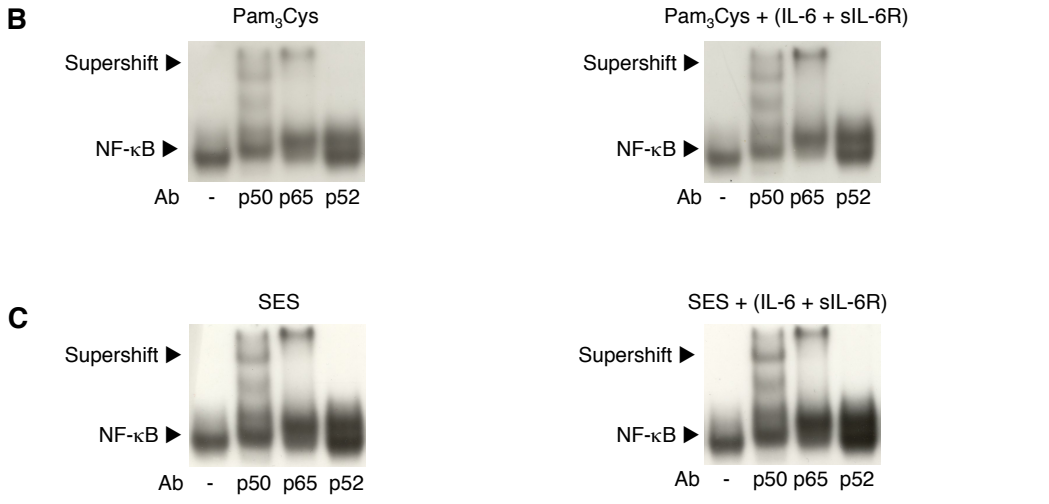

Figure 2.2.5. Effect of IL-6 signalling on TLR2-mediated NF-κB activation in HPMC.
(A) HPMC were stimulated (4h) with medium (Control), Pam_3Cys (0.5 μg/ml) or SES (1/5 dilution) alone or in combination with 50 ng/ml of IL-6, sIL6-R or IL-6 + sIL-6R. Nuclear extracts were prepared and NF-κB activation was analysed by EMSA. NF-κB fold induction relative to non stimulated cells was calculated from densitometry analysis of EMSA gels. Data presented is a representative result of four experiments performed using primary cells from different donors. **(B** and **C)** The composition of the NF-κB DNA binding complexes was studied by supershift EMSA analysis of nuclear extracts prepared from HPMC stimulated with Pam_3Cys alone or in combination with IL-6+sIL-6R **(B)**, or with SES alone or in combination with IL-6+sIL-6R **(C)**. Control samples without the addition of antibody, and samples analysed with specific antibodies for the p50, p65, and p52 subunits of NF-κB are shown. NF-κB binding and 'supershifted' complexes are indicated. Data shown are results of one experiment.

Effect of TLR2 signalling on IL-6-mediated STAT activation

The modulatory effect of IL-6/sIL-6R on TLR2-mediated HPMC responses described in the previous section suggested the possibility of cross-talk between the IL-6 and TLR2 signalling pathways. To examine this possibility, STAT activation downstream of IL-6 signalling was evaluated by EMSA following HPMC activation with Pam_3Cys or SES alone or in combination with IL-6, sIL-6R or IL-6/sIL-6R. Using a consensus oligonucleotide (SIE m67) containing a DNA binding motif for STAT1 and STAT3, a low level of STAT1/3 activation was observed for the non-stimulated, IL-6 and sIL-6R stimulated cells, when considering the sensitivity of the technique. The IL-6/sIL-6R complex triggered STAT1/3 activation, as previously reported (McLoughlin et al., 2004). Pam_3Cys did not trigger an increase of STAT1/3 activation over the basal level. Similarly, SES alone did not seem to activate STAT1/3 (Fig 2.2.6A). These results were consistent across five different experiments. STAT1/3 activation observed following cell activation with Pam_3Cys + sIL-6R was similar to Pam_3Cys alone, whereas a more pronounced increase was observed in cells stimulated with SES + sIL-6R (Fig 2.2.6A). These findings may be explained by the HPMC's basal secretion of IL-6 as well as by the SES-driven IL-6 secretion, which can combine with sIL-6R and trigger trans-signalling. Addition of the IL-6/sIL-6R complex to Pam_3Cys or SES triggered a similar response to that of IL-6/sIL-6R complex alone (Fig 2.2.6A).

'Supershift' EMSA experiments were then performed using STAT-specific antibodies to identify the STAT family member(s) involved in HPMC activation. This analysis identified the involvement of STAT3 in cell activation by Pam_3Cys and SES in combination with IL-6/sIL-6R (Fig 2.2.6B and C, right panels), as previously reported for the IL-6/sIL-6R complex (McLoughlin et al., 2004). Interestingly, STAT3 activation, albeit low, was also observed when HPMC were stimulated with Pam_3Cys or SES alone (Fig 2.2.6B and C, left panels).

2.2.4 Effect of sTLR2 on STAT activation

STAT activation was further examined over time in nuclear extracts from cells non-stimulated or stimulated with Pam_3Cys or SES. A low level of basal activation was observed, increasing slightly at later time points, but neither Pam_3Cys nor SES stimulation did up-regulate STAT1/3 DNA-binding signal above that observed for the control growth-arrested non-stimulated cells (Fig 2.2.7A). To investigate whether sTLR2, in addition to its modulatory role on NF-κB activation, could affect the status of STAT1/3 activation, HPMC were stimulated with Pam_3Cys and SES in the presence or absence of human recombinant sTLR2. A range of time points were tested but no signal was detected in the absence or presence of TLR2 ligands, and no change was observed following the addition of sTLR2 (Fig 2.2.7B).

2.2.5 Discussion

Collectively, the data described in this section demonstrated a negative modulatory role of sTLR2 in TLR2-driven HPMC responses and a potential role of IL-6 signalling in modulating the TLR2-mediated responses of these cells.

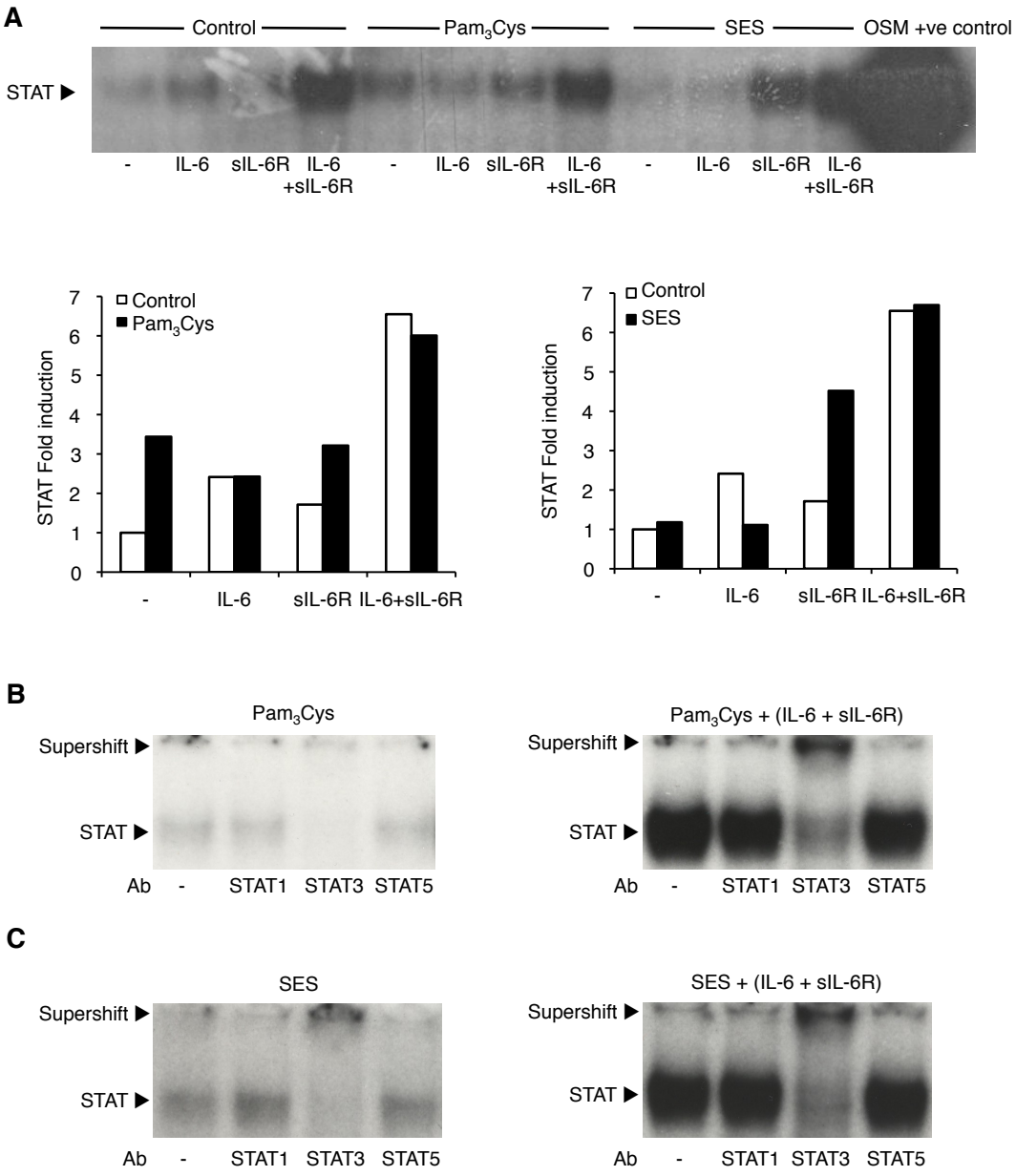

Figure 2.2.6. Effect of TLR2 signalling on IL-6-mediated STAT activation in HPMC.
(A) HPMC were stimulated (4h) with medium (Control), Pam_3Cys (0.5 μg/ml) or SES (1/5 dilution) alone or in combination with 50 ng/ml of IL-6, sIL6-R or IL-6 + sIL-6R, or with Oncostatin M (OSM) (15 min; 30 ng/ml) used as a positive control. Nuclear extracts were prepared and total STAT activation was analysed by EMSA. STAT fold induction relative to non stimulated cells was calculated from densitometry analysis of EMSA gels. Data shown are representative results of five experiments performed using primary cells from different donors. **(B** and **C)** The composition of the STAT DNA binding complexes was analysed by supershift EMSA experiments in nuclear extracts prepared from HPMC stimulated with Pam_3Cys **(B)** or with SES **(C),** alone or in combination with IL-6+sIL-6R. Control samples without the addition of antibody and samples analysed with specific antibodies for STAT 1, 3 and 5 are shown. STAT binding and 'supershifted' complexes are indicated. Data shown are results of one experiment.

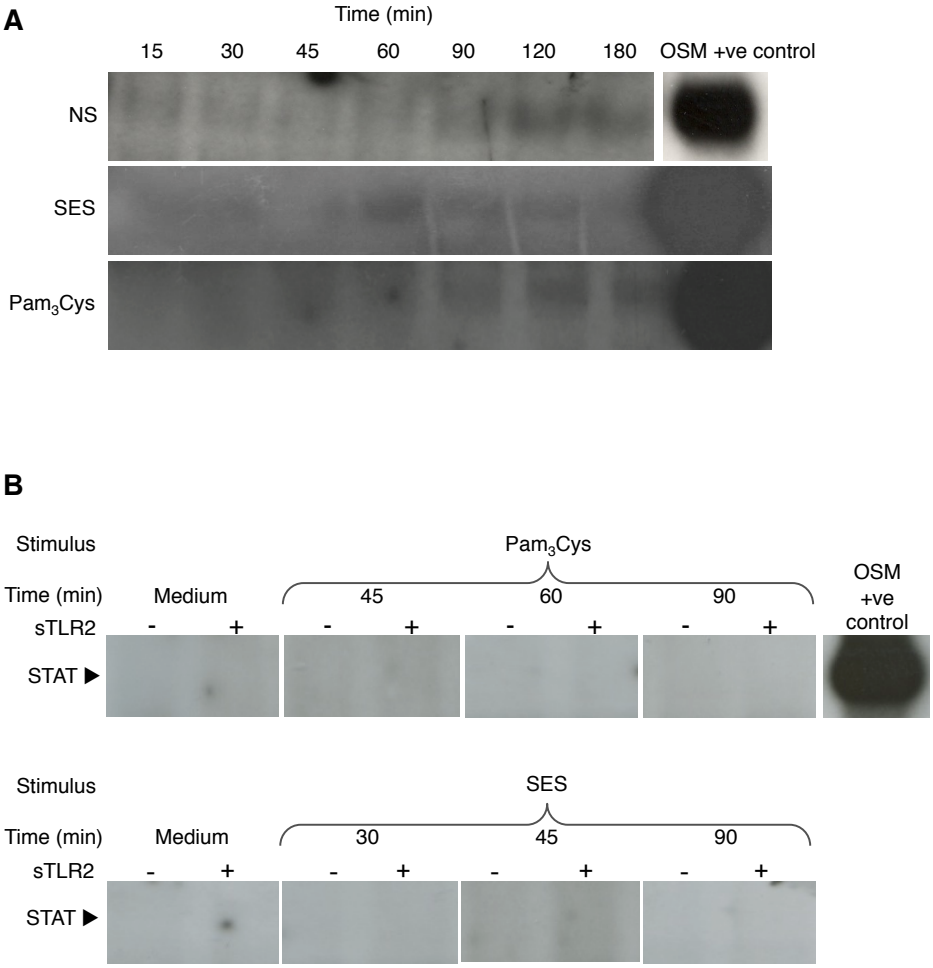

Figure 2.2.7. Examination of STAT activation in HPMC following TLR2 activation.
(A and **B)** HPMC were stimulated for the indicated time periods with Pam_3Cys (A, 2 μg/ml; B, 3 μg/ml) or SES (A, neat; B, 1/10 dilution) alone or in the presence of soluble TLR2 (sTLR2, 5 μg/ml), or with Oncostatin M (OSM) (15 min; 30 ng/ml) used as a positive control. At the indicated time points nuclear extracts were prepared and total STAT activation was analysed by EMSA. Data presented are representative results of three experiments performed using primary cells from different donors.

sTLR2 showed a substantial negative modulatory effect not only on the TLR2-mediated release of CXCL8, but also on the activation of the transcription factor NF-κB. The inhibitory effect on NF-κB activation indicated that sTLR2 has a wide spectrum of effects on HPMC responses, which may not be limited to CXCL8 production and may extend to a number of immunomediators. Notably, although HPMC showed cell-surface expression of TLR2, they do not seem to release sTLR2, as it was not detected in the culture supernatants of non-stimulated, Pam_3Cys- or SES-stimulated cells. Thus, HPMC, unlike other cell types, may lack the machinery required to shed sTLR2 from the membrane. Alternatively, HPMC might only release sTLR2 in specific conditions determined by their environment. Nevertheless, sTLR2 was readily detectable in PDE from stable and infected patients; its presence in the peritoneal cavity, presumably released by resident macrophages as well as by recruited neutrophils and monocytes during infection, may contribute to an efficient control of the local inflammatory response.

The simultaneous activation of IL-6 trans-signalling - via STAT3 - and TLR2 pathways in HPMC had a dampening effect on pro-inflammatory NF-κB activation and subsequent CXCL8 expression levels, compared with the TLR2-mediated responses to Pam_3Cys alone. This shows the potential of IL-6 trans-signalling to control the TLR2-mediated release of CXCL8 - a potent neutrophil chemoattractant - by HPMC. By contrast, IL-6 trans-signalling and Pam_3Cys-induced TLR2 activation showed a positive effect on CCL2 release. This data confirmed previous results (Hurst et al., 2001), and considering the main cell targets of these chemokines - namely neutrophils for CXCL8 and mononuclear cells for CCL2 - indicates the potential of IL-6 trans-signalling to inhibit neutrophil recruitment while increasing mononuclear cell influx. This combination of effect on various chemokine secretion could contribute to limit the detrimental effect of a prolonged presence of neutrophils in the peritoneal cavity, while promoting the initiation of the resolution phase.

IL-6 trans-signalling also showed the capacity to modulate SES-mediated responses of HPMC. Notably here, the positive effect on CCL2 release was similar to that observed on Pam_3Cys-stimulated HPMC, the negative effect on CXCL8 release was modest, only observed at the highest IL-6/sIL-6R concentration tested, and no effect on NF-κB was observed. These findings may be partly due to the complex nature of SES, comprising a variety of molecules released by *Staphylococcus epidermidis* (*S. epi*.). Various strains of *S. epi*. secrete virulence factors called phenol soluble modulins, which may signal *via* TLR2 (Hajjar et al., 2001; Otto, 2009). While some of the TLR2-triggering modulins are most likely present in SES, other factors might also be present and presumably activate an array of signaling pathways - challenging to identify - leading to the resulting effects observed here.
The regulatory effects of IL-6 trans-signalling on pro-inflammatory signals described here extended previous *in vitro* observations made in HPMC, where IL-1β- and TNFα-mediated pro-

inflammatory cytokine release was attenuated by IL-6 trans-signalling activation (Hurst et al., 2001). In addition, *in vivo* results with IL-6KO mice i.p. challenged with SES showed that deficiency of IL-6 heightened the level and prolonged the presence of pro-inflammatory cytokines and neutrophils in the peritoneal cavity (Hurst et al., 2001; Robson et al., 2001), suggesting an inhibitory effect of IL-6 signalling on pro-inflammatory responses while promoting the transition between innate and acquired immunity.

The negative modulatory effect of IL-6 signalling pathway activation via STAT3 on TLR2-mediated CXCL8 release in HPMC was also consistent with the results of a study using knockin mice genetically modified in the gp130 signalling pathway, with one strain presenting hyperactivation of STAT1/3 and a second strain with an abolished STAT1/3 signalling. Using the SES *in vivo* model of peritoneal inflammation, the study demonstrated a modulating role of IL-6 via STAT3 activation in neutrophil trafficking in the peritoneal membrane, by negatively regulating the production of the neutrophil chemoattractant CXCL1 (a mouse functional counterpart of CXCL8), leading to neutrophil clearance (Fielding et al., 2008). Lining the peritoneal membrane, mesothelial cells are the main cells in contact with the environment and leukocytes present in the cavity and could be responsible for these modulating activities (Hoentjen et al., 2005; Nishinakamura et al., 2007; Tilg et al., 1994; Xing et al., 1998; Yu et al., 2002).

In order to obtain a better understanding of the modulatory capacity of sTLR2 and IL-6 signalling, in the next phase of the project, the modulatory role of sTLR2 and IL-6 signalling in inflammation and infection was evaluated *in vivo*.

2.3 Role of TLR2, soluble TLR2 and IL-6 signalling in peritoneal inflammation and infection *in vivo*

In order to better evaluate the involvement of TLR2 and the modulatory capacity of sTLR2 in Gram-positive induced peritoneal inflammation and infection, their activity was investigated in two mouse models of acute peritoneal inflammation based on the injection of SES or live *S. epi.* (the development of the *S. epi.* model was part of this thesis and is described below in section 2.4). Furthermore, the live *in vivo* model was also used to better evaluate the impact of IL-6 signalling on *S. epi.*-induced peritoneal responses.

2.3.1 Effect of sTLR2 on SES-induced leukocyte recruitment and cytokine production

The role of sTLR2 was first evaluated in mice inoculated intraperitoneally (i.p.) with SES in the presence or absence of sTLR2. SES-induced peritoneal inflammation was monitored over time and the neutrophil, macrophage and lymphocyte numbers in the peritoneal lavages were determined by differential cell counting using cytospin. As observed in episodes of human peritonitis (Hurst et al., 2001), i.p. injection of SES resulted in an initial rapid and transient neutrophil influx, peaking at 2-3h (depending on the experiment) (Fig 2.3.1A), while mononuclear cell numbers were decreasing (Fig 2.3.1B and C), followed by a more sustained mononuclear leukocyte infiltration in the peritoneal cavity at later time points (Fig 2.3.1B and C). Neutrophils were maintained in the peritoneal cavity up to 12h following SES administration, decreasing thereafter, and were eliminated by 48h (Fig 2.3.1A, right panel). By contrast, mononuclear cells were maintained (lymphocytes) or even gradually increased (macrophages) by 48h (Fig 2.3.1B and C, right panels). The simultaneous administration of SES and sTLR2 significantly impaired the extent of neutrophil recruitment observed with SES alone at the 2h peak time, with a reduction also observed at 3h and 6h (Fig 2.3.1A, left panel), whereas later time points showed similar neutrophil numbers (Fig 2.3.1A, right panel). Unlike neutrophils, monocyte/macrophage and lymphocyte populations were not affected by the presence of sTLR2 over the entire time course (Fig 2.3.1B and C). Quantification of the neutrophil chemoattractant CXCL1/KC expression profile in the peritoneal lavages by ELISA showed a transient secretion, peaking at 1h after SES injection. Addition of sTLR2 significantly reduced the levels of CXCL1, which was consistent with the inhibitory effect of sTLR2 on neutrophils recruitment (Fig 2.3.2A). Biopsies of parietal peritoneal membrane were taken at the peak time of neutrophil recruitment following injection of SES, in order to look at the response of non-hematopoietic stromal cells (mainly mesothelial cells and fibroblasts). qRT-PCR analysis of RNA extracted from the peritoneal membrane of one mouse showed that the reduction in the levels of CXCL1 protein in the presence of sTLR2 correlated with a decrease in Cxcl1 mRNA (Fig 2.3.2A, inset). Interestingly, at the peak of neutrophil infiltration in the peritoneal cavity, the simultaneous injection of sTLR2 and SES also resulted in a reduction in Tlr2 mRNA levels in the

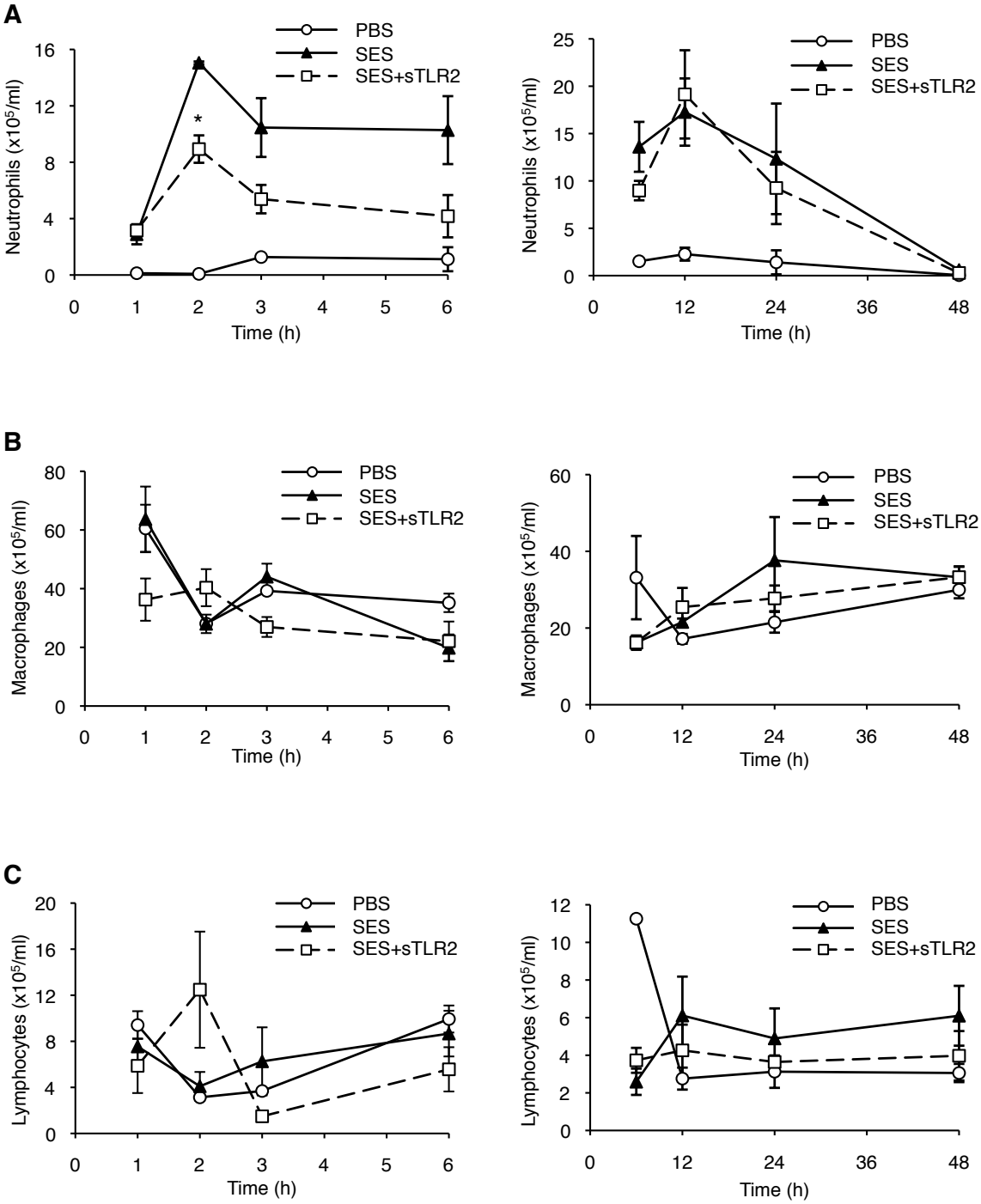

Fig 2.3.1. Effect of sTLR2 on leukocyte recruitment in the SES-induced inflammation model.
In two different experiments (1h-6h left panels and 6h-48h right panels), mice were i.p. inoculated with SES, SES + 100 ng sTLR2 or PBS (controls). At the indicated time points mice were sacrificed, the peritoneal cavity was lavaged and neutrophil **(A)**, macrophage **(B)** and lymphocyte **(C)** numbers were determined by differential cell counting using cytospin. Values are expressed as the mean ± SEM (n=3 or 4/condition; *, $p < 0.05$; SES *vs.* SES + sTLR2).

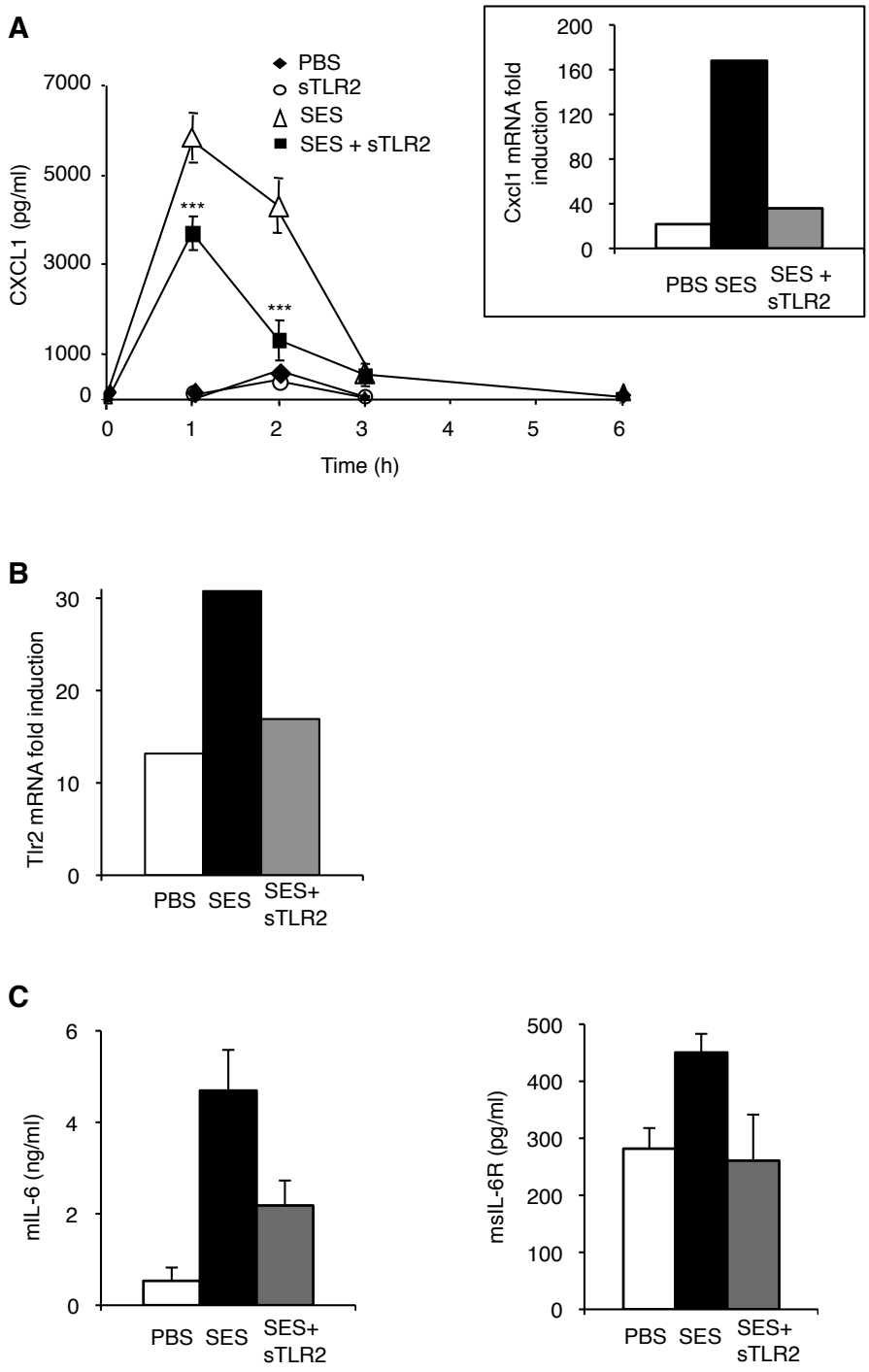

Fig 2.3.2. Effect of sTLR2 on cytokine production and Tlr2 expression in the SES-induced inflammation model.

(A-C) Mice were i.p. inoculated with SES, SES + 100 ng sTLR2 or PBS (controls). At the indicated time points in (A), and at 2h (C), the peritoneal cavity was lavaged and profiles of CXCL1 **(A)**, IL-6 and sIL-6R **(C)** expression were determined by ELISA. Values are expressed as the mean ± SEM (n=5/condition; ***, $p < 0.001$ SES *vs*. SES + sTLR2). At 2h, Cxcl1 (**A**, inset) and Tlr2 **(B)** mRNA expression levels were quantified by qRT-PCR following total RNA extraction from biopsies of the parietal peritoneal membrane. Data represents the results of one experiment.

mouse peritoneal membrane (Fig 2.3.2B), as compared with the levels in the mice injected with SES alone, which had shown a transient increase, as previously discussed in section 2.1 (Figure 2.1.17B).
The effect of sTLR2 on IL-6 and sIL-6R levels in the peritoneal lavages was also quantified. At the peak time of neutrophil recruitment, inoculation of sTLR2 in combination with SES showed a reduction (although not statistically significant) in the amount of IL-6 secreted in the peritoneal cavity, and a slight decrease in sIL-6R levels (Fig 2.3.2C).

2.3.2 Effect of sTLR2 on SES-induced NF-κB and STAT activation

To further investigate the mechanism of sTLR2 modulatory activity *in vivo*, EMSA analysis of nuclear extracts from mouse peritoneal membranes was conducted to assess NF-κB and STAT activation during the initial phase of the inflammatory response. Strong NF-κB activation was observed at 1h and 2h following i.p. injection of SES, whereas the PBS- and sTLR2-injected mice showed very low levels of transcription factor activation (Fig 2.3.3A). The simultaneous inoculation of SES and sTLR2 resulted in reduced activation of NF-κB, with more than 50% reduction at 1h (Fig 2.3.3A). These findings mirrored those observed in HPMC *in vitro* (section 2.2, Fig 2.2.1C) and were consistent with the reduction in CXCL1 levels and neutrophil recruitment observed in mice injected with SES + sTLR2 described previously (section 2.3.1).

The activation of STAT (the main signalling intermediate downstream IL-6 receptor) was investigated next. SES-induced inflammation triggered STAT1/3 activation in the peritoneal membrane (Fig 2.3.3B). At the 1h time point, SES-induced STAT1/3 activation was increased 2-fold above PBS, and further increased at 2h. The simultaneous inoculation of SES and sTLR2 resulted in reduced STAT1/3 activation, at 1h and 2h (Fig 2.3.3B). These findings were consistent with the negative effect of sTLR2 on IL-6 and sIL-6R levels observed in mice inoculated with SES described previously (section 2.3.1 and Fig 2.3.2C). However, they contrasted with those in HPMC *in vitro* (section 2.2), as no effect of SES on STAT activation and, consequently, no effect of sTLR2 on STAT in SES-treated cells (section 2.2.4) was observed in the mesothelial cells. Clearly, the lack of IL-6R in HPMC explains these contrasting findings.

2.3.3 Effect of sTLR2 on *S. epi.*-induced peritoneal infection

The modulatory activity of sTLR2 observed in the SES *in vivo* model raised the question of whether such negative effect would be detrimental to bacterial clearance. To address this issue, the activity of sTLR2 was evaluated in an acute episode of peritonitis induced by i.p. inoculation of live *S. epi*. Mice were i.p. inoculated with *S. epi*. (5×10^8 cfu/mouse) in the absence or presence of increasing doses of sTLR2. As will be described in detail in the next section, this inoculum allowed a controlled and limited infection to develop and resolve, with the infection almost completely cleared by 48h (section 2.4, Figs 2.4.20 - 22). The *S. epi*.-induced peritoneal

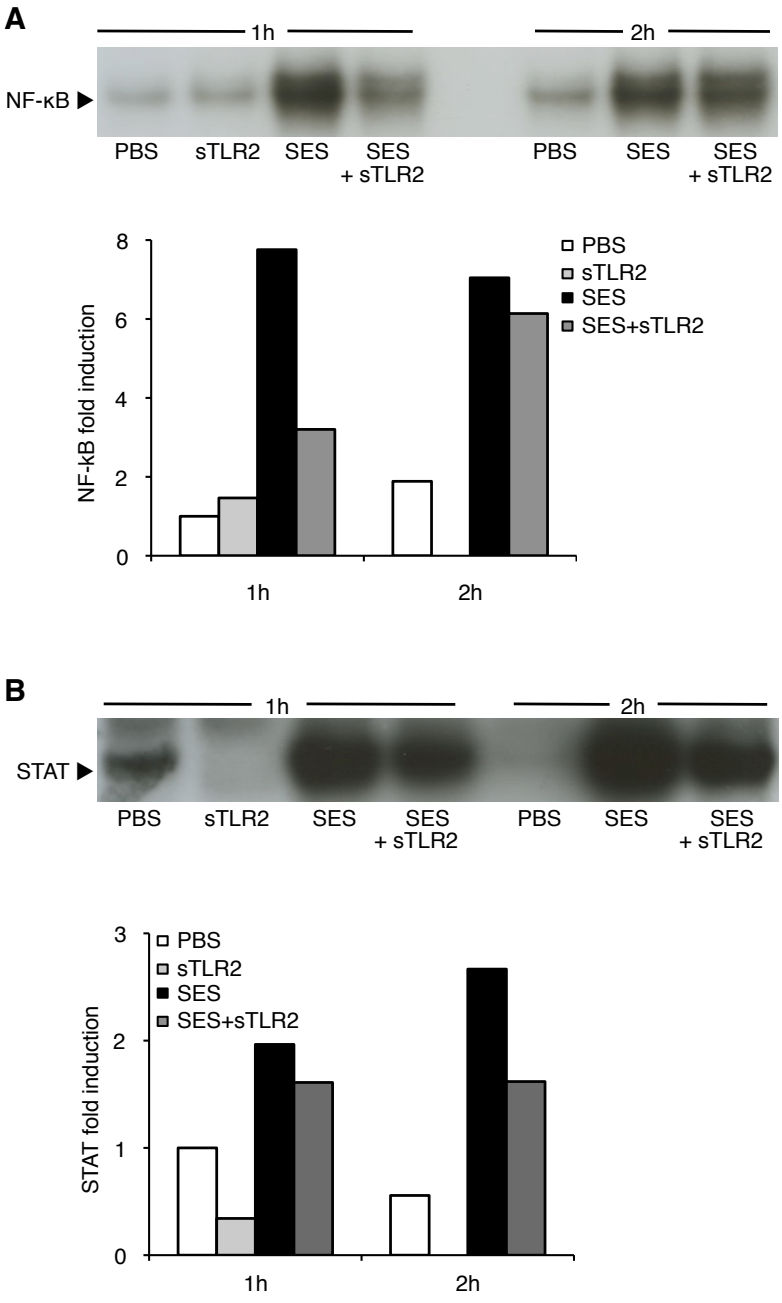

Figure 2.3.3. Effect of sTLR2 on NF-κB and STAT activation in the SES-induced inflammation model.
(A and **B)** Mice were i.p. inoculated with SES, SES + 100 ng sTLR2 or PBS (controls). At the indicated time points, NF-κB **(A)** and STAT **(B)** activation was analysed by EMSA in nuclear extracts following protein extraction from samples of parietal peritoneal membrane. NF-κB and STAT fold induction relative to PBS-injected animals was calculated from densitometry analysis of the corresponding EMSA gels. Data shown are representative results of three experiments.

inflammation and infection process was followed over 18h, the neutrophil, macrophage and lymphocyte numbers in the peritoneal lavages were determined by differential cell counting using cytospin, and bacterial numbers in the lavages and blood were determined on agar plates by using an automated spiral plater. The neutrophil recruitment kinetics and numbers differed from those in the SES *in vivo* model. Here, neutrophil influx peaked at 12h following injection, subsequently decreasing. In the presence of sTLR2, neutrophil numbers in the peritoneum were significantly reduced at the 12h peak time as well as 18h (Fig 2.3.4A, left panel). Mononuclear cells followed a similar recruitment profile to that in the SES model, and like in the SES model, their numbers were not significantly modified in the presence of any dose of sTLR2 (Fig 2.3.4A, right panel). These results, similar to those observed *in vitro* (section 2.2) and by using the SES *in vivo* model (section 2.3.2), highlighted the role of TLR2 in Gram-positive peritoneal inflammation and confirmed the negative regulatory capacity of sTLR2.

The impact of sTLR2 on bacterial clearance was evaluated next. The bacterial load in the peritoneal cavity and in the blood peaked at 3h, and was followed by a steady decrease, with the bacteria cleared from the blood by 18h. The addition of sTLR2 to the inoculum - at any tested dose - did not significantly modify the bacterial count in the peritoneal cavity. In the peripheral circulation, although the mice treated with the highest dose of sTLR2 showed increased bacterial load at the earliest time (3h) post-injection (Fig 2.3.4B right), this effect does not appear to be physiologically significant, because none of the animals showed symptoms of shock, or died from the infection, and all animals had cleared the blood infection almost completely by 6h post-injection. Moreover, plasma levels of serum amyloid A (SAA), the acute phase reactant secreted by the liver in response to bacterial infection, were similar in control (*S. epi.* only) and sTLR2-treated mice at all time points examined (Fig 2.3.4C), indicating that the relatively small increase in bacterial load in the bloodstream of 1 μg of sTLR2-treated mice did not significantly impact on the level of the systemic acute phase response.

To examine the mechanism of sTLR2 modulatory activity in this live bacteria *in vivo* model, EMSA analysis of nuclear extracts from the peritoneal membrane was conducted to assess NF-κB and STAT activation during the initial phase of the inflammatory response. A substantial increase in NF-κB activation over the control levels (PBS) was observed at 3h and 6h following inoculation of *S. epi*. The simultaneous inoculation of *S. epi.* and sTLR2 resulted in reduced activation of NF-κB at 3h, but not at 6h, at all sTLR2 doses tested (Fig 2.3.5A). To assess the possible effect of sTLR2 on the IL-6 signalling pathway, STAT activation was investigated next. *S. epi*. induced STAT1/3 activation in the peritoneal membrane at 3h and 6h, with levels greatly increased above the control (PBS), whereas the simultaneous inoculation of *S. epi.* and sTLR2 resulted in a substantial sTLR2 dose-dependent reduction in STAT1/3 activation levels at 3h and 6h (Fig 2.3.5B).

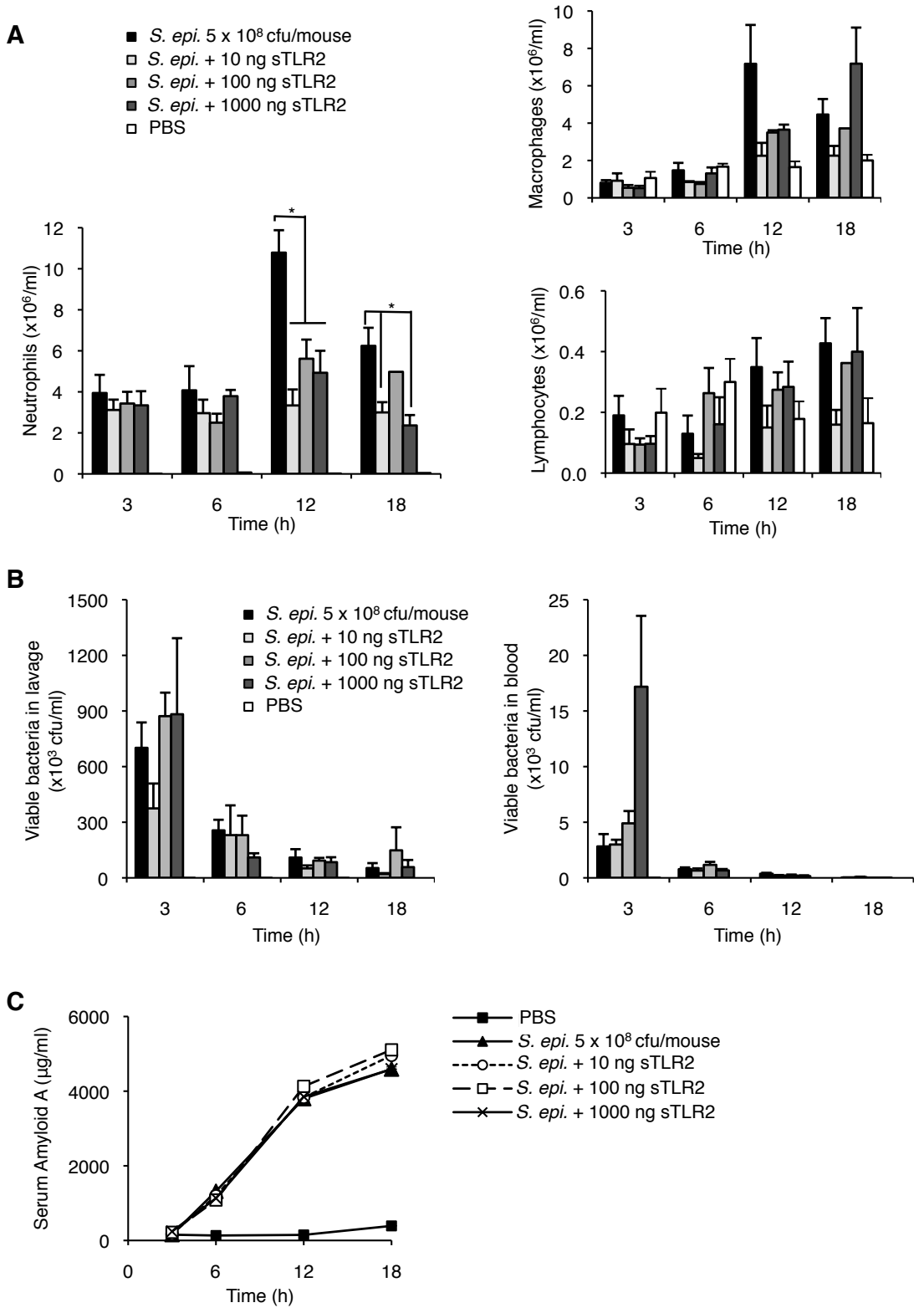

Figure 2.3.4. Effect of sTLR2 on *S. epi*.-induced peritoneal infection.
Mice were i.p. inoculated with 5 x 10^8 cfu/mouse *S. epi.,* in the presence or absence of the indicated doses of sTLR2. At the indicated time points mice were sacrificed, the peritoneal cavity was lavaged and neutrophil, macrophage and lymphocyte numbers were determined by differential cell counting using cytospin **(A),** bacteria in the peritoneal cavity and blood were counted using an automated spiral plater **(B)**, and serum levels of Serum Amyloid A (SAA) were determined by ELISA **(C)**. Values are expressed as the mean ± SEM (n=3-5/condition; *, $p < 0.05$; *S. epi.* + sTLR2 (as indicated) *vs*. *S. epi.*).

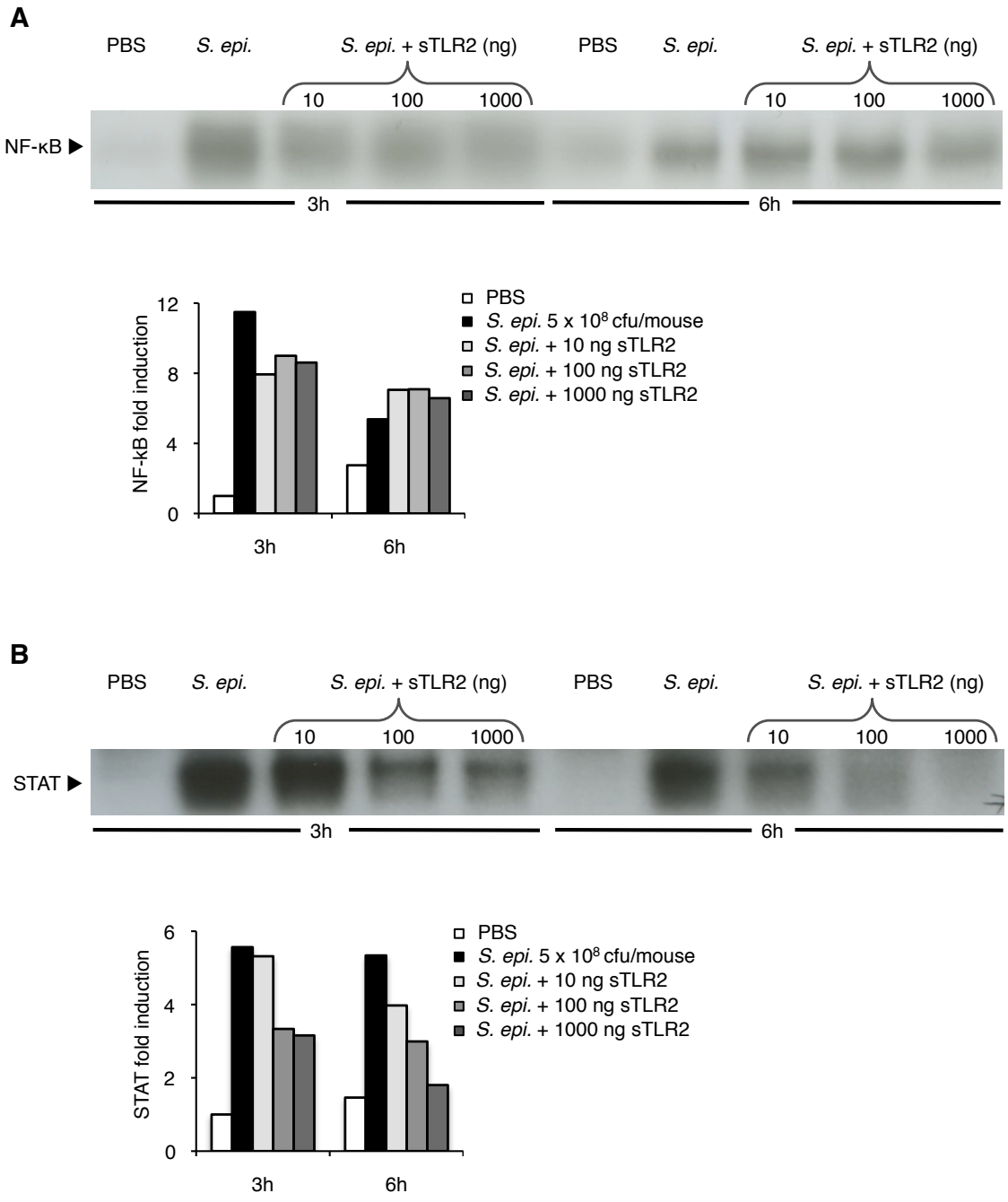

Figure 2.3.5. Effect sTLR2 on NF-κB and STAT activation in the *S. epi.*-induced peritoneal infection model.
Mice were i.p. inoculated with 5 x 10^8 cfu/mouse *S. epi.,* in the presence or absence of the indicated doses of sTLR2. At the indicated time points, NF-κB **(A)** and STAT **(B)** activation, was monitored by EMSA in nuclear extracts following protein extraction from samples of parietal peritoneal membrane. NF-κB and STAT fold induction relative to PBS-injected animals was calculated from densitometry analysis of the corresponding EMSA gels. Data shown are representative results of three experiments.

2.3.4 Effect of IL-6 signalling on *S. epi.*-induced inflammation and infection

The live bacteria *in vivo* model was also used to investigate the role of IL-6 and IL-6 signalling in bacterial-induced inflammation and bacterial clearance. To this end, *S. epi.* or PBS (control) was i.p. inoculated into WT and IL-6-deficient (IL-6KO) mice, and the induced inflammation was followed for 48h. As described in the next section (section 2.4), the mice body temperature was monitored throughout the time course as a parameter of the mice health status and as an index of bacterial infection.

The temperature variations following PBS and *S. epi.* injection in IL-6KO mice were compared with those in WT animals (Fig 2.3.6A and section 2.4). Temperature fluctuations over the time course following PBS injection were observed in both WT and IL-6KO mice, reflecting the daily variations in body temperature as well as, most likely, the limited inflammation induced by the injection of PBS. The fluctuations were more pronounced in WT mice, whereas temperature changes in IL-6KO mice remained limited. Although the general pattern was similar in both strains, IL-6KO mice temperatures were generally higher than in WT and the increases were statistically significant at 0h, 1h, 6h and 18h (Fig 2.3.6A, left panel). Inoculation of WT mice with 5 x 10^8 cfu/mouse of *S. epi.* resulted in a decrease in body temperature at 6h similar to that observed in the PBS inoculated mice, it was followed by a regular increase and reached its original level by 24-36h (Fig 2.3.6A, right panel). Despite showing an overall similar pattern, the body temperature changes in the IL-6KO mice were more severe, with significantly lower temperatures than the WT as early as 3h, reaching its lowest point at 6h, and subsequently increasing slowly and reaching similar levels to WT at 18h, and basal levels by 36-48h (Fig 2.3.6A right panel).

To monitor the inflammatory status and recovery of the mice, the serum levels of SAA, which is induced by the pro-inflammatory cytokines IL-1β, TNFα and IL-6, were quantified by ELISA. Systemic SAA levels increased slowly following bacterial injection, transiently peaking at 18h with significantly lower concentrations in the IL-6KO mice (Fig 2.3.6B), confirming the primordial role of IL-6 in the induction of the acute phase response to Gram-positive bacteria, as previously described (Kopf et al., 1994).

Next, the effect of IL-6 deficiency on leukocyte recruitment was tested. As previously observed with the SES model (McLoughlin et al., 2003), and consistent with data from sterile models of inflammation (Xing et al., 1998), IL-6 deficiency resulted in a sustained increase in neutrophil influx in the peritoneal cavity (Fig 2.3.7A). In addition, the neutrophil influx in IL-6KO mice peaked earlier (6h) than in WT (12h), and their numbers were maintained at peak levels and higher than in WT up to 24h. IL-6 deficiency also resulted in a sustained increase in macrophage and modest in lymphocyte numbers (Fig 2.3.7A). Consistent with these findings, the levels of the neutrophil chemoattractant Cxcl1 mRNA, as measured by qRT-PCR, in one parietal peritoneal membrane per time point, and those of the macrophage chemoattractant

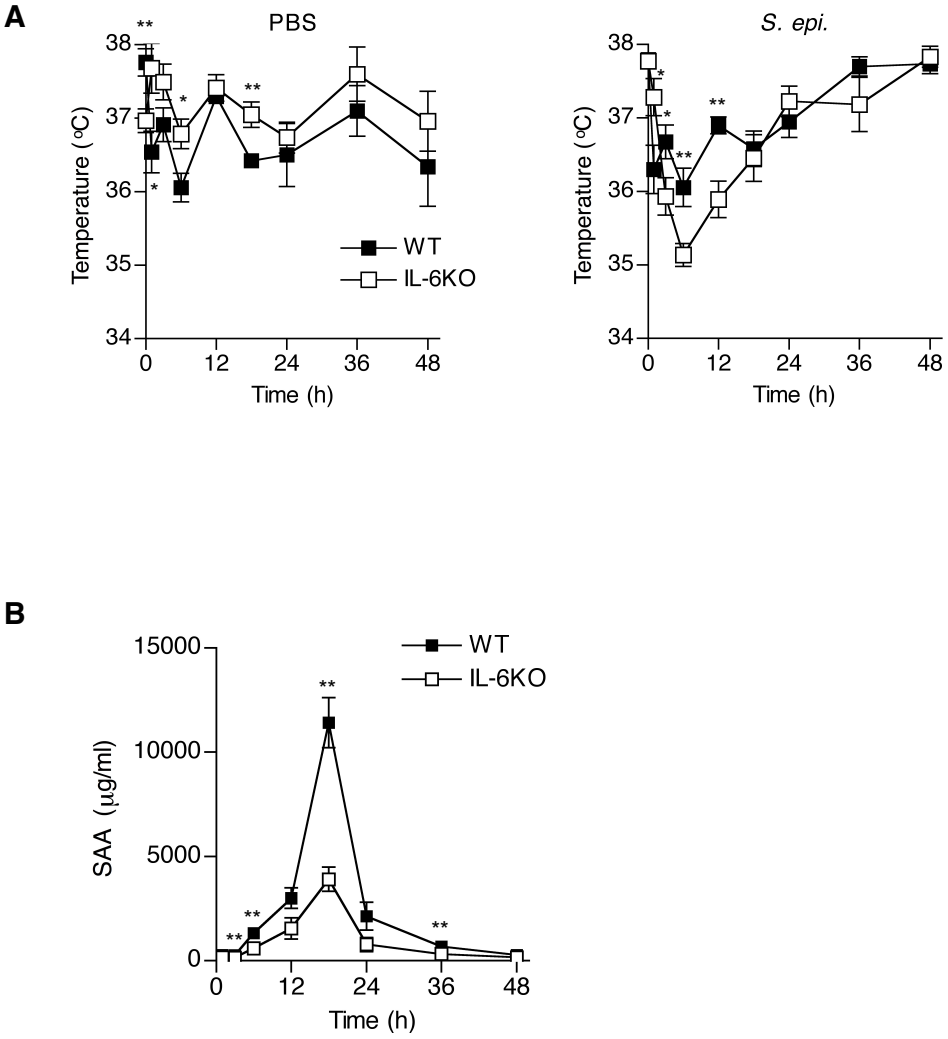

Figure 2.3.6. Effect of IL-6 deficiency on sytemic parameters.
WT and IL-6KO mice were i.p. inoculated with 5 x 10^8 cfu/mouse *S. epi.* or PBS. At the indicated time points, mice temperatures were measured using a rectal probe **(A).** Values represent the mean ±SEM (n=6-12/time point). At the same time points mice were sacrificed and serum levels of Serum Amyloid A (SAA) were determined by ELISA **(B)**. Values represent the mean ±SEM (n=3-6/time point; *, $p < 0.05$; **, $p < 0.01$; WT *vs.* IL-6KO).

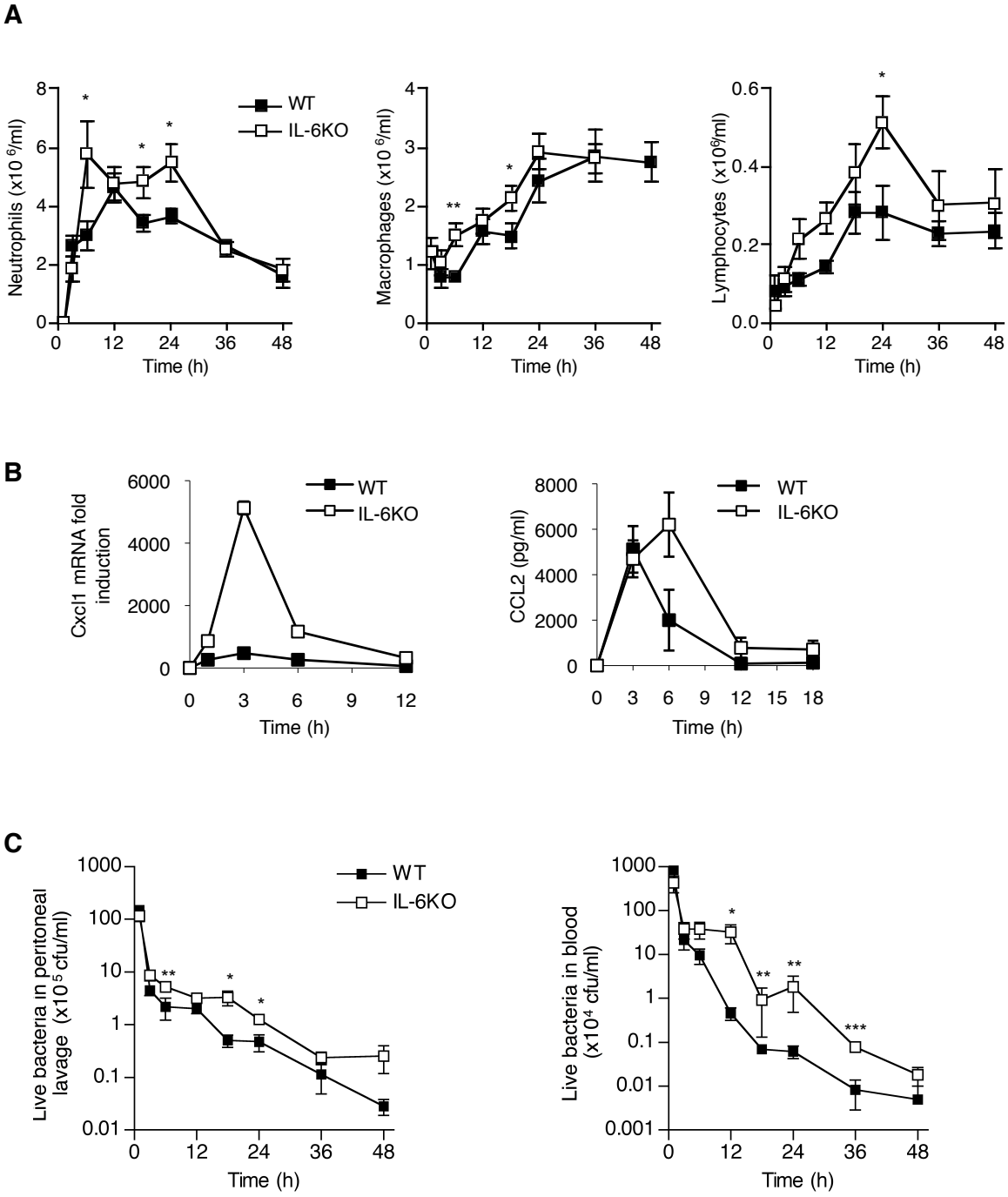

Figure 2.3.7. Effect of IL-6 deficiency on pro-inflammatory responses to *S. epi.* infection.
WT and IL-6KO mice were i.p. inoculated with 5 x 10^8 cfu/mouse *S. epi*. At the indicated time points mice were sacrificed, the peritoneal cavity was lavaged and neutrophil, macrophage and lymphocyte numbers were determined by differential cell counting using cytospin **(A)**, levels of CCL2 expression were determined by ELISA **(B,** right panel**)**, and bacteria in the peritoneal cavity and blood were counted using an automated spiral plater **(C)**. Values are expressed as the mean ± SEM (n=6-12/time point for WT and n=6-16/time point for IL-6KO; *, $p < 0.05$; **, $p < 0.01$; ***, $p < 0.001$; WT *vs*. IL-6KO). At the indicated time points, Cxcl1 mRNA expression levels were quantified by qRT-PCR following total RNA extraction from biopsies of the parietal peritoneal membrane **(B**, left panel**)**. Data represents the results of one experiment.

CCL2, measured by ELISA in the peritoneal cavity, were found increased in IL-6KO mice (Fig 2.3.7B).
To evaluate the impact of IL-6 on bacterial clearance, viable bacterial counts were determined in peritoneal lavages and whole blood at every time point. While both strains resolved this level of infection, Staphylococcal infection in WT mice was more rapidly resolved and brought under control within the first 18-24 hours, whereas IL-6KO mice showed impaired bacterial clearance and increased dissemination of infection into the bloodstream (Fig 2.3.7C).

EMSA analysis of nuclear extracts from the peritoneal membrane of mice was conducted next to assess and compare STAT1/3 activation in WT *vs*. IL-6KO mice. WT mice showed an early and transient STAT1/3 activation, peaking at 3h and decreasing subsequently, with only a residual level up to 48h. STAT1/3 activation in IL-6KO mice was found delayed, peaking at 6h, and reduced in intensity (Fig 2.3.8A). To determine the STAT family members involved, supershift EMSA experiments were conducted using a STAT1 antibody, which causes a loss of DNA binding, and a STAT3 antibody, which induces a classical supershift in electrophoresis mobility. STAT3 supershift was observed, as well as the disappearance of the STAT1 band, which identified STAT3, and to a lower extent STAT1, in both WT and IL-6KO mice (Fig 2.3.8B). Of note, unlike peritoneal stromal cells, SES-induced HPMC activation did not show STAT1 activation (Fig 2.2.5D), suggesting that other cell types, in addition to mesothelial cells, may be involved and/or that *S. epi*., as opposed to SES, may induce the activation of STAT1 as well as STAT3.
NF-κB activation was next investigated in both strains. IL-6KO mice showed higher basal levels of NF-κB activation, and while in WT mice NF-κB activation appeared to be induced earlier (at the 1h time point) than in IL-6KO, the latter showed a sustained level of activation over the 48h period (Fig 2.3.8C).
Notably, qRT-PCR analysis of RNA extracted from the peritoneal membrane of one IL-6-deficient mouse showed increased Tlr2 mRNA expression at 3h compared to that observed in a WT mouse (Fig 2.3.8D).

To examine in more detail the role of IL-6 signalling, IL-6 trans-signalling was reconstituted in the IL-6KO mice by using a genetically engineered sIL-6R-IL-6 fusion protein (IL-6 is covalently linked to sIL-6R) called HYPER-DS-sIL-6R (HDS). IL-6KO mice were i.p. inoculated with *S. epi*. (5×10^8 cfu/mouse) in the absence or presence of increasing doses of HDS. SAA serum concentrations were quantified by ELISA. As described in the previous experiment with WT and IL-6KO mice, SAA levels were greatly impaired in the absence of IL-6 (Fig 2.3.6B), indicating that alterations of systemic activation events is a prominent feature of localised episodes of infection. Following the simultaneous administration of *S. epi*. + HDS, SAA levels were reduced in the presence of HDS, suggesting an increased resolution of the acute phase response (Fig 2.3.9A). The effect of HDS on leukocyte recruitment was examined, and no significant change in neutrophil influx was observed. In comparison, HDS seemed to slightly increase the

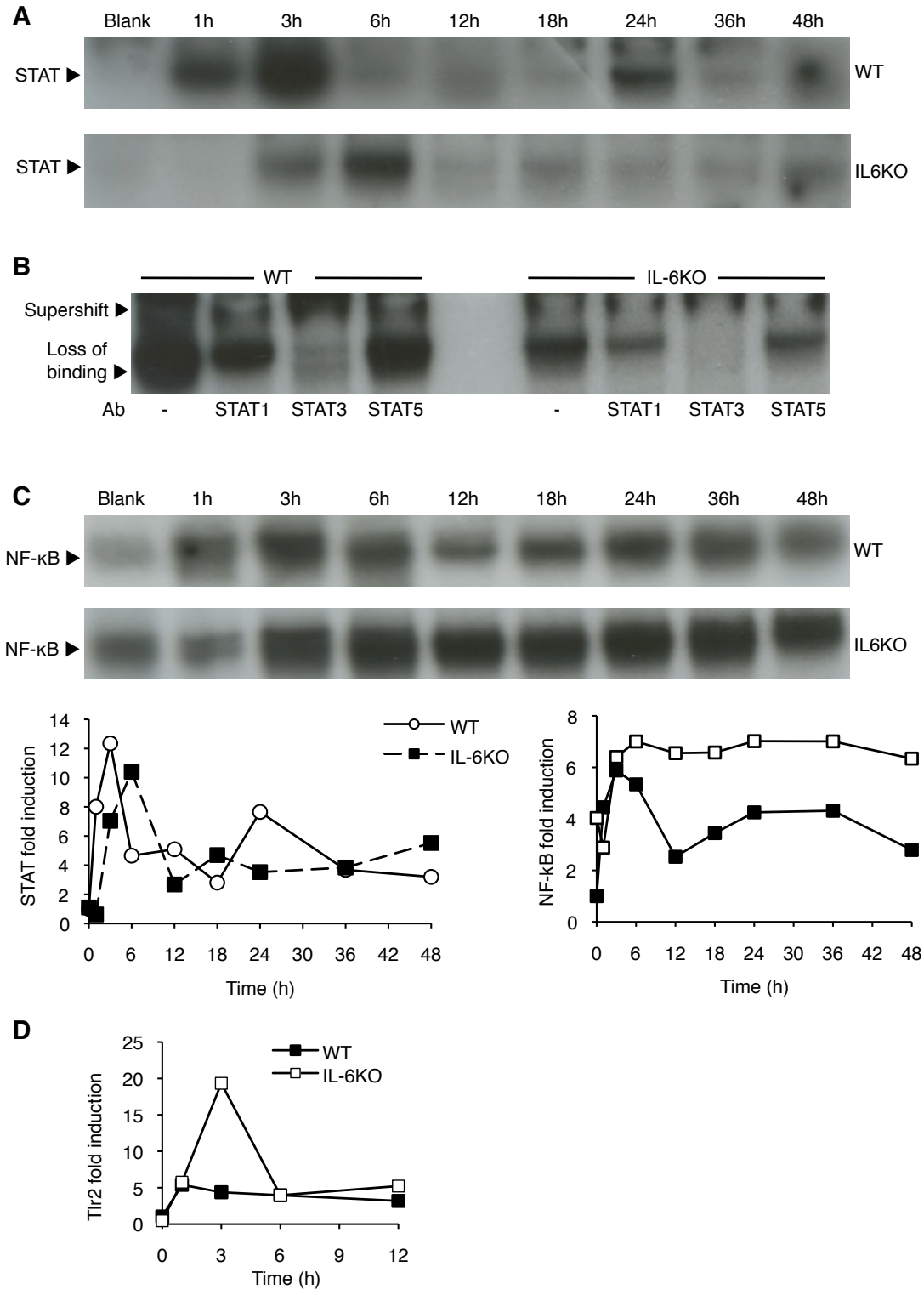

Figure 2.3.8. Effect of IL-6 deficiency on STAT and NF-κB activation, and Tlr2 expression following *S. epi*. infection.

WT and IL-6KO mice were i.p. inoculated with 5 x 10^8 cfu/mouse *S. epi*. At the indicated time points, STAT **(A)** and NF-κB **(C)** activation was analysed by EMSA in nuclear extracts following protein extraction from samples of parietal peritoneal membrane. STAT and NF-κB fold induction relative to PBS-injected animals was calculated from densitometry analysis of the corresponding EMSA gels. Data shown are representative results of three experiments. The composition of the STAT DNA binding complexes was studied by supershift analysis of the nuclear extracts **(B)**. Data shown are results of one experiment. **(D)** At the indicated time points, Tlr2 mRNA expression levels were quantified by qRT-PCR following total RNA extraction from biopsies of the parietal peritoneal membrane. The data shown is the result of one experiment.

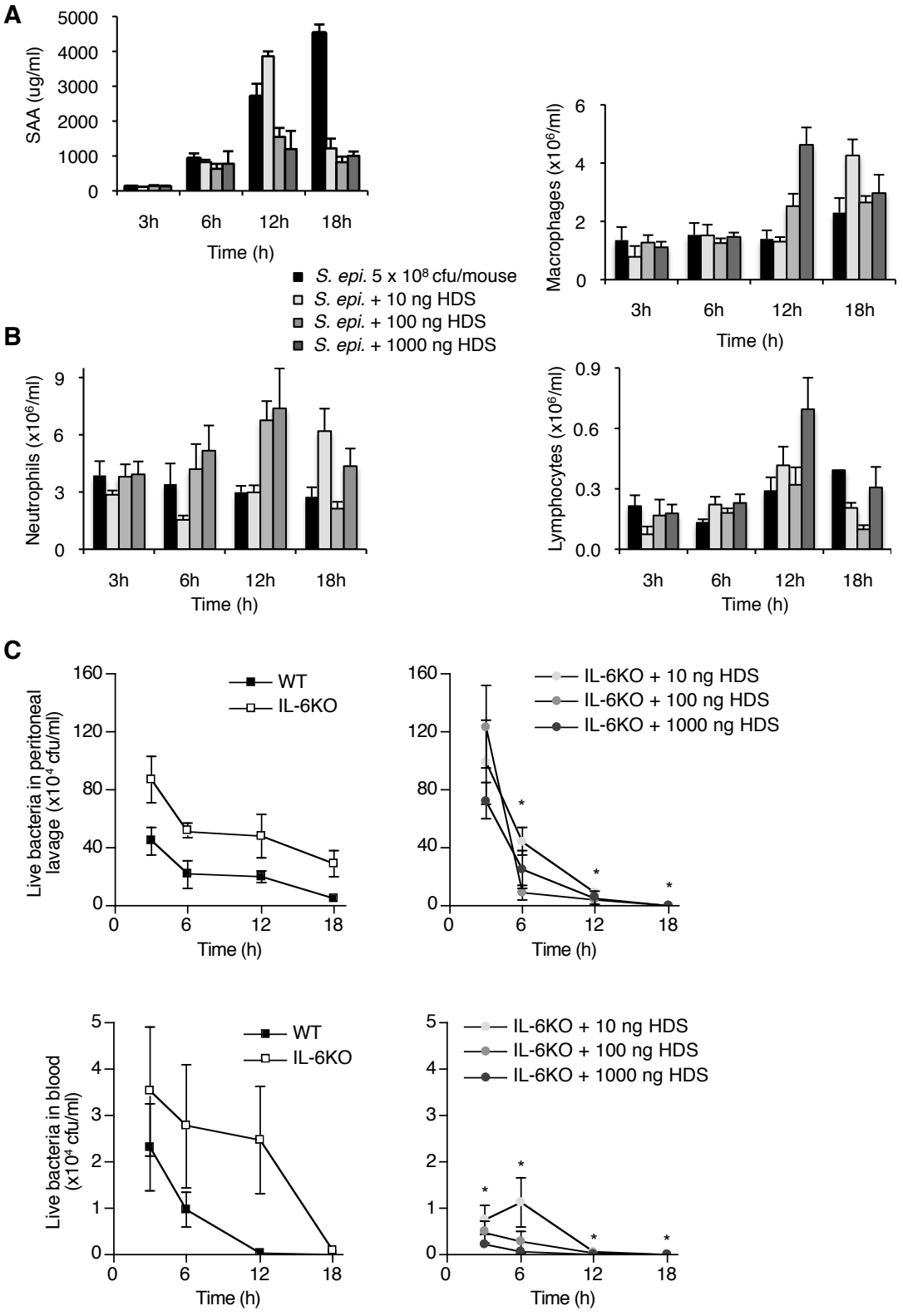

Figure 2.3.9. Effect of the IL-6/sIL-6R complex on leukocyte recruitment and bacterial clearance in the *S. epi.*-induced peritoneal infection model.
IL-6KO mice were i.p. inoculated with 5 x 10^8 cfu/mouse *S. epi.,* in the presence or absence of the indicated doses of the IL-6-sIL-6R complex (HDS). At the indicated time points mice were sacrificed, the peritoneal cavity was lavaged, SAA levels were determined by ELISA **(A)**, neutrophil, macrophage and lymphocytes numbers were determined by differential cell counting using cytospin **(B)**, and bacterial numbers in the peritoneal cavity and blood were counted using an automated spiral plater **(C)**. Values represent the mean ±SEM (n=5-11/time point for WT and n=5-18/time point for IL-6KO; *, $p < 0.05$; IL-6KO *S. epi.* + HDS (all concentrations) *vs.* IL-6KO *S. epi.*).

mononuclear cell numbers in the peritoneal cavity at the later time points (Fig 2.3.9B). To evaluate the impact of IL-6 trans-signalling on bacterial clearance and dissemination, viable bacterial counts were determined in peritoneal lavage and whole blood. Addition of HDS in the peritoneal cavity significantly improved bacterial clearance, in a dose-dependent manner, and reduced bacterial dissemination in the bloodstream, with an indication of increased improvement over the amounts of bacteria in WT mice at the highest doses tested (Fig 2.3.9C).

2.3.5 Discussion

In this section, the role of TLR2 in peritoneal responses to Gram-positive infection and the consequent negative modulatory activity of sTLR2 and its underlying mechanism, *via* inhibition of NF-κB activation, observed *in vitro,* were confirmed by using *in vivo* models of inflammation (SES) and infection (*S. epi.*). sTLR2 did not show however a negative effect on bacterial clearance, despite its negative effect on chemokine production and neutrophil recruitment. By contrast, IL-6 signalling seemed to improve clearance and reduce dissemination of bacteria as well as counteract TLR2-mediated responses by reducing peritoneal leukocyte recruitment and chemokine production. The results also suggest that in addition to leukocytes, non-hematopoietic stromal cells of the peritoneal membrane may be targets for TLR2- and IL-6-mediated activation during acute infection.

sTLR2's negative modulatory effect on NF-κB activation and neutrophil chemoattractant CXCL1 release was demonstrated and correlated with a reduction in neutrophil recruitment, confirming sTLR2 anti-inflammatory capacity. The negative modulatory effect of sTLR2 on NF-κB activation has the potential to affect the expression of many genes coding for immunomodulatory molecules, as observed with the reduced expression of IL-6 and sIL-6R mRNA levels at the peak of neutrophil recruitment. This in turn may explain sTLR2's negative effect on SES- and *S. epi*-induced STAT activation.

Notably, sTLR2 did not affect mononuclear cell trafficking, thus allowing the resolution phase of inflammation to take place. Indeed, the differential effect of sTLR2 on early and late leukocyte recruitment (positive on neutrophils and no effect on monocytes, respectively) and the consequent skewing of the leukocyte influx in favour of mononuclear cells (monocytes/macrophages) may promote efficient removal of senescent neutrophils, allowing the resolution of infection while avoiding the detrimental role of a sustained and high level of neutrophils at the inflammatory site (Raby et al., 2009).

An additional modulatory effect of sTLR2 was observed, its capacity to reduce TLR2 expression levels. This might represent an alternative mechanism used by sTLR2 to modulate TLR2-mediated inflammatory responses. Additional experiments will be required to understand how this effect on TLR2 expression takes place; a positive effect of sTLR2 on the activation or over-expression of molecules involved in protein degradation such as ubiquitination may be worth testing, as they have been described to be responsible for a reduced expression of some TLRs,

although the available data regarding TLR2 is limited and contradictory (Flo et al., 2001; Kurt-Jones et al., 2002).

Despite its anti-inflammatory capacity, sTLR2 did not affect bacterial clearance or the acute phase response in the model tested. The maintenance of efficient peritoneal removal of bacteria in the face of sTLR2 modulation is likely to be due in part to the following: 1) the fact that modulation of neutrophil recruitment by sTLR2 was significant at 12h, the peak of neutrophil influx, when the animals had cleared the infection almost completely, and 2) the activity of a number of other humoral pathway that mediate bacterial clearance and killing, e.g. complement, mannose-binding lectin, Igs as well as cell surface Fc and scavenger receptors. Clearly, *in vivo*, other immune components in addition to sTLR2 make a substantial contribution to bacterial clearance. It is also worth noting that although this study and others confirmed the critical role of TLR2 in the inflammatory response, to Gram-positive bacteria in particular, a number of studies on the potential role of TLR2 in bacterial clearance have led to contradictory results and interpretations. Initial work with TLR2- and MyD88-deficient mice indicated a positive role of TLR2 in bacterial clearance following i.v. Gram-positive infection, potentially only at high bacterial dose (10^7 cfu/mouse), and suggested a role for other TLRs (Takeuchi et al., 2000). Other studies using i.p. inoculated *S. aureus* implicated other receptors as playing more prominent roles, notably the complement receptor C5aR (Mullaly and Kubes, 2006). A more recent and extensive study however identified TLR2 as the main receptor involved in *S. epi.* clearance, but noted a possible TLR2-independent mechanism of TNFα production by peritoneal murine macrophages at high bacterial doses (10^7-10^8 cfu/ml) (Strunk et al., 2010). Conversely, a detrimental role of TLR2 in a polymicrobial sepsis model has been reported, through the inhibition of neutrophil migration towards the site of infection, with an improved survival in TLR2KO mice. This study also showed a differential role of TLR2 depending on the level of infection (Alves-Filho et al., 2009). The type of infecting microorganism(s), the level and route of infection as well as the strain of mice used in the studies may explain, at least in part, the controversial findings. Furthermore, for many organisms studied, several TLRs are activated and can co-operate, as TLR2 and TLR9 in response to *Mycobacterium tuberculosis*, and co-operation with other PRRs such as NOD1 and NOD2 has been implicated in bacterial clearance, but these co-operations still remain to be fully assessed (Gerold et al., 2007; Philpott et al., 2014). Therefore, compensatory mechanisms can exist, rendering it more complex to identify the exact role of a single receptor.

At the onset of *S. epi*. infection and TLR2-driven inflammatory response, many molecules are released and act in parallel, notably cytokines, including IL-6, which possesses pleiotropic roles. IL-6 is implicated in the regulation of body temperature by inducing fever early in the acute phase response - along with IL-1β and TNFα - *via* prostaglandin E2 generation in the brain (Dinarello et al., 1991). However, in some animals, and notably in mice, hypothermia is a feature of disease or infection and predictive of survival (Olfert and Godson, 2000; Soothill et al., 1992). Even though IL-6-deficiency did not greatly affect the body temperature of non-

infected animals, it is not surprising that it should produce a deregulated temperature pattern following infection, as was observed.

Comparative analysis between WT and IL-6KO mice showed that bacterial clearance from the peritoneal cavity was significantly impaired in IL-6KO mice, despite a heightened and more sustained neutrophil infiltration, whilst dissemination into the bloodstream was also increased, demonstrating that the absence of IL-6 was associated with a reduced capacity to fight infection. The increase in neutrophil and macrophage influx correlated with an increased NF-κB activation in the stromal cells of the peritoneal membrane, which was sustained over the 48h time course, as well as with the corresponding increased Cxcl1 mRNA levels and CCL2 secretion. These findings indicate the involvement of peritoneal stromal cells, including mesothelial cells, in leukocyte trafficking through IL-6 trans-signalling, *via* inhibition of NF-κB activation, which was demonstrated in the previous section (section 2.2). These results correlated with previous investigations in various models of pneumonia, sepsis and intracellular microbial infection, which have documented links between IL-6 and host defence against Gram-positive and Gram-negative pathogens, where neutrophil function was affected, whereas mononuclear cell and NK population did not seem impaired (Dalrymple et al., 1995; Dalrymple et al., 1996; Sutherland et al., 2008).

The reduced bacterial clearance in IL-6KO mice, despite the significantly higher number of neutrophils observed in this study, suggested that the anti-microbial neutrophil function was impaired. In this regard, a study using a *S. aureus* septic model *in vivo*, showed that the administration of a recombinant IL-6R improved neutrophil phagocytic function, bacterial clearance and survival, through a STAT3-dependent mechanism (Onogawa et al., 2013). Although delayed and reduced, STAT3 activation was not abolished, as it is triggered by other IL-6 family members, cytokines, hormones and growth factors, but coincided with the early and increased neutrophil infiltration. A protective role of STAT3 in endotoxin-induced inflammation has previously been described, where genetic deficiency of STAT3 demonstrated an impaired cytokine signalling, enhanced NF-κB activation and increased susceptibility to bacterial infections (Welte et al., 2003), as observed in this study.

Following reconstitution of IL-6 signalling in the peritoneal cavity of IL-6-deficient mice, HDS did not seem to influence the neutrophil influx, despite demonstrating an inhibitory effect on neutrophil recruitment in the SES model in other studies conducted in our laboratory. This may be due to the presence of an overwhelming amount of bacteria in a context where the neutrophil chemoattractant CXCL1 is greatly increased. However, when IL-6 signalling was re-established in IL-6-deficient mice, bacterial clearance improved significantly and in a dose-dependent manner, and was also associated with an increased resolution of the acute phase response (SAA), suggesting that increased bacterial killing at the infection site helps to stem development of systemic inflammatory events. This would indicate that IL-6 triggers responses early in the inflammatory cascade that facilitate anti-microbial host defense or the containment of acute resolving infection.

The SES *in vivo* model, described and used in the previous sections, has allowed to study acute inflammation and inflammation-related tissue damage but is restricted in its scope and do not permit to examine certain aspects such as anti microbial activities. This is the reason why the establishment of a new *in vivo* model, using live bacteria, which generated some of the results described in this section, was undertaken in the laboratory and will be described in the following section.

2.4 Development of an *in vivo* model of bacterial peritonitis

There is a need for an improved diagnostic approach to bacterial peritonitis, as this common infectious complication observed in PD may lead to fibrosis and treatment failure. This need requires a better understanding of how the immune response unravels for each specific type of infection (culture negative *vs.* positive and Gram-negative *vs.* Gram-positive infection) (Krediet, 2007; Mactier, 2009). Subsequently, novel therapies could be defined for PD patients with peritonitis. In these patients, Gram-positive bacteria are the main cause of peritonitis and coagulase-negative Staphylococcus represent almost half of all Gram-positive cases. However, Gram-negative bacteria are now responsible for 20 to 30% of all PD-related peritonitis and also a major cause of mortality (Szeto and Chow, 2007; Szeto et al., 2008). The treatment strategy for these organisms is still disputed (Szeto et al., 2008; Szeto et al., 2005), and the need to fully understand the course of immunological events occurring during infection still remains.

In order to better understand the immunological processes taking place during bacterial peritonitis, in our laboratory we have used an *in vivo* model of peritonitis, the SES model (Hurst et al., 2001; McLoughlin et al., 2003). Other *in vivo* models of peritonitis and sepsis have been described such as cecal ligation and puncture model of peritonitis/sepsis (Spight et al., 2008), zymosan-induced peritonitis (Kolaczkowska et al., 2006) and polymicrobial peritonitis (Celik et al., 2001). However, some of them are only used as a mean to study the inflammatory response in the peritoneal cavity and systemically in the blood (Celik et al., 2001). Consequently, they do not provide a representation of what is observed in PD patients (Kolaczkowska et al., 2006). Therefore, these models remain limited and inappropriate in the study of PD. As a consequence, the need for a more clinically relevant peritonitis model arose, which aimed at recreating the specific clinical situation of PD patients. This explains why in the present study *in vivo* models using an intraperitoneal route of infection/inflammation were chosen, as the inflammation in these patients occurs first in the peritoneal cavity, remaining local or spreading to other organs subsequently.

In this section, the development of a model that reflects an acute resolving bacterial peritonitis, and which allows a close inspection of both local and disseminated infection is described. This model has been used in a number of experiments described in the previous sections. The organisms chosen for this model are representative of the most common bacteria encountered in PD-related peritonitis: Gram-positive bacteria coagulase-negative *Staphylococcus epidermidis* and *Staphylococcus aureus* and Gram-negative *Escherichia coli.* Based on the SES *in vivo* model, which has been used and refined over several years, a new model using live bacteria was developed. The existing model needed technical adaptation from the SES model to address the differences due to the use of live organisms, and a specific design and refinement to reach the level of infection desired. It also required to be controlled, with the

infection spreading moderately and resolving, unlike some existing models of sepsis, which are systemic and often have death as an end point.

2.4.1 Method

2.4.1.1 Reagents and Equipment

See Chapter 4, Material and Methods.

2.4.1.2 Animals

WT C57BL/6 mice were provided by Charles River and Harlan. Following the establishment of the model in mice from Charles River, it was then tested on mice from Harlan, as mice from the latter provider had been used previously in some other experiments and gave different results. The model established using Harlan mice was however consistent with that using Charles River's, showing similar patterns of temperature variation, leukocytes recruitment and bacterial dissemination. For consistency, we selected Charles River mice to carry out the experiments described in this thesis. Whenever possible, each experiment was conducted with 50% males and 50% females.

2.4.1.3 General aseptic technique

Before and after any procedure was carried out, work surfaces were thoroughly cleaned with 1% (v:v) hypochlorite and gloved hands sprayed with 70% (v:v) ethanol. All waste was disposed of in autoclavable bags.

2.4.1.4 Bacteria

The different strain of bacteria used for this model were kept in a dormant state at -80^{o}C as 50% glycerol stocks, and experimental batches maintained at room temperature on agar slopes.

2.4.1.5 Agar plate inoculation and incubation

Using a flame-sterilised loop, bacteria were aseptically transferred to an agar plate, which was streaked to isolate single colonies. The plate was incubated at 37^{o}C for 48h, with a check for growth after 24h.

2.4.1.6 First and second broth inoculation and incubation

A single colony of *S. epi* collected from an agar plate with a flame-sterilised loop was aseptically inoculated in 10 ml of liquid broth (see Material and Methods, section 4.1) and incubated 24h at 37^{o}C in a shaking incubator. This bacteria culture was then used to inoculate nutrient broth for each specific experiment (100 μl/10 ml broth) and left initially for 18h, and later reduced to 15h, in the shaking incubator. This overnight bacterial culture consistently grew to approximately 1 x 10^{9} cfu/ml following 15h incubation (see section 2.4.2.1a), consistent with previous reports (Masuda and Tomioka, 1978) and with the reported doubling time of 25-30 min (Irwin et al.,

2010). Consequently, calculations of bacteria preparations for injection were made assuming this estimated concentration, verified by OD reading, agar plate count and ATP measurement for each individual experiment (see section 2.4.1.8). Using the same protocol, *Staphylococcus aureus* (*S. aureus*) reached 5 x10^9 cfu/ml following 15h incubation (see section 2.4.2.1b) and *Escherichia coli* (*E. coli*) 2 x 10^9 cfu/ml (see section 2.4.2.1c). All inoculums were prepared according to the procedure described for *S. epi.*, and the protocol described in the following subsections is based on the use of *S. epi*.

2.4.1.7 Bacteria preparation for inoculation

Bacteria were harvested during their log phase growth after 15h incubation and spun down for 10 min at 4,000 x g at room temperature. The supernatant was carefully removed, avoiding disturbing the pellet, which was washed in sterile PBS. The bacteria were spun again and resuspended in PBS for a total of 3 times. A final centrifugation at 4,000 x g for 10 min at room temperature was done before resuspending the pellet in the volume of sterile PBS calculated for each specific experiment. Bacterial suspensions were then left on ice in readiness for immediate i.p. administration.

2.4.1.8 Inoculum verification

a. OD measurement

Assuming a concentration at 1 x 10^9 cfu/ml following 15h incubation, serial dilutions were prepared (1 x 10^9 to 1 x 10^4 cfu/ml) in PBS, the OD were measured in a spectrophotometer set at 600 nm and compared with the counts obtained by agar plate reading (see section 2.4.1.8b). Table 2.4.1 below shows representative OD values obtained.

Table 2.4.1 Representative OD values of overnight bacterial cultures

cfu/ml	OD	OD	OD	OD	OD
1 x 10^9	1.44	1.575	1.121	1.016	1.117
1 x 10^8	0.164	0.197	0.126	0.132	0.158
1 x 10^7	0.023	0.023	0.006	0.003	0.015
1 x 10^6	0.004	0.006	0.003	0.001	0.001
1 x 10^5	0.001	0.004	0	0.0015	0
1 x 10^4	0	0.005	0	0	0

b. Bacterial counts on agar plate

Assuming a concentration at 1 x 10^9 cfu/ml following 15h incubation, the specific dilution used for each experiment was manually or spiral plated on an agar plate to confirm the exact concentration obtained. The plate was incubated at 37^{o}C overnight or up to 24h, until colonies were big enough to be counted.

c. ATP bioassay

An alternative technique used for assessing the amount of bacteria to be injected was the determination of ATP levels of overnight bacterial cultures. One millilitre of each bacterial dilution (1×10^9 - 1×10^4 cfu/ml) was used for ATP assays. All samples were centrifuged at 17,900 x g for 10 min, the supernatants were discarded, and 100 μl of Benzalkonium Chloride-extract/EDTA were added to the pellets followed by 100 μl of 25 mM Hepes/10mM EDTA. The samples were then stored at -20°C until analysis using the ATP Bioluminescence Assay Kit CLS II (Roche Diagnostics).

2.4.1.9 Preparation of injection

a. Mice body temperature readings

According to the Home Office and animal license regulations, if the mice become hypothermic (<32°C) for prolonged periods (over 12h), they should be culled and excluded from the study. Body temperature readings were carried out on scruffed animals using a thermometer probe, previously cleaned with 70% (v:v) ethanol and coated with lubricating gel, which was inserted rectally and hold until the reading was stable. The probe was cleaned between each animal. Before injecting the mice with bacteria, their body temperature was recorded and monitored at indicated time points throughout the procedure, as a measure of animal health status.

b. Anaesthetisation of mice

A group of 5 to 6 mice was anaesthetised with isoflurane in an anaesthetic chamber with an oxygen flow of 2.5 to 3 l/min, following the local animal house regulations. Once unconscious and their breathing rate had slightly decreased, the isoflurane level was lowered to maintain the mice in an unconscious state.

2.4.1.10 Intra peritoneal injection of anaesthetised mice

As soon as the mice were unconscious, they were taken one at a time out of the anaesthetic chamber, their lower abdomen was sprayed with 70% (v:v) ethanol, and they were injected with the indicated bacterial inoculum via the intraperitoneal route. Mice were then put in their respective experimental cage and monitored for full recovery from anaesthesia.

2.4.1.11 Mice body temperature readings and culling process

At designated end time points, the body temperature of each mouse was taken as described above (section 2.4.1.9a). They were put in a CO_2 chamber to be culled in batches of 2 to 3 mice with a CO_2 flow rate of 2 to 2.5 l/min.

2.4.1.12 Blood retrieval by cardiac puncture

Mice were sprayed with 70% (v:v) ethanol prior to proceeding to cardiac puncture. A needle coated with heparin to prevent adverse clotting was inserted in the heart and up to 0.6 ml of

blood drawn. The volume obtained was recorded, to allow for dilution volumes to be considered when calculating bacterial counts. Blood was kept on ice until further processing.

2.4.1.13 Peritoneal lavages

An incision was made in the abdominal skin, which was pulled away to completely expose the peritoneal membrane. Two millilitres of cold PBS was injected in the peritoneal cavity with a syringe via a flexible catheter, and the membrane was massaged to ensure sufficient flushing of the cavity. The liquid in the cavity was carefully aspirated to collect the cell suspension, and the recovered volume recorded. Lavages were kept on ice for further processing.

2.4.1.14 Peritoneal membrane recovery for bacterial count

About 2 cm^2 of membrane was cut out and placed in 1 ml of sterile ice cold PBS, homogenised, then spread on an agar plate and incubated at 37^oC for 24h to quantify bacterial growth.

2.4.1.15 Kidney recovery for bacterial count

The mice's kidneys were carefully cut out and the renal capsule, ureter and blood vessels removed. They were then placed in 1 ml of sterile ice cold PBS and kept on ice and homogenised. Subsequently, the kidney homogenate was spread on an agar plate to quantify bacterial levels following 24h growth at 37^oC.

2.4.1.16 Sample processing

The various samples collected (blood, peritoneal lavages, kidneys and peritoneal membrane) were then processed for leukocyte and bacterial counts and storage.

Before establishing the appropriate dose of bacteria to use and refine the model to suit the requirements, the most adequate techniques to measure the different outputs in this model had to be determined.

a. Technical issue: haemocytometer *vs.* cell counter counts

First, two different techniques to count the cells from the peritoneal lavage were compared. Fig 2.4.1, Fig 2.4.2 and Fig 2.4.3 illustrate the results obtained after counting with a haemocytometer or by using a Coulter counter. As shown in Fig 2.4.1A and C, Fig 2.4.2A and C and Fig 2.4.3A and B, following injection of increasing numbers of bacteria, the counts with the haemocytometer were consistently lower than those obtained with the Coulter counter, when looking at total cell counts or a specific cell type. Statistical analysis of the data was conducted by using the Bland-Altman test, which assesses the agreement between two methods of measurement. Fig 2.4.1B and D, Fig 2.4.2B and D show that the two methods are not equivalent, as there is an imbalance between them, indicated by the % of difference concentrated on only one side of the x axis. It was difficult to assess exactly how the differences between the two methods originated, but despite these divergences, the overall results with

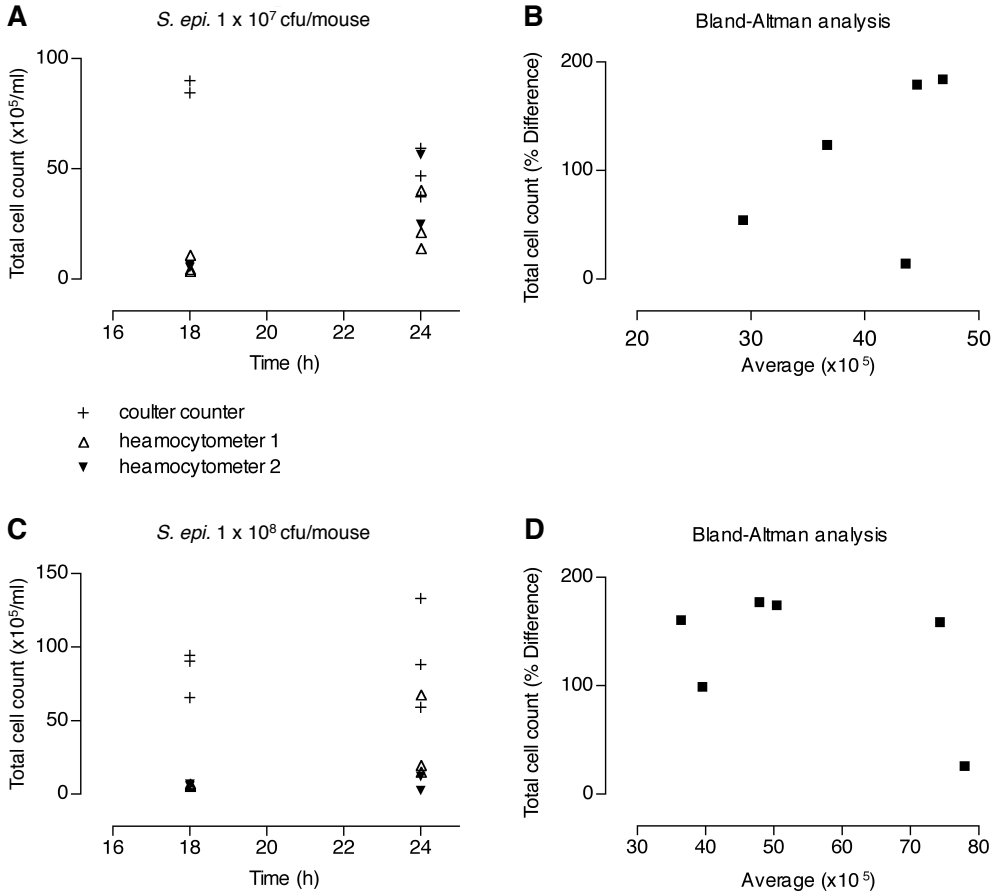

Figure 2.4.1. Comparison of two methods for cell counting.
Mice (n=3/condition) were i.p. injected with the indicated doses of *S. epi*. At the indicated time points, mice were sacrificed, the peritoneal cavity was lavaged and leukocyte numbers were counted using a Coulter counter or a heamocytometer **(A,C)**. A Bland-Altman statistical test was used to analyse the data **(B,D)**.

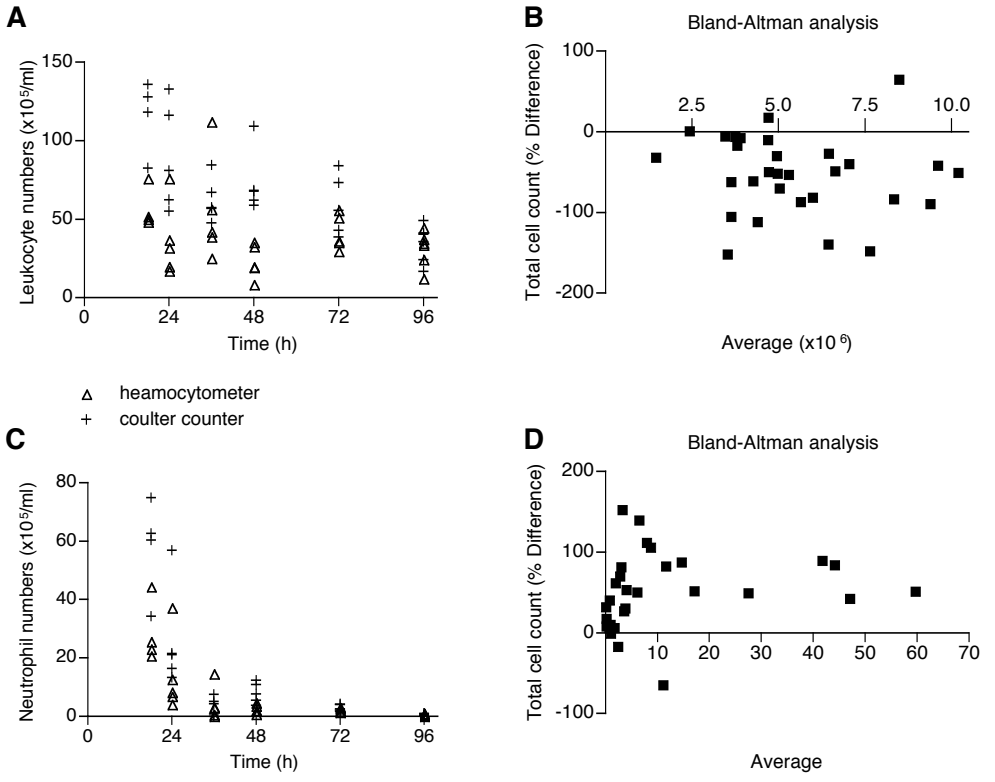

Figure 2.4.2. Optimisation of cell counting.
Following a time course of infection with *S. epi.* (1 x 10^8 cfu/mouse), total cell **(A)** and neutrophil **(C)** numbers were determined using the two indicated methods. A Bland-Altman statistical test was used to analyse the data **(B** and **D)** (n=5/condition).

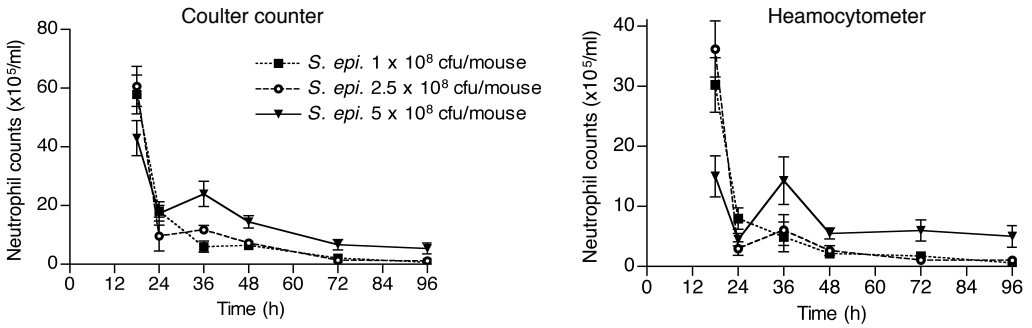

Figure 2.4.3. Determination of neutrophil numbers using two counting methods.
Mice were i.p. inoculated with the indicated doses of *S. epi*. At the indicated time points, mice were sacrificed, the peritoneal cavity was lavaged and total leukocyte numbers were determined by using a Coulter counter or a heamocytometer as indicated. Neutrophils in the preparation were identified by differential cell counting on cytospined slides. Their numbers were estimated according to the corresponding leukocyte counts. Values represent the mean ±SEM (n=5/time point).

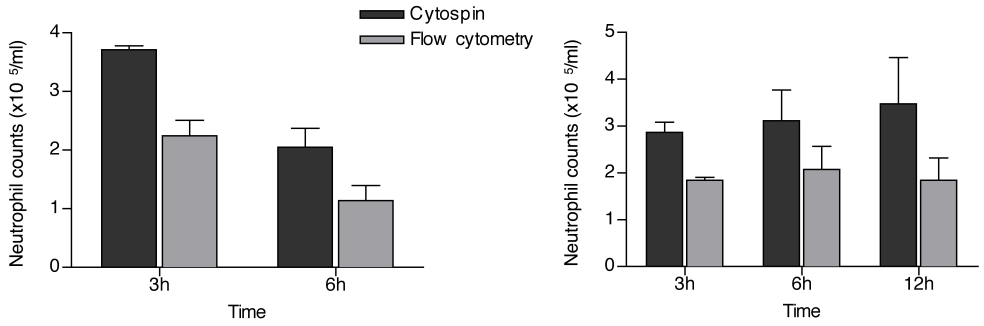

Figure 2.4.4. Comparison of two methods to differentiate leukocyte populations.
Mice were i.p. inoculated with *S. epi.* (5 x 10^7 cfu/mouse). At the indicated time points, mice were sacrificed, the peritoneal cavity was lavaged and neutrophil numbers were determined by differential cell counting using cytospin or flow cytometry. Left and right panels show the results of two independent experiments. Values represent the mean ±SEM (n=2-4/time point).

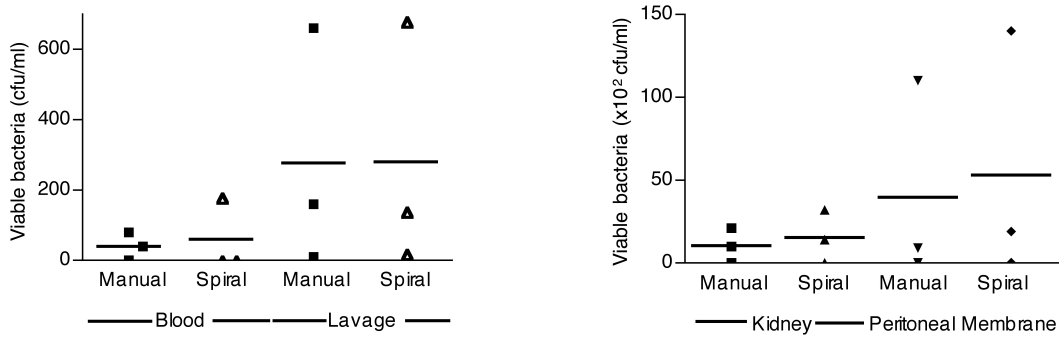

Figure 2.4.5. Comparison of two methods to determine bacterial dissemination.
Mice (n=3/condition) were i.p. inoculated with *S. epi.* (1 x 10^7 cfu/mouse). Subsequently, mice were sacrificed and bacteria were counted in the indicated organs by manual spreading on agar plates or using an automated spiral plater.

both methods were similar, as shown in Fig 2.4.2C or by the comparison of neutrophil recruitment in Fig 2.4.3A and B. Subsequent to this comparison, we used the Coulter counter to determine cell numbers, as this was a faster method, more appropriate to the setting of our protocol and time constrictions.

b. Technical issue: Differential cell counting by cytospin *vs.* flow cytometry

To distinguish leukocyte populations in the peritoneal lavages, differential cell counting (DCC) following cytospin or using flow cytometry may be performed. Fig 2.4.4 shows the results of two experiments where the two techniques were used and compared. At the indicated times points in each experiment, peritoneal lavages were divided in half and neutrophil, macrophage and lymphocyte numbers were determined using either technique. Comparison of results in Fig 2.4.4 (left and right panels) shows that lower counts were obtained by using flow cytometry than cytospin. One reason might be that some cells had been lost during staining in preparation for flow cytometry. Given these results, and considering the cost of flow cytometry and time necessary to stain the cells, as well as the long time courses of the experiments (involving overnight work), it was decided to determine cell numbers by the cytospin method.

c. Technical issue: manual *vs.* spiral plating of bacteria

In order to determine the bacterial load in the different tissues over the time during infection, the organs were homogenised and spread manually on agar plates. A spiral plater was acquired later (Whitley Automated Spiral Plater II, Don Whitley Scientific Limited, UK), which automatically spreads the liquid in a concentric and decreasing manner, facilitating counting (high counts in particular). Fig 2.4.5 shows the result of using the manual and automated techniques on the same experiment. Although the counts are comparable, manual spreading resulted in slightly lower counts than spiral spreading, which might be due to an increased difficulty to identify separate colonies when spreading manually and thus less evenly. Spreading the cells manually is also a lengthier and less accurate technique, while spiral plating standardises counting methods and decreases consumables costs. Hence spiral plating was used in all subsequent experiments.

2.4.1.17 Microbiology, dilutions, plating, incubation and counting

In most experiments only lavages and blood were assessed for bacterial load. For spiral plating, 50 μl of neat sample were used. Plates were incubated at 37°C for 24h to 48h before storage at 4°C prior to cell counting using a specified template and counts converted with appropriate counting tables from the spiral plater user manual (Don Whitley Scientific Limited, WASP II user manual). Later on, this process was done using a plate counter (Don Whitley Acolyte plate counter) and software set for counting pour plates with the appropriate dilutions factored into the program. The calculations were also averaged for duplicate samples. Remaining samples of peritoneal lavages were centrifuged, rendered cell-free and supernatants stored at -80°C for further analysis by ELISA (see Material and Methods, section 4.13). Leukocyte pellets were

resuspended in PBS prior to analysis by flow cytometry (see Material and Methods, section 4.13). Blood samples were centrifuged. The serum (cell-free supernatant) was stored at -80^{o}C for further analysis by ELISA. For DCC following cytospin, slides were let to dry at room temperature following centrifugation, and later stained with modified Wright-Giemsa for 30 sec, followed by a 5 min wash in water. Neutrophils, macrophages and lymphocytes in the preparations were identified according to their morphology and staining pattern and counted under a phase constrast microscope. Fig 2.4.6 shows a representative slide used for DCC by the cytospin technique.

2.4.2 Results

Fig 2.4.7 recapitulates the protocol followed to develop the new *in vivo* model.

2.4.2.1 Standardisation-Bacterial growth

a. *Staphylococcus epidermidis*

One bacterium focus of the present study was *S. epi.,* since amongst coagulase-negative staphylococcus organisms, it remains a predominant cause of peritonitis in PD patients (Li et al., 2010). Initially, an overnight culture of 1 x 10^9 cfu/ml was established in liquid broth and the OD at 600 nm was measured. Dilutions of 1 x 10^5, 1 x 10^6 and 1 x 10^8 cfu/ml were prepared in 10 ml broth and the OD measured. Each of these cultures was returned to a shaking incubator at 37^{o}C and the OD measured every hour for 7h and then at 24h. Fig 2.4.8 (left panel) shows that only the 1 x 10^8 cfu/ml culture grew from the start in a linear fashion up to 24h, whereas the 1 x 10^5 and 1 x 10^6 cfu/ml cultures took 5h to 6h to start growing. At 24h, the bacterial counts of these cultures suggested that they had stopped growing in a linear fashion. Subsequently, 1 x 10^6 and 1 x 10^8 cfu/ml dilutions of the overnight 1 x 10^9 cfu/ml culture were prepared and the OD monitored every hour over a 10h period (Fig 2.4.8 right panel). As in the previous experiment, the 1 x 10^6 cfu/ml culture took 4h to start growing, whereas the 1 x 10^8 cfu/ml culture grew from the start. Both cultures showed a linear growth for about 7h. From the overnight culture, an additional 1 x 10^4 cfu/ml dilution was prepared and 1, 10 and 100 µl aliquots were plated on agar and the bacterial numbers counted following overnight incubation (Table 2.4.2).

Table 2.4.2 Correlation between nominal bacterial numbers and counts on plates following overnight growth.

Volume of 1 x 10^4 cfu/ml dilution	Expected bacterial numbers	Actual bacterial counts on plate
1 µl	10	16
10 µl	100	94
100 µl	1000	624

The counts were similar to the numbers expected from a 1 x 10^4 cfu/ml culture, indicating that the estimated concentration of the starting dilution (1 x 10^9 cfu/ml) was accurate. Following two additional experiments that confirmed the correlation between OD readings and bacterial

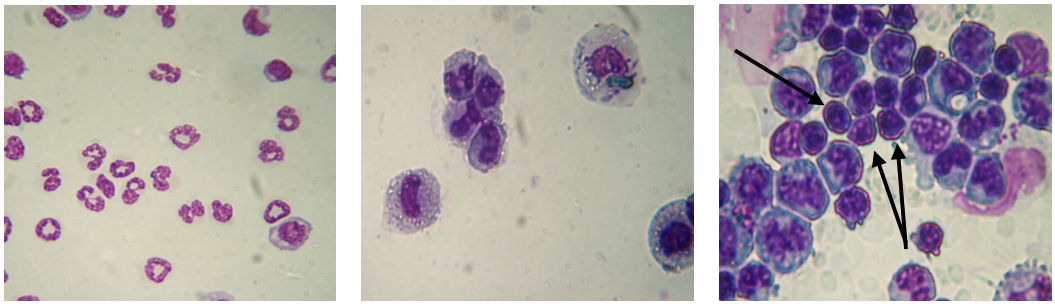

Neutrophils | Macrophages | Lymphocytes

Figure 2.4.6. Leukocytes on cytospin preparations.
Neutrophils, macrophages and lymphocytes (indicated by black arrows) were identified according to their morphology and staining (Wright-Giemsa) pattern in cytospin preparations from peritoneal lavages of mice i.p. injected with *S. epi., S. aureus* or *E. coli.*

Bacterial growth optimisation

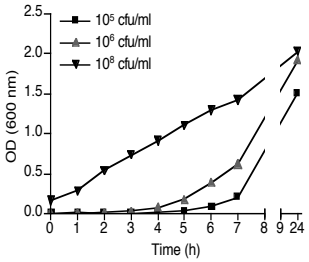

Dose determination/ Dose optimisation

OD reading → Bacterial counts

OD reading = cfu/ml

Experiment

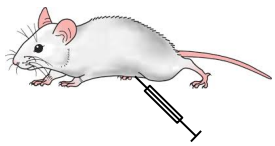

Injection of increasing dose of bacteria
Checking dissemination in different organs and blood
Checking resolution of inflammation

Monitoring the effect of increasing doses of bacteria

During experiment:	Monitoring survival Monitoring temperature throughout the experiment
Bacterial dose optimisation:	Monitoring bacterial dosage for injection and organ dissemination Adjusting bacterial dose

---

Figure 2.4.7. Summary of the process followed for setting up a live bacteria infection model using *S. epi.*, *S. aureus* and *E. coli.*

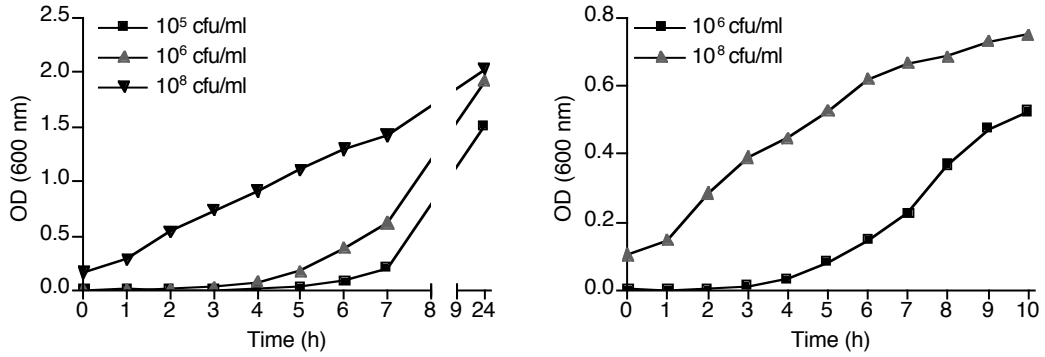

Figure 2.4.8. *S. epi.* (ATCC 12228) growth curve.
From an overnight *S. epi.* 1 x 10^9 cfu/ml culture, several dilutions were prepared as indicated, and at the indicated time points the growth of the cultures was monitored by OD reading. Results shown in left and right panels correspond to two independent experiments.

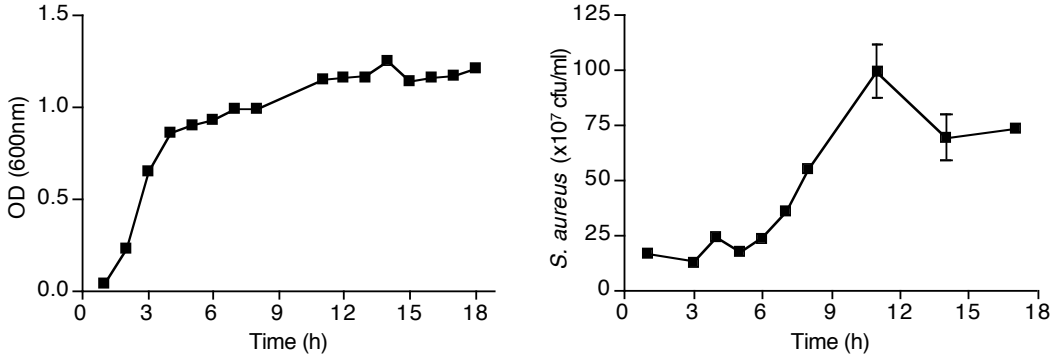

Fig 3.2.9. *S. aureus* (ATCC 25923) growth curve.
Bacterial cultures of *S. aureus* with defined ODs measured at the indicated time points (left panel) were grown on agarose in triplicate for 24h and bacterial numbers were determined (right panel).

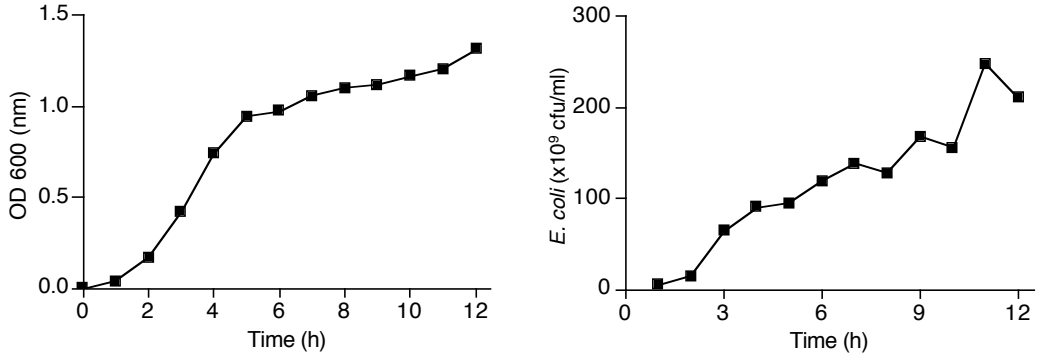

Figure 2.4.10. *E. coli* (ATCC 25922) growth curve.
Bacterial cultures of *E. coli* with defined ODs measured at the indicated time points (left panel) were grown on agarose in triplicate for 24h and bacterial numbers were determined (right panel).

numbers, bacteria was taken from an agar slope and cultured for 15h. This protocol was adopted as part of the final setting of the *in vivo* model and used in the methodology described under sections 2.4.1.5 and 2.4.1.6.

b. *Staphylococcus aureus*

S. aureus is another leading Gram-positive bacteria responsible for peritoneal infection and represents a serious complication in PD (Szeto et al., 2007). Understanding *S. aureus*-triggered peritonitis is a prority, as its clinical course has not yet been fully clarified. Following establishment of the *S. epi.* infection model, the same procedure was used to establish a corresponding model with *S. aureus* (ATCC 25923), choosing a mild and commonly used strain for quality control and positive control in the evaluation of specific agar plates. Bacteria were cultured as indicated previously in section 2.4.1.5 and adapted section 2.4.1.6. To study bacterial growth over time, an overnight growth between 1 x 10^8 and 1 x 10^9 cfu/ml was assumed, and a 1:10 dilution was prepared, cultured and growth monitored over 18h with the OD measured every hour (Fig 2.4.9 left panel). The culture grew from the start, with a sharp increase in concentration in the first 4h, followed by a slower growth during the next 10h and a plateau in the last 4h. At defined time points, a sample of the culture was taken and plated in triplicate to determine the bacterial concentration (Fig 2.4.9 right panel). The results indicated that the culture reached about 1 x 10^9 cfu/ml by 12h, subsequently, the concentration decreased slightly. Five liquid broth cultures were established, the OD of the overnight (last 15h) culture was measured, and a sample of the culture was plated in triplicate to verify the bacterial concentration. Table 2.4.3 shows the results obtained:

Table 2.4.3 OD values and bacterial counts of a 15h *S. aureus* culture

OD	counts (cfu/ml)	counts (cfu/ml)	counts (cfu/ml)	Average counts (cfu/ml)
1.144	4.23 x 10^9	4.45 x 10^9	5.77 x 10^9	4.82 x10^9
1.153	4.43 x 10^9	5.26 x 10^9	5.47 x 10^9	5.05 x10^9
1.192	6.64 x 10^9	5.99 x 10^9	4.13 x 10^9	5.59 x10^9
1.153	4.23 x 10^9	4.16 x 10^9	5.18 x 10^9	4.52 x10^9
1.192	5.55 x 10^9	5.52 x 10^9	5.62 x 10^9	5.56 x10^9
			Total average	*5.11 x10^9*

Based on these results, it was concluded that a 15h culture reached approximately 5 x 10^9 cfu/ml. ATCC documentation indicated that the culture protocol followed for *S. epi.* preparation was also appropriate for *S. aureus,* which was confirmed by the results of bacterial growth.

Of note, OD measurements of bacterial growth were initially complemented with ATP measurements of serial dilutions of bacteria, as described in section 2.4.1.8c. However, following measurements of ATP activity in more than 10 experiments, this technique proved to be unreliable and it was abandoned.

c. *Escherichia coli*

PD-related peritonitis and its severe complications are also caused by Gram-negative bacteria, with *E. coli* alone being responsible for almost 7% of culture positive episodes (Szeto and Chow, 2007). As previously described for the two other strains of bacteria tested, a growth curve of *E. coli* (ATCC 25922) was established. A bacterial culture was prepared as indicated in section 2.4.1.5 and adapted section 2.4.1.6. To study the bacterial growth over time, a 1:100 dilution of an overnight culture was prepared. The new culture was monitored over a 12h period, and the OD measured every hour (Fig 2.4.10 left panel). The culture grew from the start, with a regular increase in concentration for about 6h, followed by a slower growth during the subsequent 6h. At defined time points, a sample of the culture was plated and checked for the bacterial concentration (Fig 2.4.10 right panel). The results showed that the culture reached a growth peak of about 2 x 10^9 cfu/ml after 11h-12h, This concentration is consistent with what has been reported in the literature (Masuda and Tomioka, 1978).

2.4.2.2 *Staphylococcus epidermidis* infection

A series of experiments were conducted to develop a model of acute peritonitis. In defining the appropriate dose of bacteria, it was taken into consideration that a substantial level of inflammation should be induced without being lethal, and that the dissemination in other organs and blood should be kept limited.

a. Pilot study 1: Aseptic techniques and bacterial dissemination

Pilot study 1 was designed to ascertain the optimal aseptic technique for injections and evaluate bacterial dissemination. Two groups of five animals were i.p. injected with PBS, with the injection site either swabbed or sprayed with 70% (v:v) ethanol before injection. The body temperature (rectal probe) and leukocyte counts in the peritoneal cavity (peritoneal lavages) were monitored over a 24h and 48h period, respectively. As shown in Fig 2.4.11A, the baseline temperature (pre-inoculation) for the two PBS groups differed significantly, with the swabbed group showing lower temperatures. The cause of this discrepancy is not clear. However, at 6h and 24h both groups showed similar values. Leukocyte numbers were similar after 48h, with no sign of inflammation in the lavages (Fig 2.4.11B). Given these similar results, the mice abdomen was sprayed with ethanol in subsequent experiments.

In order to determine the appropriate dose of bacteria to inject that reflects the clinical setting of PD-related peritonitis, and to assess the level of dissemination in different organs, 1 x 10^7 or 1 x 10^8 cfu of *S. epi.*/mouse were injected. Similar body temperature was observed in both groups (5 mice/group) over the time course (Fig 2.4.12A). As expected, the peritoneal leukocyte counts show more inflammation i.e., higher neutrophil and macrophage numbers after 48h, when 1 x 10^8 cfu/mouse were injected (Fig 2.4.12B). Blood, peritoneal lavages, peritoneal membrane and kidney samples were collected. All material retrieved was spread on agar plates to assess

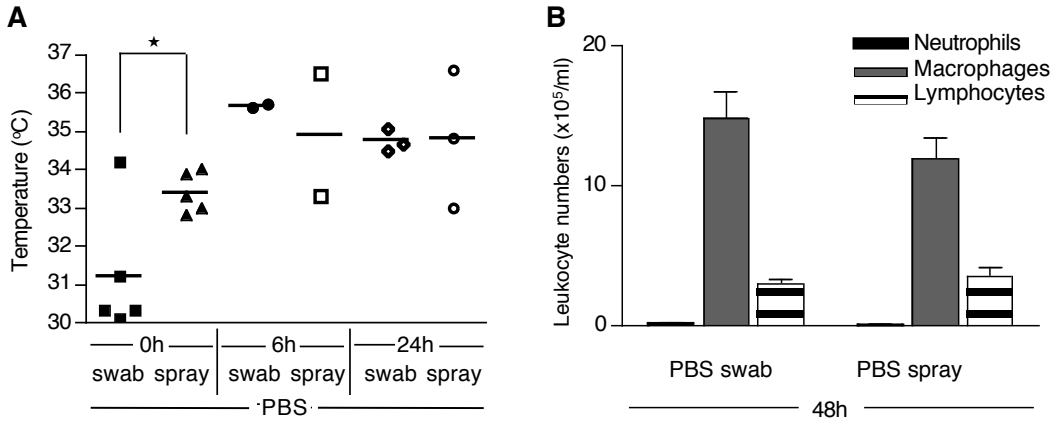

Figure 2.4.11. Evaluation of two aseptic techniques.
Before i.p. injection of PBS, mice abdomen were swabbed or sprayed with ethanol as indicated. At the indicated time points, mice temperatures were measured using a rectal probe (*, p <0.05) **(A)**. At 48h, mice were sacrificed, the peritoneal cavity was lavaged and leukocyte numbers were determined by differential cell counting using cytospin **(B)**. Values represent the mean ±SEM (n=5/condition).

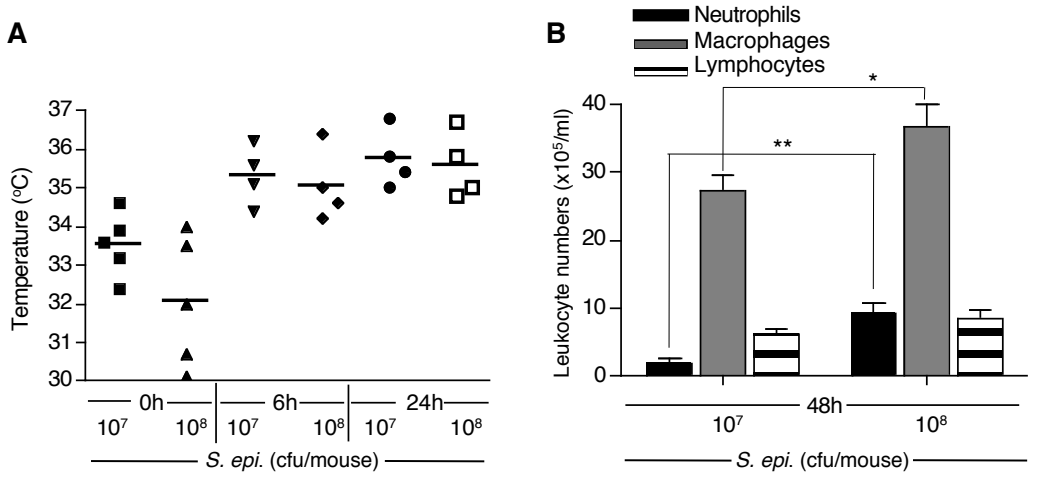

Figure 2.4.12. Comparison of body temperatures and leukocyte recruitment following infection with two *S. epi.* doses.
Mice were i.p. inoculated with the indicated doses of *S. epi*. At the indicated time points, mice temperatures were measured using a rectal probe **(A)**. At 48h, mice were sacrificed, the peritoneal cavity was lavaged and leukocyte numbers were determined by differential cell counting using cytospin **(B)**. Values represent the mean ±SEM (n=5/condition) (*, p <0.05; **, p <0.01).

bacterial dissemination (as described in section 2.4.1.16c). Only one colony was found in the neat lavage for each group, and all other samples showed no bacterial growth.

b. Pilot study 2: Dose determination

Pilot study 2 was conducted to determine the optimal dose of bacteria to use in the experiments. To better study the inflammation process and bacterial dissemination, an additional time point was included to understand initial immunological events. The baseline body temperature was well below the 32^{o}C threshold (lowest body temperature accepted by the regulatory body), and remained under that level throughout the procedure, increasing slightly at 5h and 18h, and decreasing significantly at 24h (Fig 2.4.13). These low body temperature values might have resulted from a technical artefact, the probe might not have been used appropriately to record actual values (accurate depth and adequate time for temperature stabilisation).

In the next set of experiments, mice (n=3/group) were i.p. injected with *S. epi.* at 1 x 10^7 or 1 x 10^8 cfu/mouse, and after 18h and 24h, leukocyte numbers in the peritoneal lavages were determined (2.3.14A–C). As expected, the higher dose of bacteria (1 x 10^8 cfu/mouse) induced larger peritoneal influx of neutrophils and macrophages, the latter after 24h, which is consistent with their later recruitment (Fig 2.4.14A and B). Following the injection of 1 x 10^7 cfu/mouse, the inflammation was in its resolution phase after 24h, with decreasing neutrophil and macrophage numbers (Fig 2.4.14A and B), whereas injection of *S. epi.* at 1 x 10^8 cfu/mouse prolonged the inflammation process, with as many neutrophils at 24h as at 18h (Fig 2.4.14A) and still increasing numbers of macrophages and lymphocytes at 24h (Fig 2.4.14B and C). This was confirmed by the microbiology counts, which showed approximately 5 times more bacteria after 24h in the peritoneal membranes of the 1 x 10^8 cfu-inoculated mice than in those from 1 x 10^7 cfu/mouse (Fig 2.4.15 left and right). Of note, Fig 2.4.15B also shows the resolution of inflammation, as there are almost no remaining bacteria in the lavages after 18h and 24h.

c. Pilot study 3: Toxicity-survival

The previous pilot studies showed that the mice were in good health throughout the time course of the experiments and showed mild inflammation (no sign of distress, pain or suffering, leukocytes numbers returning to baseline levels, no extensive bacterial dissemination). Therefore, the pilot study 3 was designed to explore whether a controlled dissemination and resolution of the infection may still be achieved when a higher dose of bacteria is used. To this end, *S. epi.* at 1 x 10^9 or 1 x 10^{10} cfu/mouse or PBS (control injection) were i.p. injected, and the infection was monitored over a 24h period. At 3h, the mice body temperature was measured. Mice injected with 1 x 10^9 cfu showed diminished activity and looked poorly (piloerection and slightly hunched), but their temperature remained at the basal level (Fig 2.4.16A) and similar to that of the PBS group (Fig 2.4.16C). The mice injected with 1 x 10^{10} cfu looked extremely poor after 3h with severe signs of sickness, such as piloerection, were slow and hunched, and their temperature started to drop (Fig 2.4.16B). This group of mice were considered too poorly, and

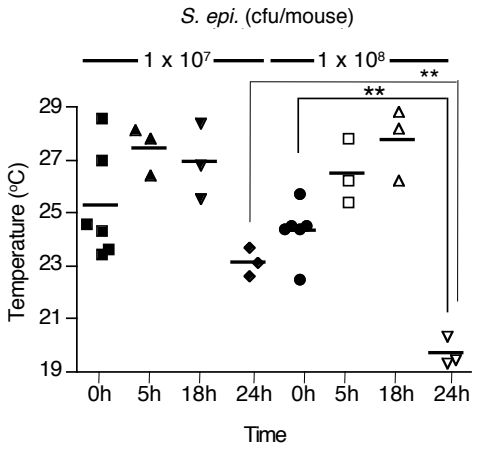

Figure 2.4.13. Body temperature patterns over a 24h time course.
Mice were i.p. inoculated with the indicated doses of *S. epi*. At the indicated time points, mice temperatures were measured using a rectal probe (**, p <0.01). (n=3-6/time point).

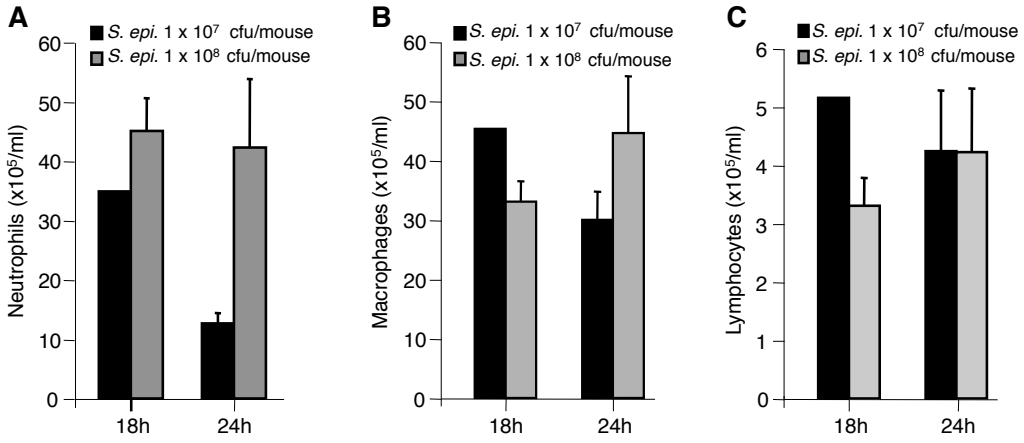

Figure 2.4.14. Leukocytes recruitment following *S. epi.* infection.
Mice were i.p. inoculated with the indicated doses of *S. epi*. At the indicated time points, the peritoneal cavity was lavaged and neutrophil **(A)**, macrophage **(B)** and lymphocyte **(C)** numbers were determined by differential cell counting using cytospin. Values represent the mean ±SEM (n=3/time point).

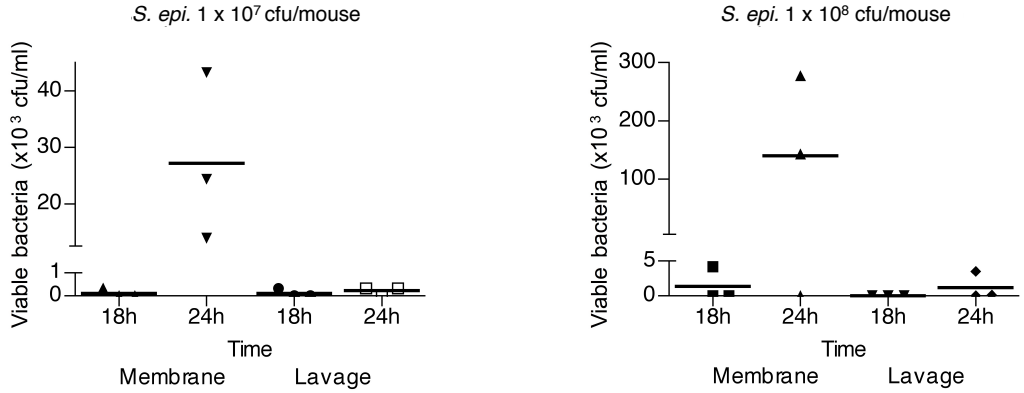

Figure 2.4.15. Bacterial dissemination following *S. epi.* infection.
Mice were i.p. inoculated with the indicated doses of *S. epi*. At the indicated time points, mice were sacrificed and bacteria were counted in the indicated organs by manual spreading on agar plates (n=3/time point).

thus they were culled and no more data was collected. The mice of the 1 x 10^9 cfu/mouse group were kept over the 24h period, but their temperature dropped significantly at 18h and 24h when compared with that at 3h and pre-inoculation (Fig 2.4.16A). The PBS group remained stable throughout the experiment (Fig 2.4.16C).

With regard to bacterial dissemination, too many bacteria were present in the different samples collected from the 1 x 10^9 cfu/mouse group at either 18h or 24h, and could not be counted. Fig 2.4.16D shows however that there was some bacterial clearance at 24h, as some mice had no bacteria in their blood, peritoneal lavage or kidney. Leukocyte numbers could not be determined, as the slides presented debris and necrotic cells extremely difficult to identify. It was concluded that both inoculums, the 1 x 10^9 and 1 x 10^{10} cfu/mouse, resulted in an inflammatory episode more severe than that required for the planned experiments of this thesis and additional experiments of our laboratory. Overall it would not reflect what was observed in most PD patients with peritonitis.

d. Pilot study 4: Bacterial dose optimisation for a 24h study

Following the standardisation of bacterial growth described in section 2.4.2.1a, a pilot study was conducted to further refine the dose of bacteria to be used in the *in vivo* model. This study aimed at increasing the inflammation process, although slightly, compared with what was observed using the doses described in the pilot study 2. To this end, *S. epi.* at 2.5 x 10^8 and 5 x 10^8 cfu/mouse were injected (n=5/group), and the infection was monitored over a 24h period. To confirm the dose of the inoculum, the OD of the two different doses was measured and serial dilutions were made, down to 1 x 10^4 cfu/ml, plated overnight and counted. Table 2.4.4 shows the results obtained.

Table 2.4.4 Summary of checks to verify bacterial doses

Dose (cfu/mouse)	Expected bacterial numbers in 1 µl	Actual counts in 1 µl	Expected bacterial numbers in 10 µl	Actual counts in 10 µl	Expected bacterial numbers in 100 µl	Actual counts in 100 µl	OD
S. epi. 2.5 x 10^8	10	26	100	324	1000	1776	0.691
S. epi. 5 x 10^8	10	28	100	195	1000	1248	1.245

The bacterial counts indicated that the dose of bacteria injected was higher (up to 2 fold) than expected.

The baseline temperatures were around 36°C, showing a drop of 2 to 3°C (depending on the bacterial dose) after 6h and an increase to slightly above baseline levels at 18h, which was maintained up to 24h (Fig 2.4.17A and B). Leukocyte counts indicated that the inflammation was not resolved in 24h, as expected from the results of pilot study 2. Indeed, neutrophil numbers (Fig 2.4.17C) were not yet decreasing, while macrophage and lymphocyte numbers (Fig 2.4.17D and E, respectively) were still increasing by 24h, reflecting the initial events of the inflammatory process. The bacterial counts from the retrieved organ samples provided additional information about the inflammatory process. With the exception of blood, significantly

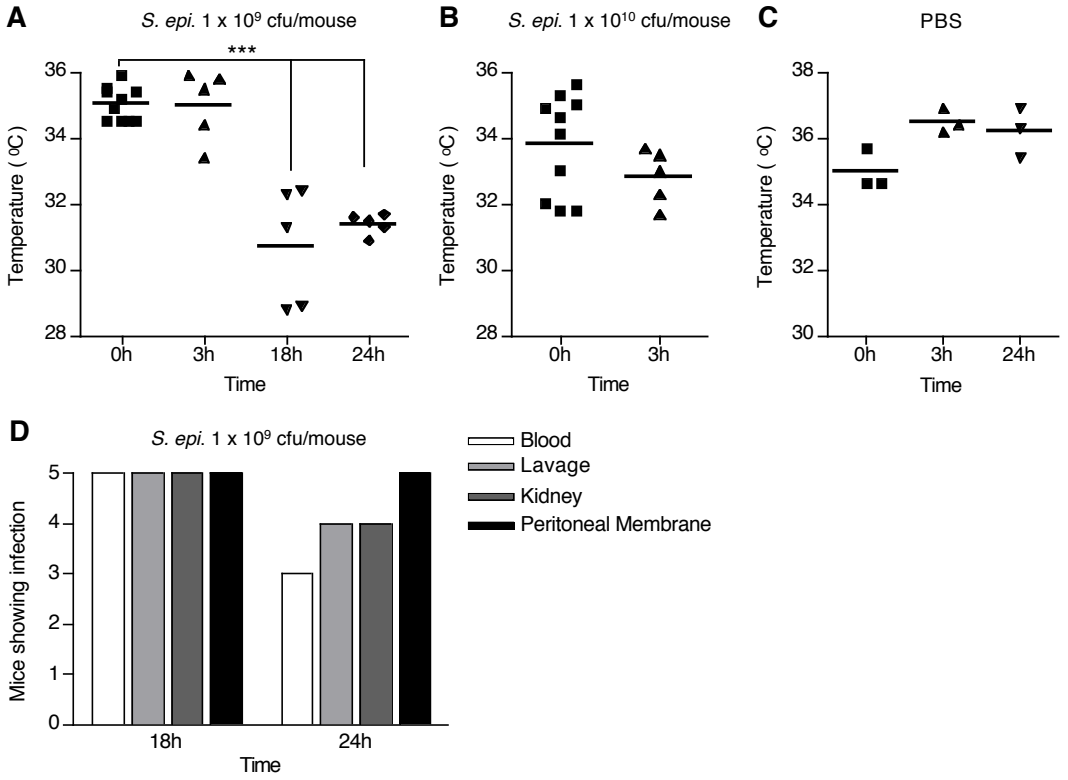

Figure 2.4.16. Toxicity and survival study.
Mice were i.p. inoculated with *S. epi.* (1 x 10^9 **(A)** and 1 x 10^{10} **(B)** cfu/mouse) (n=5/time point) and PBS (n=3/time point) **(C)** (n=3-10/condition). At the indicated time points, mice temperatures were measured using a rectal probe (***, p <0.001 0h *vs.* indicated time points). At the indicated time points, mice were sacrificed and bacteria presence was determined in the indicated organs (n=5/condition) **(D)**.

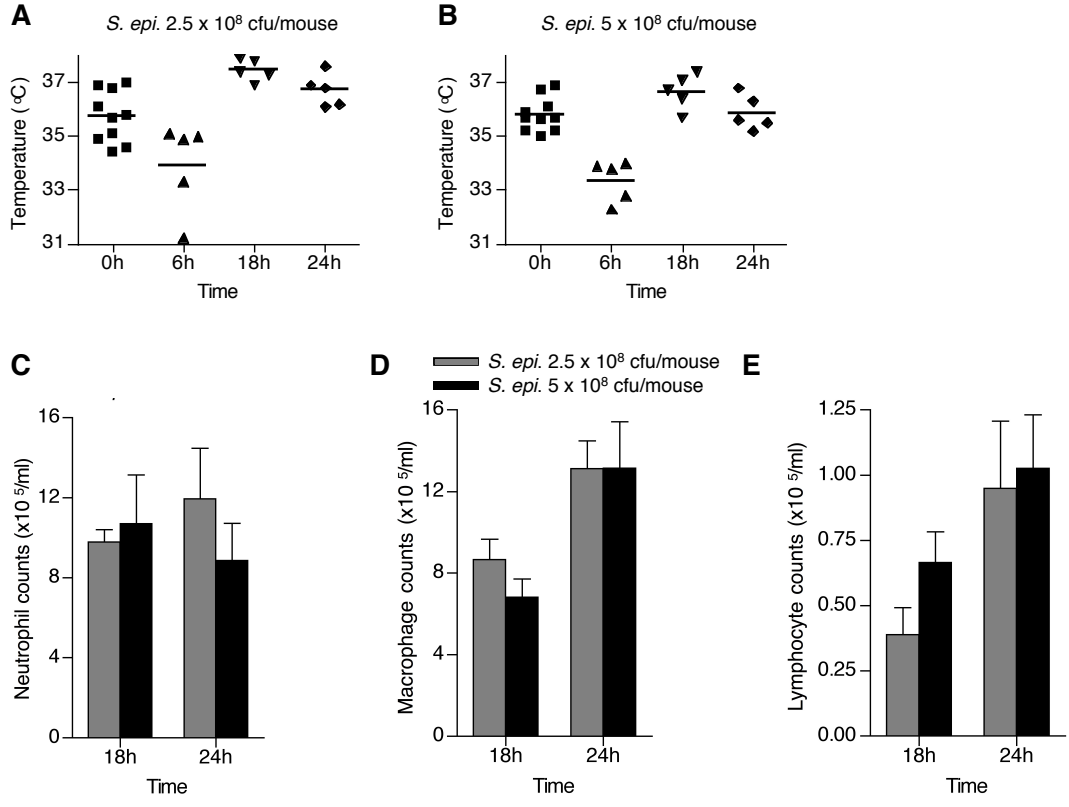

Figure 2.4.17. Body temperatures and leukocyte recruitment following *S. epi.* infection.
Mice were i.p. inoculated with the indicated doses of *S. epi*. At the indicated time points, mice temperatures were measured using a rectal probe **(A, B)** (n=5-10/time point). At the indicated time points, the peritoneal cavity was lavaged and neutrophil **(C)**, macrophage **(D)** and lymphocyte **(E)** numbers were determined by differential cell counting using cytospin. Values represent the mean ±SEM (n=5/time point).

higher counts were always observed with a higher bacterial dose injected (Fig 2.4.18). At 24h following injection with *S. epi.* 2.5 x 10^8 cfu/mouse, there were almost no remaining bacteria in the blood and kidney (Fig 2.4.18A and C), while the numbers were decreasing in the peritoneal lavage and membrane (Fig 2.4.18E and G), indicating resolution of inflammation. By contrast, the numbers of bacteria were very high in the organs following the injection of *S. epi.* at 5 x 10^8 cfu/mouse, and while decreasing in the kidney (Fig 2.4.18D), they were still increasing at 24h in the blood (Fig 2.4.18B), lavage and peritoneal membrane (Fig 2.4.18F and H), thus reflecting an ongoing inflammatory process, with dissemination and lack of containment by anti-microbial mechanisms.

e. Pilot study 5: Bacterial dose optimisation for a 96h study

As the experiments so far have been performed over a 24h period, and with some doses of bacteria resulting in an unresolved inflammatory process at the end of the study, the pilot study 5 was conducted over a longer time course, to ensure complete resolution of the infection and facilitate interpretation of the findings. For this experiment, PBS was injected as control, along with *S. epi. at* 1 x 10^8, 2.5 x 10^8 and 5 x 10^8 cfu/mouse over a 96h period. To confirm the inoculum doses, dilutions of a theoretical 1 x 10^4 cfu/ml dose were prepared, plated and counted. Table 2.4.5 shows the results obtained.

Table 2.4.5 Summary of checks to verify bacterial doses

Dose (cfu/mouse)	Expected bacterial numbers in 1 µl	Actual counts in 1 µl	Expected bacterial numbers in 10 µl	Actual counts in 10 µl	Expected bacterial numbers in 100 µl	Actual counts in 100 µl
S. epi. 1 x 10^8	10	18	100	172	1000	1584
S. epi. 2.5 x 10^8	10	23	100	168	1000	1184
S. epi. 5 x 10^8	10	20	100	165	1000	1202

The bacterial counts indicated that the doses of bacteria to be injected were higher (up to 1.7 fold) than estimated. For all subsequent experiments the OD of each dose was measured and the concentration checked on agar plates. The bacterial concentrations were then adjusted to correspond to the appropriate OD, and thus a dose closer to the one required was prepared.

For all doses of bacteria injected the pattern of mouse body temperature over time was similar (Fig 2.4.19A-C). Indeed, temperature levels at 6h were similar to basal levels, dropped by 3^{o}C - 4^{o}C at 10h, increased slightly above the basal levels by 18h, and remained at this level up to 96h. Leukocytes counts in the peritoneal cavity were only monitored from 18h to 96h, as the early time points had been studied in pilot studies 2 and 3. The highest neutrophil numbers were found at 18h, corresponding to the 1 x 10^8 and 2.5 x 10^8 cfu/mouse doses (Fig 2.4.20A). The numbers decreased by 24h and remained relatively low. The 5 x 10^8 cfu/mouse showed a different pattern, with a comparatively lower number of neutrophils at 18h, the number decreased by 24h but went back up at 36h, decreasing again by 48h and remaining at this level until 96h (Fig 2.4.20A). As expected, the overall number of neutrophils over the course of the

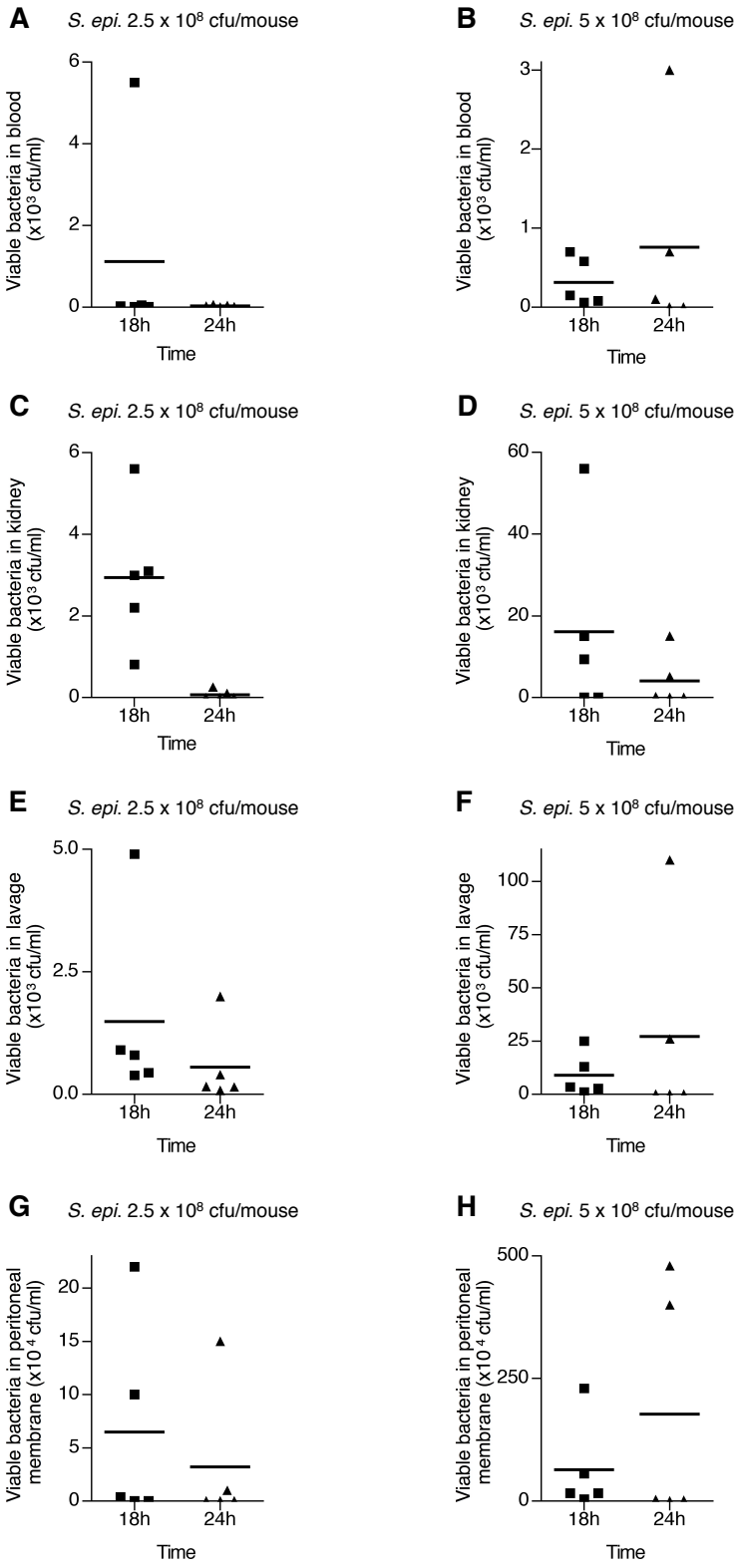

Figure 2.4.18. Bacterial dissemination following *S. epi.* infection.
Mice were i.p. inoculated with the indicated doses of *S. epi*. At the indicated time points, mice were sacrificed and bacteria were counted in the indicated organs by manual spreading on agar plates (n=5/time point).

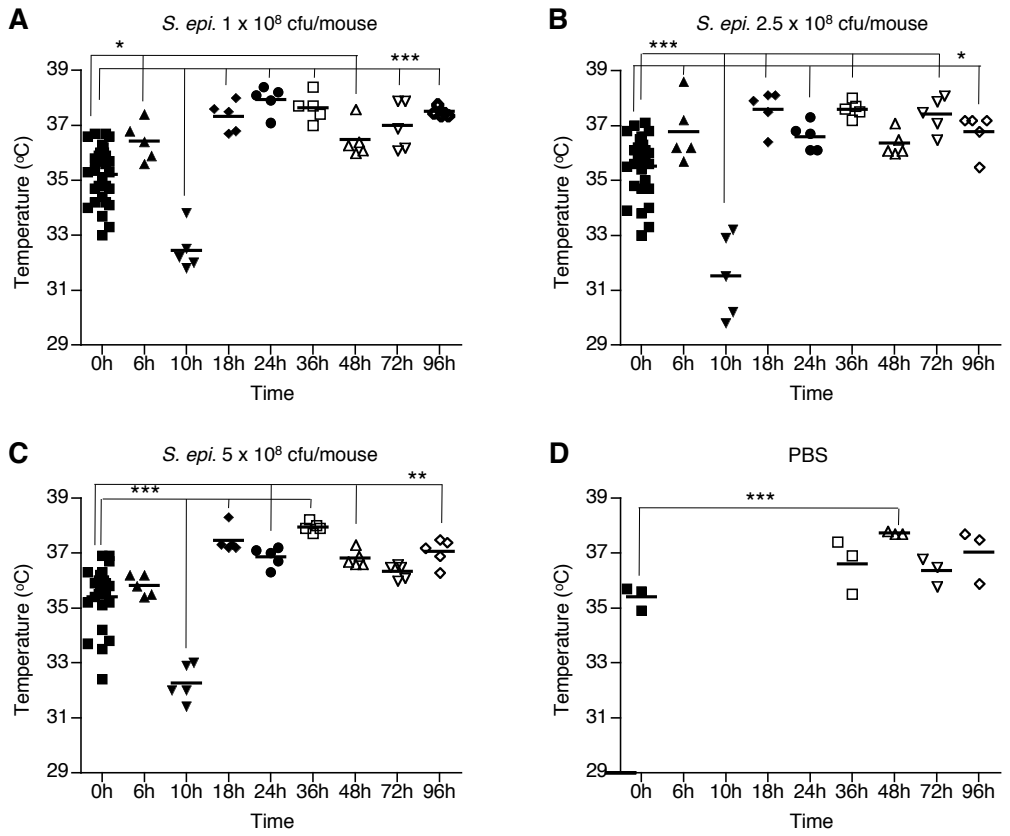

Figure 2.4.19. Body temperature patterns over a 96h time course following *S. epi.* infection.
Mice were i.p. inoculated with the indicated doses of *S. epi.* **(A, B, C)** or with PBS **(D)** (n=3/time point). At the indicated time points, mice temperatures were measured using a rectal probe (n=5-30/time point **(A)**, n=5-30/time point **(B)**, n=5-25/time point **(C)** and (n=3/time point **(D)**) (*, p <0.05; **, p <0.01; ***, p <0.001 0h *vs.*indicated time points).

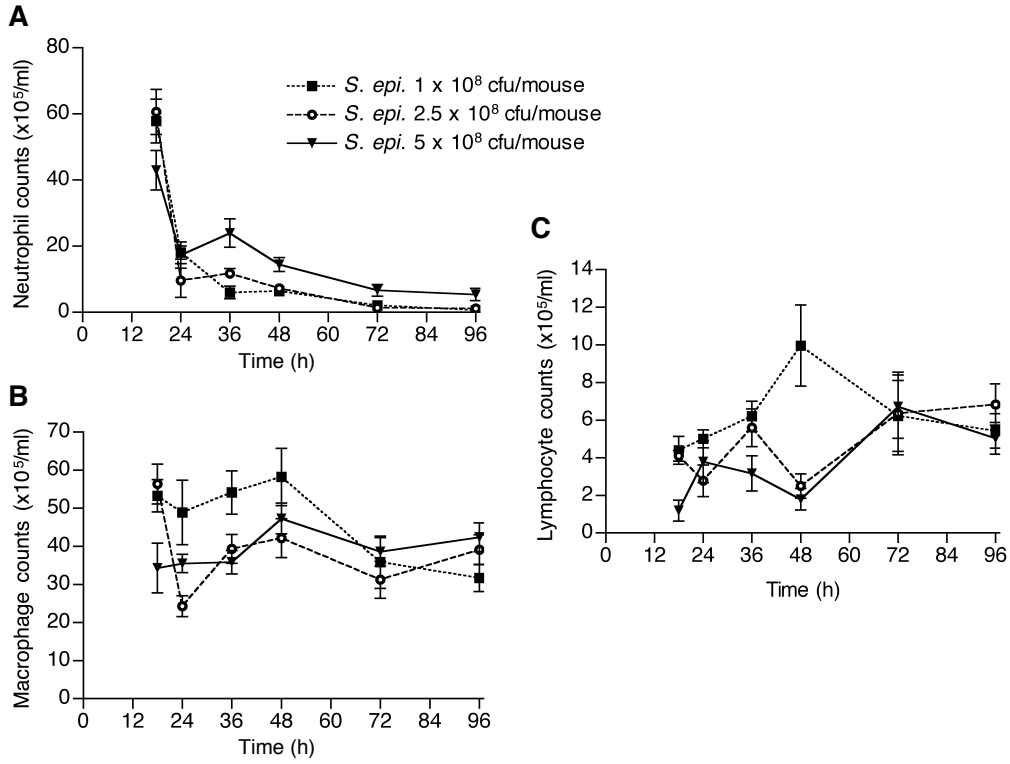

Figure 2.4.20. Leukocyte recruitment pattern over a 96h time course following *S. epi.* infection.
Mice were i.p. inoculated with the indicated dsoses of *S. epi.* At the indicated time points, mice were sacrificed, the peritoneal cavity was lavaged and neutrophil **(A)**, macrophage (B) and lymphocyte **(C)** numbers were determined by differential cell counting using cytospin **(B)**. Values represent the mean ±SEM (n=5/time point).

study was slightly higher with the highest dose of bacteria. Unlike the neutrophil counts, the pattern of macrophage and lymphocyte numbers over the time were similar (Fig 2.4.20B and C), with no major differences between the different doses of bacteria injected. As previously established with the SES model, these two leukocyte populations peaked later than the neutrophils (at 36h-48h for macrophages and 48h-72h for lymphocytes; Fig 2.4.20B and C). Surprisingly, the lowest dose showed an overall slightly higher number of macrophages and lymphocytes than the two other doses.

Examination of the bacterial counts in the blood, kidney, peritoneal lavage and membrane (Fig 2.4.21 and 2.4.22) showed, except for the lavages, no remaining bacteria by the end of the experiment. Overall, apart from the occasional outliers, a higher bacterial dose resulted in an increased bacterial count in the organs, and a longer bacterial clearance. With a regular decrease, no bacteria remained in the blood later than 48h (Fig 2.4.21A, C and E), whereas the kidney showed some viable bacteria over the time. (Fig 2.4.21B, D and F). The peritoneal lavages and peritoneal membrane (Fig 2.4.22A-F) showed a considerable number of viable bacteria over the course of the study at any dose used, with the highest dose showing the highest bacterial numbers. The lower bacterial dose showed an initial increase in the peritoneal lavages, which was sustained until 72h, followed by an abrupt decline by 96h. By contrast, the intermediate dose showed a regular decline of bacterial numbers over the time course (Fig 2.4.22A and C). In the peritoneal membrane bacterial dissemination initially increased from 18h, followed by a decrease, peaking at later time points with increasing bacterial doses (Fig 2.4.22 B, D and F).

These pilot studies demonstrated the establishment of a controlled model of peritoneal inflammation and infection, acute, non lethal, and with a resolving infection manifested by moderate temperature variations, leukocyte numbers returning to baseline, and clearance of bacteria. 5 x 10^8 cfu/mouse of *S. epi.* was determined as the highest appropriate dose for this model.

2.4.2.3 Pilot study to establish a mild peritonitis model with *S. aureus*

A literature search showed that up to 3 x 10^9 cfu/mouse were used as sub-lethal doses of *S. aureus* to induce peritoneal inflammation over at least a 24h time course (Crosara-Alberto et al., 2002; Mullaly and Kubes, 2006). In the first pilot study, three different bacterial doses were injected, 1 x 10^8, 5 x 10^8 and 1 x 10^9 cfu/mouse, (n=3/group), with 5 time points over a 24h period for testing body temperature levels, leukocyte numbers and bacterial numbers in tissue samples.

The body temperature pattern showed an initial decrease reaching the lowest level at approximately 6h. Subsequently, mice injected with the lowest and intermediate bacterial doses showed an increased in temperature levels with values closer to basal by 18h, and decreasing again by 24h (Fig 2.4.23A and B). The mice injected with the highest bacterial dose showed a more important decrease in body temperature (Fig 2.4.23C), probably reflecting a more severe infection. This was consistent with the findings on leukocytes recruited to the peritoneal cavity,

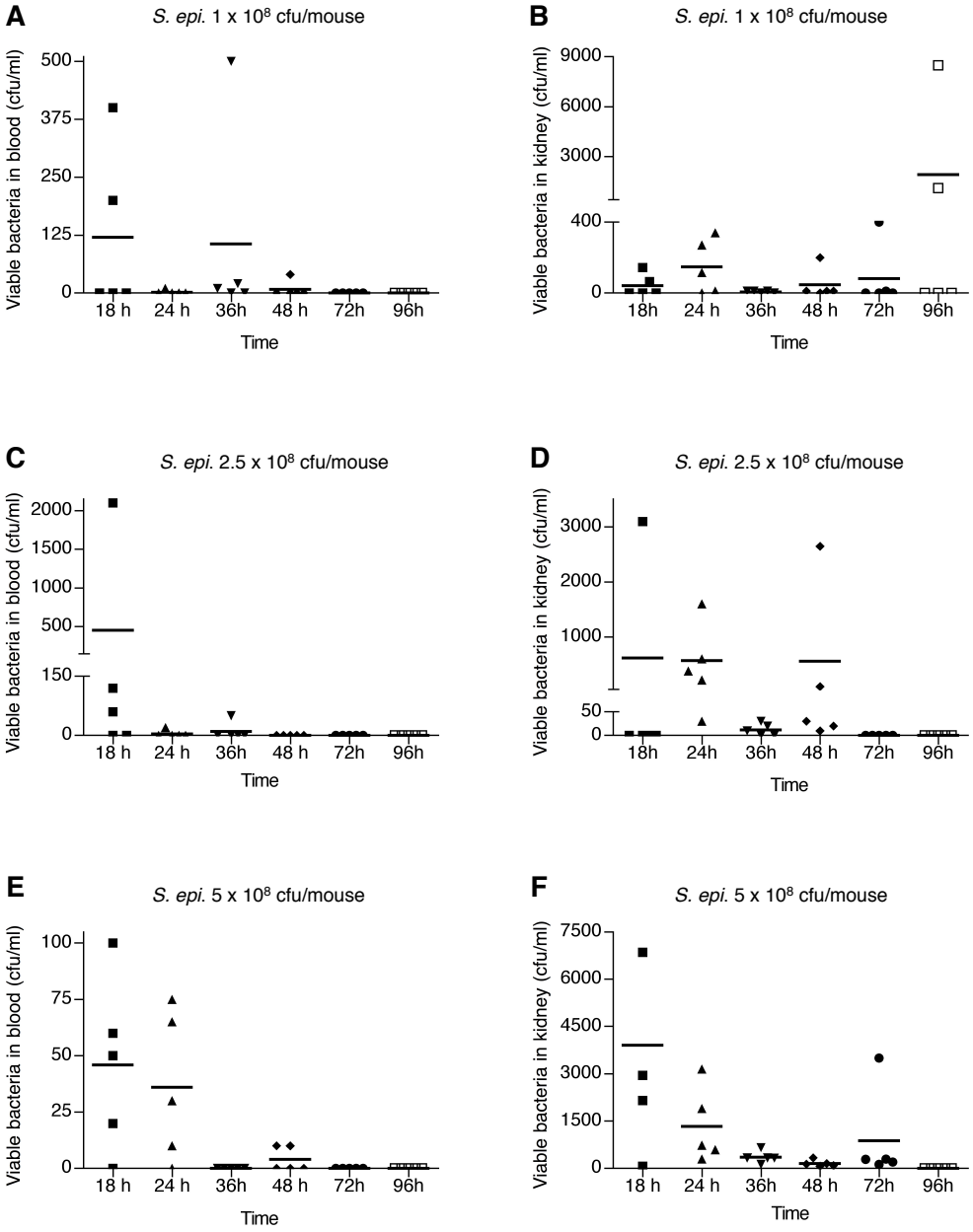

Figure 2.4.21. Bacterial dissemination over a 96h time course following *S. epi.* infection.
Mice were i.p. inoculated with the indicated doses of *S. epi*. At the indicated time points, mice were sacrificed and bacteria were counted in the indicated organs by manual spreading on agar plates (n=5/time point).

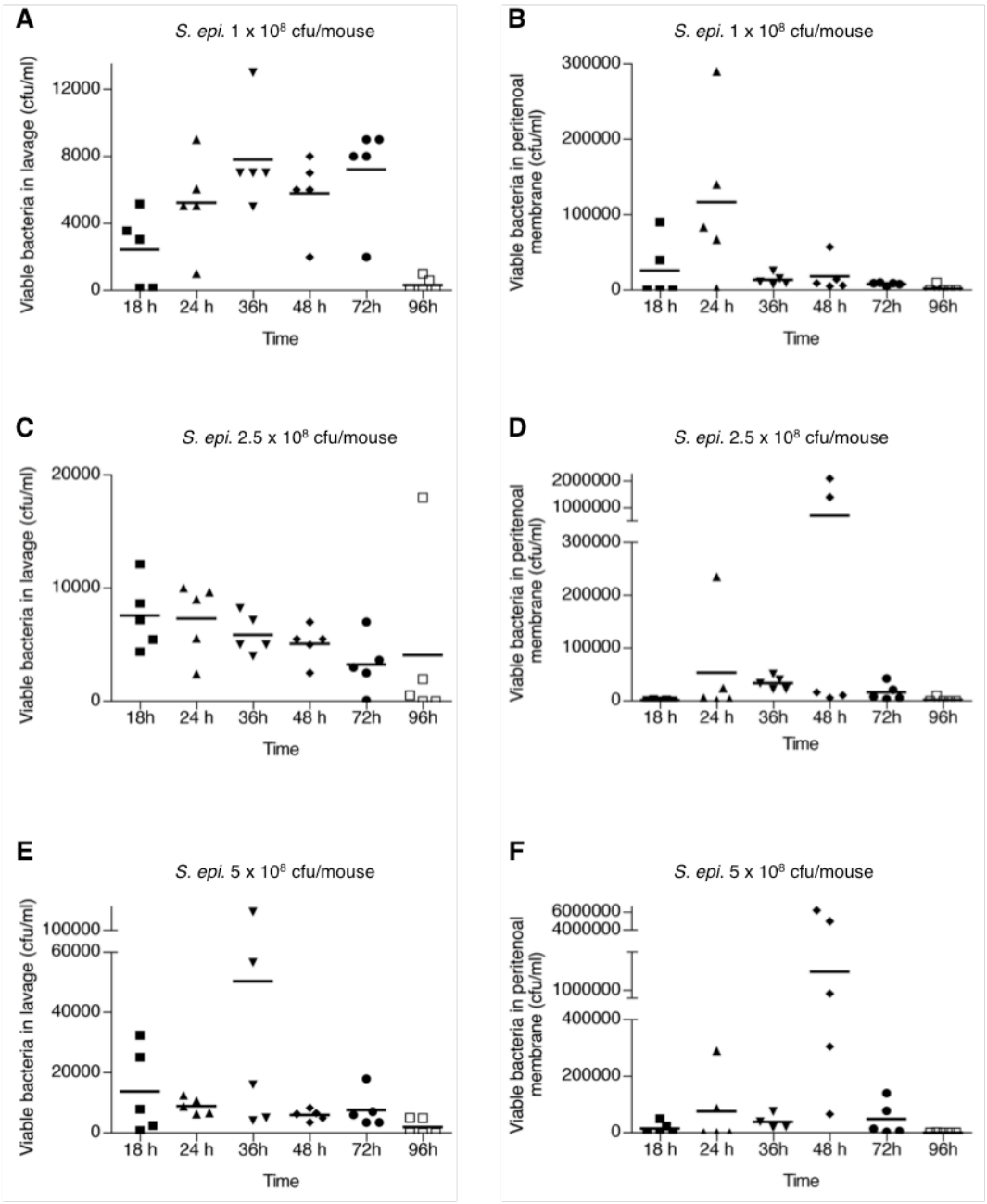

Figure 2.4.22. Bacterial dissemination over a 96h time course following *S. epi.* infection.
Mice were i.p. inoculated with the indicated doses of *S. epi.* At the indicated time points, mice were sacrificed and bacteria were counted in the indicated organs by manual spreading on agar plates (n=5/time point).

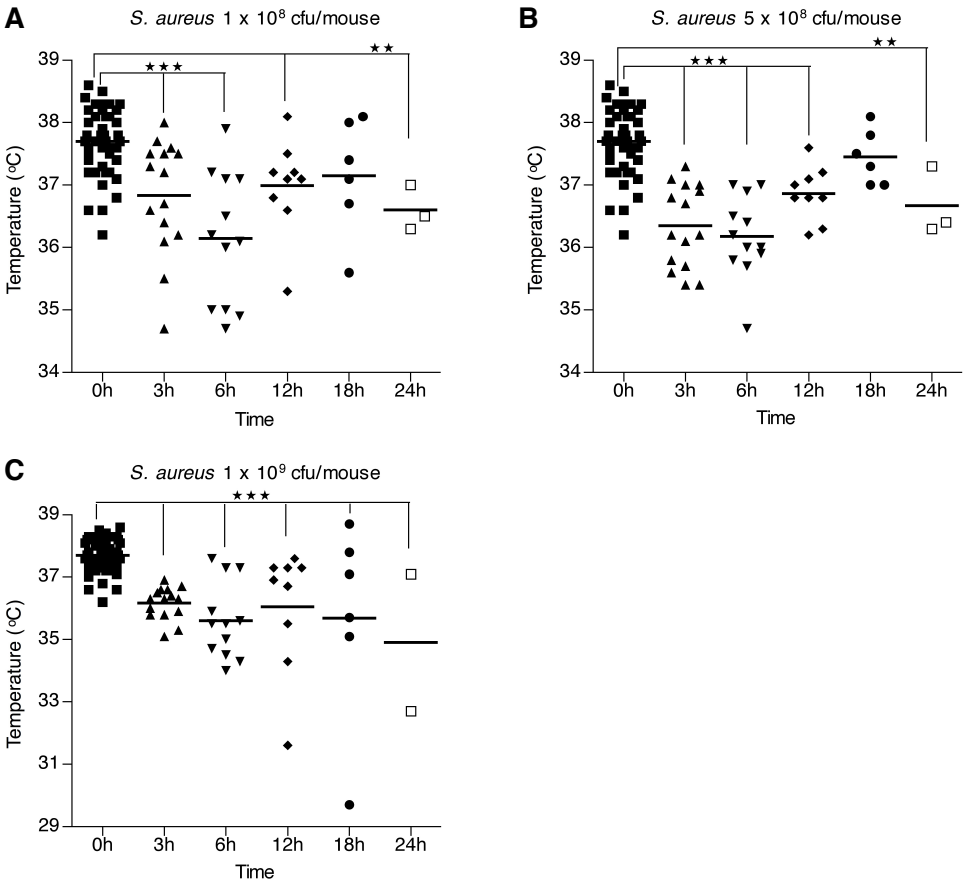

Fig 3.2.23. Body temperature patterns over a 24h time course following *S. aureus* infection.
Mice were i.p. inoculated with the indicated doses of *S.aureus*. At the indicated time points, mice temperatures were measured using a rectal probe (n=3-46/time point **(A)**, n=3-46/time point **(B)** and n=2-46/time point **(C)**) (**, p <0.01; ***, p <0.001 0h *vs.*indicated time points).

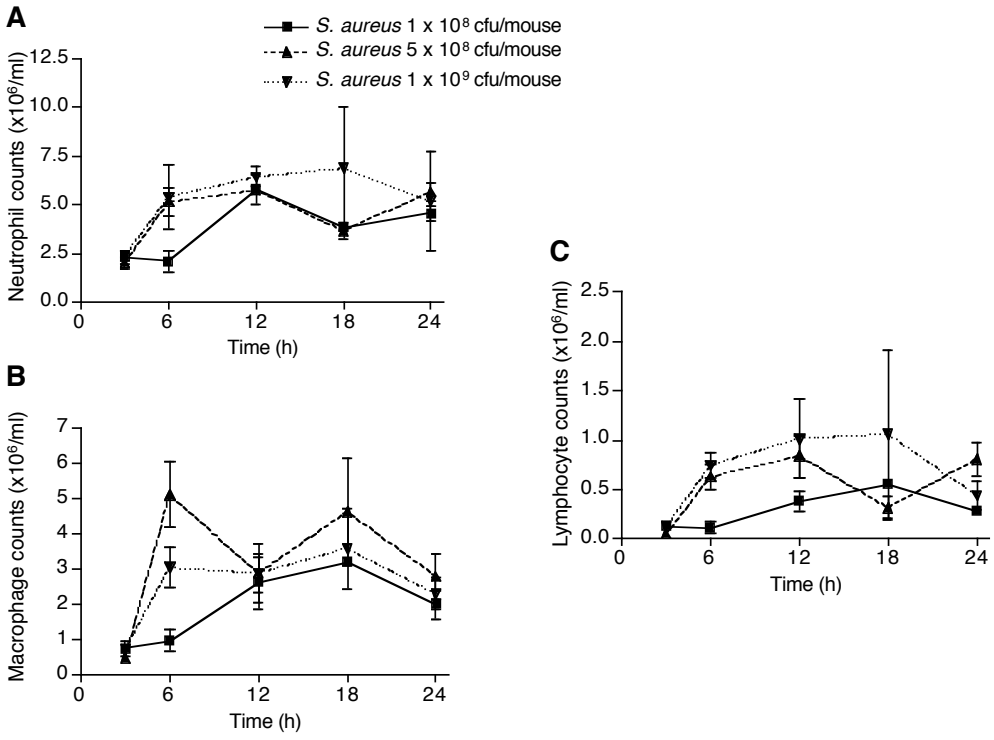

Figure 2.4.24. Leukocyte recruitment patterns over a 24h time course following *S. aureus* infection.
Mice were i.p. inoculated with the indicated doses of *S.aureus*. At the indicated time points, mice were sacrificed, the peritoneal cavity was lavaged and neutrophil **(A)**, macrophage **(B)** and lymphocyte **(C)** numbers were determined by differential cell counting using cytospin. Values represent the mean ±SEM (n=3/time point).

with faster neutrophil, macrophage and lymphocyte influxes when 5 x 10^8 and 1 x 10^9 cfu/mouse were injected (Fig 2.4.24A-C), and mostly higher leukocyte numbers recruited when more bacteria were injected. Of note, by 24h neutrophil numbers remained relatively high (Fig 2.4.24A), indicating that the inflammation was not totally resolved. The bacterial load data (Fig 2.4.25) showed that most mice have cleared bacteria from the blood and peritoneal lavage by 24h, but there were a few outliers with some bacteria remaining in the blood (Fig 2.4.25A and E) as well as the lavage (Fig 2.4.25F). This data suggests that although the bacteria have mostly been cleared by 24h, the inflammation process is prolonged with neutrophils remaining in the peritoneal cavity for longer and the resolution phase occurring later. Increasing the inoculum of bacteria increased the severity of the infection, as shown in Fig 2.4.25 and by inspecting the mice. Indeed, all groups were doing poorly between 6h and 18h, with mice moving slowly and presenting some piloerection and infected eyes. While 1 x 10^8 and 5 x 10^8 cfu/mouse groups also presented these signs of sickness, they were less severe and the mice were recovering by 24h. The 1 x 10^9 cfu/mouse group showed signs of sickness as early as 6h, and were still poor at 24h. An inoculum of 5 x 10^8 cfu/mouse of *S. aureus* was deemed appropriate for subsequent studies.

2.4.2.4 Pilot study of *E. coli* - induced peritonitis

Aiming for a moderate model of *E. coli* peritonitis, a literature search was conducted and showed that sub-lethal doses of *E. coli* up to 2 x 10^8 cfu/mouse have been used to induce peritoneal inflammation (Demir et al., 2007; Hemmi et al., 2002). The pilot study consisted of three different inoculums, 1 x 10^7, 5 x 10^7 and 1 x 10^8 cfu/mouse (n=4/group) to be followed for 48h, with several time points to test infection/inflammation parameters. The mice injected with 1 x 10^7 cfu/mouse showed a body temperature pattern different from that observed with the previous strains of bacteria, no significant changes throughout the time course were observed (Fig 2.4.26A), even though they showed signs of sickness between 12h and 18h, recovering thereafter. The groups injected with the intermediate and higher doses showed a body temperature pattern previously observed, a decrease in temperature between 3h and 6h and a subsequent increase (Fig 2.4.26B and C). As early as 6h, however, some mice of these two groups showed severe signs of sickness, and a few were found dead. At this point, it was decided to cull the remaining mice of the 1 x 10^8 cfu/mouse group except for one, and most of the 5 x 10^7 cfu/mouse ones, keeping only those that appeared to be well and with a temperature above 34°C. For this reason, the experiment was stopped at the 26h time point. The leukocyte counts were incomplete, as many slides proved very difficult to count (dead cells, cell debris). The data obtained however reflected the severity of the infection (Fig 2.4.27), with neutrophils at their highest levels at 24h-26h (Fig 2.4.27A). Macrophage and lymphocyte levels were still rising after 24h (Fig 2.4.27B and C). The bacterial counts were also much higher than those previously observed with the other strain of bacteria, still very high at 24h for the lowest inoculum (Fig 2.4.28A and B). Most of the mice of the 5 x 10^7 and 1 x 10^8 cfu/mouse groups had

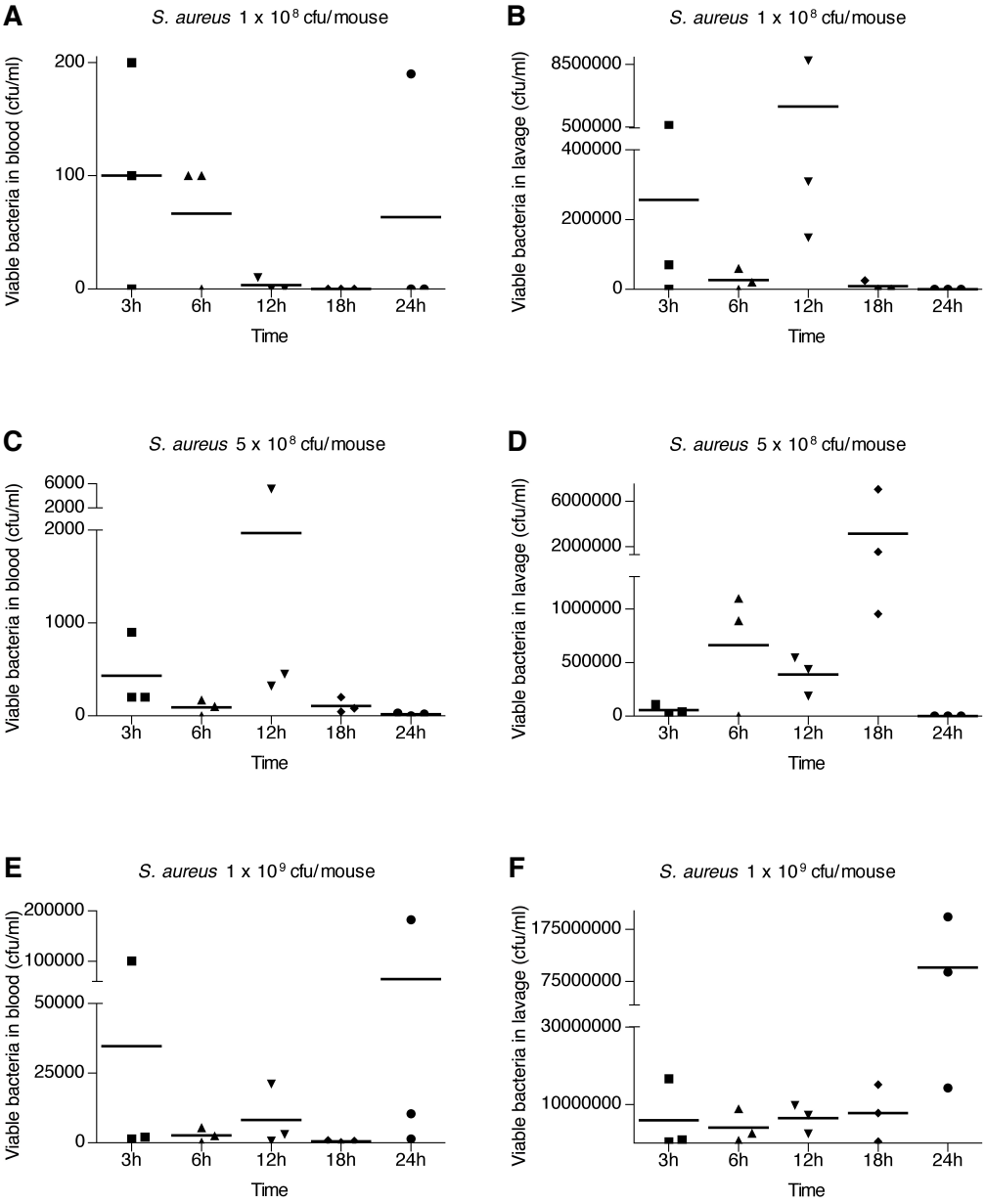

Figure 2.4.25. Bacterial dissemination over a 24h time course following *S. aureus* infection.
Mice were i.p. inoculated with the indicated doses of *S.aureus*. At the indicated time points, mice were sacrificed and bacteria were counted in the indicated organs using an automated spiral plater (n=3/time point).

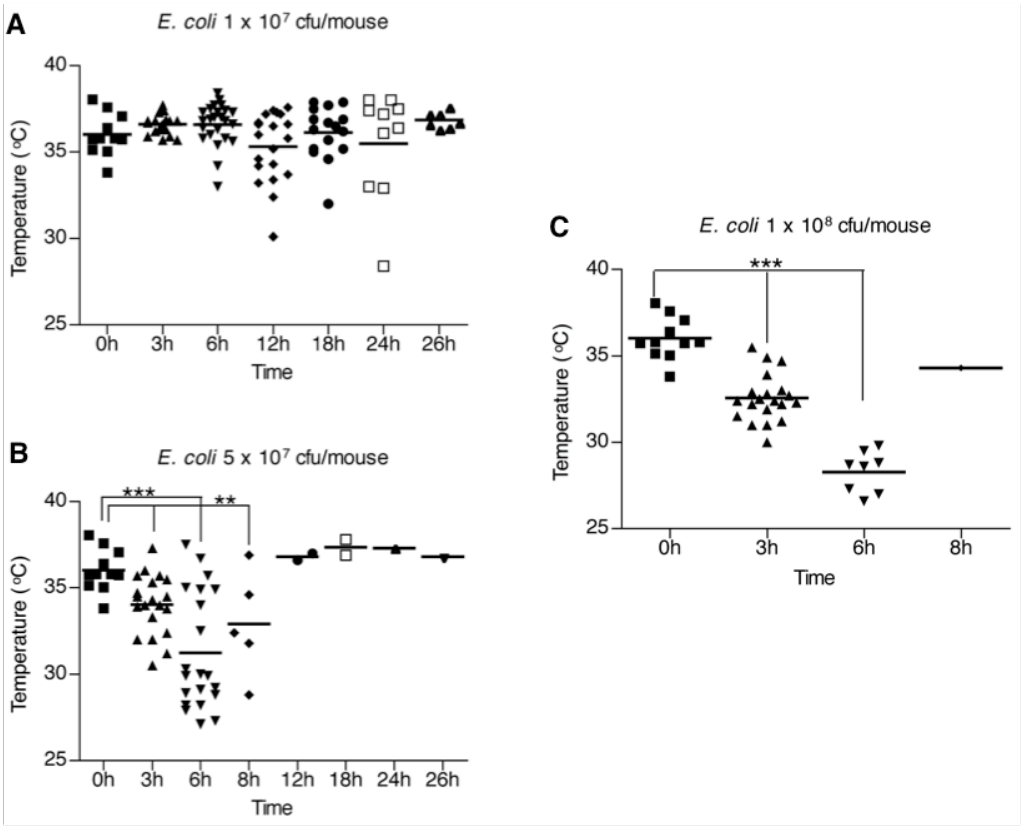

Figure 2.4.26. Body temperature patterns following infection with increasing doses of *E. coli*.
Mice were i.p. inoculated with the indicated doses of *E. coli*. At the indicated time points, mice temperatures were measured using a rectal probe (n=10-24/time point **(A)**, n=2-21/time point **(B)**, n=8-20/time point **(C)**) (**, p <0.01; ***, p <0.001 0h *vs.*indicated time points).

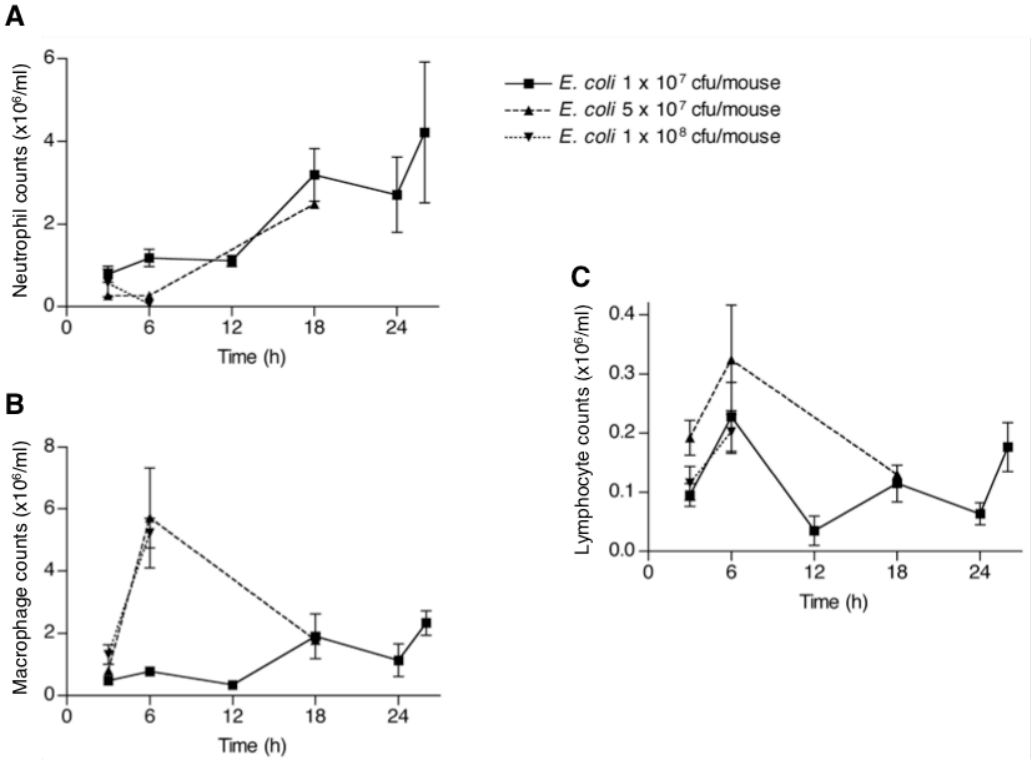

Figure 2.4.27. Leukocyte recruitment patterns following infection with increasing doses of *E. coli*.
Mice were i.p. inoculated with the indicated doses of *E. coli*. At the indicated time points, mice were sacrificed, the peritoneal cavity was lavaged and neutrophil **(A)**, macrophage **(B)** and lymphocyte **(C)** numbers were determined by differential cell counting using cytospin. Values represent the mean ±SEM (n=5-21/time point).

to be culled at 6h, as explained previously, and at this time point the bacterial load was still high (Fig 2.4.28C, D, E and F).

This experiment demonstrated that the levels of infection attained with these inoculums were much higher than anticipated, and sepsis was observed in many animals. *E. coli* was not extensively used in our laboratory and further setting up and revision of the model using this bacterium was subsequently conducted by others.

2.4.3 Discussion

The clinical outcomes of Gram-positive and Gram-negative peritonitis in PD patients are markedly different when considering hospital admission, catheter removal or relapse, which underlines the relevance of studying both types of organisms in our *in vivo* models. In order to obtain a more controllable process, the initial set up of this model was limited to the use of three relatively attenuated organisms, although the ultimate aim was to study all the varying strains as well as events encountered in the clinical setting by using more virulent organisms.

The setting up of the *in vivo* model started with relatively small experiments, with limited number of mice and time points to assess the severity of the inflammation process induced with lower doses of bacteria. The model then increased in complexity by increasing the concentration of the bacterial inoculum to adjust the doses to the level of inflammation required, before extending the time frame for a better understanding of the inflammation/infection process. As the dose of bacteria injected increased, the intensity of the inflammation heightened with extended bacterial dissemination and systemic activation. This was reflected in more marked body temperature changes. Furthermore, a larger leukocyte recruitment and new patterns of recruitment and dissemination were observed, reflecting different time frames of immunological events and possibly leukocyte subpopulations activation status. The temporal evaluation of the body temperature, leukocyte influx, bacterial clearance from the peritoneal cavity and bacterial dissemination into blood, allowed a refinement of animal use in the experiments and facilitated the interpretation of the regulation of peritoneal infection. The use of more mice in the experiments may have resulted in an increase in the reliability and accuracy of the data, given that the variability between animals and genders is quite important. However, it was planned to use a limited number of mice in the experiments, and thus animals used were kept to a minimum compatible with valid data.

Before establishing the *in vivo* model in our laboratory, a preliminary experiment was conducted in Boston (USA) under the expert supervision of Dr Arthur Tzianabos and staff from his laboratory, where another live *S. epi*. *in vivo* model for intra-abdominal abscess formation studies had already been established. The aim was to determine the pattern of leukocyte recruitment and measure chemokine secretion following i.p. injection of *S. epi.* and to compare them with the SES model. Overall, the results were similar to those obtained by using the SES

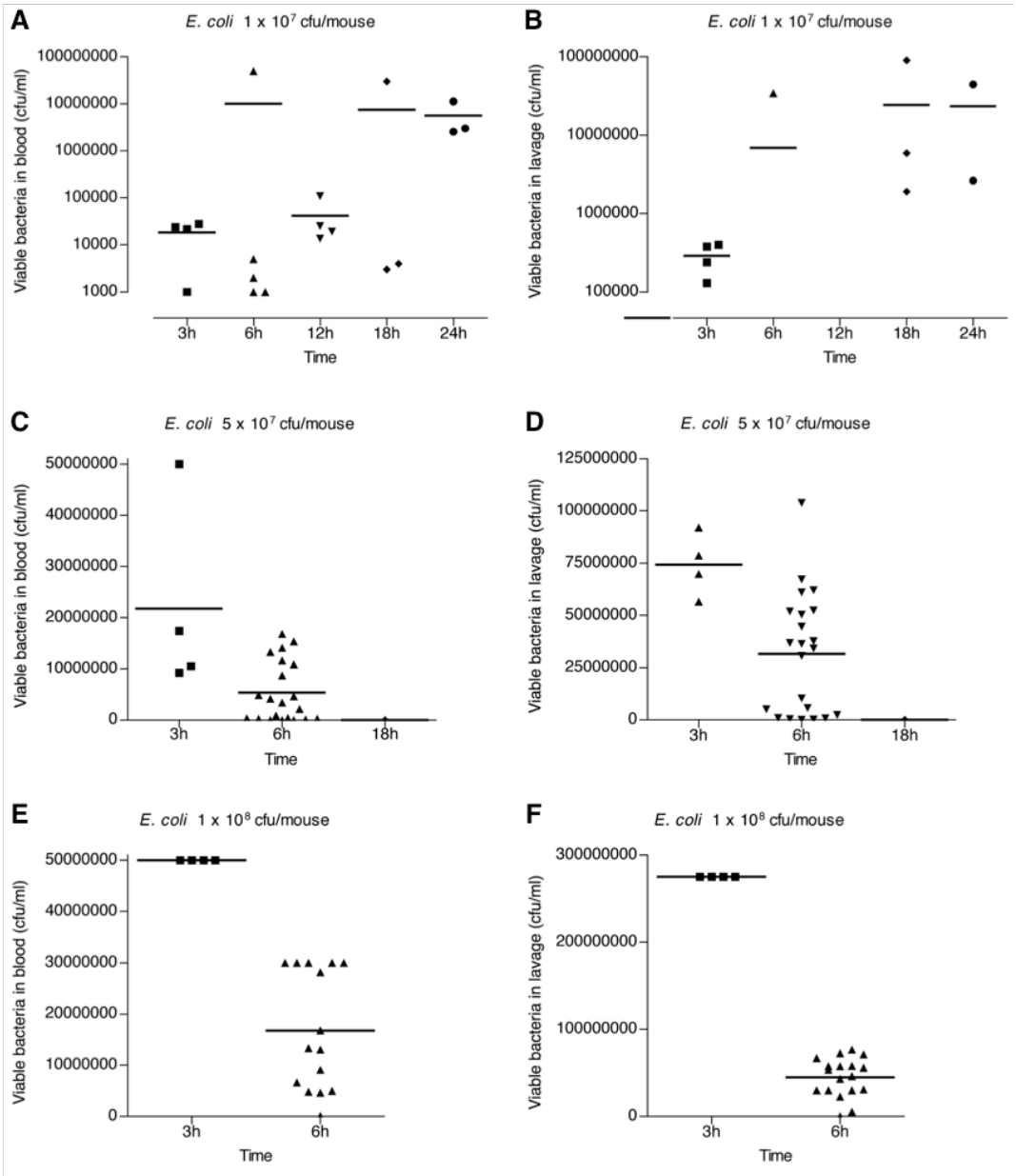

Figure 2.4.28. Bacterial dissemination following infection with increasing doses of *E. coli*.
Mice were i.p. injected with the indicated doses of *E. coli*. At the indicated time points, mice were sacrificed and bacteria were counted in the indicated organs using an automated spiral plater (n=3-5/time point **(A)**, n=2-5/time point **(B)**, n=1-21/time point **(C)**, n=1-22/time point **(D)**, n=4-15/time point **(E)**, n=4-18/time point **(F)**).

model. This preliminary experiment confirmed the possibility to reproduce with live bacteria what is observed in PD patients.

In addition to the SES model, the *in vivo* model established in our laboratory and described here recreated more accurately the infections occurring in PD patients, thus allowing studies on acute inflammation, infection, inflammation-induced tissue damage and anti-microbial immunity as well as their control mechanisms.

Chapter 3

GENERAL DISCUSSION AND FUTURE WORK

A number of studies have demonstrated the capacity of epithelial, endothelial and various other cell types lining body cavities to contribute to immune defences (Card et al., 2014; Peterson and Artis, 2014). Notably, in the last thirty years the development of PD as an alternative treatment for ESRD patients has brought substantial interest in the immunobiology of peritoneal mesothelial cells and their role in inflammation (Muijsken et al., 1991; Topley and Williams, 1994; Valle et al., 1995). The capacity of HPMC to ingest bacteria has been described (Visser et al., 1996), and TLRs' critical ability to detect and initiate inflammatory responses to various types of pathogens has been amply demonstrated, in particular in leukocytes (Akira et al., 2006). However, the pathogen recognition ability of HPMC, the potential role of TLRs in this activity, the specific role of HPMC in the early stages of the inflammatory response and the regulation of the putative pathogen recognition by HPMC have not been fully investigated.

The aims of the present study were to characterise TLR expression and responses in HPMC, and evaluate the capacity of known modulators of pro-inflammatory responses, namely sTLR2 and IL-6/sIL-6R, to regulate TLR-mediated HPMC and peritoneal responses *in vitro* and *in vivo*. This study demonstrated the capacity of HPMC to recognise and respond to a vast array of bacterial pathogens *via* expression and function of a specific set of TLRs and NOD receptors. Although HPMC did not appear to be able to release sTLR2 and sIL-6R, which are known to be secreted during the course of an inflammatory response, they were able to respond to both soluble modulators, leading to modulation of the inflammatory response in a timely manner. *In vivo*, sTLR2 and IL-6/sIL-6R showed the capacity to reduce neutrophil influx, at least in part *via* modulating signalling in the mesothelial/stromal cells of the peritoneal membrane. Notably, following the establishment of a mouse model of peritoneal bacterial infection, IL-6 signalling was confirmed to be beneficial to bacterial clearance. The proposed role of TLRs and IL-6/sIL-6R in HPMC and their early involvement in inflammation is recapitulated in Figure 3.1.

Primary HPMC, as opposed to an established cell line, were used in part to account for human inter-individual variability. Indeed, variability has been well documented in biological systems (Endres et al., 1989; Raby et al., 2011; Shikotra et al., 2012), and notably in response to drugs, leading to tailored treatment in modern medicine (Rocca et al., 2013; Rosenbaum and Lipton, 2012). It is important to account for variability when trying to understand a molecular mechanism. Variability was observed in TLR2 cell-surface expression (Fig 2.1.2), as well as in the basal levels of chemokine secretion, notably with up to 40 fold difference in basal CXCL8 secretion between various primary cell preparations. These differences may account for inter-subject variations in the observed response to a particular stimulus, as cells isolated from a particular donor might have a different sensitivity to a stimulus as the result of a different threshold to trigger a response. The interpretation of cellular responses are particularly challenging when a complex stimulus such as SES is used, as opposed to a single stimulus e.g. Pam_3Cys, as SES probably triggers responses *via* several signalling pathways in addition to TLR2, whereas Pam_3Cys signals through TLR2 only. The multiplicity and nature of ligands in

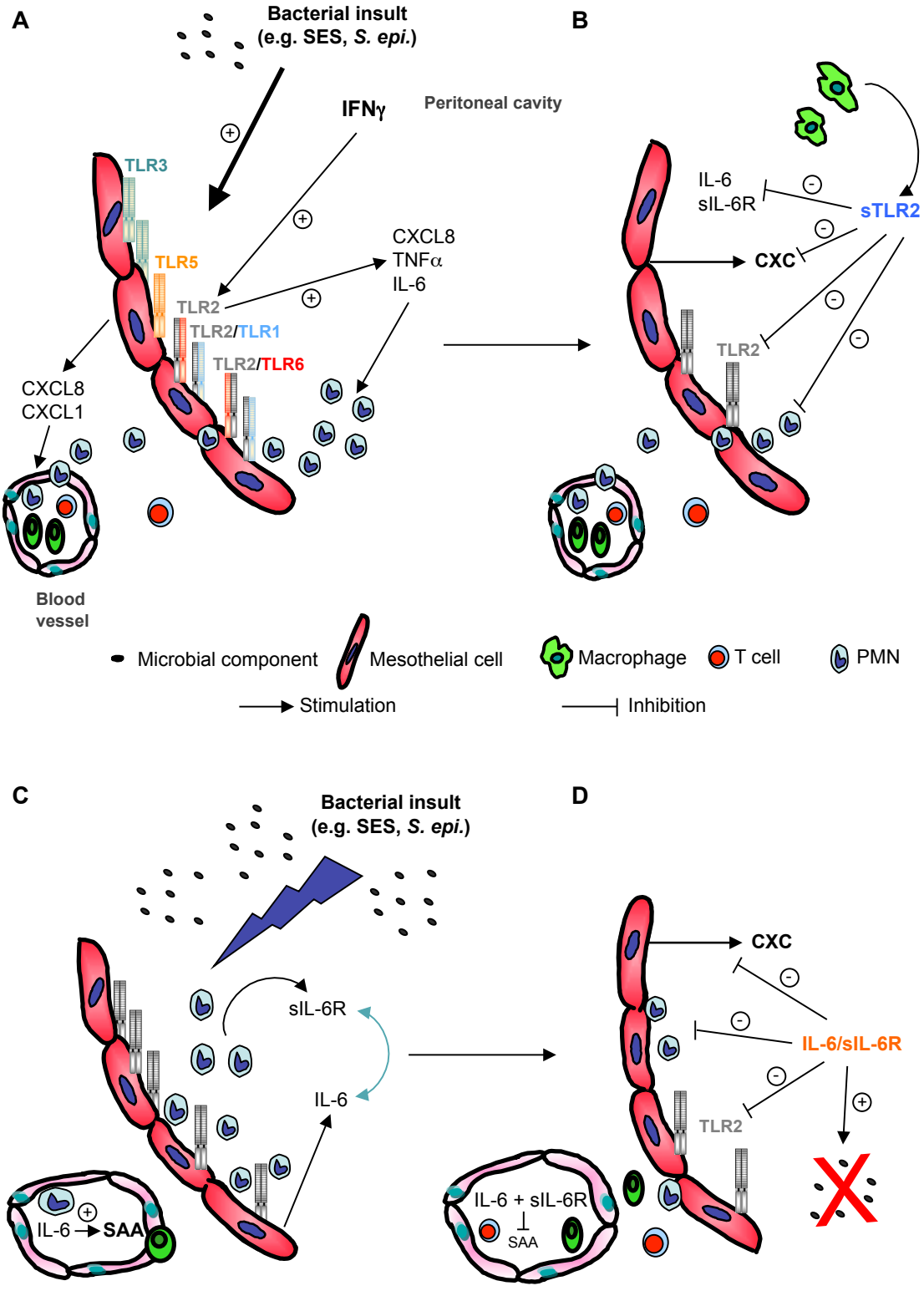

Figure 3.1. Proposed role of TLRs, sTLR2 and IL-6 trans-signalling in TLR-mediated peritoneal responses. **(A)** Bacterial insult triggers cytokine and chemokine secretion by resident macrophages and stromal cells (shown, mesothelial cells) from the peritoneal membrane, inducing neutrophil influx into the peritoneal cavity. Upon activation by a variety of modulators present at the onset of infection, particularly SES and IFNγ, TLR2 expression on HPMC is temporarily increased. This results in an increased production of various chemokines and cytokines dependent on NF-κB activation - such as CXCL8, IL-6 and TNFα - that contributes to the peritoneal cytokine network. **(B)** sTLR2, released into the peritoneal cavity during inflammation (most likely by myeloid cells), contributes to a negative feedback by inhibiting CXC chemokines (CXCL8/CXCL1), IL-6 and sIL-6R production, neutrophil infiltration as well as modulating TLR2 cell-surface expression. **(C)** Subsequent to peritoneal infection and upon migration and activation, neutrophils (and macrophages) shed sIL-6R, which combines with IL-6 - produced by mesothelial cells and macrophages - to form the IL-6/sIL-6R complex. **(D)** This complex inhibits CXC chemokine secretion, neutrophil infiltration, TLR2 cell-surface expression and increases bacterial clearance. At the systemic level, IL-6 triggers the acute phase reactant serum amyloid A (SAA) secretion whereas the IL-6/sIL-6R complex increases acute phase response resolution.

preparations like SES clearly contribute to the inter-individual variability observed. A number of parameters are responsible for this variability such as age, gender, co-morbidities and genetic characteristics. Examining the response in enough individuals to observe a trend or a definite response, although not always achievable, may circumvent it. A potential consequence of the variability in TLR expression and sTLR2 secretion for pro- *vs.* anti-inflammatory mediator response between individuals might be a differing capacity to clear infection efficiently and successfully resolve inflammation. Amongst the parameters responsible for variability, an important one to consider is age, as there is evidence that immunological responses are greatly affected by it - both in terms of cell population numbers and functions - which led to the creation of the new separate research area that is immunoscenescence (Solana et al., 2012). This is particularly important when considering an aging population, like PD patients who are often elderly. For example, preliminary work by Witowski's group showed that HPMC seem to behave differently when stimulated at early and late (senescent cells) passages, with a heightened basal level of IL-6 secretion and lack of response to stimulation by PD effluent by the latter when compared to "younger" cells (Rudolf and Witowski, 2013). In addition, it has been shown that breast cancer cells, naturally unresponsive to IL-6 stimulation, increase their IL-6R expression during cellular senescence, rendering them responsive to classic IL-6 signalling, whereas they were previously only responsive to trans-signalling (Garbers et al., 2013), potentially triggering a detrimental cascade of events. This will be important to consider when exploring new therapeutic avenues.

Despite the mentioned variability, the data presented in this study adds further evidence of the role of the mesothelium in the regulation of inflammation in the peritoneal cavity, and emphasise the importance and relevance of cell-type/organ specific studies, as conflicting data often arise from different experimental model systems. In addition, experiments done with KO mice replenished with the missing protein/molecule do not necessarily recapitulate the observations in WT animals, implying the existence of underlying mechanisms better understood at a specific cell-type/organ level. Indeed, in CAPD, increased local IL-6 levels in the peritoneal cavity are associated with lower membrane function but not with survival, whereas systemic levels correlate with survival (Lambie et al., 2013). In addition, since individual pathologies may possess unique aetiologies, it is critical that changes in the immune response are monitored within a defined clinical context.

The critical role played by the mesothelium in inflammation is further demonstrated by the capacity of human peritoneal fibroblasts to secrete CXC and CC chemokines - notably CXCL8, CXCL1, IL-6, CCL2 - in response to inflammatory mediators secreted by macrophages, demonstrating the fibroblasts' contribution to leukocyte trafficking into the peritoneal cavity (Jorres et al., 1996; Witowski et al., 2009; Witowski et al., 2001).

SES- and *S. epi*.-induced TLR2 stimulation leading to NF-κB activation, chemokine secretion and leukocyte recruitment, and the modulatory effect of sTLR2 demonstrated in this study are convincing evidence that TLR2 is involved in peritoneal responses to Gram-positive bacterial infection. Notably, in addition to the well-documented observations of the activity of TLR2 in leukocyte populations (Zarember and Godowski, 2002) confirmed here, the present results demonstrate the activity of TLR2 in stromal cells of the peritoneal membrane.

This study also demonstrated that sTLR2 regulates peritoneal TLR2-mediated pro-inflammatory responses induced by microbial components from Gram-positive bacteria *in vitro* and *in vivo*. In addition, a role of sTLR2 in macrophage and neutrophil functions has been shown, with a modest inhibitory effect on the phagocytic capacity of macrophages, but a significant reduction in superoxide production by neutrophils (Raby et al., 2009), thus showing sTLR2 potential to modulate critical effector functions. The presence of sTLR2 in non-infected and infected effluents of PD patients points at a role of sTLR2 as part of a negative feedback mechanism to control peritoneal inflammation and therefore limit the potential damage to peritoneal tissues that may result from a prolonged response to infection. Considering that inflammation is an aggravating factor in PD and increases treatment failure, it would be of interest to monitor sTLR2 levels over the course of PD therapy and evaluate the potential as marker of treatment outcomes by linking sTLR2 levels to membrane function and survival. Given that HPMC are known to play an important role during the early phase of peritoneal inflammation, notably in leukocyte trafficking into the peritoneal cavity (Douvdevani et al., 1994; Topley et al., 1993a; Topley and Williams, 1994), their ability to respond to sTLR2 demonstrated in this study supports an additional role of this cell type, as critical player in the modulation of the inflammatory response.

Beside a role in processes such as metabolism, embryonic development and memory consolidation, IL-6 and its receptors are involved in inflammation by controlling differentiation, proliferation, migration and apoptosis of target cells (Scheller et al., 2013). Previous studies demonstrated the involvement of IL-6 signalling in the resolution of inflammation (Hurst et al., 2001; McLoughlin et al., 2005; Xing et al., 1998) and the data presented here further substantiate this role. Unpublished data from our laboratory using the *S. epi*. *in vivo* model of peritoneal inflammation in WT and IL-6KO mice demonstrated the importance of non-hematopoietic stromal cells of the peritoneal membrane in IL-6-mediated processes by showing that IL-6-trans-signalling and STAT3 activity in the peritoneal membrane may be responsible for the anti-bacterial activity of the infiltrating neutrophils. The study showed that upon *S. epi*. infection, sIL-6R is shed by resident macrophages and infiltrating neutrophils. Subsequently, these cells became unresponsive not only to IL-6 classic but also trans-signalling, and dependant on stromal cell trans-signalling and STAT3 activity for efficient phagocytic and respiratory burst activity by neutrophils (Hammond et al., manuscript in preparation).

IL-6 is a marker of disease progression, and a humanised anti-IL-6R antibody is now used to treat rheumatoid arthritis (Tanaka et al., 2012). However, blocking of IL-6 signalling has been associated with increased bacterial infections (Lang et al., 2012), an important issue to consider in prolonged/lifetime treatment therapies such as rheumatoid arthritis and other autoimmune diseases. The findings presented in this thesis by using IL-6KO mice are consistent with the IL-6 blocking experiments reported previously, as they show that the lack of IL-6 reduces bacterial clearance substantially. Bacterial clearance is a major parameter to control in order to promote a timely resolution of inflammation and limit the damage of host tissue. Retention of leukocytes at sites of immunological challenges is also a risk factor of chronic inflammation and fibrosis. Well-designed *in vivo* models of peritoneal infection/inflammation are critical to a better understanding of the host's response to bacterial challenge, which is vital to reduce the impact of the concomitant inflammation in the peritoneal cavity. The development, validation and use in this study of a mild-moderate mouse model of peritoneal infection using *S. epi.*, *S. aureus* and *E. coli*, has allowed us to make key observations of clinical relevance to bacterial peritonitis. Notably, by collecting data on leukocyte profiling over time during infection, local and systemic bacterial dissemination/clearance rates, body temperature change profile and changes in the acute phase response, it was demonstrated that therapeutic modulation of the IL-6/sIL-6R signalling pathway could accelerate bacterial clearance as a result of its effect on leukocyte trafficking. The change in the spectrum of infecting organisms in PD patients correlates with the increased development of antibiotic resistance, which is driving the increased demand for novel therapeutic strategies to combat these types of infections. The new live *in vivo* model described here, specifically with the use of both Gram-negative and Gram-positive bacteria and also clinically relevant antibiotic resistant organisms, will help to evaluate whether modulating leukocyte trafficking and/or bacterial clearance through the use of molecules such as sTLR2 and IL-6/sIL6R complex improves the resolution process and is a viable therapeutic option for all infections. The validation of this model should subsequently inform the development of therapeutic interventions to reduce inflammation, through a faster and more efficient resolution, and prevent progression to membrane and technique failure.

IL-6 and sIL-6R possess the capacity to orchestrate both beneficial and detrimental outcomes. Plasma IL-6 levels are increased in numerous diseases, including CAPD, and considered to be a prognostic marker of poor outcomes (Pecoits-Filho et al., 2002). Sepsis is a complex syndrome, with a heterogeneous immune response (Remick et al., 2002). Elevated IL-6 levels in peritonitis mouse models of sepsis have been found associated with a higher mortality risk (Remick et al., 2002), although this correlation was demonstrated only for the early but not late sepsis mortality (Osuchowski et al., 2006). Therefore, IL-6 presence is often associated with detrimental outcomes, indeed, genetic polymorphism leading to increased IL-6 mRNA levels in the peritoneal membrane and IL-6 protein levels in dialysate and plasma are associated with higher membrane permeability and worse solute transport function (Gillerot et al., 2005). Despite high serum IL-6 concentration, studies have described an impaired IL-6/STAT3

signalling in sepsis that correlates with increased mortality - possibly due to an alteration of the gp130 signalling receptor phosphorylation status and/or inhibition of the JAK/STAT pathway (Abcejo et al., 2009; Ling et al., 2002). Serum sIL-6R levels are also increased during inflammation, as well as local levels in various autoimmune disorders and cancers, and correlate with poor survival (Kallen, 2002). Given its detrimental role in various diseases, blockade of IL-6 signalling with an anti-IL-6R antibody is now a common therapy, notably for rheumatoid arthritis, and has proven very effective (Serada et al., 2008; Takagi et al., 1998). In light of more recent research, and the differing activities of classic *vs.* trans- signalling, blocking of the latter pathway using soluble gp130 linked to the Fc portion of IgG (sgp130Fc) (Jostock et al., 2001) has shown promising results in preclinical animal models of chronic inflammatory diseases such as inflammatory bowel disease (IBD), rheumatoid arthritis (RA) and inflammation-associated cancer such as colon cancer, and is currently in phase I clinical trials for IBD and RA (Scheller et al., 2013). Separating clearly the role of classic IL-6 signalling *vs.* trans-signalling, however, remains a challenge. Through the design and use of the proteins Hyper-IL-6 (chimera IL-6/sIL-6R fusion protein) and soluble gp130Fc studies have demonstrated that IL-6 trans-signalling drives chronic inflammation and autoimmune disorders (Jones et al., 2011). Whether one of the two IL-6 signalling pathways is really detrimental remains to be determined. Some differences could be explained by the fact that different stages of the inflammatory process and disease progression - initiation, progression/resolution *vs.* chronic inflammation - are controlled by different cell-types, namely leukocytes/hematopoietic cells and hepatocytes, which express membrane-bound IL-6R, and non-hematopoietic cells, which express gp130 and are only activated *via* trans-signalling once the IL-6R has been shed by leukocytes. The immune activity of non-hematopoietic cells may not be as tightly regulated as in leukocytes, and a slight deregulation may trigger harmful signalling events. In addition, once sIL-6R has been shed, all cells in the environment may have the capacity to trigger IL-6-mediated responses *via* trans-signalling, amplifying a potentially detrimental effect of IL-6 signalling irrespective of the pathway classic or trans- signalling. Finally, the trans-signalling detrimental effect could be due to a deregulation of leukocyte activation status, primarily neutrophils, leading to an excessive sIL-6R shedding and a cascade of detrimental signalling events. Deciphering the role of the two different types of signalling, as well as cell-type activity, might be beneficial to inform future therapeutic options, and as knowledge increases, it might prove useful to block classic *vs.* trans- signalling at various stages of the disease.

In HPMC, the simultaneous activation of the TLR2 and IL-6 signalling pathways - via NF-κB and STAT3 activation, respectively - showed an inhibitory effect on the NF-κB-driven secretion of the neutrophil chemoattractant CXCL8 and induction of the monocyte and T cell chemoattractant CCL2. These findings suggested an additional role of HPMC in response to Gram-positive infection, in the transition from the recruitment of leukocytes typically associated with innate immunity to those important in acquired immunity. This transition appears to facilitate the successful resolution of inflammation and the return to normal tissue homeostasis

without organ damage (DiTirro et al., 1998). The *in vivo* results using IL-6-deficient mice partly correlated with the *in vitro* findings, in particular regarding the role of IL-6 in controlling neutrophil recruitment, as IL-6 deficiency resulted in increased peritoneal neutrophil recruitment and CXCL1 levels. By contrast, *in vivo,* IL-6 deficiency also resulted in increased CCL2 levels and monocyte/lymphocyte recruitment, indicating a negative effect of IL-6 on mononuclear cells recruitment *in vivo*. CCL2 secretion and regulation - and its effect on mononuclear cell influx - *in vivo*, appear to be complex mechanisms and do not seem to be governed by IL-6 signalling exclusively. The use of whole bacteria (*S. epi*.) and the involvement of other peritoneal cells in addition to HPMC may have also contributed to the effect observed *in vivo*, as it is possible that microbial components other than those activating via TLR2 may have triggered signalling pathways in peritoneal cells that directly or indirectly modulate IL-6 signalling.

sTLR2 also demonstrated a differing modulatory effect on neutrophil and mononuclear cell recruitment, as sTLR2 - *via* inhibition of CXCL8 secretion - reduced neutrophil influx, as shown in this study, whereas it had no effect on mononuclear cell recruitment, despite triggering a heightened CCL2 secretion, as shown by Raby *et al*. (Raby et al., 2009). Other chemokines - such as CCL3 and CCL5 - play an important role in inducing monocyte/macrophage infiltration to the site of infection and it would be of interest to study the effect of sTLR2 on their recruitment profiles. Another cytokine belonging to the IL-6 family affects the profile of leukocyte recruitment. Indeed, oncostatin M has been shown to limit monocytic cell infiltration by inhibiting CCL5 secretion by HPMC (Hams et al., 2008). In addition, human peritoneal fibroblasts have been shown to release CCL5 in response to inflammatory mediators present in the inflamed peritoneal cavity (Kawka et al., 2014). Alternatively, chemokine receptor expression might be affected, rather than the ligand. CCR1, CCR2 and CCR5 are CC chemokine receptors mediating the recruitment of blood monocytes towards infected tissues. It will be of interest to test whether the expression of these receptors is affected by sTLR2 and by IL-6/sIL-6R in TLR2-mediated responses, as TLR2 has been shown to negatively regulate these receptors (Fox et al., 2011). The chemokine network generated following an inflammatory insult will have compensatory roles, with the positive effect of one chemokine counteracted by other mediators. The results of the present study also suggest a differing regulation of the various chemokines expressed during an inflammatory episode between the various cell-types involved, resulting in an increased complexity when examining responses at the organ level.

The modulatory effect of IL-6 and its STAT3 downstream signalling pathway on TLR2-mediated responses indicated by the findings of this study, has also been suggested in a number of studies and disease settings. In cancer, with tumorigenesis often reliant on/or involving a chronic inflammatory component, a common feature is the deregulated co-activation of STAT3 and NF-κB (Mansell and Jenkins, 2013). Notably, one study on gastric cancer demonstrated that STAT3 activation directly increased TLR2 expression in gastric epithelial cells (Tye et al., 2012). In this regard, it will be of interest to investigate the effect of IL-6/sIL-6R on TLR2

expression in HPMC as well as in the *in vivo* settings used in this study. Preliminary results of HPMC stimulation with Pam_3Cys or SES in the presence or absence of the IL-6/sIL-6R complex showed that Pam_3Cys-mediated and SES-mediated Tlr2 mRNA levels did not seem to be significantly affected by IL-6/sIL-6R. These results imply that the modulatory effect of IL-6 signalling on TLR2-mediated responses may not be exerted through modulation of TLR2 expression, but the data will need to be confirmed before a clear interpretation can be made. Another indication of the interplay between TLR2 and IL-6 signalling pathways is the observation that the production of a number of non-microbial TLR2 agonists is regulated by STAT3, such as the TLR2 agonist SAA (Hagihara et al., 2005). It will also be of interest to further study the regulation of this acute phase reactant in our *in vivo* settings.

A number of issues and questions were raised by the present study that deserve to be addressed through future work:

1. The results of the *in vitro* studies have indicated that SES responses are mediated primarily *via* TLR2. However, the extent of the TLR2 involvement and the possibility that additional signalling pathways are involved cannot be excluded at present. Stimulation of the astrocyte-like cell line U373, which expresses TLR1, TLR3, TLR4 and TLR5, but not TLR2 or CD14, gave an additional indication of the main role of TLR2 (Kurt-Jones et al., 2004). Following stimulation with increasing doses of LPS, Pam_3Cys and SES, these cells showed a dose-dependent secretion of CXCL8 in response to LPS but not to Pam_3Cys, and SES only triggered a response at the highest dose used. Preliminary *in vivo* experiments of i.p. injection of SES into C3H/HeJ mice, which are naturally deficient in TLR4 signalling (Poltorak et al., 1998), showed a response to SES in terms of neutrophil recruitment over a 6h time period, further confirming the lack of involvement of TLR4 in SES responses. To further study the specificity of SES-induced responses it would be of interest to block specific signalling pathways using TLRs and NODs siRNAs *in vitro*, as well as TLR2KO mice *in vivo.*

2. Following previous work on the role of sTLR2 and the elucidation of its mechanism of action (LeBouder et al., 2006; Raby et al., 2009), this study has further demonstrated in HPMC and in two *in vivo* models that sTLR2 is able to dampen inflammation by reducing NF-κB activation, neutrophil chemoattractant levels and the number of neutrophils infiltrating the peritoneal cavity. The lack of effect of sTLR2 on bacterial clearance has not been extensively investigated. As there is debate about the exact role of TLR2 in bacterial clearance, it will be of interest to evaluate the role of sTLR2 in IL-6KO animals, where there is an increased neutrophil influx and delayed bacterial clearance, and to determine sTLR2's capacity to modulate a deregulated inflammatory response.

3. It will be of interest to examine the regulation of TLR expression further during *in vivo* inflammation. To this end, peritoneal inflammation using the established SES or *S. epi*. models may be induced in WT mice and several strain of knockin mice genetically modified in the gp130 signalling pathway. At specific time points, inflammatory mediator expression and leukocyte trafficking will be examined to define the immune activation process, and TLR2 expression levels will be assessed in the peritoneal membrane. Preliminary experiments using the SES *in vivo* model indicate a reduction of TLR2 expression in the peritoneal membrane when STAT3 is over-expressed, suggesting a possible down-regulation of TLR2 expression by IL-6/STAT3 signalling. Changes in expression levels of SOCS3 - a STAT3-dependent inhibitor of IL-6 signalling - will also be monitored as SOCS3 has been described as being part of a negative feedback loop to regulate TLR signalling (Baetz et al., 2004; Rothlin et al., 2007).

4. One of the main complications of PD therapy is the development of fibrosis of the peritoneal membrane (de Lima et al., 2013), leading to loss of peritoneal function. Fibrosis is linked to the duration of treatment and incidence of bacterial peritonitis (Davies et al., 1996; Williams et al., 2002). IL-6 signalling was shown to play a critical role in the development of fibrosis through STAT1 inhibition of homeostatic extracellular matrix turnover (Fielding et al., 2014). The involvement of TLRs, and TLR2/4 in particular, in peritoneal fibrosis remains to be determined. To examine the influence of TLR signalling on the development of fibrosis, repeated rounds of inflammation will be induced in WT and TLR2/4KO mice. At defined time points up to 49 days, peritoneal lavages will be collected as well as membrane biopsies, specifically mesothelial cell layer obtained by laser dissection. Immuno-detection approaches and quantitative mRNA analysis will be used to assess changes in TLR and fibrotic markers expression, such as collagen, transforming growth factor β and SMAD7. Such changes will be correlated with alterations in leukocyte trafficking and inflammatory mediator expression. The thickness of the submesothelial compact zone will be measured, scored and compared in WT and TLR2/4KO mice.

5. The anti-inflammatory capacity of sTLR2 and its presence in the PD effluent described in this study raise the question of whether sTLR2 levels in PDE correlate with treatment outcome and/or can be used as early and sensitive prognostic marker of infection in these patients. In this regard, it will be of substantial interest to monitor sTLR2 levels in the PDE of stable and infected patients.

In conclusion, this study demonstrated that the interaction of Gram-positive bacteria with TLR2 expressed on the mesothelium is an early feature of the induction and orchestration of the inflammatory response in the peritoneal cavity. A growing number of studies highlight the relevance of examining different pathways in relation to each other, as none acts in isolation, and what is observed results from a combination of interplays and cross-talks between various pathways. Understanding the regulatory processes governing the onset of inflammation and the

molecular mechanisms behind the altered responses observed in chronic diseases may inform the design of novel therapeutics against acute and chronic inflammatory conditions that will aim at reducing detrimental events while preserving microbial recognition and effective immune responses. Such therapeutics may prove useful in PD.

Chapter 4

MATERIALS AND METHODS

4.1 Antibodies, reagents and equipment

The antibodies used and their sources are listed in Table 4.1 and 4.8. All chemicals were reagent grade. The synthetic bacterial lipopeptides Pam_3-Cys-Ser-$(Lys)_4$ HCl (Pam_3Cys) and Pam_2-Cys-Phe-Glu-$(Pro)_3$-Ala-$(Thr)_3$ (Pam_2Cys) were purchased from EMC Microcollections GmbH, (Tübingen, Germany). Ultra-pure LPS (from *Escherichia coli* O111:B4 strain), bacterial peptidoglycan and Flagellin (from *Salmonella typhimurium*) were purchased from Invitrogen™, Life Technologies (Paisley, UK). Human natural soluble CD14 (sCD14), purified from human milk as described previously (Labéta et al., 2000) and human recombinant sTLR2, produced and purified as described in Raby *et al*. (Raby et al., 2009), were prepared in our laboratories. sTLR2 corresponds to the full extracellular domain of human TLR2. Recombinant IL-1β, TNFα, IFNγ, IL-6, sIL-6R (proteolytic shedding form) and Oncostatin M were purchased from R&D Systems (Minneapolis, MN, USA). The unimolecular protein HYPER-DS-sIL-6R (HDS) is a genetically engineered sIL-6R-IL-6 fusion protein designed so that IL-6 is linked to the differentially spliced form (DS) of sIL-6R, was GMP-manufactured by Biovian Ldt. (Turku, Finland). DRAQ5 was from Biostatus Ltd. (Shepshed, UK). Fluorosave was from Merck Millipore (Nottingham, UK). Electrophoresis grade agarose (Ultrapure agarose) was from GIBCO/BRL (Paisley, UK). EDTA, DTT, recombinant ribonuclease inhibitor (RNAsin) and Klenow fragment (DNA polymerase I large) were from Promega Ltd (Southampton, UK). Ficoll Type 400, random hexamers and deoxynucleotides (dATP, dGTP, dCTP, dTTP) were from Amersham Biosciences UK Ltd (Chalfont St.Giles, UK). Nitrocellulose membrane (Hybond ECL) was from Amersham Pharmacia, UK Ltd., (Little Chalfont, UK). RNAse-free DNAse I, Superscript II reverse transcriptase and Superscript III 1st strand synthesis strand system were from Invitrogen™, Life Technologies. All cell culture media and reagents were purchased from Invitrogen™, Life Technologies, unless otherwise stated. 1X PCR buffer was from Applied Biosystems (Warrington, UK). The cell culture flasks (Falcon) were from Becton Dickinson (Oxford, UK). Human AB serum was from tcs biosciences Ltd (Buckingham, UK). RNase-free DNase Set and RNAEasy minicolumns were from Qiagen (Valencia, CA, USA). $\alpha[^{32}P]$-dTTP was from Perkin Elmer (Waltham, MA, USA). 6X DNA loading buffer and the centrifuge for cytospin were from Thermo Fisher Scientific (Waltham, MA, USA). X-ray films were from GE Healthcare (Chalfont St Giles, UK). *Staphylococcus epidermidis* (12228), *Staphylococcus aureus* (25923) and *Escherichia coli* (25922) were purchased from ATCC (ATCC, Teddington, UK). Heparin (5,000 units/ml) was from Sagent Pharmaceutical (Schaumburg, IL, USA). Modified Wright-Giemsa stain (Accustain), BAC-extract (Benzalkonium Chloride, 1 mg/ml), transferrin, insulin, hydrocortisone, Tri Reagent, 3M Whatman paper and Tyrode's salt were purchased from (Sigma-Aldrich, Poole, UK). The ATP Bioluminescence Assay Kit CLS II was purchased from Roche Diagnostics (Burgess Hill, UK). Nutrient Broth No. 2, diagnostic sensitivity testing agar plate, agar slopes, 50% glycerol slopes on plastic beads, Mueller-Hinton Agar plates and Columbia Agar with 5% Horse blood were from Oxoid Limited (Basingstoke, UK). The tissue homogeniser (PowerGen125) was purchased from Fisher Scientific

Table 4.1 List of antibodies and immunoreagents

Antibodies to	Clone/code	Isotype	Source
Human TLR2	T2.5	Mouse IgG1	eBioscience, CA, USA
Human TLR2	TL2.1	Mouse IgG2a	eBioscience
Human TLR2 peptide N-terminus 20-mer peptide)	TLR2p	Rabbit IgGs	Dr. M.O. Labéta, Institute of Infection & Immunity, School of Medicine, Cardiff University, UK {LeBouder, 2003 #14}
Human TLR4	HTA 125	Mouse IgG2a	eBioscience
Human TLR1	GD2.F4	Mouse IgG1	eBioscience
Human TLR6	hPer6	Rat IgG2a	eBioscience
Human CD14	MY4	Mouse IgG2b	Beckman Coulter, High Wycombe, UK
Human CD14-PE	M5E2	Mouse IgG2a	BD Biosciences, Oxford, UK
Human CA125-PE	OC125	Mouse IgG1	Fujirebio Diagnostic Inc., Malvern, PA, USA
Human gp130-PE	28126.111	Mouse IgG1	R&D Systems, Dorset, UK
Human gp130	H-255	Rabbit IgGs	Santa Cruz Biotechnology, Santa Cruz, CA, USA
Rabbit IgGs	-	Goat IgGs	Santa Cruz Biotechnology
Mouse F4/80-FITC	CI:A3-1	Rat IgG2b	Serotec, Oxford, UK
Mouse CD11b-APC	M1/70	Rat IgG2b	BD Pharmingen, Oxford, UK
Mouse IgG-Alexa 568	-	Goat IgGs	Kindly provided by Prof V. O'Donnell, Institute of Infection & Immunity, School of Medicine, Cardiff University, UK
Rabbit IgGs-HRP	-	Donkey IgG	ECL system, Amersham
Rat IgG-FITC	11-4811	Mouse IgG	eBioscience
Immunoreagents	**Clone/code**	**Isotype**	**Source**
Rat IgG (purified)	eBR2a	IgG2a	eBioscience
Mouse IgG (purified)	14-4714	IgG1	eBioscience
Mouse IgG (purified)	14-4724	IgG2a	eBioscience
Mouse IgG (purified)	16-4732	IgG2b	eBioscience
Rat IgG (purified)	LO-DNP-16	IgG2a	Serotec
Anti-Mouse IgG/RPE	R0480	Goat $F(ab')_2$	Dako, Glostrup, Denmark
Rat IgG-PE	-	Goat IgG	Dako
Normal rabbit serum	-	-	Dako

(Loughborough, UK). The rectal probe thermometer (TES 1319 K type) was purchased from Vet Tech Solutions, (Congleton, UK). The Whitley Automated Spiral Plater (WASP II) and aColyte 3 colony counter were purchased from Don Whitley Scientific Limited (Shipley, UK). The Beckman UV-DU64 spectrophotometer was from Beckman Instruments Ltd (High Wycombe, UK). The mini gel system was from Thermo Life Sciences Ltd (Basingstoke, UK). The ChemiDoc^{TM} Gel documentation system, the Bio-Rad Mini Protean II gel apparatus and the Bradford assay were from Bio-Rad Laboratories Ltd (Hercules, CA, USA). The inverted light microscope (Axiovert 25) was from Carl Zeiss Ltd (Cambridge, UK). The Coulter counter (Coulter Z2) was from Beckman Coulter (High Wycombe, UK). The NanoDrop-1000 spectrophotometer was from Fisher Thermo (Wilmington, DE, USA)

4.2 Cell and tissue culture

4.2.1 HPMC isolation, growth conditions and sub-culture

HPMC were isolated from consenting patients undergoing elective abdominal surgery by serial tryptic digestion of greater omental tissue obtained using an adapted version of Stylianou's original method (Stylianou et al., 1990), as previously described (Topley et al., 1993a). Briefly, tissue sections were washed in sterile Dulbecco's phosphate-buffered saline (PBS; 2.5 mM KH_2PO_4, 137 mM NaCl, 8 mM Na_2HPO_4 pH 7.4, then digested in 20 ml 0.1% (w/v) trypsin/ 0.02% (w/v) EDTA, diluted in PBS and incubated 15 min at 37°C with continuous rotation. HPMC were harvested by centrifugation at 800 x g for 6 min at room temperature (RT). The omentum was transferred to a new tube for a second digestion step identical to the first one. Pelleted cells of each piece of omentum were suspended in 5 ml growth medium. Cells were cultured in Earle's buffered 199 medium containing 10% (v/v) foetal calf serum (FCS) (Hyclone, Logan, UT, USA; < 0.06 U/ml endotoxin), supplemented with 2 mM L-Glutamine, 100 U/ml penicillin, 100 µg/ml streptomycin, 5 µg/ml transferrin, 5 µg/ml insulin and 0.4 µg/ml hydrocortisone (Li et al., 1998). Cell monolayers were grown in 25 cm^2 cell culture flasks (T25) and incubated at 37°C in a 5% CO_2 incubator until confluent, when the cells were passaged at a 1:3 ratio.

In order to remove potentially contaminating fibroblasts and macrophages from primary cultures, HPMC purity was enhanced by performing "differential sub-culture/adherence" (Lang and Topley, 1998). On reaching confluence, the primary culture cells in T25 flasks were transferred to 75 cm^2 culture flasks (T75 Falcon). Growth medium was aspirated and cells in T25 flasks were washed in sterile PBS, followed by trypsinisation with 10% (v/v) trypsin/EDTA diluted in sterile PBS. Cell detachment was monitored by light microscopy following brief incubation at 37°C. Following detachment, 10 ml of growth medium was added to neutralise the trypsin. The cell suspension was transferred to a 30 ml tube and spun at 600 x g for 6 min at room temperature, the supernatant removed and the cell pellet resuspended in fresh growth medium, before transfer to a T75 culture flask and incubated at 37°C, 5% CO_2.

The morphology of HPMC monolayer cultures was examined using an inverted light microscope. Confluent HPMC were typically polygonal in shape and displayed the classical "cobblestone" appearance, as shown on Figure 1.3 (Introduction).

4.2.2 SV40-transformed HPMC

SV40-transformed HPMC cell line (kindly provided by Dr. Jean-Phillipe Rougier, Department of Nephrology and Dialysis, Unité INSERM 64, Hôpital Tenon, Paris, France) (Rougier et al., 1997), are derived from a primary HPMC culture transformed with a plasmid containing a modified SV40 virus sequence, containing a deletion in the late region and a 1 bp insertion, which disrupts the origin of replication site within the SV40 genome. These cells retain many of the characteristics of primary HPMC including morphology and the expression of Cytokeratins 8 and 18 and Vimentin (Fischereder et al., 1997). They were used to test the bioactivity of SES preparations (section 4.12). SV40-transformed HPMC were cultured under the same conditions as HPMC in 10% FCS DMEM with 25 mM HEPES supplemented with 2 mM L-Glutamine, 100 U/ml penicillin, 100 µg/ml streptomycin, 5 µg/ml transferrin, 5 µg/ml insulin and 0.4 µg/ml hydrocortisone. Cells were grown (incubated at 37°C, 5% CO_2) in T25 culture flasks until confluent and passaged as previously described for HPMC (section 4.2.1).

4.2.3 Isolation and culture of Peripheral Blood Mononuclear Cells

Peripheral blood mononuclear cells (PBMC) were isolated by Ficoll density-gradient centrifugation from whole blood of healthy volunteers. Briefly, blood was collected in tubes containing EDTA (0.5 M) as an anticoagulant and centrifuged at 400 x g (10 min, RT). The upper phase was discarded and the leukocytes were diluted in an equal volume of PBS and then 6 ml were carefully layered onto 5 ml of room temperature Ficoll-Paque PLUS (Ficoll PM400 and sodium diatrizoate with a density of 1.077 g/ml; Sigma-Aldrich) and centrifuged (400 x g, 30 min, RT) without brake. PBMC sediment at the interface, whereas neutrophils pellet at the bottom. The interface between the upper layer of plasma and the Ficoll was carefully removed, transferred to a new tube and washed three times with PBS (first wash: 400 x g, 10 min, RT; second and third washes: 300 x g, 8 min, RT). PBMC were resuspended in PBS at a concentration of 2 x 10^6 cells/ml in preparation for flow cytometry analysis (described in section 4.5) or directly resuspended in Tri Reagent for RNA extraction (described in section 4.6). Alternatively, mononuclear cells were obtained by adherence (2h, 37°C) on cell culture flasks of PBMC that had been resuspended in RPMI-1640 medium supplemented with 2 mM L-Glutamine, 100 U/ml penicillin, 100 µg/ml streptomycin and 0.5% human AB serum.

4.2.4 Culture of transfected Human Embryonic Kidney Cells

Human Embryonic Kidney (HEK) 293 plasmid control transfected cells (HEK-pDR2) and HEK-TLR2-transfected cells were generated in our laboratories as previously described (LeBouder et al., 2003). HEK-TLR4/MD2-transfected cells were kindly provided by Prof. Douglas T.

Golenbock (Department of Medicine, Division of Infectious Diseases and Immunology, University of Massachusetts Medical School, USA). HEK293-transfected cells were cultured in complete medium: DMEM containing 4500 mg/ml Glucose supplemented by 2 mM L-Glutamine and 10% FCS and specific additives as follows: 400 µg/ml hygromycin B (Calbiochem, San Diego, CA) for HEK-TLR2 (LeBouder et al., 2003) or 200 µg/ml Geneticin (G418) (Sigma Aldrich) for HEK-TLR4/MD2.

4.3 Cell activation

4.3.1 Activation of HPMC

HPMC monolayers were cultured in T25 (for flow cytometry analysis), 6-well plates (for RNA analysis and protein extraction), or 24- and 48-well plates (for cytokine and chemokines secretion), until they reached confluence. Prior to experimentation, HPMC were growth arrested for 48h in serum free culture medium. All experiments were performed with confluent HPMC from the second passage, except when testing for TLR2 and TLR4 expression (Figure 2.1.3) when cells were used immediately following tryptic digestion, as described in section 2.1.1.
Confluent growth-arrested HPMC were cultured (37°C for 24h) in triplicate in medium containing 0.1% FCS (unless stated otherwise) in the presence or absence of the stimuli indicated in the figure legends and Results section. To test for cytokine and chemokine secretion, cell culture supernatants were harvested, centrifuged (300 x g, 5 min, RT) to remove cellular debris and the supernatant stored at -80°C until assayed using commercially available ELISA kits for human CXCL8, human CCL2, human CCL5 (BD OptEIA, BD Biosciences, Oxford, UK); TNFα and human IL-6 (DuoSet, R&D Systems) and human sIL-6R (DuoSet, R&D Systems; it does not distinguish between the two sIL-6R isoforms) according to the manufacturer's instructions. For sTLR2 expression experiments (Figure 2.2.1A), the cell-free culture supernatants were analysed by Western blotting as described below in section 4.10.

For Ab blocking experiments shown in Figure 2.1.13A, HPMC were pre-incubated (1h 30min) with an anti CD14-specific blocking mAb (MY4, IgG2b, 10 µg/ml) or its isotype-matched control, before adding SES and incubating for up to 24h.
For cell activation experiments in the presence of sTLR2 shown in Figure 2.2.1C, sTLR2 (5 µg/ml) was pre-incubated for 30 min at 37°C with Pam_3Cys or SES in medium without serum before adding the stimulatory mixture to the cells for the time indicated in the figure.
For cell activation shown in Figures 2.2.3 to 2.2.6, IL-6 and sIL-6R (at the concentrations indicated in the figure legend) were mixed and pre-incubated for 15 min at room temperature to allow complex formation, before incubation with the cells.

4.3.2 Activation of PBMC

For the blocking experiments shown in Figure 2.1.13B, PBMC were seeded at 2 x 10^6 cells/ml and incubated for 2h before removing non-adherent cells by washing twice with PBS. PBMC were then pre-incubated or not with the anti CD14 blocking mAb (MY4, 10 µg/ml) or its isotype-matched control for 1h at 37°C, and the stimulus was then added as indicated in the figure legend. Cells were cultured in phenol red free RPMI-1640 medium supplemented with 0.5% human AB serum and stimulated for 20h as indicated in the figure legend. CXCL8 levels in the cell-free culture supernatants were quantified by ELISA.

4.3.3 Stimulation of transfected Human Embryonic Kidney Cells

For the cell activation experiments described in Figure 2.1.9C, confluent cells were trypsinised and washed 5 times with PBS to eliminate serum sCD14 before stimulation with dilutions of SES or left untreated (medium alone). HEK-TLR2 were seeded in triplicate at 500,000 cells/well on 48-well plates, and directly stimulated in suspension for 15h. CXCL8 was quantified by ELISA in the cell-free culture supernatants.

4.4 Detection of TLR expression by immunocytochemistry

Non-stimulated and stimulated cells were trypsinised, washed with PBS and resuspended in PBS at a concentration of 1 x 10^6 cells/ml. Hundred microlitres of cell suspension were cytospined, and the cells were then fixed on slides with acetone for 5 min at -20°C, washed in PBS once (5 min, RT) and left in PBS overnight at 4°C. To reduce non-specific binding of Abs, the cells were incubated (1h, RT) with PBS containing 1% (w/v) BSA (bovine serum albumin fraction V) and 10% (v:v) normal rabbit serum before incubation (1h, RT) with either the appropriate Ab (T2.5, IgG1, 5 ug/ml) or an isotype matched control. Slides were washed three times over a 45 min period and were then incubated with Alexa 568-conjugated secondary Ab (kindly provided by Prof V. O'Donnell, Institute of Infection and Immunity, School of Medicine, Cardiff University, UK) for 30-45 min at 37°C in the dark. Slides were washed for a 45 min period changing buffer every 10-15 min, and cells were stained for 5 min at room temperature with DRAQ5, a marker of DNA content. Slides were washed once in PBS and once in water, dried and a drop of Fluorosave was added on the cells before placing a coverslip and sealing. Slides were kept in the dark and imaging was performed using an Axiovert 100 inverted microscope connected to a Bio-Rad MRC 1024ES laser scanning system (Bio-Rad Microscience, Hemel Hempstead, UK) and using a standard analysis software (Lasersharp 2000, Bio-Rad Microscience).

4.5 Flow cytometry analysis

In preparation for flow cytometric analyses, HPMC were trypsinised or scraped from cell culture flasks. HPMC or PBMC were washed and resuspended in PBS at a density of 2 x 10^6 cells/ml.

Fifty microlitres of cell aliquots were distributed in wells of round bottom 96-well plates. Cells were incubated for 5 min at 4°C with 50 µl of blocking buffer (50% FACS buffer: PBS pH 7.3, 10 mM EDTA, 1% BSA, 15 mM sodium azide; 25% normal rabbit serum and 25% human AB serum). For immuno-labelling, 50 µl of the indicated primary unconjugated Abs and their isotype-matched controls or primary fluorochrome-conjugated were added to the wells (1 µg mAb per 10^6 cells in 100 µl total) and incubated for 30 min at 4°C in the dark. Cells were washed twice in FACS buffer (1300 x g, 5 min, 5°C) and resuspended in 250 µl of FACS buffer. Where necessary, cells were incubated for a further 30 min at 4°C in the dark with appropriate fluorochrome-conjugated secondary Abs. The stained cells were analysed by using a FACSCalibur® flow cytometer (Becton Dickinson) using previously defined settings for HPMC (Hurst et al., 2002). Data were acquired from 10,000 to 20,000 events and staining compared against isotype control antibodies. Data were further analysed using the CellQuest Pro software (BD Bioscience) and expressed as mean fluorescence intensity values.

4.6 RNA Analysis

4.6.1 RNA isolation from HPMC and mouse peritoneal membrane

Total cellular RNA was extracted using the TRI Reagent (Sigma Aldrich) and following a chloroform-isopropanol isolation protocol. HPMC monolayers were washed with PBS before adding 1 ml TRI Reagent and incubated for 5 min at room temperature. The resulting cell lysate was collected in a microcentrifuge tube, chloroform was added - 1:5 ratio (v/v) - and the samples were mixed by inversion and left on ice for 5 min to allow separation of two phases. The samples were then centrifuged (12,000 x g, 15 min, 4°C, no braking), the colourless upper phase - containing the RNA - was carefully removed, without disturbing the interface, and transferred to a new tube. RNA precipitation was achieved by adding an equal volume of isopropanol and incubating at -20°C 1h to overnight. RNA was pelleted by centrifugation at 12,000 x g, 20 min at 4°C and the supernatant discarded. The pellet was then washed twice by adding 1.5 ml of 75% (v/v) ice-cold ethanol followed by brief vortexing and centrifugation at 12,000 x g, 20 min at 4°C. The ethanol was removed and the RNA pellet allowed to air dry for approximately 1h before re-suspension in 10 µl of double distilled H_2O. For RNA extraction from mouse peritoneal membrane, approximately 1 cm^2 of membrane was homogenised in 2 ml TRI reagent, followed by the isolation protocol described previously.

4.6.2 Nucleic acid quantification and RNA integrity assessment methods

For RT-PCR experiments, the RNA concentration was determined by spectrophotometric analysis using a Beckman UV-DU64 spectrophotometer. In an appropriate cuvette, 1 µl of RNA or DNA was diluted in 54 µl of sterile water. The absorbance was read at 260 nm and 280 nm. A 260/280 ratio above 1.8 was indicative of a sufficiently pure sample. The concentration was calculated using the following formula:

[RNA or DNA] (µg/ml)= Abs_{260} x Molar extinction coefficient x dilution factor
Molar extinction coefficient for RNA = 40. Molar extinction coefficient for DNA = 50. Dilution factor = 55

An Abs_{260} of between 0.1-1.0 was required to be in the linear range of the Beer-Lambert law, which states that a linear relationship exits between absorbance and the concentration of an absorbing substance, relying on both the distance light travels through the substance (path length) and the absorption coefficient of the substance. Samples were diluted where necessary and discarded if Abs_{260} was below 0.1.

RNA integrity was determined by flat bed electrophoresis using a mini gel system with a 2% agarose gel composed of 1 g electrophoresis grade agarose, 50 ml of 1X TAE buffer (40 mM Tris-Acetate, 1 mM EDTA) and 5 µl ethidium bromide (5 mg/ml). One microgram of RNA was loaded into a single well of the mini gel together with 5 µl of loading buffer - 15% (v/v) Ficoll Type 400 in ddH_2O, 0.25% (v/v) Orange G. RNA integrity was visualised under ultra violet light in the ChemiDoc™ Gel documentation system. The quality of the RNA was assessed by observing the ethidium bromide staining pattern of 28S and 18S ribosomal RNA, with two clearly distinct bands indicative of good RNA integrity.
For qRT-PCR experiments, RNA concentration and integrity was determined as described below in section 4.7.2.

4.6.3 Reverse transcription

Before performing RT-PCR reactions, the RNA was treated with RNAse-free DNAse I following the manufacturer's instructions. Reverse transcription was then performed using the random hexamer method as described previously (Topley et al., 1993a). Briefly, 1 µg of total RNA in a total volume of 20 µl comprising 100 µM random hexamers, 5 mM mixed deoxynucleotides (dATP, dGTP, dCTP and dTTP), 1X PCR buffer (20 mM Tris-HCl, pH 8.4, 50 mM KCl, containing 1.5 mM $MgCl_2$) and 10 mM DTT (Dithiothreitol; Invitrogen) was heated to 95^{o}C for 5 min to linearise the RNA. Following immediate cooling on ice, 40 units of recombinant ribonuclease inhibitor (RNAsin) and 200 units of Superscript II reverse transcriptase were added. The RNA was then reverse transcribed by heating to 20^{o}C for 10 min to enable primer annealing to the linearised RNA, and to 42^{o}C for 60 min to allow primer extension from the random hexamers by reverse transcription. The reaction was stopped by denaturation at 95^{o}C for 5 minutes and 4^{o}C for 2 min. Negative control reactions were performed by replacing the Superscript reverse transcriptase enzyme with distilled water. Two microlitres of the resulting complementary (c) DNA was used in each PCR reaction.

4.7 DNA Analysis

4.7.1 Primer design and PCR

All primer sequences were designed using the internet based Primer 3 software (Rozen and Skaletsky, 2000) (http://biotools.umassmed.edu/bioapps/primer3_www.cgi) and purchased from Invitrogen. Primers were designed to have a GC content of 50-60% and a T_M (annealing temperature) of approximately 60^oC. Primer sequences are detailed in Table 4.2 for RT-PCR and Table 4.3 for qRT-PCR. All primers (lyophilised upon arrival) were reconstituted in ddH_2O to give a stock concentration of approximately 100 µM. A working concentration of 10 µM was prepared for all primers.

For each 50 µl PCR reaction, 2 µl of cDNA generated by reverse transcription (section 4.6.3) was used. Each reaction comprised 1X PCR Buffer containing 5 mM $MgCl_2$, 0.2 mM dNTPs, 1.25 U AmpliTaq Gold and 1 µM oligonucleotide primers (all from Invitrogen™, Life Technologies). Negative control reactions were performed by replacing the cDNA with 2 µl of ddH_2O. PCR amplification was performed as described in Table 4.2.

Five microlitres of PCR products were analysed by 2% agarose gel electrophoresis as described above in section 4.6.2. Typically, the gel was run at 90 volts for 45-60 min. The agarose gels were visualised/photographed using a ChemiDoc^{TM} Gel documentation system.

4.7.2 Quantitative real-time PCR

Human cells

The quantity and quality of total RNA, isolated as described in section 4.6.1, was assessed with the NanoDrop-1000 spectrophotometer and on agarose gel as described in section 4.6.2. Reverse transcription was performed using 1µg of RNA with the High Capacity cDNA Reverse Transcription kit from Applied Biosystems and following the manufacturer's protocol. cDNA was diluted 5 times before performing real-time PCR using Power SYBR green PCR master mix from Applied Biosystems and following the manufacturer's protocol. The primers used for real-time PCR are listed in Table 4.3 as well as the standard amplification process, using an Applied Biosystems ABI 7900 HT.

Mouse peritoneal membrane

Total RNA was isolated from snap-frozen mouse peritoneal membranes as described in section 4.6.1. Fifty micrograms of total RNA was DNase-treated using an RNase-free DNase Set and washed using RNAEasy minicolumns. The DNase-treated RNA was quantified by spectrophotometry (Nanodrop) and its quality assessed with the Agilent Bioanalyzer 2100 using the RNA Nano LabChip kits and the Eukaryote total RNA assay (Agilent Technologies Inc, Santa Clara, CA, USA). One microgram of DNase-treated RNA was used to generate cDNA using the Superscript III 1st strand synthesis strand system. Two microlitres of cDNA (1:4 dilution) was used in quantitative PCR reactions using 384-well plates, Taqman primer and

Table 4.2 Primer sequence and protocol used for RT-PCR

Primer	Sequence (5'-3')	
	Forward	Reverse
TLR2	TGGCCAGCAGGTTCAGGATG	TCGCAGCTCTCAGATTTACCC
TLR4	CCTCCAGGTTCTTGATTACAG	GTGCCGCCCCAGGACACT
TLR6	AGAACTCACCAGAGGTCCAACC	GAAGGCATATCCTTCGTCATGAG
Actin	CGGCCAGCCAGGTCCAGA	GTGGGCATGGGTCAGAAGGATT
PCR amplification: 32 cycles (TLR2, TLR4 and TLR6) or 22 cycles (Actin) at 94°C for 40s, 56°C for 40 s and 72°C for 90 s		

Table 4.3 Primer sequence and protocol used for qRT-PCR in human cells

Human mRNA	Sequence (5'-3') Forward	Reverse	Accession number
Tlr1	CAATGCTGCTGTTCAGCTCTTC	GCCCAATATGCCTTTGTTATCC	NM_003263.3
Tlr2	AATCCTCCAATCAGGCTTCTCT	TGTAGGTCACTGTTGCTAATGTAGGT	NM_003264.3
Tlr3	GAAAGGCTAGCAGTCATCCAAC	GTCAGCAACTTCATGGCTAACA	NM_003265.2
Tlr4	AGAACCTGGACCTGAGCTTTAATC	GAGGTGGCTTAGGCTCTGATATG	NM_138554.2
Tlr5	ACAAGATTCATACTCCTGATGCTACTG	CCAGGAAAGCTGGGCAACTA	NM_003268.3
Tlr6	ATTGTTAAAAGCTTCCATTTTGTTTG	CTAAGACTTTGGTTTTCAGCGGTAG	NM_006068.2
Tlr7	TCTCATGCTCTGCTCTCTTCAAC	TTGTCTCTTCAGTGTCCACATTGGAAA	NM_016562.3
Tlr8	GCTTGACTTACGTGGAAACAAACTAC	AACTTAAATCGAGGTGCTTCAGACTAC	NM_016610.2
Tlr9	TATTCATGGACGGCAACTGTTATT	TACTTGAGTGACAGGTGGGTGAG	NM_017442.2
Tlr10	CGATTCCACGCATTTATTTCATAC	TAGCTTTCATAAAGGCAAATCAAGATAG	NM_001017388.1
Gapdh	CCTCTGACTTCAACAGCGACAC	TGTCATACCAGGAAATGAGCTTGA	NM_002046.3
PCR amplification:	3 stages: Stage 1, 1 cycle, 95°C for 10 min, Stage 2, 40 cycles, 95°C for 15 s, 60°C for 1 s, Stage 3, 1 cycle, 95°C for 15 s, 60°C for 15 s, 95°C for 15 s		

probe sets for Eukarytotic 18s RNA (only for Fig 2.1.17), GAPDH and murine TLR2 and Taqman Universal PCR master mix (all from Applied Biosytems) and the Applied Biosystems ABI 7900 HT machine using a standard program as detailed in Table 4.4.

Analysis of real-time PCR

GAPDH was used as endogenous reference for normalisation. Baseline and threshold for Ct values were determined using the Sequence Detection System 2.3 software provided by Applied Biosystems. Results are expressed as relative induction to the housekeeping gene GAPDH ($2^{-}{}^{Ct}$) or using the $2^{-}{}^{\Delta\Delta Ct}$ Method (Livak and Schmittgen, 2001).

4.8 NF-κB reporter assay

For experiments shown on Figure 2.1.10, HEK-TLR2 and HEK-TLR4/MD2 cells were seeded at 1 x 10^5 cells/well in 24-well plates the day before transfection. Twenty-four hours later, approximately 2 x 10^5 cells/well were transfected, using 2 µl of Lipofectamine™ per well and 2 µl of Plus Reagent™ per µg of construct (Lipofectamine transfection reagent, Invitrogen™, Life Technologies), with 0.25 µg of a construct directing expression of the firefly luciferase reporter under the control of the NK-κB promoter (pNF-κBLuc; Stratagene, La Jolla, CA) and 0.05 µg of a construct directing expression of *Renilla* luciferase (pRL-SV40; Promega, Southampton, UK). Forty-eight hours post-transfection, the cells were stimulated for 16h at 37°C with SES at the dilutions indicated in the figure legend. Luciferase activity was measured using the Dual-Luciferase® reporter assay system (Promega), according to the manufacturer's instructions.

4.9 Preparation of nuclear extracts

4.9.1 HPMC nuclear extracts

Following stimulation, cells were washed and scraped into ice-cold PBS and pelleted by centrifugation (4500 x g, 1 min, 4°C). The cells were resuspended in ice-cold buffer A (detailed in Table 4.5) and lysed on ice for 10 min. After vortexing, samples were centrifuged (13,000 x g, 5 min, 4°C), the supernatant - cytosolic extract - was transferred to a new tube and the pellet resuspended in buffer B (detailed in Table 4.5) and incubated on ice for 20 min with vortexing every 5 min, for high salt extraction of nuclear proteins. Cell debris were removed by centrifugation (13,000 x g, 5 min, 4°C), and the supernatant - nuclear extract - was stored at -80°C before measuring protein concentrations using a Bradford assay following the manufacturer's instructions.

Table 4.4 Primer sequence and protocol used for qRT-PCR in mouse peritoneal membranes

Mouse mRNA	Taqman Assay ID	Company
Tlr2	Mm00442346_m1	Applied Biosytems
Cxcl1	Mm00433858_g1	Applied Biosytems
Gapdh	43522339E	Applied Biosytems
Eukarytotic 18S	VIC-labeled, 4310893E	Applied Biosytems
PCR amplification:	3 stages: Stage 1, 1 cycle, 50°C for 2 min; Stage 2, 1 cycle, 95°C for 10 min; Stage 3, 40 cycles, 95°C for 15 s, 60°C for 1 min	

4.9.2 Nuclear extracts from murine peritoneal membrane

Nuclear proteins were extracted from snap-frozen peritoneal membrane sections taken during *in vivo* experiments. Membrane sections were kept frozen on dry ice, placed in a mortar containing liquid nitrogen and ground to a fine powder with a pestle. The tissue extracts were collected, resuspended in buffer A (Table 4.5), lysed on ice for 30 min and vortexed for 10 s. Samples were centrifuged (13,000 x g, 5 min, 4^{o}C), the supernatant - cytosolic extract - collected and the pellet resuspended in buffer B (Table 4.5) and incubated on ice for 30 min with regular vortexing. Cell debris were removed by centrifugation (13,000 x g, 5 min, 4^{o}C), the supernatant - nuclear extract - was stored at -80^{o}C and protein concentrations were determined as for HPMC nuclear extracts (above section. 4.9.1).

4.10 Electrophoretic Mobility Shift Assay (EMSA)

4.10.1 Annealing of primers and radio-labelling of oligonucleotide probes

All work involving radioactive material was performed behind Perspex shield. Double stranded oligonucleotide primers (sequences detailed in Table 4.6) were labelled using an end-labelling technique. Reverse complementary oligonucleotide sequences were annealed in order to create overhanging 5' single stranded sequences (identified by lower case in 5'-3' sequences listed in Table 4.6). Primers were annealed at a concentration of 100 ng/µl in the presence of 100 mM NaCl at 95^{o}C for 10 min. The annealed probe was cooled slowly overnight at room temperature and stored at -20^{o}C. The labeling reaction was prepared as follows: oligonucleotide probe (25 ng), dNTP mix (dATP, dCTP, dGTP; 2.5 mM each), 10X Klenow buffer (500 mM Tris-HCl, pH 7.2, 100 mM $MgSO_4$, 1 mM DTT), NaCl (100 mM) made up to 46 µl with ddH_2O. Binding of 30 µCi of $\alpha[^{32}P]$-dTTP was catalysed by 2 units of Klenow fragment (DNA polymerase I large). The 50-µl reaction was incubated at room temperature for 1h, and the reaction was stopped by addition of EDTA (10 mM, pH 8) and STE buffer (100 mM NaCl, 10 mM Tris-HCl, 1 mM EDTA, pH 8). Probes were purified from any free contaminating radioactivity using size exclusion columns (GE Healthcare) and stored at -20^{o}C.

4.10.2 Analysis of DNA-protein complexes by electrophoresis

All samples were run on vertical 8% (w/v) polyacrylamide gels (cast and run on Hoeffer Sturdier gel apparatus), the composition of which is described in Table 4.7. Wells were washed with 0.5X TBE (Tris-Boric Acid EDTA running buffer, detailed in Table 4.7).

The EMSA technique allows evaluating the formation of protein/DNA complexes by showing restricted electrophoretic mobility. A binding reaction was thus prepared, consisting of 1X binding buffer (10 mM HEPES, pH 7.9, 50 mM KCl, 10% glycerol, 0.2 mg/ml acetylated BSA, 1 mM DTT, 0.2 mM PMSF), poly dI/dC (1 mg/ml), nuclear extracts (2 µg HPMC or 10 µg peritoneal membrane extract) and ddH_2O. After 10 min incubation at room temperature to allow

Table 4.5 Buffer composition for nuclear protein extraction

Cytolasmic protein buffer A	Nuclear protein buffer B	Source
10 mM HEPES, pH 8	20 mM HEPES, pH 8	Sigma-Aldrich
1.5 mM $MgCl_2$	1.5 mM $MgCl_2$	
10 mM KCl	420 mM NaCl	
0.01% (v/v) NP40	0.2 mM EDTA, pH 8	
	25% (v/v) Glycerol	
Addition of protease and phospphatase inhibitors:	Addition of protease and phospphatase inhibitors:	
0.8 µM PMSF	0.8 µM PMSF	
40 µM Na_3VO_4	40 µM Na_3VO_4	
0.2 mM NaF	0.2 mM NaF	
2 µM DTT	2 µM DTT	
0.025% protease inhibitor cocktail*	0.025% protease inhibitor cocktail*	

*Protease inhibitor cocktail containing 4-(2-aminoethyl) benzenesulfonyl fluoride (AEBSF), pepstatin A, E64, bestatin, leupeptin and aprotinin.

Table 4.6 Oligonucleotide sequence of primers

Transcription factor	Orientation	Sequence*
NF-κB	Forward	5'-gaTCCATGG**GGAATTCCC**C-3'
	Reverse	5'-gaG**GGGAATTCC**CCATGGA-3'
SIE (M67)-STAT	Forward	5'-cgaCAT**TTCCCGTAA**ATCG-3'
	Reverse	5'-cgaCGAT**TTACGGGAA**ATG-3'

* Transcription factor binding motifs are shown in bold type

Table 4.7 EMSA gel composition

Composition	Amount	Source
dH_2O	44.25 ml	Bio-Rad
40% Acrylamide/Bis Acrylamide (29:1)	15 ml	
5X TBE*	7.5 ml	
50% glycerol	7.5 ml	
10% ammonium persulphate	0.75 ml	
TEMED	60 µl	

*5X TBE: (0.45 M Tris-HCl, 0.45 M Boric acid, 0.01 M EDTA, pH8)

blocking of non-specific binding sites, the radiolabelled oligonucleotide probe containing a binding motif for a transcription factor - NF-κB or SIE (M67) - was added. Samples were incubated with the probe for a further 20 min when the binding reaction was stopped by adding 6X DNA loading buffer, prior to loading onto the gel. Gels were run at 180 volts for 3h 30 min and transferred to 3M Whatman paper and dried on a vacuum drier at -80^{o}C for 2h. Dried gels were exposed to X-ray film overnight to several days at -80^{o}C, and developed by autoradiography.

Quantification of band intensities was performed for each individual time point or stimulation condition by gel scanning followed by analysis using the ImageJ software (ImageJ, NIH, USA). For HPMC stimulations, changes in stimuli-mediated transcription factor activation were expressed as a ratio over non-stimulated cells. For *in vivo* experiments, changes of transcription factor activation following specific stimulations as detailed in figure legends were expressed relative to PBS-injected WT mice.

4.10.3 Analysis of transcription factor subunits

The composition of individual transcription factors subunits in protein/DNA complexes was determined by "supershift" assays using specific rabbit polyclonal antibodies against the NF-κB subunits p65, p50, RelB, p52 and cRel or STAT subunits STAT1, STAT3 and STAT5 as detailed in Table 4.8. If the subunit is present, antibody binding to the protein bound to the probe will either directly block DNA binding - loss of DNA binding observed with STAT1 Ab (Figure 2.3.8) - or result in the formation of a larger complex which migrates slower during gel electrophoresis - the supershift. The binding reaction was prepared as described above in section 4.10.2. Following the 10 min blocking step, nuclear extracts were incubated (20 min, RT) with specific Abs before adding the radio-labelled probe and processing as described in section 4.10.2.

4.11 SDS-PAGE and Western blotting

PD fluids were collected from stable and infected patients and centrifuged (2 x 1000 x g, 15 min, 4°C) to remove the cells. SDS-PAGE was carried out using the Bio-Rad Mini Protean II gel apparatus. To detect sTLR2, samples were diluted 1:20 with Laemmi reducing sample buffer (2% SDS, 100 mM DTT, 50 mM Tris-HCl, pH 6.8, 10% glycerol and 0.1% bromophenol blue) and boiled for 4 min prior to 10% SDS-PAGE. Forty microlitres were run on the gel, and pre-stained molecular weight markers (Bio-Rad) were run in parallel. Electrophoresis was carried out using SDS running buffer (25 mM Tris base, 192 mM glycine, 0.1% SDS). Gels were briefly washed twice in PBS before Western blotting.

Following electrophoresis and in preparation for Western blot, the gels were incubated at room temperature with transfer buffer (48 mM Tris base, 39 mM glycine, 20% (v/v) methanol) for a total of 20 min with three changes of buffer. Extra thick filter paper (Bio-Rad) and the

Table 4.8 Antibodies used for supershift analysis

Transcription factor	Subunit	Clone*	Isotype
NF-κB	p50	NL2	Rabbit IgG
	p52	C5	Mouse IgG2a
	p65	A	Rabbit Ig G
	cRel	N-466	Rabbit Ig G
	RelB	C-19	Rabbit Ig G
SIE (M67)	STAT1	M-22	Rabbit Ig G
	STAT3	C-20	Rabbit Ig G
	STAT5	C-17	Rabbit Ig G

*All antibodies were from Santa-Cruz Biotechnology and used at a concentration of 20 ng/ml

nitrocellulose membrane used for transfer were kept in transfer buffer for 20 min before transfer. Electrotransfer was conducted in a semi-dry transfer cell apparatus (Transblot SD, Bio-Rad) for 30 min at 13 volts. Following transfer, the membranes were blocked for 1h at room temperature with blocking buffer consisting of PBS/0.1% Tween-20 (PBS-T) in 2% milk. The membranes were then washed (1 x 15 min and 2 x 5 min) and incubated with the TLR2-specific rabbit polyclonal Ab TLR2p (1/3000 dilution in 2% milk) overnight at 4°C with gentle rocking. Following washing (as above), the membranes were incubated for 1h at room temperature with an anti rabbit IgGs Ab-horseradish peroxidase-conjugated. Subsequently, the membrane was washed (PBS-T, 1 x 15 min and 4 x 5 min, RT) before detection by enhanced chemiluminescence (ECL system, Amersham) following the manufacturer's instructions.

4.12 Preparation of *S. epi*. cell-free supernatant (SES)

A lyophilized cell-free supernatant (SES) was prepared from *S. epi*. - isolated from a CAPD patient with peritonitis (Mackenzie et al., 1990) - as previously described (Hurst et al., 2001). Briefly, a colony of *S. epi*. grew to stationary phase in Nutrient Broth No. 2 at 37°C in a shaking incubator overnight. Bacteria were centrifuged at 1800 x g, 20 min at 20°C and the pellet resuspended in Tyrode's salt solution without gelatin (1.8 mM $CaCl_2 \cdot 2H_2O$, 1 mM $MgCl_2 \cdot 6H_2O$, 2.6 mM KCl, 137 mM NaCl, 0.42 mM NaH_2PO_4, 5.5 mM D-glucose, with 12 mM $NaHCO_3$), diluted to an absorbance of 0.5 at 560 nm, and incubated at 37°C for 24h. Bacterial suspensions were centrifuged (5000 x g, 30 min, 20°C) and the supernatant was filtered prior to dialysis against distilled water. Ten millilitres aliquots were freeze-dried and the lyophilised powder was stored at -80°C. SES preparations were free of live bacteria as assessed by the lack of bacterial growth on diagnostic sensitivity testing agar plate. SES was reconstituted in cell culture media (*in vitro* experiments) or sterile PBS (*in vivo* experiments) and filtered (0.2 µm). For cell activation, one aliquot of SES was resuspended in 2.5 ml of the appropriate medium (neat SES). For *in vivo* experiments and i.p. injections, one aliquot of SES was resuspended in 0.75 ml of sterile PBS and 0.5 ml of this neat SES was injected in each mouse.

To evaluate the bioactivity of SES, CXCL8 secretion in response to SES was quantified using SV40-transformed HPMC, grown as described in sections 4.2.2. Adherent monolayers were growth arrested for 48h and stimulated for 24h with serial dilutions of SES. Supernatants were collected, rendered cell free by centrifugation and CXCL8 levels were quantified by ELISA. To maintain experimental reproducibility, SES was only used when CXCL8 secretion by SV40 HPMC exceeded 2500 ± 500 pg/ml.

4.13 *In vivo* experiments

Experiments were performed using groups of mixed genders, 8 to 12 week-old inbred WT C57BL6/J (Charles River Ltd, Margate, UK and Harlan, Shardlow, UK) and IL-6KO mice with the same genetic background, which were bred in house. Procedures were conducted following

Home Office approval under project license number PPL 30/2269. Peritoneal inflammation was induced by i.p. inoculation of 500 µl of SES in the presence or absence of sTLR2 (in WT mice), or HDS (in IL-6KO mice), as indicated in the figure legends. Control animals were i.p. injected with 500 µl PBS. At the indicated time points, the mice were sacrificed and the peritoneal cavity was lavaged with 2 ml of PBS and kept on ice until further processing. Total leukocyte numbers were determined using a Coulter counter, slides for differential cell counting were prepared by cytospin and stained with Wright-Giemsa. Leukocyte subsets - neutrophils, macrophages and lymphocytes - were counted according to cell morphology as visualised by light microscopy. For results shown on Fig 2.4.4, leukocyte numbers were quantified by flow cytometry analysis by double staining with FITC-conjugated anti-mouse F4/80 mAb (monocytes/macrophages) and an APC-conjugated anti-mouse CD11b mAb (monocytes/macrophages and granulocytes). Levels of CXCL1, CCL2, IL-6 and sIL-6R in cell-free peritoneal lavage samples were quantified by ELISA (DuoSet, R&D Systems). Sections of peritoneal membrane were collected and snap-frozen in liquid nitrogen and stored at -80^{o}C until processing for analysis of RNA expression by qRT-PCR (described in section 4.6), or transcription factor activation by EMSA (described in sections 4.9. and 4.10).

The detailed description of the development of, and experiments performed using the *in vivo* model of *S. epi*. infection are detailed in the Results section (section 2.4) and in figure legends. In addition, for Serum Amyloid A (SAA) determinations, immediately after the mice were sacrificed blood samples were collected by cardiac puncture using heparin-coated syringes and centrifuged at 900 x g for 10 min at 4^{o}C. Plasma was collected and stored at -80^{o}C until SAA was quantified by ELISA (Biosource, UK).

4.14 Statistical Analysis

Data presented are expressed as means (±SD or ±SEM, as indicated in the figures) and statistical analyses were performed using a two-tailed Student's *t* test. A *p* value of less than 0.05 was considered significantly different.

BIBLIOGRAPHY

Abcejo, A.S., Andrejko, K.M., Raj, N.R., and Deutschman, C.S. (2009). Failed interleukin-6 signal transduction in murine sepsis: attenuation of hepatic glycoprotein 130 phosphorylation. Crit Care Med *37*, 1729-1734.

Abraham, S.N., and St John, A.L. (2010). Mast cell-orchestrated immunity to pathogens. Nat Rev Immunol *10*, 440-452.

Akira, S., and Takeda, K. (2004). Toll-like receptor signalling. Nat Rev Immunol *4*, 499-511.

Akira, S., Uematsu, S., and Takeuchi, O. (2006). Pathogen Recognition and Innate Immunity Cell *124*, 783–801.

Akoh, J.A. (2012). Peritoneal dialysis associated infections: An update on diagnosis and management. World J Nephrol *1*, 106-122.

Alexopoulou, L., Holt, A.C., Medzhitov, R., and Flavell, R.A. (2001). Recognition of double-stranded RNA and activation of NF-kappaB by Toll-like receptor 3. Nature *413*, 732-738.

Alexopoulou, L., Thomas, V., Schnare, M., Lobet, Y., Anguita, J., Schoen, R.T., Medzhitov, R., Fikrig, E., and Flavell, R.A. (2002). Hyporesponsiveness to vaccination with Borrelia burgdorferi OspA in humans and in TLR1- and TLR2-deficient mice. Nat Med *8*, 878-884.

Alves-Filho, J.C., Freitas, A., Souto, F.O., Spiller, F., Paula-Neto, H., Silva, J.S., Gazzinelli, R.T., Teixeira, M.M., Ferreira, S.H., and Cunha, F.Q. (2009). Regulation of chemokine receptor by Toll-like receptor 2 is critical to neutrophil migration and resistance to polymicrobial sepsis. Proc Natl Acad Sci U S A *106*, 4018-4023.

Amara, U., Rittirsch, D., Flierl, M., Bruckner, U., Klos, A., Gebhard, F., Lambris, J.D., and Huber-Lang, M. (2008). Interaction between the coagulation and complement system. Adv Exp Med Biol *632*, 71-79.

Andersen-Nissen, E., Smith, K.D., Bonneau, R., Strong, R.K., and Aderem, A. (2007). A conserved surface on Toll-like receptor 5 recognizes bacterial flagellin. J Exp Med *204*, 393-403.

Andersen-Nissen, E., Smith, K.D., Strobe, K.L., Barrett, S.L., Cookson, B.T., Logan, S.M., and Aderem, A. (2005). Evasion of Toll-like receptor 5 by flagellated bacteria. Proc Natl Acad Sci U S A *102*, 9247-9252.

Anderson, K.V., Jurgens, G., and Nusslein-Volhard, C. (1985). Establishment of dorsal-ventral polarity in the Drosophila embryo: genetic studies on the role of the Toll gene product. Cell *42*, 779-789.

Andersson, U., and Tracey, K.J. (2011). HMGB1 is a therapeutic target for sterile inflammation and infection. Annu Rev Immunol *29*, 139-162.

Arnold, M.A., and Bryce, D. (2010). Arnold's Glossary of Anatomy.

Askarian, F., van Sorge, N.M., Sangvik, M., Beasley, F.C., Henriksen, J.R., Sollid, J.U., van Strijp, J.A., Nizet, V., and Johannessen, M. (2014). A Staphylococcus aureus TIR Domain Protein Virulence Factor Blocks TLR2-Mediated NF-kappaB Signaling. J Innate Immun.

Baetz, A., Frey, M., Heeg, K., and Dalpke, A.H. (2004). Suppressor of cytokine signaling (SOCS) proteins indirectly regulate toll-like receptor signaling in innate immune cells. J Biol Chem *279*, 54708-54715.

Baeuerle, P.A., and Henkel, T. (1994). Function and activation of NF-kappa B in the immune system. Annu Rev Immunol *12*, 141-179.

Barbalat, R., Lau, L., Locksley, R.M., and Barton, G.M. (2009). Toll-like receptor 2 on inflammatory monocytes induces type I interferon in response to viral but not bacterial ligands. Nat Immunol *10*, 1200-1207.

Barbano, G., Cappa, F., Prigione, I., Tedesco, F., Pausa, M., Gugliemino, R., Pistoia, V., Gusmano, R., and Perfumo, F. (1999). Peritoneal mesothelial cells produce complement factors and express CD59 that inhibits C5b-9-mediated cell lysis. Adv Perit Dial *15*, 253-257.

Barton, G.M., and Kagan, J.C. (2009). A cell biological view of Toll-like receptor function: regulation through compartmentalization. Nat Rev Immunol *9*, 535-542.

Basok, A., Shnaider, A., Man, L., Chaimovitz, C., and Douvdevani, A. (2001). CD40 is expressed on human peritoneal mesothelial cells and upregulates the production of interleukin-15 and RANTES. Journal Of The American Society Of Nephrology: JASN *12*, 695-702.

Baumann, C.L., Aspalter, I.M., Sharif, O., Pichlmair, A., Bluml, S., Grebien, F., Bruckner, M., Pasierbek, P., Aumayr, K., Planyavsky, M.*, et al.* (2010). CD14 is a coreceptor of Toll-like receptors 7 and 9. J Exp Med *207*, 2689-2701.

Beelen, R.H., Oosterling, S.J., van Egmond, M., van den Born, J., and Zareie, M. (2005). Omental milky spots in peritoneal pathophysiology (spots before your eyes). Perit Dial Int *25*, 30-32.

Beutler, B. (2004). Innate immunity: an overview. Mol Immunol *40*, 845-859.

Beutler, B.A. (2009). TLRs and innate immunity. Blood *113*, 1399-1407.

Biron, C.A. (2010). More things in heaven and earth: defining innate and adaptive immunity. Nat Immunol *11*, 1080-1082.

Blasius, A.L., and Beutler, B. (2010). Intracellular toll-like receptors. Immunity *32*, 305-315.

Boen, S.T. (1988). Peritoneal Dialysis (Kluwer Academic Publishers).

Borg, C., Jalil, A., Laderach, D., Maruyama, K., Wakasugi, H., Charrier, S., Ryffel, B., Cambi, A., Figdor, C., Vainchenker, W.*, et al.* (2004). NK cell activation by dendritic cells (DCs) requires the formation of a synapse leading to IL-12 polarization in DCs. Blood *104*, 3267-3275.

Bottazzi, B., Doni, A., Garlanda, C., and Mantovani, A. (2010). An integrated view of humoral innate immunity: pentraxins as a paradigm. Annu Rev Immunol *28*, 157-183.

Brikos, C., and O'Neill, L.A. (2008). Signalling of toll-like receptors. Handb Exp Pharmacol, 21-50.

Broche, F., and Tellado, J.M. (2001). Defense mechanisms of the peritoneal cavity. Curr Opin Crit Care *7*, 105-116.

Brown, M.S., and Goldstein, J.L. (1979). Receptor-mediated endocytosis: insights from the lipoprotein receptor system. Proc Natl Acad Sci U S A *76*, 3330-3337.

Byrne, C., Steenkamp, R., Castledine, C., Ansell, D., and Feehally, J. (2010). UK Renal Registry 12th Annual Report (December 2009): Chapter 4: UK ESRD prevalent rates in 2008: national and centre-specific analyses. Nephron Clin Pract *115 Suppl 1*, c41-67.

Cailhier, J.F., Partolina, M., Vuthoori, S., Wu, S., Ko, K., Watson, S., Savill, J., Hughes, J., and Lang, R.A. (2005). Conditional macrophage ablation demonstrates that resident macrophages initiate acute peritoneal inflammation. J Immunol *174*, 2336-2342.

Canton, J., Neculai, D., and Grinstein, S. (2013). Scavenger receptors in homeostasis and immunity. Nat Rev Immunol *13*, 621-634.

Card, C.M., Yu, S.S., and Swartz, M.A. (2014). Emerging roles of lymphatic endothelium in regulating adaptive immunity. J Clin Invest *124*, 943-952.

Carpenter, S., Carlson, T., Dellacasagrande, J., Garcia, A., Gibbons, S., Hertzog, P., Lyons, A., Lin, L.L., Lynch, M., Monie, T.*, et al.* (2009). TRIL, a functional component of the TLR4 signaling complex, highly expressed in brain. J Immunol *183*, 3989-3995.

Carpenter, S., Wochal, P., Dunne, A., and O'Neill, L.A. (2011). Toll-like receptor 3 (TLR3) signaling requires TLR4 Interactor with leucine-rich REPeats (TRIL). J Biol Chem *286*, 38795-38804.

Carroll, M.V., and Sim, R.B. (2011). Complement in health and disease. Adv Drug Deliv Rev *63*, 965-975.

Celik, I., Stover, C., Botto, M., Thiel, S., Tzima, S., Kunkel, D., Walport, M., Lorenz, W., and Schwaeble, W. (2001). Role of the classical pathway of complement activation in experimentally induced polymicrobial peritonitis. Infect Immun *69*, 7304-7309.

Chalaris, A., Garbers, C., Rabe, B., Rose-John, S., and Scheller, J. (2011). The soluble Interleukin 6 receptor: generation and role in inflammation and cancer. Eur J Cell Biol *90*, 484-494.

Chalifour, A., Jeannin, P., Gauchat, J.F., Blaecke, A., Malissard, M., N'Guyen, T., Thieblemont, N., and Delneste, Y. (2004). Direct bacterial protein PAMP recognition by human NK cells involves TLRs and triggers alpha-defensin production. Blood *104*, 1778-1783.

Chen, Q., Wang, W.C., Bruce, R., Li, H., Schleider, D.M., Mulbury, M.J., Bain, M.D., Wallace, P.K., Baumann, H., and Evans, S.S. (2004). Central role of IL-6 receptor signal-transducing chain gp130 in activation of L-selectin adhesion by fever-range thermal stress. Immunity *20*, 59-70.

Cheng, N., He, R., Tian, J., Ye, P.P., and Ye, R.D. (2008). Cutting edge: TLR2 is a functional receptor for acute-phase serum amyloid A. J Immunol *181*, 22-26.

Chiang, C., and Beachy, P.A. (1994). Expression of a novel Toll-like gene spans the parasegment boundary and contributes to hedgehog function in the adult eye of Drosophila. Mech Dev *47*, 225-239.

Chien, Y.H., Zeng, X., and Prinz, I. (2013). The natural and the inducible: interleukin (IL)-17-producing gammadelta T cells. Trends Immunol *34*, 151-154.

Chockalingam, A., Cameron, J.L., Brooks, J.C., and Leifer, C.A. (2011). Negative regulation of signaling by a soluble form of toll-like receptor 9. Eur J Immunol *41*, 2176-2184.

Coban, C., Ishii, K.J., Kawai, T., Hemmi, H., Sato, S., Uematsu, S., Yamamoto, M., Takeuchi, O., Itagaki, S., Kumar, N.*, et al.* (2005). Toll-like receptor 9 mediates innate immune activation by the malaria pigment hemozoin. J Exp Med *201*, 19-25.

Cole, J.E., Georgiou, E., and Monaco, C. (2010). The expression and functions of toll-like receptors in atherosclerosis. Mediators Inflamm *2010*, 393946.

Crosara-Alberto, D.P., Darini, A.L., Inoue, R.Y., Silva, J.S., Ferreira, S.H., and Cunha, F.Q. (2002). Involvement of NO in the failure of neutrophil migration in sepsis induced by Staphylococcus aureus. Br J Pharmacol *136*, 645-658.

Cui, L., Johkura, K., Liang, Y., Teng, R., Ogiwara, N., Okouchi, Y., Asanuma, K., and Sasaki, K. (2002). Biodefense function of omental milky spots through cell adhesion molecules and leukocyte proliferation. Cell Tissue Res *310*, 321-330.

Dalrymple, S.A., Lucian, L.A., Slattery, R., McNeil, T., Aud, D.M., Fuchino, S., Lee, F., and Murray, R. (1995). Interleukin-6-deficient mice are highly susceptible to Listeria monocytogenes infection: correlation with inefficient neutrophilia. Infect Immun *63*, 2262-2268.

Dalrymple, S.A., Slattery, R., Aud, D.M., Krishna, M., Lucian, L.A., and Murray, R. (1996). Interleukin-6 is required for a protective immune response to systemic Escherichia coli infection. Infect Immun *64*, 3231-3235.

Davies, L.C., Jenkins, S.J., Allen, J.E., and Taylor, P.R. (2013). Tissue-resident macrophages. Nat Immunol *14*, 986-995.

Davies, S.J., Bryan, J., Phillips, L., and Russell, G.I. (1996). Longitudinal changes in peritoneal kinetics: the effects of peritoneal dialysis and peritonitis. Nephrology, Dialysis, Transplantation: Official Publication Of The European Dialysis And Transplant Association - European Renal Association *11*, 498-506.

Davies, S.J., Suassuna, J., Ogg, C.S., and Cameron, J.S. (1989). Activation of immunocompetent cells in the peritoneum of patients treated with CAPD. Kidney Int *36*, 661-668.

de Lima, S.M., Otoni, A., Sabino Ade, P., Dusse, L.M., Gomes, K.B., Pinto, S.W., Marinho, M.A., and Rios, D.R. (2013). Inflammation, neoangiogenesis and fibrosis in peritoneal dialysis. Clin Chim Acta *421*, 46-50.

Degli-Esposti, M.A., and Smyth, M.J. (2005). Close encounters of different kinds: dendritic cells and NK cells take centre stage. Nat Rev Immunol *5*, 112-124.

Demir, M., Sert, S., Kaleli, I., Demir, S., Cevahir, N., Yildirim, U., and Sahin, B. (2007). Liver lipid peroxidation in experimental Escherichia coli peritonitis: the role of myeloperoxidase and nitric oxide inhibition. Med Sci Monit *13*, BR225-229.

Devuyst, O., Margetts, P.J., and Topley, N. (2010). The pathophysiology of the peritoneal membrane. J Am Soc Nephrol *21*, 1077-1085.

Diao, H., and Kohanawa, M. (2005). Endogenous interleukin-6 plays a crucial protective role in streptococcal toxic shock syndrome via suppression of tumor necrosis factor alpha production. Infect Immun *73*, 3745-3748.

Diebold, S.S., Kaisho, T., Hemmi, H., Akira, S., and Reis e Sousa, C. (2004). Innate antiviral responses by means of TLR7-mediated recognition of single-stranded RNA. Science *303*, 1529-1531.

Dinarello, C.A. (1991). Interleukin-1 and interleukin-1 antagonism. Blood *77*, 1627-1652.

Dinarello, C.A., Cannon, J.G., Mancilla, J., Bishai, I., Lees, J., and Coceani, F. (1991). Interleukin-6 as an endogenous pyrogen: induction of prostaglandin E2 in brain but not in peripheral blood mononuclear cells. Brain Res *562*, 199-206.

DiTirro, J., Rhoades, E.R., Roberts, A.D., Burke, J.M., Mukasa, A., Cooper, A.M., Frank, A.A., Born, W.K., and Orme, I.M. (1998). Disruption of the cellular inflammatory response to Listeria monocytogenes infection in mice with disruptions in targeted genes. Infect Immun *66*, 2284-2289.

Douvdevani, A., Rapoport, J., Konforty, A., Argov, S., Ovnat, A., and Chaimovitz, C. (1994). Human peritoneal mesothelial cells synthesize IL-1 alpha and beta. Kidney International *46*, 993-1001.

Doyle, S.L., and O'Neill, L.A. (2006). Toll-like receptors: from the discovery of NFkappaB to new insights into transcriptional regulations in innate immunity. Biochem Pharmacol *72*, 1102-1113.

Dulay, A.T., Buhimschi, C.S., Zhao, G., Oliver, E.A., Mbele, A., Jing, S., and Buhimschi, I.A. (2009). Soluble TLR2 is present in human amniotic fluid and modulates the intraamniotic inflammatory response to infection. J Immunol *182*, 7244-7253.

Durieux, J.J., Vita, N., Popescu, O., Guette, F., Calzada-Wack, J., Munker, R., Schmidt, R.E., Lupker, J., Ferrara, P., Ziegler-Heitbrock, H.W., and et al. (1994). The two soluble forms of the lipopolysaccharide receptor, CD14: characterization and release by normal human monocytes. Eur J Immunol *24*, 2006-2012.

Echchannaoui, H., Frei, K., Schnell, C., Leib, S.L., Zimmerli, W., and Landmann, R. (2002). Toll-like receptor 2-deficient mice are highly susceptible to Streptococcus pneumoniae meningitis because of reduced bacterial clearing and enhanced inflammation. J Infect Dis *186*, 798-806.

Elinav, E., Strowig, T., Henao-Mejia, J., and Flavell, R.A. (2011). Regulation of the antimicrobial response by NLR proteins. Immunity *34*, 665-679.

Endres, S., Cannon, J.G., Ghorbani, R., Dempsey, R.A., Sisson, S.D., Lonnemann, G., Van der Meer, J.W., Wolff, S.M., and Dinarello, C.A. (1989). In vitro production of IL 1 beta, IL 1 alpha, TNF and IL2 in healthy subjects: distribution, effect of cyclooxygenase inhibition and evidence of independent gene regulation. Eur J Immunol *19*, 2327-2333.

Ernst, M., and Jenkins, B.J. (2004). Acquiring signalling specificity from the cytokine receptor gp130. Trends Genet *20*, 23-32.

Erridge, C., Spickett, C.M., and Webb, D.J. (2007). Non-enterobacterial endotoxins stimulate human coronary artery but not venous endothelial cell activation via Toll-like receptor 2. Cardiovasc Res *73*, 181-189.

Eulenfeld, R., Dittrich, A., Khouri, C., Muller, P.J., Mutze, B., Wolf, A., and Schaper, F. (2012). Interleukin-6 signalling: more than Jaks and STATs. Eur J Cell Biol *91*, 486-495.

Fabbri, M., Paone, A., Calore, F., Galli, R., Gaudio, E., Santhanam, R., Lovat, F., Fadda, P., Mao, C., Nuovo, G.J.*, et al.* (2012). MicroRNAs bind to Toll-like receptors to induce prometastatic inflammatory response. Proc Natl Acad Sci U S A *109*, E2110-2116.

Faure, E., Thomas, L., Xu, H., Medvedev, A., Equils, O., and Arditi, M. (2001). Bacterial lipopolysaccharide and IFN-gamma induce Toll-like receptor 2 and Toll-like receptor 4 expression in human endothelial cells: role of NF-kappa B activation. J Immunol *166*, 2018-2024.

Fearon, D.T. (1998). The complement system and adaptive immunity. Semin Immunol *10*, 355-361.

Fielding, C.A., Jones, G.W., McLoughlin, R.M., McLeod, L., Hammond, V.J., Uceda, J., Williams, A.S., Lambie, M., Foster, T.L., Liao, C.T.*, et al.* (2014). Interleukin-6 signaling drives fibrosis in unresolved inflammation. Immunity *40*, 40-50.

Fielding, C.A., McLoughlin, R.M., McLeod, L., Colmont, C.S., Najdovska, M., Grail, D., Ernst, M., Jones, S.A., Topley, N., and Jenkins, B.J. (2008). IL-6 regulates neutrophil trafficking during acute inflammation via STAT3. J Immunol *181*, 2189-2195.

Fieren, M.W. (2012). The local inflammatory responses to infection of the peritoneal cavity in humans: their regulation by cytokines, macrophages, and other leukocytes. Mediators Inflamm *2012*, 1-9.

Fischereder, M., Luckow, B., Sitter, T., Schroppel, B., Banas, B., and Schlondorff, D. (1997). Immortalization and characterization of human peritoneal mesothelial cells. Kidney Int *51*, 2006-2012.

Fitzgerald, K.A., Palsson-McDermott, E.M., Bowie, A.G., Jefferies, C.A., Mansell, A.S., Brady, G., Brint, E., Dunne, A., Gray, P., Harte, M.T., *et al.* (2001). Mal (MyD88-adapter-like) is required for Toll-like receptor-4 signal transduction. Nature *413*, 78-83.

Fitzgerald, K.A., Rowe, D.C., Barnes, B.J., Caffrey, D.R., Visintin, A., Latz, E., Monks, B., Pitha, P.M., and Golenbock, D.T. (2003). LPS-TLR4 signaling to IRF-3/7 and NF-kappaB involves the toll adapters TRAM and TRIF. J Exp Med *198*, 1043-1055.

Flannery, S., and Bowie, A.G. (2010). The interleukin-1 receptor-associated kinases: critical regulators of innate immune signalling. Biochem Pharmacol *80*, 1981-1991.

Flo, T.H., Halaas, O., Torp, S., Ryan, L., Lien, E., Dybdahl, B., Sundan, A., and Espevik, T. (2001). Differential expression of Toll-like receptor 2 in human cells. J Leukoc Biol *69*, 474-481.

Foster, S.L., Hargreaves, D.C., and Medzhitov, R. (2007). Gene-specific control of inflammation by TLR-induced chromatin modifications. Nature *447*, 972-978.

Fox, J.M., Letellier, E., Oliphant, C.J., and Signoret, N. (2011). TLR2-dependent pathway of heterologous down-modulation for the CC chemokine receptors 1, 2, and 5 in human blood monocytes. Blood *117*, 1851-1860.

Galli, S.J., Borregaard, N., and Wynn, T.A. (2011). Phenotypic and functional plasticity of cells of innate immunity: macrophages, mast cells and neutrophils. Nat Immunol *12*, 1035-1044.

Gallo, R.L., and Hooper, L.V. (2012). Epithelial antimicrobial defence of the skin and intestine. Nat Rev Immunol *12*, 503-516.

Ganter, G. (1923). Ueber die Beseitigung giftiger Stoffe aus dem Blute durch Dialyse (On the elimination of toxic substances from the blood by dialysis). Münchener Medizinische Wochenschrift *70*, 1478-1480.

Gantner, B.N., Simmons, R.M., Canavera, S.J., Akira, S., and Underhill, D.M. (2003). Collaborative induction of inflammatory responses by dectin-1 and Toll-like receptor 2. J Exp Med *197*, 1107-1117.

Garbers, C., Spudy, B., Aparicio-Siegmund, S., Waetzig, G.H., Sommer, J., Holscher, C., Rose-John, S., Grotzinger, J., Lorenzen, I., and Scheller, J. (2013). An interleukin-6 receptor-dependent molecular switch mediates signal transduction of the IL-27 cytokine subunit p28 (IL-30) via a gp130 protein receptor homodimer. J Biol Chem *288*, 4346-4354.

Gay, N.J., Gangloff, M., and O'Neill, L.A. (2011). What the Myddosome structure tells us about the initiation of innate immunity. Trends In Immunology *32*, 104-109.

Gay, N.J., Gangloff, M., and Weber, A.N. (2006). Toll-like receptors as molecular switches. Nat Rev Immunol *6*, 693-698.

Gay, N.J., and Keith, F.J. (1991). Drosophila Toll and IL-1 receptor. Nature *351*, 355-356.

Gazzinelli, R.T., Ropert, C., and Campos, M.A. (2004). Role of the Toll/interleukin-1 receptor signaling pathway in host resistance and pathogenesis during infection with protozoan parasites. Immunol Rev *201*, 9-25.

Gerold, G., Zychlinsky, A., and de Diego, J.L. (2007). What is the role of Toll-like receptors in bacterial infections? Semin Immunol *19*, 41-47.

Gewirtz, A.T., Navas, T.A., Lyons, S., Godowski, P.J., and Madara, J.L. (2001a). Cutting edge: bacterial flagellin activates basolaterally expressed TLR5 to induce epithelial proinflammatory gene expression. J Immunol *167*, 1882-1885.

Gewirtz, A.T., Simon, P.O., Jr., Schmitt, C.K., Taylor, L.J., Hagedorn, C.H., O'Brien, A.D., Neish, A.S., and Madara, J.L. (2001b). Salmonella typhimurium translocates flagellin across intestinal epithelia, inducing a proinflammatory response. J Clin Invest *107*, 99-109.

Gilleron, M., Quesniaux, V.F., and Puzo, G. (2003). Acylation state of the phosphatidylinositol hexamannosides from Mycobacterium bovis bacillus Calmette Guerin and mycobacterium tuberculosis H37Rv and its implication in Toll-like receptor response. J Biol Chem *278*, 29880-29889.

Gillerot, G., Goffin, E., Michel, C., Evenepoel, P., Biesen, W.V., Tintillier, M., Stenvinkel, P., Heimburger, O., Lindholm, B., Nordfors, L.*, et al.* (2005). Genetic and clinical factors influence the baseline permeability of the peritoneal membrane. Kidney Int *67*, 2477-2487.

Gilliet, M., Cao, W., and Liu, Y.J. (2008). Plasmacytoid dendritic cells: sensing nucleic acids in viral infection and autoimmune diseases. Nat Rev Immunol *8*, 594-606.

Gonzaga, R., Matzinger, P., and Perez-Diez, A. (2011). Resident peritoneal NK cells. J Immunol *187*, 6235-6242.

Goodman, R.B., Wood, R.G., Martin, T.R., Hanson-Painton, O., and Kinasewitz, G.T. (1992). Cytokine-stimulated human mesothelial cells produce chemotactic activity for neutrophils including NAP-1/IL-8. J Immunol *148*, 457-465.

Goodridge, H.S., and Underhill, D.M. (2008). Fungal Recognition by TLR2 and Dectin-1. Handb Exp Pharmacol, 87-109.

Grassmann, A., Gioberge, S., Moeller, S., and Brown, G. (2005). ESRD patients in 2004: global overview of patient numbers, treatment modalities and associated trends. Nephrol Dial Transplant *20*, 2587-2593.

Greenhill, C.J., Rose-John, S., Lissilaa, R., Ferlin, W., Ernst, M., Hertzog, P.J., Mansell, A., and Jenkins, B.J. (2011). IL-6 trans-signaling modulates TLR4-dependent inflammatory responses via STAT3. J Immunol *186*, 1199-1208.

Gregoire, C., Chasson, L., Luci, C., Tomasello, E., Geissmann, F., Vivier, E., and Walzer, T. (2007). The trafficking of natural killer cells. Immunol Rev *220*, 169-182.

Guan, Y., Ranoa, D.R., Jiang, S., Mutha, S.K., Li, X., Baudry, J., and Tapping, R.I. (2010). Human TLRs 10 and 1 share common mechanisms of innate immune sensing but not signaling. J Immunol *184*, 5094-5103.

Ha, H., Yu, M.R., and Lee, H.B. (2001). High glucose-induced PKC activation mediates TGF-beta 1 and fibronectin synthesis by peritoneal mesothelial cells. Kidney Int *59*, 463-470.

Hagihara, K., Nishikawa, T., Sugamata, Y., Song, J., Isobe, T., Taga, T., and Yoshizaki, K. (2005). Essential role of STAT3 in cytokine-driven NF-kappaB-mediated serum amyloid A gene expression. Genes Cells *10*, 1051-1063.

Hailman, E., Lichenstein, H.S., Wurfel, M.M., Miller, D.S., Johnson, D.A., Kelley, M., Busse, L.A., Zukowski, M.M., and Wright, S.D. (1994). Lipopolysaccharide (LPS)-binding protein accelerates the binding of LPS to CD14. J Exp Med *179*, 269-277.

Hajjar, A.M., O'Mahony, D.S., Ozinsky, A., Underhill, D.M., Aderem, A., Klebanoff, S.J., and Wilson, C.B. (2001). Cutting edge: functional interactions between toll-like receptor (TLR) 2 and TLR1 or TLR6 in response to phenol-soluble modulin. J Immunol *166*, 15-19.

Hams, E., Colmont, C.S., Dioszeghy, V., Hammond, V.J., Fielding, C.A., Williams, A.S., Tanaka, M., Miyajima, A., Taylor, P.R., Topley, N., and Jones, S.A. (2008). Oncostatin M receptor-beta signaling limits monocytic cell recruitment in acute inflammation. J Immunol *181*, 2174-2180.

Haslinger, B., Mandl-Weber, S., Sellmayer, A., and Sitter, T. (2001). Hyaluronan fragments induce the synthesis of MCP-1 and IL-8 in cultured human peritoneal mesothelial cells. Cell Tissue Res *305*, 79-86.

Hausmann, M.J., Rogachev, B., Weiler, M., Chaimovitz, C., and Douvdevani, A. (2000). Accessory role of human peritoneal mesothelial cells in antigen presentation and T-cell growth. Kidney International *57*, 476-486.

Hayashi, F., Smith, K.D., Ozinsky, A., Hawn, T.R., Yi, E.C., Goodlett, D.R., Eng, J.K., Akira, S., Underhill, D.M., and Aderem, A. (2001). The innate immune response to bacterial flagellin is mediated by Toll-like receptor 5. Nature *410*, 1099-1103.

Hazeki, K., Nigorikawa, K., and Hazeki, O. (2007). Role of phosphoinositide 3-kinase in innate immunity. Biological & Pharmaceutical Bulletin *30*, 1617-1623.

Haziot, A., Chen, S., Ferrero, E., Low, M.G., Silber, R., and Goyert, S.M. (1988). The monocyte differentiation antigen, CD14, is anchored to the cell membrane by a phosphatidylinositol linkage. J Immunol *141*, 547-552.

He, R.L., Zhou, J., Hanson, C.Z., Chen, J., Cheng, N., and Ye, R.D. (2009). Serum amyloid A induces G-CSF expression and neutrophilia via Toll-like receptor 2. Blood *113*, 429-437.

Healy, J.C., and Reznek, R.H. (2000). Peritoneal Anatomy. Imaging *12*, 1-9.

Heinrich, P.C., Behrmann, I., Haan, S., Hermanns, H.M., Muller-Newen, G., and Schaper, F. (2003). Principles of interleukin (IL)-6-type cytokine signalling and its regulation. Biochem J *374*, 1-20.

Hemmi, H., Kaisho, T., Takeuchi, O., Sato, S., Sanjo, H., Hoshino, K., Horiuchi, T., Tomizawa, H., Takeda, K., and Akira, S. (2002). Small anti-viral compounds activate immune cells via the TLR7 MyD88-dependent signaling pathway. Nat Immunol *3*, 196-200.

Hemmi, H., Takeuchi, O., Kawai, T., Kaisho, T., Sato, S., Sanjo, H., Matsumoto, M., Hoshino, K., Wagner, H., Takeda, K., and Akira, S. (2000). A Toll-like receptor recognizes bacterial DNA. Nature *408*, 740-745.

Hochrein, H., Schlatter, B., O'Keeffe, M., Wagner, C., Schmitz, F., Schiemann, M., Bauer, S., Suter, M., and Wagner, H. (2004). Herpes simplex virus type-1 induces IFN-alpha production via Toll-like receptor 9-dependent and -independent pathways. Proc Natl Acad Sci U S A *101*, 11416-11421.

Hoebe, K., Du, X., Georgel, P., Janssen, E., Tabeta, K., Kim, S.O., Goode, J., Lin, P., Mann, N., Mudd, S.*, et al.* (2003). Identification of Lps2 as a key transducer of MyD88-independent TIR signalling. Nature *424*, 743-748.

Hoebe, K., Georgel, P., Rutschmann, S., Du, X., Mudd, S., Crozat, K., Sovath, S., Shamel, L., Hartung, T., Zahringer, U., and Beutler, B. (2005). CD36 is a sensor of diacylglycerides. Nature *433*, 523-527.

Hoebe, K., Janssen, E., and Beutler, B. (2004). The interface between innate and adaptive immunity. Nat Immunol *5*, 971-974.

Hoentjen, F., Sartor, R.B., Ozaki, M., and Jobin, C. (2005). STAT3 regulates NF-kappaB recruitment to the IL-12p40 promoter in dendritic cells. Blood *105*, 689-696.

Hoffmann, J., and Akira, S. (2013). Innate immunity. Curr Opin Immunol *25*, 1-3.

Holm, C.K., Paludan, S.R., and Fitzgerald, K.A. (2013). DNA recognition in immunity and disease. Curr Opin Immunol *25*, 13-18.

Homma, T., Kato, A., Hashimoto, N., Batchelor, J., Yoshikawa, M., Imai, S., Wakiguchi, H., Saito, H., and Matsumoto, K. (2004). Corticosteroid and cytokines synergistically enhance toll-like receptor 2 expression in respiratory epithelial cells. Am J Respir Cell Mol Biol *31*, 463-469.

Honda, K., Nitta, K., Horita, S., Yumura, W., Nihei, H., Nagai, R., Ikeda, K., and Horiuchi, S. (1999). Accumulation of advanced glycation end products in the peritoneal vasculature of continuous ambulatory peritoneal dialysis patients with low ultra-filtration. Nephrol Dial Transplant *14*, 1541-1549.

Horng, T., Barton, G.M., and Medzhitov, R. (2001). TIRAP: an adapter molecule in the Toll signaling pathway. Nat Immunol *2*, 835-841.

Hornung, V., Rothenfusser, S., Britsch, S., Krug, A., Jahrsdorfer, B., Giese, T., Endres, S., and Hartmann, G. (2002). Quantitative expression of toll-like receptor 1-10 mRNA in cellular subsets of human peripheral blood mononuclear cells and sensitivity to CpG oligodeoxynucleotides. J Immunol *168*, 4531-4537.

Hoshino, K., Takeuchi, O., Kawai, T., Sanjo, H., Ogawa, T., Takeda, Y., Takeda, K., and Akira, S. (1999). Cutting edge: Toll-like receptor 4 (TLR4)-deficient mice are hyporesponsive to lipopolysaccharide: evidence for TLR4 as the Lps gene product. J Immunol *162*, 3749-3752.

Hu, X., Paik, P.K., Chen, J., Yarilina, A., Kockeritz, L., Lu, T.T., Woodgett, J.R., and Ivashkiv, L.B. (2006). IFN-gamma suppresses IL-10 production and synergizes with TLR2 by regulating GSK3 and CREB/AP-1 proteins. Immunity *24*, 563-574.

Huber-Lang, M., Sarma, J.V., Zetoune, F.S., Rittirsch, D., Neff, T.A., McGuire, S.R., Lambris, J.D., Warner, R.L., Flierl, M.A., Hoesel, L.M.*, et al.* (2006). Generation of C5a in the absence of C3: a new complement activation pathway. Nat Med *12*, 682-687.

Hugot, J.P., Chamaillard, M., Zouali, H., Lesage, S., Cezard, J.P., Belaiche, J., Almer, S., Tysk, C., O'Morain, C.A., Gassull, M.*, et al.* (2001). Association of NOD2 leucine-rich repeat variants with susceptibility to Crohn's disease. Nature *411*, 599-603.

Huntzinger, E., and Izaurralde, E. (2011). Gene silencing by microRNAs: contributions of translational repression and mRNA decay. Nat Rev Genet *12*, 99-110.

Hurst, S.M., McLoughlin, R.M., Monslow, J., Owens, S., Morgan, L., Fuller, G.M., Topley, N., and Jones, S.A. (2002). Secretion of oncostatin M by infiltrating neutrophils: regulation of IL-6 and chemokine expression in human mesothelial cells. J Immunol *169*, 5244-5251.

Hurst, S.M., Wilkinson, T.S., McLoughlin, R.M., Jones, S., Horiuchi, S., Yamamoto, N., Rose-John, S., Fuller, G.M., Topley, N., and Jones, S.A. (2001). Il-6 and its soluble receptor orchestrate a temporal switch in the pattern of leukocyte recruitment seen during acute inflammation. Immunity *14*, 705-714.

Hussain, T., Nasreen, N., Lai, Y., Bellew, B.F., Antony, V.B., and Mohammed, K.A. (2008). Innate immune responses in murine pleural mesothelial cells: Toll-like receptor-2 dependent induction of beta-defensin-2 by staphylococcal peptidoglycan. Am J Physiol Lung Cell Mol Physiol *295*, L461-470.

Ikeda, Y., Adachi, Y., Ishii, T., Miura, N., Tamura, H., and Ohno, N. (2008). Dissociation of Toll-like receptor 2-mediated innate immune response to Zymosan by organic solvent-treatment without loss of Dectin-1 reactivity. Biol Pharm Bull *31*, 13-18.

Inohara, N., Ogura, Y., Chen, F.F., Muto, A., and Nunez, G. (2001). Human Nod1 confers responsiveness to bacterial lipopolysaccharides. J Biol Chem *276*, 2551-2554.

Ip, Y.T., Reach, M., Engstrom, Y., Kadalayil, L., Cai, H., Gonzalez-Crespo, S., Tatei, K., and Levine, M. (1993). Dif, a dorsal-related gene that mediates an immune response in Drosophila. Cell *75*, 753-763.

Irwin, P.L., Nguyen, L.H., Paoli, G.C., and Chen, C.Y. (2010). Evidence for a bimodal distribution of Escherichia coli doubling times below a threshold initial cell concentration. BMC Microbiol *10*, 207.

Iwami, K.I., Matsuguchi, T., Masuda, A., Kikuchi, T., Musikacharoen, T., and Yoshikai, Y. (2000). Cutting edge: naturally occurring soluble form of mouse Toll-like receptor 4 inhibits lipopolysaccharide signaling. J Immunol *165*, 6682-6686.

Izzi, V., Masuelli, L., Tresoldi, I., Foti, C., Modesti, A., and Bei, R. (2012). Immunity and malignant mesothelioma: from mesothelial cell damage to tumor development and immune response-based therapies. Cancer Lett *322*, 18-34.

Jain, A.K., Blake, P., Cordy, P., and Garg, A.X. (2012). Global trends in rates of peritoneal dialysis. J Am Soc Nephrol *23*, 533-544.

Jansen, M.A., Hart, A.A., Korevaar, J.C., Dekker, F.W., Boeschoten, E.W., and Krediet, R.T. (2002). Predictors of the rate of decline of residual renal function in incident dialysis patients. Kidney Int *62*, 1046-1053.

Jaresova, I., Rozkova, D., Spisek, R., Janda, A., Brazova, J., and Sediva, A. (2007). Kinetics of Toll-like receptor-4 splice variants expression in lipopolysaccharide-stimulated antigen presenting cells of healthy donors and patients with cystic fibrosis. Microbes Infect *9*, 1359-1367.

Jarrossay, D., Napolitani, G., Colonna, M., Sallusto, F., and Lanzavecchia, A. (2001). Specialization and complementarity in microbial molecule recognition by human myeloid and plasmacytoid dendritic cells. Eur J Immunol *31*, 3388-3393.

Jeannin, P., Jaillon, S., and Delneste, Y. (2008). Pattern recognition receptors in the immune response against dying cells. Curr Opin Immunol *20*, 530-537.

Jenkins, B.J., Roberts, A.W., Greenhill, C.J., Najdovska, M., Lundgren-May, T., Robb, L., Grail, D., and Ernst, M. (2007). Pathologic consequences of STAT3 hyperactivation by IL-6 and IL-11 during hematopoiesis and lymphopoiesis. Blood *109*, 2380-2388.

Jones, S.A. (2005). Directing transition from innate to acquired immunity: defining a role for IL-6. J Immunol *175*, 3463-3468.

Jones, S.A., Richards, P.J., Scheller, J., and Rose-John, S. (2005). IL-6 transsignaling: the in vivo consequences. J Interferon Cytokine Res *25*, 241-253.

Jones, S.A., and Rose-John, S. (2002). The role of soluble receptors in cytokine biology: the agonistic properties of the sIL-6R/IL-6 complex. Biochim Biophys Acta *1592*, 251-263.

Jones, S.A., Scheller, J., and Rose-John, S. (2011). Therapeutic strategies for the clinical blockade of IL-6/gp130 signaling. J Clin Invest *121*, 3375-3383.

Jorres, A., Ludat, K., Lang, J., Sander, K., Gahl, G.M., Frei, U., DeJonge, K., Williams, J.D., and Topley, N. (1996). Establishment and functional characterization of human peritoneal fibroblasts in

culture: regulation of interleukin-6 production by proinflammatory cytokines. J Am Soc Nephrol *7*, 2192-2201.

Jostock, T., Mullberg, J., Ozbek, S., Atreya, R., Blinn, G., Voltz, N., Fischer, M., Neurath, M.F., and Rose-John, S. (2001). Soluble gp130 is the natural inhibitor of soluble interleukin-6 receptor transsignaling responses. European Journal of Biochemistry *268*, 160-167.

Kabelitz, D. (2007). Expression and function of Toll-like receptors in T lymphocytes. Curr Opin Immunol *19*, 39-45.

Kallen, K.J. (2002). The role of transsignalling via the agonistic soluble IL-6 receptor in human diseases. Biochim Biophys Acta *1592*, 323-343.

Kang, D.H., Hong, Y.S., Lim, H.J., Choi, J.H., Han, D.S., and Yoon, K.I. (1999). High glucose solution and spent dialysate stimulate the synthesis of transforming growth factor-beta1 of human peritoneal mesothelial cells: effect of cytokine costimulation. Perit Dial Int *19*, 221-230.

Kato, S., Yuzawa, Y., Tsuboi, N., Maruyama, S., Morita, Y., Matsuguchi, T., and Matsuo, S. (2004). Endotoxin-induced chemokine expression in murine peritoneal mesothelial cells: the role of toll-like receptor 4. J Am Soc Nephrol *15*, 1289-1299.

Kawagoe, T., Takeuchi, O., Takabatake, Y., Kato, H., Isaka, Y., Tsujimura, T., and Akira, S. (2009). TANK is a negative regulator of Toll-like receptor signaling and is critical for the prevention of autoimmune nephritis. Nat Immunol *10*, 965-972.

Kawai, T., and Akira, S. (2007). TLR signaling. Semin Immunol *19*, 24-32.

Kawai, T., and Akira, S. (2009). The roles of TLRs, RLRs and NLRs in pathogen recognition. Int Immunol *21*, 317-337.

Kawai, T., and Akira, S. (2010). The role of pattern-recognition receptors in innate immunity: update on Toll-like receptors. Nat Immunol *11*, 373-384.

Kawai, T., and Akira, S. (2011). Toll-like receptors and their crosstalk with other innate receptors in infection and immunity. Immunity *34*, 637-650.

Kawka, E., Witowski, J., Fouqet, N., Tayama, H., Bender, T.O., Catar, R., Dragun, D., and Jorres, A. (2014). Regulation of chemokine CCL5 synthesis in human peritoneal fibroblasts: a key role of IFN-gamma. Mediators Inflamm *2014*, 590654.

Kayagaki, N., Phung, Q., Chan, S., Chaudhari, R., Quan, C., O'Rourke, K.M., Eby, M., Pietras, E., Cheng, G., Bazan, J.F.*, et al.* (2007). DUBA: a deubiquitinase that regulates type I interferon production. Science *318*, 1628-1632.

Kenny, E.F., and O'Neill, L.A. (2008). Signalling adaptors used by Toll-like receptors: an update. Cytokine *43*, 342-349.

Kokkinopoulos, I., Jordan, W.J., and Ritter, M.A. (2005). Toll-like receptor mRNA expression patterns in human dendritic cells and monocytes. Mol Immunol *42*, 957-968.

Kolaczkowska, E., Chadzinska, M., Scislowska-Czarnecka, A., Plytycz, B., Opdenakker, G., and Arnold, B. (2006). Gelatinase B/matrix metalloproteinase-9 contributes to cellular infiltration in a murine model of zymosan peritonitis. Immunobiology *211*, 137-148.

Kollisch, G., Kalali, B.N., Voelcker, V., Wallich, R., Behrendt, H., Ring, J., Bauer, S., Jakob, T., Mempel, M., and Ollert, M. (2005). Various members of the Toll-like receptor family contribute to the innate immune response of human epidermal keratinocytes. Immunology *114*, 531-541.

Kopf, M., Baumann, H., Freer, G., Freudenberg, M., Lamers, M., Kishimoto, T., Zinkernagel, R., Bluethmann, H., and Kohler, G. (1994). Impaired immune and acute-phase responses in interleukin-6-deficient mice. Nature *368*, 339-342.

Krediet, R.T. (2007). 30 years of peritoneal dialysis development: the past and the future. Perit Dial Int *27 Suppl 2*, S35-41.

Krieg, A.M. (2002). CpG motifs in bacterial DNA and their immune effects. Annu Rev Immunol *20*, 709-760.

Krutzik, S.R., Ochoa, M.T., Sieling, P.A., Uematsu, S., Ng, Y.W., Legaspi, A., Liu, P.T., Cole, S.T., Godowski, P.J., Maeda, Y.*, et al.* (2003). Activation and regulation of Toll-like receptors 2 and 1 in human leprosy. Nat Med *9*, 525-532.

Kulkarni, R., Behboudi, S., and Sharif, S. (2011). Insights into the role of Toll-like receptors in modulation of T cell responses. Cell Tissue Res *343*, 141-152.

Kuroishi, T., Tanaka, Y., Sakai, A., Sugawara, Y., Komine, K., and Sugawara, S. (2007). Human parotid saliva contains soluble toll-like receptor (TLR) 2 and modulates TLR2-mediated interleukin-8 production by monocytic cells. Mol Immunol *44*, 1969-1976.

Kurt-Jones, E.A., Mandell, L., Whitney, C., Padgett, A., Gosselin, K., Newburger, P.E., and Finberg, R.W. (2002). Role of toll-like receptor 2 (TLR2) in neutrophil activation: GM-CSF enhances TLR2 expression and TLR2-mediated interleukin 8 responses in neutrophils. Blood *100*, 1860-1868.

Kurt-Jones, E.A., Sandor, F., Ortiz, Y., Bowen, G.N., Counter, S.L., Wang, T.C., and Finberg, R.W. (2004). Use of murine embryonic fibroblasts to define Toll-like receptor activation and specificity. J Endotoxin Res *10*, 419-424.

Labéta, M.O., Vidal, K., Nores, J.E., Arias, M., Vita, N., Morgan, B.P., Guillemot, J.C., Loyaux, D., Ferrara, P., Schmid, D*., et al.* (2000). Innate recognition of bacteria in human milk is mediated by a milk-derived highly expressed pattern recognition receptor, soluble CD14. J Exp Med *191*, 1807-1812.

Lai, K.N., and Leung, J.C. (2010a). Inflammation in peritoneal dialysis. Nephron Clin Pract *116*, c11-18.

Lai, K.N., and Leung, J.C. (2010b). Peritoneal adipocytes and their role in inflammation during peritoneal dialysis. Mediators Inflamm *2010*, 495416.

Lam, M.F., Leung, J.C., Lo, W.K., Tam, S., Chong, M.C., Lui, S.L., Tse, K.C., Chan, T.M., and Lai, K.N. (2007). Hyperleptinaemia and chronic inflammation after peritonitis predicts poor nutritional status and mortality in patients on peritoneal dialysis. Nephrology, Dialysis, Transplantation: Official Publication Of The European Dialysis And Transplant Association - European Renal Association *22*, 1445-1450.

Lambie, M., Chess, J., Donovan, K.L., Kim, Y.L., Do, J.Y., Lee, H.B., Noh, H., Williams, P.F., Williams, A.J., Davison, S*., et al.* (2013). Independent effects of systemic and peritoneal inflammation on peritoneal dialysis survival. J Am Soc Nephrol *24*, 2071-2080.

Lambie, M.L., John, B., Mushahar, L., Huckvale, C., and Davies, S.J. (2010). The peritoneal osmotic conductance is low well before the diagnosis of encapsulating peritoneal sclerosis is made. Kidney Int *78*, 611-618.

Lande, R., Gregorio, J., Facchinetti, V., Chatterjee, B., Wang, Y.H., Homey, B., Cao, W., Su, B., Nestle, F.O., Zal, T*., et al.* (2007). Plasmacytoid dendritic cells sense self-DNA coupled with antimicrobial peptide. Nature *449*, 564-569.

Lang, M.J., and Topley, N. (1998). Isolation, culture and characterisation of human peritoneal mesothelial cells. Cell and Tissue Culture Manual: Specialized Vertebrate Cultures-Integumentary Systems and Muscular Tissue *vol 11B*, 10.11-10.13

Lang, V.R., Englbrecht, M., Rech, J., Nusslein, H., Manger, K., Schuch, F., Tony, H.P., Fleck, M., Manger, B., Schett, G., and Zwerina, J. (2012). Risk of infections in rheumatoid arthritis patients treated with tocilizumab. Rheumatology (Oxford) *51*, 852-857.

LeBouder, E., Rey-Nores, J.E., Raby, A.C., Affolter, M., Vidal, K., Thornton, C.A., and Labeta, M.O. (2006). Modulation of neonatal microbial recognition: TLR-mediated innate immune responses are specifically and differentially modulated by human milk. J Immunol *176*, 3742-3752.

LeBouder, E., Rey-Nores, J.E., Rushmere, N.K., Grigorov, M., Lawn, S.D., Affolter, M., Griffin, G.E., Ferrara, P., Schiffrin, E.J., Morgan, B.P., and Labeta, M.O. (2003). Soluble forms of Toll-like receptor (TLR)2 capable of modulating TLR2 signaling are present in human plasma and breast milk. J Immunol *171*, 6680-6689.

Lee, C.C., Avalos, A.M., and Ploegh, H.L. (2012). Accessory molecules for Toll-like receptors and their function. Nat Rev Immunol *12*, 168-179.

Lee, H.K., Dunzendorfer, S., Soldau, K., and Tobias, P.S. (2006). Double-stranded RNA-mediated TLR3 activation is enhanced by CD14. Immunity *24*, 153-163.

Lemaitre, B., Nicolas, E., Michaut, L., Reichhart, J.M., and Hoffmann, J.A. (1996). The dorsoventral regulatory gene cassette spatzle/Toll/cactus controls the potent antifungal response in Drosophila adults. Cell *86*, 973-983.

Li, F.K., Davenport, A., Robson, R.L., Loetscher, P., Rothlein, R., Williams, J.D., and Topley, N. (1998). Leukocyte migration across human peritoneal mesothelial cells is dependent on directed chemokine secretion and ICAM-1 expression. Kidney International *54*, 2170-2183.

Li, P.K., Szeto, C.C., Piraino, B., Bernardini, J., Figueiredo, A.E., Gupta, A., Johnson, D.W., Kuijper, E.J., Lye, W.C., Salzer, W.*, et al.* (2010). Peritoneal dialysis-related infections recommendations: 2010 update. Perit Dial Int *30*, 393-423.

Liew, F.Y., Liu, H., and Xu, D. (2005a). A novel negative regulator for IL-1 receptor and Toll-like receptor 4. Immunol Lett *96*, 27-31.

Liew, F.Y., Xu, D., Brint, E.K., and O'Neill, L.A. (2005b). Negative regulation of toll-like receptor-mediated immune responses. Nat Rev Immunol *5*, 446-458.

Lin, C.Y., and Huang, T.P. (1990). Serial peritoneal macrophage function studies in CAPD patients with peritonitis. Adv Perit Dial *6*, 114-119.

Lin, C.Y., Kift-Morgan, A., Moser, B., Topley, N., and Eberl, M. (2013a). Suppression of pro-inflammatory T-cell responses by human mesothelial cells. Nephrology, Dialysis, Transplantation: Official Publication Of The European Dialysis And Transplant Association - European Renal Association *28*, 1743-1750.

Lin, S.C., Lo, Y.C., and Wu, H. (2010). Helical assembly in the MyD88-IRAK4-IRAK2 complex in TLR/IL-1R signalling. Nature *465*, 885-890.

Lin, X.W., Xu, W.C., Luo, J.G., Guo, X.J., Sun, T., Zhao, X.L., and Fu, Z.J. (2013b). WW domain containing E3 ubiquitin protein ligase 1 (WWP1) negatively regulates TLR4-mediated TNF-alpha and IL-6 production by proteasomal degradation of TNF receptor associated factor 6 (TRAF6). PLoS One *8*, e67633.

Ling, P.R., Smith, R.J., Mueller, C., Mao, Y., and Bistrian, B.R. (2002). Inhibition of interleukin-6-activated janus kinases/signal transducers and activators of transcription but not mitogen-activated protein kinase signaling in liver of endotoxin-treated rats. Crit Care Med *30*, 202-211.

Litman, G.W., Rast, J.P., and Fugmann, S.D. (2010). The origins of vertebrate adaptive immunity. Nat Rev Immunol *10*, 543-553.

Livak, K.J., and Schmittgen, T.D. (2001). Analysis of relative gene expression data using real-time quantitative PCR and the 2(-Delta Delta C(T)) Method. Methods *25*, 402-408.

Lotz, M., Gutle, D., Walther, S., Menard, S., Bogdan, C., and Hornef, M.W. (2006). Postnatal acquisition of endotoxin tolerance in intestinal epithelial cells. J Exp Med *203*, 973-984.

Mackenzie, R., Holmes, C.J., Jones, S., Williams, J.D., and Topley, N. (2003). Clinical indices of in vivo biocompatibility: the role of ex vivo cell function studies and effluent markers in peritoneal dialysis patients. Kidney International Supplement, S84-93.

Mackenzie, R.K., Coles, G.A., and Williams, J.D. (1990). Eicosanoid synthesis in human peritoneal macrophages stimulated with S. epidermidis. Kidney Int *37*, 1316-1324.

Mactier, R. (2009). Peritonitis is still the achilles' heel of peritoneal dialysis. Peritoneal Dialysis International *29*, 262-266.

Man, L., Lewis, E., Einbinder, T., Rogachev, B., Chaimovitz, C., and Douvdevani, A. (2003). Major involvement of CD40 in the regulation of chemokine secretion from human peritoneal mesothelial cells. Kidney International *64*, 2064-2071.

Manfredi, A.A., Rovere-Querini, P., Bottazzi, B., Garlanda, C., and Mantovani, A. (2008). Pentraxins, humoral innate immunity and tissue injury. Curr Opin Immunol *20*, 538-544.

Mansell, A., and Jenkins, B.J. (2013). Dangerous liaisons between interleukin-6 cytokine and toll-like receptor families: a potent combination in inflammation and cancer. Cytokine Growth Factor Rev *24*, 249-256.

Marin, V., Montero-Julian, F.A., Gres, S., Boulay, V., Bongrand, P., Farnarier, C., and Kaplanski, G. (2001). The IL-6-soluble IL-6Ralpha autocrine loop of endothelial activation as an intermediate between acute and chronic inflammation: an experimental model involving thrombin. J Immunol *167*, 3435-3442.

Martin, J., Yung, S., Robson, R.L., Steadman, R., and Davies, M. (2000). Production and regulation of matrix metalloproteinases and their inhibitors by human peritoneal mesothelial cells. Perit Dial Int *20*, 524-533.

Martinon, F., Burns, K., and Tschopp, J. (2002). The inflammasome: a molecular platform triggering activation of inflammatory caspases and processing of proIL-beta. Mol Cell *10*, 417-426.

Martinon, F., Mayor, A., and Tschopp, J. (2009). The inflammasomes: guardians of the body. Annu Rev Immunol *27*, 229-265.

Masuda, G., and Tomioka, S. (1978). Quantitative assessment of bactericidal activities of beta-lactam antibiotics by agar plate method. Antimicrob Agents Chemother *14*, 587-595.

McCully, M.L., and Madrenas, J. (2006). Dendritic cells as arbiters of peritoneal immune responses. Perit Dial Int *26*, 8-25.

McGettrick, A.F., and O'Neill, L.A. (2010). Localisation and trafficking of Toll-like receptors: an important mode of regulation. Curr Opin Immunol *22*, 20-27.

McGregor, S.J., Topley, N., Jorres, A., Speekenbrink, A.B., Gordon, A., Gahl, G.M., Junor, B.J., Briggs, J.D., and Brock, J.H. (1996). Longitudinal evaluation of peritoneal macrophage function and activation during CAPD: maturity, cytokine synthesis and arachidonic acid metabolism. Kidney Int *49*, 525-533.

McLoughlin, R. (2005). Resolving peritoneal inflammation: flicking the right "switches". Perit Dial Int *25*, 223-229.

McLoughlin, R.M., Hurst, S.M., Nowell, M.A., Harris, D.A., Horiuchi, S., Morgan, L.W., Wilkinson, T.S., Yamamoto, N., Topley, N., and Jones, S.A. (2004). Differential regulation of neutrophil-activating chemokines by IL-6 and its soluble receptor isoforms. J Immunol *172*, 5676-5683.

McLoughlin, R.M., Jenkins, B.J., Grail, D., Williams, A.S., Fielding, C.A., Parker, C.R., Ernst, M., Topley, N., and Jones, S.A. (2005). IL-6 trans-signaling via STAT3 directs T cell infiltration in acute inflammation. Proc Natl Acad Sci U S A *102*, 9589-9594.

McLoughlin, R.M., Witowski, J., Robson, R.L., Wilkinson, T.S., Hurst, S.M., Williams, A.S., Williams, J.D., Rose-John, S., Jones, S.A., and Topley, N. (2003). Interplay between IFN-gamma and IL-6 signaling governs neutrophil trafficking and apoptosis during acute inflammation. J Clin Invest *112*, 598-607.

Medzhitov, R. (2007). Recognition of microorganisms and activation of the immune response. Nature *449*, 819-826.

Medzhitov, R. (2008). Origin and physiological roles of inflammation. Nature *454*, 428-435.

Medzhitov, R., Preston-Hurlburt, P., and Janeway, C.A., Jr. (1997). A human homologue of the Drosophila Toll protein signals activation of adaptive immunity. Nature *388*, 394-397.

Melmed, G., Thomas, L.S., Lee, N., Tesfay, S.Y., Lukasek, K., Michelsen, K.S., Zhou, Y., Hu, B., Arditi, M., and Abreu, M.T. (2003). Human intestinal epithelial cells are broadly unresponsive to Toll-like receptor 2-dependent bacterial ligands: implications for host-microbial interactions in the gut. J Immunol *170*, 1406-1415.

Meylan, E., Curran, J., Hofmann, K., Moradpour, D., Binder, M., Bartenschlager, R., and Tschopp, J. (2005). Cardif is an adaptor protein in the RIG-I antiviral pathway and is targeted by hepatitis C virus. Nature *437*, 1167-1172.

Miggin, S.M., and O'Neill, L.A. (2006). New insights into the regulation of TLR signaling. J Leukoc Biol *80*, 220-226.

Minot, C.S. (1880). A sketch of comparative embryology. The American Naturalist *14*, 871-880.

Modur, V., Li, Y., Zimmerman, G.A., Prescott, S.M., and McIntyre, T.M. (1997). Retrograde inflammatory signaling from neutrophils to endothelial cells by soluble interleukin-6 receptor alpha. J Clin Invest *100*, 2752-2756.

Morgan, L.W., Wieslander, A., Davies, M., Horiuchi, T., Ohta, Y., Beavis, M.J., Craig, K.J., Williams, J.D., and Topley, N. (2003). Glucose degradation products (GDP) retard remesothelialization independently of D-glucose concentration. Kidney International *64*, 1854-1866.

Moro, K., Yamada, T., Tanabe, M., Takeuchi, T., Ikawa, T., Kawamoto, H., Furusawa, J., Ohtani, M., Fujii, H., and Koyasu, S. (2010). Innate production of T(H)2 cytokines by adipose tissue-associated c-Kit(+)Sca-1(+) lymphoid cells. Nature *463*, 540-544.

Morris, G.E., Whyte, M.K., Martin, G.F., Jose, P.J., Dower, S.K., and Sabroe, I. (2005). Agonists of toll-like receptors 2 and 4 activate airway smooth muscle via mononuclear leukocytes. Am J Respir Crit Care Med *171*, 814-822.

Mortier, S., Lameire, N.H., and De Vriese, A.S. (2004). The effects of peritoneal dialysis solutions on peritoneal host defense. Perit Dial Int *24*, 123-138.

Muijsken, M.A., Heezius, H.J., Verhoef, J., and Verbrugh, H.A. (1991). Role of mesothelial cells in peritoneal antibacterial defence. J Clin Pathol *44*, 600-604.

Mulla, M.J., Myrtolli, K., Tadesse, S., Stanwood, N.L., Gariepy, A., Guller, S., Norwitz, E.R., and Abrahams, V.M. (2013). Cutting-edge report: TLR10 plays a role in mediating bacterial peptidoglycan-induced trophoblast apoptosis. Am J Reprod Immunol *69*, 449-453.

Mullaly, S.C., and Kubes, P. (2006). The role of TLR2 in vivo following challenge with Staphylococcus aureus and prototypic ligands. Journal of Immunology *177*, 8154-8163.

Munib, S. (2006). Continuous ambulatory peritoneal dialysis (CAPD) Gomal Journal of Medical Sciences July–Dec 2006 *4*, 82-85.

Mutsaers, S.E. (2002). Mesothelial cells: their structure, function and role in serosal repair. Respirology *7*, 171-191.

Mutsaers, S.E. (2004). The mesothelial cell. The International Journal Of Biochemistry & Cell Biology *36*, 9-16.

Muzio, M., Bosisio, D., Polentarutti, N., D'Amico, G., Stoppacciaro, A., Mancinelli, R., van't Veer, C., Penton-Rol, G., Ruco, L.P., Allavena, P., and Mantovani, A. (2000). Differential expression and regulation of toll-like receptors (TLR) in human leukocytes: selective expression of TLR3 in dendritic cells. J Immunol *164*, 5998-6004.

Nagy, J., and Jackman, R. (1998). Anatomy and Physiology of the Peritoneal Membrane. Seminars in Dialysis *11*, 49-56

Nakata, T., Yasuda, M., Fujita, M., Kataoka, H., Kiura, K., Sano, H., and Shibata, K. (2006). CD14 directly binds to triacylated lipopeptides and facilitates recognition of the lipopeptides by the receptor complex of Toll-like receptors 2 and 1 without binding to the complex. Cell Microbiol *8*, 1899-1909.

Nakatsu, F., and Ohno, H. (2003). Adaptor protein complexes as the key regulators of protein sorting in the post-Golgi network. Cell Struct Funct *28*, 419-429.

Nasreen, N., Mohammed, K.A., Hardwick, J., Van Horn, R.D., Sanders, K.L., Doerschuk, C.M., Hott, J.W., and Antony, V.B. (2001). Polar production of interleukin-8 by mesothelial cells promotes the transmesothelial migration of neutrophils: role of intercellular adhesion molecule-1. J Infect Dis *183*, 1638-1645.

Netea, M.G., Van der Graaf, C., Van der Meer, J.W., and Kullberg, B.J. (2004). Recognition of fungal pathogens by Toll-like receptors. Eur J Clin Microbiol Infect Dis *23*, 672-676.

Nguyen, L.T., Haney, E.F., and Vogel, H.J. (2011). The expanding scope of antimicrobial peptide structures and their modes of action. Trends Biotechnol *29*, 464-472.

Ni, M., MacFarlane, A.W.t., Toft, M., Lowell, C.A., Campbell, K.S., and Hamerman, J.A. (2012). B-cell adaptor for PI3K (BCAP) negatively regulates Toll-like receptor signaling through activation of PI3K. Proc Natl Acad Sci U S A *109*, 267-272.

Nishinakamura, H., Minoda, Y., Saeki, K., Koga, K., Takaesu, G., Onodera, M., Yoshimura, A., and Kobayashi, T. (2007). An RNA-binding protein alphaCP-1 is involved in the STAT3-mediated suppression of NF-kappaB transcriptional activity. Int Immunol *19*, 609-619.

Nomura, F., Akashi, S., Sakao, Y., Sato, S., Kawai, T., Matsumoto, M., Nakanishi, K., Kimoto, M., Miyake, K., Takeda, K., and Akira, S. (2000). Cutting edge: endotoxin tolerance in mouse peritoneal macrophages correlates with down-regulation of surface toll-like receptor 4 expression. Journal Of Immunology (Baltimore, Md : 1950) *164*, 3476-3479.

O'Neill, L.A. (2008). When signaling pathways collide: positive and negative regulation of toll-like receptor signal transduction. Immunity *29*, 12-20.

O'Neill, L.A., and Bowie, A.G. (2007). The family of five: TIR-domain-containing adaptors in Toll-like receptor signalling. Nat Rev Immunol *7*, 353-364.

O'Neill, L.A., Golenbock, D., and Bowie, A.G. (2013). The history of Toll-like receptors - redefining innate immunity. Nat Rev Immunol *13*, 453-460.

O'Neill, L.A., Sheedy, F.J., and McCoy, C.E. (2011). MicroRNAs: the fine-tuners of Toll-like receptor signalling. Nat Rev Immunol *11*, 163-175.

O'Reilly, S., Cant, R., Ciechomska, M., Finnegan, J., Oakley, F., Hambleton, S., and van Laar, J.M. (2014). Serum Amyloid A (SAA) induces IL-6 in dermal fibroblasts via TLR2, IRAK4 and NF-kappaB. Immunology.

Oh, K.H., Jung, J.Y., Yoon, M.O., Song, A., Lee, H., Ro, H., Hwang, Y.H., Kim, D.K., Margetts, P., and Ahn, C. (2010). Intra-peritoneal interleukin-6 system is a potent determinant of the baseline peritoneal solute transport in incident peritoneal dialysis patients. Nephrology, Dialysis, Transplantation: Official Publication Of The European Dialysis And Transplant Association - European Renal Association *25*, 1639-1646.

Olfert, E.D., and Godson, D.L. (2000). Humane endpoints for infectious disease animal models. ILAR J *41*, 99-104.

Onogawa, T. (2005). Local delivery of soluble interleukin-6 receptors to improve the outcome of alpha-toxin producing Staphylococcus aureus infection in mice. Immunobiology *209*, 651-660.

Onogawa, T., Saito-Taki, T., Yamamoto, H., and Wada, T. (2013). IL6 trans-signaling promotes functional recovery of hypofunctional phagocytes through STAT3 activation during peritonitis. Inflamm Res *62*, 797-810.

Oshiumi, H., Matsumoto, M., Funami, K., Akazawa, T., and Seya, T. (2003a). TICAM-1, an adaptor molecule that participates in Toll-like receptor 3-mediated interferon-beta induction. Nat Immunol *4*, 161-167.

Oshiumi, H., Sasai, M., Shida, K., Fujita, T., Matsumoto, M., and Seya, T. (2003b). TIR-containing adapter molecule (TICAM)-2, a bridging adapter recruiting to toll-like receptor 4 TICAM-1 that induces interferon-beta. J Biol Chem *278*, 49751-49762.

Osuchowski, M.F., Welch, K., Siddiqui, J., and Remick, D.G. (2006). Circulating cytokine/inhibitor profiles reshape the understanding of the SIRS/CARS continuum in sepsis and predict mortality. J Immunol *177*, 1967-1974.

Otto, M. (2009). Staphylococcus epidermidis--the 'accidental' pathogen. Nat Rev Microbiol *7*, 555-567.

Ozinsky, A., Underhill, D.M., Fontenot, J.D., Hajjar, A.M., Smith, K.D., Wilson, C.B., Schroeder, L., and Aderem, A. (2000). The repertoire for pattern recognition of pathogens by the innate immune system is defined by cooperation between toll-like receptors. Proc Natl Acad Sci U S A *97*, 13766-13771.

Park, B., Buti, L., Lee, S., Matsuwaki, T., Spooner, E., Brinkmann, M.M., Nishihara, M., and Ploegh, H.L. (2011). Granulin is a soluble cofactor for toll-like receptor 9 signaling. Immunity *34*, 505-513.

Park, J.H., Kim, Y.G., Shaw, M., Kanneganti, T.D., Fujimoto, Y., Fukase, K., Inohara, N., and Nunez, G. (2007). Nod1/RICK and TLR Signaling Regulate Chemokine and Antimicrobial Innate Immune Responses in Mesothelial Cells. J Immunol *179*, 514-521.

Park, M.S., Lee, H.A., Chu, W.S., Yang, D.H., and Hwang, S.D. (2000). Peritoneal accumulation of AGE and peritoneal membrane permeability. Perit Dial Int *20*, 452-460.

Parolini, S., Santoro, A., Marcenaro, E., Luini, W., Massardi, L., Facchetti, F., Communi, D., Parmentier, M., Majorana, A., Sironi, M.*, et al.* (2007). The role of chemerin in the colocalization of NK and dendritic cell subsets into inflamed tissues. Blood *109*, 3625-3632.

Parroche, P., Lauw, F.N., Goutagny, N., Latz, E., Monks, B.G., Visintin, A., Halmen, K.A., Lamphier, M., Olivier, M., Bartholomeu, D.C.*, et al.* (2007). Malaria hemozoin is immunologically inert but radically enhances innate responses by presenting malaria DNA to Toll-like receptor 9. Proc Natl Acad Sci U S A *104*, 1919-1924.

Pecoits-Filho, R., Barany, P., Lindholm, B., Heimburger, O., and Stenvinkel, P. (2002). Interleukin-6 is an independent predictor of mortality in patients starting dialysis treatment. Nephrology, Dialysis, Transplantation: Official Publication Of The European Dialysis And Transplant Association - European Renal Association *17*, 1684-1688.

Pecoits-Filho, R., Carvalho, M.J., Stenvinkel, P., Lindholm, B., and Heimburger, O. (2006). Systemic and intraperitoneal interleukin-6 system during the first year of peritoneal dialysis. Perit Dial Int *26*, 53-63.

Peterson, L.W., and Artis, D. (2014). Intestinal epithelial cells: regulators of barrier function and immune homeostasis. Nat Rev Immunol *14*, 141-153.

Petrilli, V., Dostert, C., Muruve, D.A., and Tschopp, J. (2007). The inflammasome: a danger sensing complex triggering innate immunity. Curr Opin Immunol *19*, 615-622.

Philpott, D.J., Sorbara, M.T., Robertson, S.J., Croitoru, K., and Girardin, S.E. (2014). NOD proteins: regulators of inflammation in health and disease. Nat Rev Immunol *14*, 9-23.

Podack, E.R. (1984). Molecular composition of the tubular structure of the membrane attack complex of complement. J Biol Chem *259*, 8641-8647.

Podack, E.R., and Tschopp, J. (1984). Membrane attack by complement. Mol Immunol *21*, 589-603.

Poltorak, A., He, X., Smirnova, I., Liu, M.Y., Van Huffel, C., Du, X., Birdwell, D., Alejos, E., Silva, M., Galanos, C*., et al.* (1998). Defective LPS signaling in C3H/HeJ and C57BL/10ScCr mice: mutations in Tlr4 gene. Science (New York, N Y) *282*, 2085-2088.

Popovich, R.P., Moncrief, J.W., Nolph, K.D., Ghods, A.J., Twardowski, Z.J., and Pyle, W.K. (1978). Continuous ambulatory peritoneal dialysis. Annals of Internal Medicine *88*, 449-456.

Qureshi, S.T., Lariviere, L., Leveque, G., Clermont, S., Moore, K.J., Gros, P., and Malo, D. (1999). Endotoxin-tolerant mice have mutations in Toll-like receptor 4 (Tlr4). J Exp Med *189*, 615-625.

Raby, A.C., Holst, B., Davies, J., Colmont, C., Laumonnier, Y., Coles, B., Shah, S., Hall, J., Topley, N., Kohl, J*., et al.* (2011). TLR activation enhances C5a-induced pro-inflammatory responses by negatively modulating the second C5a receptor, C5L2. Eur J Immunol *41*, 2741-2752.

Raby, A.C., Le Bouder, E., Colmont, C., Davies, J., Richards, P., Coles, B., George, C.H., Jones, S.A., Brennan, P., Topley, N., and Labeta, M.O. (2009). Soluble TLR2 reduces inflammation without compromising bacterial clearance by disrupting TLR2 triggering. J Immunol *183*, 506-517.

Raftery, A.T., Slater, N.D., and Cope, G.H. (1989). Clinical Anatomy of the Peritoneal Mesothelium: A Review. Clinical Anatomy *2*, 69-45.

Ramos, B.F., Zhang, Y., Qureshi, R., and Jakschik, B.A. (1991). Mast cells are critical for the production of leukotrienes responsible for neutrophil recruitment in immune complex-induced peritonitis in mice. J Immunol *147*, 1636-1641.

Rangel-Moreno, J., Moyron-Quiroz, J.E., Carragher, D.M., Kusser, K., Hartson, L., Moquin, A., and Randall, T.D. (2009). Omental milky spots develop in the absence of lymphoid tissue-inducer cells and support B and T cell responses to peritoneal antigens. Immunity *30*, 731-743.

Rawlings, D.J., Schwartz, M.A., Jackson, S.W., and Meyer-Bahlburg, A. (2012). Integration of B cell responses through Toll-like receptors and antigen receptors. Nat Rev Immunol *12*, 282-294.

Remick, D.G., Bolgos, G.R., Siddiqui, J., Shin, J., and Nemzek, J.A. (2002). Six at six: interleukin-6 measured 6 h after the initiation of sepsis predicts mortality over 3 days. Shock *17*, 463-467.

Roberts, G.W., Baird, D., Gallagher, K., Jones, R.E., Pepper, C.J., Williams, J.D., and Topley, N. (2009). Functional effector memory T cells enrich the peritoneal cavity of patients treated with peritoneal dialysis. J Am Soc Nephrol *20*, 1895-1900.

Robinson, B. (1897). The peritoneum: Histology and physiology.

Robson, R.L., McLoughlin, R.M., Witowski, J., Loetscher, P., Wilkinson, T.S., Jones, S.A., and Topley, N. (2001). Differential regulation of chemokine production in human peritoneal mesothelial cells: IFN-gamma controls neutrophil migration across the mesothelium in vitro and in vivo. J Immunol *167*, 1028-1038.

Rocca, B., Dragani, A., and Pagliaccia, F. (2013). Identifying determinants of variability to tailor aspirin therapy. Expert Rev Cardiovasc Ther *11*, 365-379.

Rock, F.L., Hardiman, G., Timans, J.C., Kastelein, R.A., and Bazan, J.F. (1998). A family of human receptors structurally related to Drosophila Toll. Proc Natl Acad Sci U S A *95*, 588-593.

Romano, M., Sironi, M., Toniatti, C., Polentarutti, N., Fruscella, P., Ghezzi, P., Faggioni, R., Luini, W., van Hinsbergh, V., Sozzani, S*., et al.* (1997). Role of IL-6 and its soluble receptor in induction of chemokines and leukocyte recruitment. Immunity *6*, 315-325.

Rose-John, S., Scheller, J., Elson, G., and Jones, S.A. (2006). Interleukin-6 biology is coordinated by membrane-bound and soluble receptors: role in inflammation and cancer. J Leukoc Biol *80*, 227-236.

Rosenbaum, S.B., and Lipton, M.L. (2012). Embracing chaos: the scope and importance of clinical and pathological heterogeneity in mTBI. Brain Imaging Behav *6*, 255-282.

Rothlin, C.V., Ghosh, S., Zuniga, E.I., Oldstone, M.B., and Lemke, G. (2007). TAM receptors are pleiotropic inhibitors of the innate immune response. Cell *131*, 1124-1136.

Rougier, J.P., Moullier, P., Piedagnel, R., and Ronco, P.M. (1997). Hyperosmolality suppresses but TGF beta 1 increases MMP9 in human peritoneal mesothelial cells. Kidney Int *51*, 337-347.

Rozen, S., and Skaletsky, H. (2000). Primer3 on the WWW for general users and for biologist programmers. Methods Mol Biol *132*, 365-386.

Rudolf, A., and Witowski, J. (2013). The impacts of dialysis fluids on senescent mesothelial cells. In 11th European Peritoneal Dialysis meeting (Maastricht, The Netherlands).

Ryckelynck, J.P., Lobbedez, T., and Hurault de Ligny, B. (2005). [Peritoneal dialysis]. Nephrol Ther *1*, 252-263.

Sabroe, I., Jones, E.C., Usher, L.R., Whyte, M.K., and Dower, S.K. (2002). Toll-like receptor (TLR)2 and TLR4 in human peripheral blood granulocytes: a critical role for monocytes in leukocyte lipopolysaccharide responses. J Immunol *168*, 4701-4710.

Saitoh, T., Tun-Kyi, A., Ryo, A., Yamamoto, M., Finn, G., Fujita, T., Akira, S., Yamamoto, N., Lu, K.P., and Yamaoka, S. (2006). Negative regulation of interferon-regulatory factor 3-dependent innate antiviral response by the prolyl isomerase Pin1. Nat Immunol *7*, 598-605.

Sakai, A., Han, J., Cato, A.C., Akira, S., and Li, J.D. (2004). Glucocorticoids synergize with IL-1beta to induce TLR2 expression via MAP Kinase Phosphatase-1-dependent dual Inhibition of MAPK JNK and p38 in epithelial cells. BMC Mol Biol *5*, 2.

Sammour, T., Kahokehr, A., Soop, M., and Hill, A.G. (2010). Peritoneal damage: the inflammatory response and clinical implications of the neuro-immuno-humoral axis. World J Surg *34*, 704-720.

Sancho, D., and Reis e Sousa, C. (2012). Signaling by myeloid C-type lectin receptors in immunity and homeostasis. Annu Rev Immunol *30*, 491-529.

Sandor, F., and Buc, M. (2005). Toll-like receptors. II. Distribution and pathways involved in TLR signalling. Folia Biol (Praha) *51*, 188-197.

Sasai, M., Linehan, M.M., and Iwasaki, A. (2010). Bifurcation of Toll-like receptor 9 signaling by adaptor protein 3. Science *329*, 1530-1534.

Saxena, R. (2008). Pathogenesis and treatment of peritoneal membrane failure. Pediatr Nephrol *23*, 695-703.

Saxena, R., and West, C. (2006). Peritoneal dialysis: a primary care perspective. J Am Board Fam Med *19*, 380-389.

Scheller, J., Garbers, C., and Rose-John, S. (2013). Interleukin-6: From basic biology to selective blockade of pro-inflammatory activities. Semin Immunol.

Schroder, K., Sweet, M.J., and Hume, D.A. (2006). Signal integration between IFNgamma and TLR signalling pathways in macrophages. Immunobiology *211*, 511-524.

Sen, R., and Baltimore, D. (1986). Inducibility of kappa immunoglobulin enhancer-binding protein Nf-kappa B by a posttranslational mechanism. Cell *47*, 921-928.

Serada, S., Fujimoto, M., Mihara, M., Koike, N., Ohsugi, Y., Nomura, S., Yoshida, H., Nishikawa, T., Terabe, F., Ohkawara, T.*, et al.* (2008). IL-6 blockade inhibits the induction of myelin antigen-specific Th17 cells and Th1 cells in experimental autoimmune encephalomyelitis. Proc Natl Acad Sci U S A *105*, 9041-9046.

Serhan, C.N., Chiang, N., and Van Dyke, T.E. (2008). Resolving inflammation: dual anti-inflammatory and pro-resolution lipid mediators. Nat Rev Immunol *8*, 349-361.

Seth, R.B., Sun, L., Ea, C.K., and Chen, Z.J. (2005). Identification and characterization of MAVS, a mitochondrial antiviral signaling protein that activates NF-kappaB and IRF 3. Cell *122*, 669-682.

Shaykhiev, R., and Bals, R. (2007). Interactions between epithelial cells and leukocytes in immunity and tissue homeostasis. J Leukoc Biol *82*, 1-15.

Shi, M., Deng, W., Bi, E., Mao, K., Ji, Y., Lin, G., Wu, X., Tao, Z., Li, Z., Cai, X.*, et al.* (2008). TRIM30 alpha negatively regulates TLR-mediated NF-kappa B activation by targeting TAB2 and TAB3 for degradation. Nat Immunol *9*, 369-377.

Shikotra, A., Choy, D.F., Ohri, C.M., Doran, E., Butler, C., Hargadon, B., Shelley, M., Abbas, A.R., Austin, C.D., Jackman, J.*, et al.* (2012). Increased expression of immunoreactive thymic stromal lymphopoietin in patients with severe asthma. J Allergy Clin Immunol *129*, 104-111 e101-109.

Shimazu, R., Akashi, S., Ogata, H., Nagai, Y., Fukudome, K., Miyake, K., and Kimoto, M. (1999). MD-2, a molecule that confers lipopolysaccharide responsiveness on Toll-like receptor 4. J Exp Med *189*, 1777-1782.

Sims, J.E., March, C.J., Cosman, D., Widmer, M.B., MacDonald, H.R., McMahan, C.J., Grubin, C.E., Wignall, J.M., Jackson, J.L., Call, S.M., and et al. (1988). cDNA expression cloning of the IL-1 receptor, a member of the immunoglobulin superfamily. Science *241*, 585-589.

Sinnakirouchenan, R., and Holley, J.L. (2011). Peritoneal dialysis versus hemodialysis: risks, benefits, and access issues. Adv Chronic Kidney Dis *18*, 428-432.

Smyth, M.J., Cretney, E., Kelly, J.M., Westwood, J.A., Street, S.E., Yagita, H., Takeda, K., van Dommelen, S.L., Degli-Esposti, M.A., and Hayakawa, Y. (2005). Activation of NK cell cytotoxicity. Mol Immunol *42*, 501-510.

Soehnlein, O., and Lindbom, L. (2010). Phagocyte partnership during the onset and resolution of inflammation. Nat Rev Immunol *10*, 427-439.

Solana, R., Tarazona, R., Gayoso, I., Lesur, O., Dupuis, G., and Fulop, T. (2012). Innate immunosenescence: effect of aging on cells and receptors of the innate immune system in humans. Semin Immunol *24*, 331-341.

Soothill, J.S., Morton, D.B., and Ahmad, A. (1992). The HID50 (hypothermia-inducing dose 50): an alternative to the LD50 for measurement of bacterial virulence. Int J Exp Pathol *73*, 95-98.

Spight, D., Trapnell, B., Zhao, B., Berclaz, P., and Shanley, T.P. (2008). Granulocyte-macrophage-colony-stimulating factor-dependent peritoneal macrophage responses determine survival in experimentally induced peritonitis and sepsis in mice. Shock *30*, 434-442.

Spiller, S., Elson, G., Ferstl, R., Dreher, S., Mueller, T., Freudenberg, M., Daubeuf, B., Wagner, H., and Kirschning, C.J. (2008). TLR4-induced IFN-gamma production increases TLR2 sensitivity and drives Gram-negative sepsis in mice. Journal of Experimental Medicine *205*, 1747-1754.

Steward, R. (1987). Dorsal, an embryonic polarity gene in Drosophila, is homologous to the vertebrate proto-oncogene, c-rel. Science *238*, 692-694.

Stewart, C.R., Stuart, L.M., Wilkinson, K., van Gils, J.M., Deng, J., Halle, A., Rayner, K.J., Boyer, L., Zhong, R., Frazier, W.A.*, et al.* (2010). CD36 ligands promote sterile inflammation through assembly of a Toll-like receptor 4 and 6 heterodimer. Nat Immunol *11*, 155-161.

Strunk, T., Power Coombs, M.R., Currie, A.J., Richmond, P., Golenbock, D.T., Stoler-Barak, L., Gallington, L.C., Otto, M., Burgner, D., and Levy, O. (2010). TLR2 mediates recognition of live Staphylococcus epidermidis and clearance of bacteremia. PLoS One *5*, e10111.

Stuart, L.M., Deng, J., Silver, J.M., Takahashi, K., Tseng, A.A., Hennessy, E.J., Ezekowitz, R.A., and Moore, K.J. (2005). Response to Staphylococcus aureus requires CD36-mediated phagocytosis triggered by the COOH-terminal cytoplasmic domain. J Cell Biol *170*, 477-485.

Stylianou, E., Jenner, L.A., Davies, M., Coles, G.A., and Williams, J.D. (1990). Isolation, culture and characterization of human peritoneal mesothelial cells. Kidney Int *37*, 1563-1570.

Sun, J., Duffy, K.E., Ranjith-Kumar, C.T., Xiong, J., Lamb, R.J., Santos, J., Masarapu, H., Cunningham, M., Holzenburg, A., Sarisky, R.T.*, et al.* (2006). Structural and functional analyses of the human Toll-like receptor 3. Role of glycosylation. J Biol Chem *281*, 11144-11151.

Sun, S.C. (2008). Deubiquitylation and regulation of the immune response. Nat Rev Immunol *8*, 501-511.

Sutherland, R.E., Olsen, J.S., McKinstry, A., Villalta, S.A., and Wolters, P.J. (2008). Mast cell IL-6 improves survival from Klebsiella pneumonia and sepsis by enhancing neutrophil killing. J Immunol *181*, 5598-5605.

Szeto, C.C., and Chow, K.M. (2007). Gram-negative peritonitis--the Achilles heel of peritoneal dialysis? Perit Dial Int *27 Suppl 2*, S267-271.

Szeto, C.C., Chow, K.M., Kwan, B.C., Law, M.C., Chung, K.Y., Yu, S., Leung, C.B., and Li, P.K. (2007). Staphylococcus aureus peritonitis complicates peritoneal dialysis: review of 245 consecutive cases. Clin J Am Soc Nephrol *2*, 245-251.

Szeto, C.C., Kwan, B.C., Chow, K.M., Lau, M.F., Law, M.C., Chung, K.Y., Leung, C.B., and Li, P.K. (2008). Coagulase negative staphylococcal peritonitis in peritoneal dialysis patients: review of 232 consecutive cases. Clin J Am Soc Nephrol *3*, 91-97.

Szeto, C.C., Leung, C.B., Chow, K.M., Kwan, B.C., Law, M.C., Wang, A.Y., Lui, S.F., and Li, P.K. (2005). Change in bacterial aetiology of peritoneal dialysis-related peritonitis over 10 years: experience from a centre in South-East Asia. Clin Microbiol Infect *11*, 837-839.

Tabeta, K., Georgel, P., Janssen, E., Du, X., Hoebe, K., Crozat, K., Mudd, S., Shamel, L., Sovath, S., Goode, J.*, et al.* (2004). Toll-like receptors 9 and 3 as essential components of innate immune defense against mouse cytomegalovirus infection. Proc Natl Acad Sci U S A *101*, 3516-3521.

Takagi, N., Mihara, M., Moriya, Y., Nishimoto, N., Yoshizaki, K., Kishimoto, T., Takeda, Y., and Ohsugi, Y. (1998). Blockage of interleukin-6 receptor ameliorates joint disease in murine collagen-induced arthritis. Arthritis Rheum *41*, 2117-2121.

Takeuchi, O., and Akira, S. (2010). Pattern recognition receptors and inflammation. Cell *140*, 805-820.

Takeuchi, O., Hoshino, K., and Akira, S. (2000). Cutting edge: TLR2-deficient and MyD88-deficient mice are highly susceptible to Staphylococcus aureus infection. J Immunol *165*, 5392-5396.

Takeuchi, O., Kawai, T., Muhlradt, P.F., Morr, M., Radolf, J.D., Zychlinsky, A., Takeda, K., and Akira, S. (2001). Discrimination of bacterial lipoproteins by Toll-like receptor 6. Int Immunol *13*, 933-940.

Takeuchi, O., Sato, S., Horiuchi, T., Hoshino, K., Takeda, K., Dong, Z., Modlin, R.L., and Akira, S. (2002). Cutting edge: role of Toll-like receptor 1 in mediating immune response to microbial lipoproteins. J Immunol *169*, 10-14.

Tanaka, T., Narazaki, M., and Kishimoto, T. (2012). Therapeutic targeting of the interleukin-6 receptor. Annu Rev Pharmacol Toxicol *52*, 199-219.

Tang, S., Leung, J.C., Chan, L.Y., Tsang, A.W., Chen, C.X., Zhou, W., Lai, K.N., and Sacks, S.H. (2004). Regulation of complement C3 and C4 synthesis in human peritoneal mesothelial cells by peritoneal dialysis fluid. Clin Exp Immunol *136*, 85-94.

Tavares, L.S., Silva, C.S., de Souza, V.C., da Silva, V.L., Diniz, C.G., and Santos, M.O. (2013). Strategies and molecular tools to fight antimicrobial resistance: resistome, transcriptome, and antimicrobial peptides. Front Microbiol *4*, 412.

ter Wee, P.M., Beelen, R.H., and van den Born, J. (2003). The application of animal models to study the biocompatibility of bicarbonate-buffered peritoneal dialysis solutions. Kidney Int Suppl, S75-83.

Terlizzi, M., Casolaro, V., Pinto, A., and Sorrentino, R. (2014). Inflammasome: Cancer's friend or foe? Pharmacol Ther.

Tian, J., Avalos, A.M., Mao, S.Y., Chen, B., Senthil, K., Wu, H., Parroche, P., Drabic, S., Golenbock, D., Sirois, C.*, et al.* (2007). Toll-like receptor 9-dependent activation by DNA-containing immune complexes is mediated by HMGB1 and RAGE. Nat Immunol *8*, 487-496.

Tilg, H., Trehu, E., Atkins, M.B., Dinarello, C.A., and Mier, J.W. (1994). Interleukin-6 (IL-6) as an anti-inflammatory cytokine: induction of circulating IL-1 receptor antagonist and soluble tumor necrosis factor receptor p55. Blood *83*, 113-118.

Topley, N., Brown, Z., Jorres, A., Westwick, J., Davies, M., Coles, G.A., and Williams, J.D. (1993a). Human peritoneal mesothelial cells synthesize interleukin-8. Synergistic induction by interleukin-1 beta and tumor necrosis factor-alpha. Am J Pathol *142*, 1876-1886.

Topley, N., Jorres, A., Luttmann, W., Petersen, M.M., Lang, M.J., Thierauch, K.H., Muller, C., Coles, G.A., Davies, M., and Williams, J.D. (1993b). Human peritoneal mesothelial cells synthesize interleukin-6: induction by IL-1 beta and TNF alpha. Kidney Int *43*, 226-233.

Topley, N., Liberek, T., Davenport, A., Li, F.K., Fear, H., and Williams, J.D. (1996a). Activation of inflammation and leukocyte recruitment into the peritoneal cavity. Kidney Int Suppl *56*, S17-21.

Topley, N., Mackenzie, R.K., and Williams, J.D. (1996b). Macrophages and mesothelial cells in bacterial peritonitis. Immunobiology *195*, 563-573.

Topley, N., Petersen, M.M., Mackenzie, R., Neubauer, A., Stylianou, E., Kaever, V., Davies, M., Coles, G.A., Jorres, A., and Williams, J.D. (1994). Human peritoneal mesothelial cell prostaglandin synthesis: induction of cyclooxygenase mRNA by peritoneal macrophage-derived cytokines. Kidney Int *46*, 900-909.

Topley, N., and Williams, J.D. (1994). Role of the peritoneal membrane in the control of inflammation in the peritoneal cavity. Kidney Int Suppl *48*, S71-78.

Tosi, M.F. (2005). Innate immune responses to infection. J Allergy Clin Immunol *116*, 241-249; quiz 250.

Trikha, M., Corringham, R., Klein, B., and Rossi, J.F. (2003). Targeted anti-interleukin-6 monoclonal antibody therapy for cancer: a review of the rationale and clinical evidence. Clin Cancer Res *9*, 4653-4665.

Trinchieri, G., and Sher, A. (2007). Cooperation of Toll-like receptor signals in innate immune defence. Nat Rev Immunol *7*, 179-190.

Trompouki, E., Hatzivassiliou, E., Tsichritzis, T., Farmer, H., Ashworth, A., and Mosialos, G. (2003). CYLD is a deubiquitinating enzyme that negatively regulates NF-kappaB activation by TNFR family members. Nature *424*, 793-796.

Troutman, T.D., Hu, W., Fulenchek, S., Yamazaki, T., Kurosaki, T., Bazan, J.F., and Pasare, C. (2012). Role for B-cell adapter for PI3K (BCAP) as a signaling adapter linking Toll-like receptors (TLRs) to serine/threonine kinases PI3K/Akt. Proc Natl Acad Sci U S A *109*, 273-278.

Tsoi, S., Park, K.C., Kay, H.H., O'Brien, T.J., Podor, E., Sun, G., Douglas, S.E., Brown, L.L., and Johnson, S.C. (2006). Identification of a transcript encoding a soluble form of toll-like receptor 5 (TLR5) in Atlantic salmon during Aeromonas salmonicida infection. Vet Immunol Immunopathol *109*, 183-187.

Tsujita, T., Ishii, A., Tsukada, H., Matsumoto, M., Che, F.S., and Seya, T. (2006). Fish soluble Toll-like receptor (TLR)5 amplifies human TLR5 response via physical binding to flagellin. Vaccine *24*, 2193-2199.

Tsukada, T., Fushida, S., Harada, S., Yagi, Y., Kinoshita, J., Oyama, K., Tajima, H., Fujita, H., Ninomiya, I., Fujimura, T., and Ohta, T. (2012). The role of human peritoneal mesothelial cells in the fibrosis and progression of gastric cancer. Int J Oncol *41*, 476-482.

Tye, H., and Jenkins, B.J. (2013). Tying the knot between cytokine and toll-like receptor signaling in gastrointestinal tract cancers. Cancer Sci *104*, 1139-1145.

Tye, H., Kennedy, C.L., Najdovska, M., McLeod, L., McCormack, W., Hughes, N., Dev, A., Sievert, W., Ooi, C.H., Ishikawa, T.O.*, et al.* (2012). STAT3-driven upregulation of TLR2 promotes gastric tumorigenesis independent of tumor inflammation. Cancer Cell *22*, 466-478.

Valle, M.T., Degl'Innocenti, M.L., Bertelli, R., Facchetti, P., Perfumo, F., Fenoglio, D., Kunkl, A., Gusmano, R., and Manca, F. (1995). Antigen-presenting function of human peritoneum mesothelial cells. Clin Exp Immunol *101*, 172-176.

van Aubel, R.A., Keestra, A.M., Krooshoop, D.J., van Eden, W., and van Putten, J.P. (2007). Ligand-induced differential cross-regulation of Toll-like receptors 2, 4 and 5 in intestinal epithelial cells. Mol Immunol *44*, 3702-3714.

van der Wal, J.B., and Jeekel, J. (2007). Biology of the peritoneum in normal homeostasis and after surgical trauma. Colorectal Dis *9 Suppl 2*, 9-13.

Vijay-Kumar, M., Sanders, C.J., Taylor, R.T., Kumar, A., Aitken, J.D., Sitaraman, S.V., Neish, A.S., Uematsu, S., Akira, S., Williams, I.R., and Gewirtz, A.T. (2007). Deletion of TLR5 results in spontaneous colitis in mice. J Clin Invest *117*, 3909-3921.

Virtue, A., Wang, H., and Yang, X.F. (2012). MicroRNAs and toll-like receptor/interleukin-1 receptor signaling. J Hematol Oncol *5*, 66.

Visser, C.E., Brouwer-Steenbergen, J.J., Betjes, M.G., Koomen, G.C., Beelen, R.H., and Krediet, R.T. (1995a). Cancer antigen 125: a bulk marker for the mesothelial mass in stable peritoneal dialysis patients. Nephrology Dialysis Transplantation *10*, 64-69.

Visser, C.E., Brouwer-Steenbergen, J.J., Schadee-Eestermans, I.L., Meijer, S., Krediet, R.T., and Beelen, R.H. (1996). Ingestion of Staphylococcus aureus, Staphylococcus epidermidis, and Escherichia coli by human peritoneal mesothelial cells. Infect Immun *64*, 3425-3428.

Visser, C.E., Steenbergen, J.J., Betjes, M.G., Meijer, S., Arisz, L., Hoefsmit, E.C., Krediet, R.T., and Beelen, R.H. (1995b). Interleukin-8 production by human mesothelial cells after direct stimulation with staphylococci. Infection & Immunity *63*, 4206-4209.

Welte, T., Zhang, S.S., Wang, T., Zhang, Z., Hesslein, D.G., Yin, Z., Kano, A., Iwamoto, Y., Li, E., Craft, J.E.*, et al.* (2003). STAT3 deletion during hematopoiesis causes Crohn's disease-like pathogenesis and lethality: a critical role of STAT3 in innate immunity. Proc Natl Acad Sci U S A *100*, 1879-1884.

Whitham, S., Dinesh-Kumar, S.P., Choi, D., Hehl, R., Corr, C., and Baker, B. (1994). The product of the tobacco mosaic virus resistance gene N: similarity to toll and the interleukin-1 receptor. Cell *78*, 1101-1115.

Williams, J.D., Craig, K.J., Topley, N., Von Ruhland, C., Fallon, M., Newman, G.R., Mackenzie, R.K., and Williams, G.T. (2002). Morphologic changes in the peritoneal membrane of patients with renal disease. J Am Soc Nephrol *13*, 470-479.

Williams, J.D., Craig, K.J., Topley, N., and Williams, G.T. (2003a). Peritoneal dialysis: changes to the structure of the peritoneal membrane and potential for biocompatible solutions. Kidney International Supplement, S158-161.

Williams, J.D., Craig, K.J., von Ruhland, C., Topley, N., and Williams, G.T. (2003b). The natural course of peritoneal membrane biology during peritoneal dialysis. Kidney International Supplement, S43-49.

Wilson, J.L., Heffler, L.C., Charo, J., Scheynius, A., Bejarano, M.T., and Ljunggren, H.G. (1999). Targeting of human dendritic cells by autologous NK cells. J Immunol *163*, 6365-6370.

Witowski, J., Jorres, A., Coles, G.A., Williams, J.D., and Topley, N. (1996). Superinduction of IL-6 synthesis in human peritoneal mesothelial cells is related to the induction and stabilization of IL-6 mRNA. Kidney International *50*, 1212-1223.

Witowski, J., Korybalska, K., Wisniewska, J., Breborowicz, A., Gahl, G.M., Frei, U., Passlick-Deetjen, J., and Jorres, A. (2000). Effect of glucose degradation products on human peritoneal mesothelial cell function. J Am Soc Nephrol *11*, 729-739.

Witowski, J., Ksiazek, K., Warnecke, C., Kuzlan, M., Korybalska, K., Tayama, H., Wisniewska-Elnur, J., Pawlaczyk, K., Trominska, J., Breborowicz, A., and Jorres, A. (2007). Role of mesothelial cell-derived granulocyte colony-stimulating factor in interleukin-17-induced neutrophil accumulation in the peritoneum. Kidney Int *71*, 514-525.

Witowski, J., Tayama, H., Ksiazek, K., Wanic-Kossowska, M., Bender, T.O., and Jorres, A. (2009). Human peritoneal fibroblasts are a potent source of neutrophil-targeting cytokines: a key role of IL-1beta stimulation. Lab Invest *89*, 414-424.

Witowski, J., Thiel, A., Dechend, R., Dunkel, K., Fouquet, N., Bender, T.O., Langrehr, J.M., Gahl, G.M., Frei, U., and Jorres, A. (2001). Synthesis of C-X-C and C-C chemokines by human peritoneal fibroblasts: induction by macrophage-derived cytokines. Am J Pathol *158*, 1441-1450.

Wornle, M., Sauter, M., Kastenmuller, K., Ribeiro, A., Roeder, M., Schmid, H., Krotz, F., Mussack, T., Ladurner, R., and Sitter, T. (2009). Novel role of toll-like receptor 3, RIG-I and MDA5 in poly (I:C) RNA-induced mesothelial inflammation. Mol Cell Biochem *322*, 193-206.

Wu, J., Yang, X., Zhang, Y.F., Wang, Y.N., Liu, M., Dong, X.Q., Fan, J.J., and Yu, X.Q. (2010). Glucose-based peritoneal dialysis fluids downregulate toll-like receptors and trigger hyporesponsiveness to pathogen-associated molecular patterns in human peritoneal mesothelial cells. Clin Vaccine Immunol *17*, 757-763.

Wynn, T.A., and Ramalingam, T.R. (2012). Mechanisms of fibrosis: therapeutic translation for fibrotic disease. Nat Med *18*, 1028-1040.

Xing, Z., Gauldie, J., Cox, G., Baumann, H., Jordana, M., Lei, X.F., and Achong, M.K. (1998). IL-6 is an antiinflammatory cytokine required for controlling local or systemic acute inflammatory responses. J Clin Invest *101*, 311-320.

Yamamoto, M., Sato, S., Hemmi, H., Hoshino, K., Kaisho, T., Sanjo, H., Takeuchi, O., Sugiyama, M., Okabe, M., Takeda, K., and Akira, S. (2003a). Role of adaptor TRIF in the MyD88-independent toll-like receptor signaling pathway. Science *301*, 640-643.

Yamamoto, M., Sato, S., Hemmi, H., Uematsu, S., Hoshino, K., Kaisho, T., Takeuchi, O., Takeda, K., and Akira, S. (2003b). TRAM is specifically involved in the Toll-like receptor 4-mediated MyD88-independent signaling pathway. Nat Immunol *4*, 1144-1150.

Yamamoto, M., Sato, S., Mori, K., Hoshino, K., Takeuchi, O., Takeda, K., and Akira, S. (2002). Cutting edge: a novel Toll/IL-1 receptor domain-containing adapter that preferentially activates the IFN-beta promoter in the Toll-like receptor signaling. J Immunol *169*, 6668-6672.

Yanai, H., Ban, T., Wang, Z., Choi, M.K., Kawamura, T., Negishi, H., Nakasato, M., Lu, Y., Hangai, S., Koshiba, R.*, et al.* (2009). HMGB proteins function as universal sentinels for nucleic-acid-mediated innate immune responses. Nature *462*, 99-103.

Yao, V., Platell, C., and Hall, J.C. (2003). Role of peritoneal mesothelial cells in peritonitis. Br J Surg *90*, 1187-1194.

Yoshimura, A., Lien, E., Ingalls, R.R., Tuomanen, E., Dziarski, R., and Golenbock, D. (1999). Cutting edge: recognition of Gram-positive bacterial cell wall components by the innate immune system occurs via Toll-like receptor 2. J Immunol *163*, 1-5.

Young, V.J., Brown, J.K., Saunders, P.T., and Horne, A.W. (2013). The role of the peritoneum in the pathogenesis of endometriosis. Hum Reprod Update *19*, 558-569.

Yu, Z., Zhang, W., and Kone, B.C. (2002). Signal transducers and activators of transcription 3 (STAT3) inhibits transcription of the inducible nitric oxide synthase gene by interacting with nuclear factor kappaB. Biochem J *367*, 97-105.

Yuk, J.M., Shin, D.M., Lee, H.M., Kim, J.J., Kim, S.W., Jin, H.S., Yang, C.S., Park, K.A., Chanda, D., Kim, D.K.*, et al.* (2011). The orphan nuclear receptor SHP acts as a negative regulator in inflammatory signaling triggered by Toll-like receptors. Nat Immunol *12*, 742-751.

Yung, S., and Chan, T.M. (2009). Intrinsic cells: mesothelial cells -- central players in regulating inflammation and resolution. Perit Dial Int *29 Suppl 2*, S21-27.

Zanoni, I., Ostuni, R., Marek, L.R., Barresi, S., Barbalat, R., Barton, G.M., Granucci, F., and Kagan, J.C. (2011). CD14 controls the LPS-induced endocytosis of Toll-like receptor 4. Cell *147*, 868-880.

Zareie, M., Fabbrini, P., Hekking, L.H., Keuning, E.D., Ter Wee, P.M., Beelen, R.H., and van den Born, J. (2006). Novel role for mast cells in omental tissue remodeling and cell recruitment in experimental peritoneal dialysis. J Am Soc Nephrol *17*, 3447-3457.

Zarember, K.A., and Godowski, P.J. (2002). Tissue expression of human Toll-like receptors and differential regulation of Toll-like receptor mRNAs in leukocytes in response to microbes, their products, and cytokines. Journal Of Immunology (Baltimore, Md : 1950) *168*, 554-561.

Zlotnik, A., and Yoshie, O. (2000). Chemokines: a new classification system and their role in immunity. Immunity *12*, 121-127.

Zunt, S.L., Burton, L.V., Goldblatt, L.I., Dobbins, E.E., and Srinivasan, M. (2009). Soluble forms of Toll-like receptor 4 are present in human saliva and modulate tumour necrosis factor-alpha secretion by macrophage-like cells. Clin Exp Immunol *156*, 285-293.